Magnetic Nanomaterials.
Some Biomedical Applications: Magnetofection, Magnetic Hyperthermia, and Ferrogels for Drug Delivery

Francisco H. Sánchez
G3M, Physics Department and La Plata Institute of Physics, FCE,UNLP, CONICET, Argentina

Physics Building, 1905

Using magnetization of magnetic phase (NPs) M_p

$$M_p = \gamma^3 M$$

hence

$$H_i \approx \frac{\kappa\beta\lambda_1^S}{\gamma^3} M_p = -N_{Def} M_p$$

Determined by shape and NP dilution

$$N_{Def} = \frac{N_D}{\gamma^3}$$

Determined by shape

$$if\ \ \gamma > 3.16 \Rightarrow N_{Def} < 0.1 N_D$$

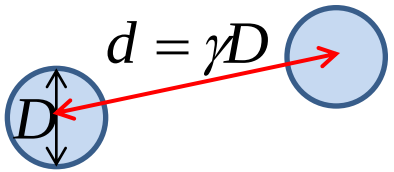

or $$N_{Def} = \left(\frac{D}{d}\right)^3 N_D$$

Case of interest

NPs are aggregated in clusters, and clusters interact among them. N_D is the demagnetizing factor which corresponds both to sample shape and to cluster average shape.

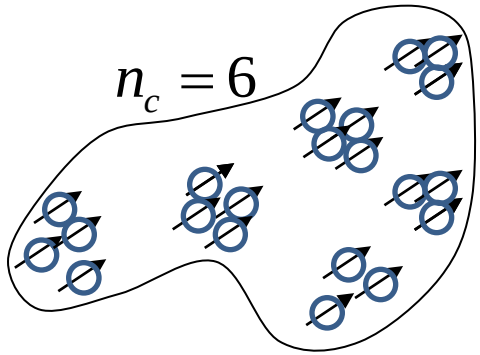

NP nuber $n_p = n_c n_{pc}$

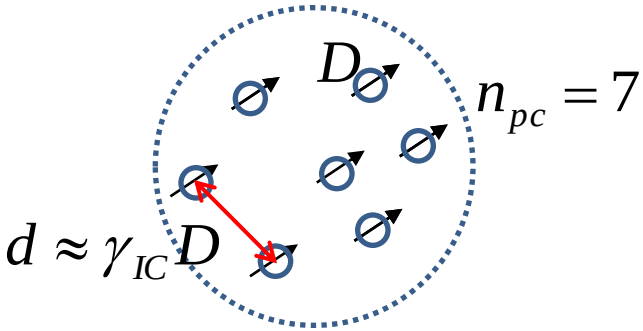

$$D_C^3 = n_{pc} \gamma_{IC}^3 D^3$$

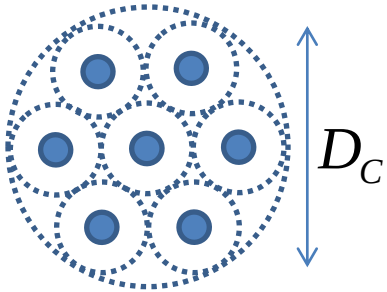

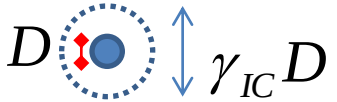

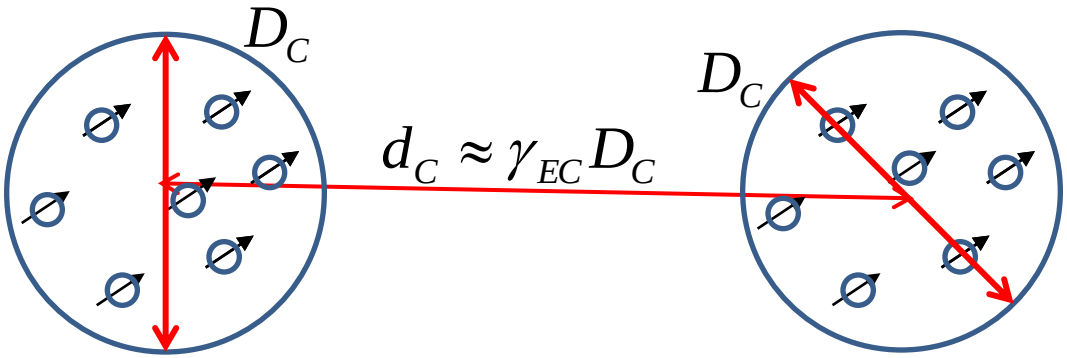

Leads to

$$N_{Def} \approx \frac{N_D^{cluster}}{\gamma_{IC}^3} + \frac{N_D^{sample} - N_D^{cluster}}{\gamma_{IC}^3 \gamma_{EC}^3}$$

This is the sought result, it gives the dependency of the effective demagnetizing factor in terms of cluster and sample ones, and the characteristic distances (dilution factors) of the problem.

Analysis with Langevin model. Comparison with Allia's proposition

$$\vec{H} = \vec{H}^{ap} + \vec{H}^{dip}$$

$$M_p = M_{pS} L\left(\frac{\mu_0 \vec{\mu} \cdot \vec{H}}{kT} \right) = M_{pS} L\left(\frac{\mu_0 \mu \left(H^{ap} + H^{dip} \right)}{kT} \right)$$

$$\vec{H}^{dip} = -N_{Def} \vec{M}_p$$

Assumptions $\vec{M}_p \uparrow\uparrow \vec{H} \uparrow\downarrow \vec{H}^{dip}$

$$M_p(H,T) = M_{pS} L\left(\frac{\mu_0 \mu \left(H^{ap} - N_{Def} M_p \right)}{kT} \right) = \frac{\mu}{V_p} L\left(\frac{\mu_0 \mu \left(H^{ap} - N_{Def} M_p \right)}{kT} \right)$$

When Langevin function argument is << 1

$$M_p = \frac{\mu_0 \mu^2 \left(H^{ap} - N_{Def} M_p \right)}{3kTV_p}$$

$$M_p = \frac{H^{ap}}{\frac{3kTV_p}{\mu_0 \mu^2} + N_{Def}}$$

$$\frac{1}{\chi_p} = \frac{3kT}{\mu_0 M_{pS}^2 V_p} + N_{Def}$$

$$\frac{1}{\chi_p} = \frac{3kTN_p}{\mu_0 M_{pS}^2} + N_{Def} \qquad N_p = 1/V_p$$

Measured susceptibility of magnetic phase.

$$\frac{\rho}{\chi} = \frac{3kN_{pp}}{\mu_0}\left(\frac{T}{M_S^2}\right) + \gamma_{EC}^3 N_D$$

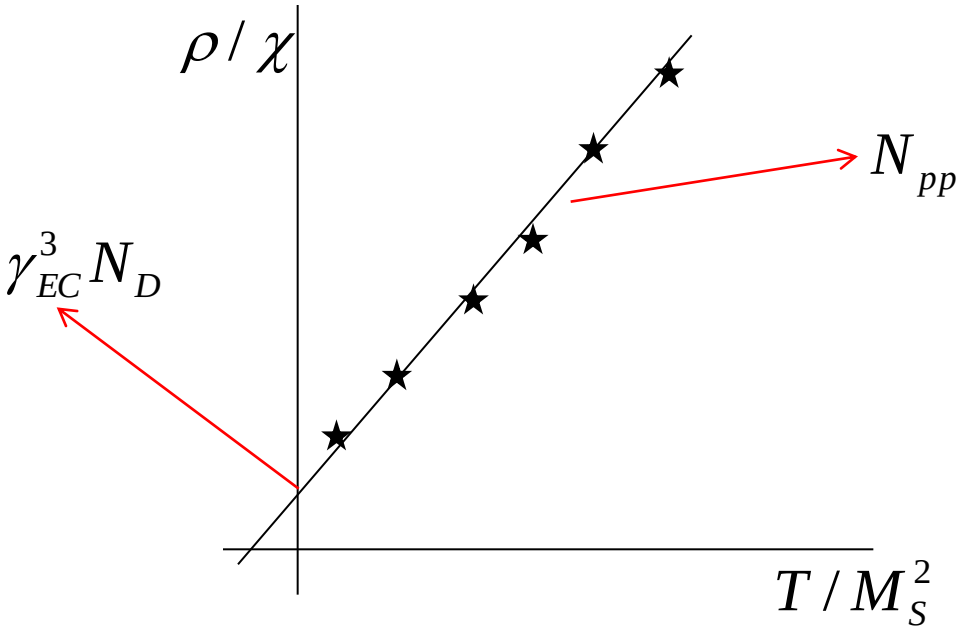

F.H. Sánchez

Shape effects

Ferrogel PVA/maghemite 15.7% mass concentration

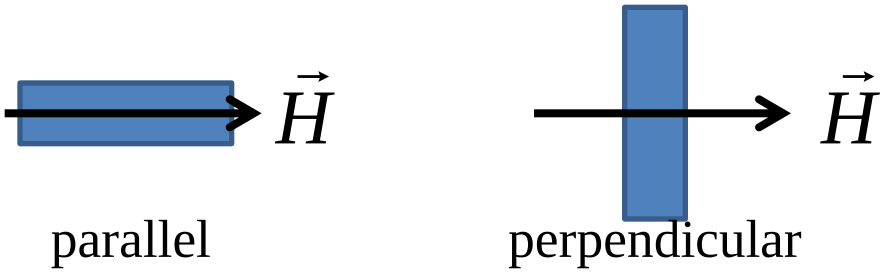

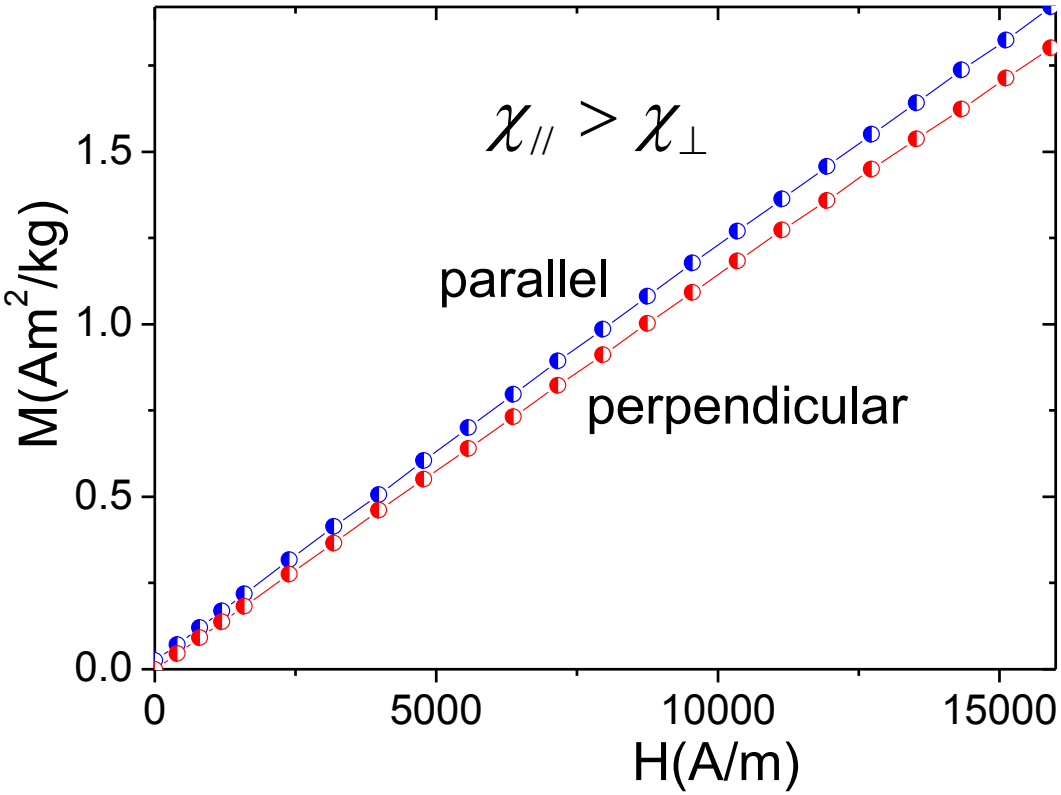

F.H. Sánchez

$$\chi_{//} \approx 1.13\times10^{3} m^{3}/kg$$

$$\chi_{\perp} \approx 1.08\times10^{3} m^{3}/kg$$

$$N_{Def\perp} - N_{Def//} \approx \frac{10^{3}}{4\pi\rho}\left(\frac{1}{\chi_{\perp}} - \frac{1}{\chi_{//}}\right)$$

Assuming a uniform distribution of NPs

$$\gamma^{3} \approx \frac{N_{D\perp} - N_{D//}}{N_{Def\perp} - N_{Def//}}$$

De la forma de la muestra

Demagnetizing factors for rectangular ferromagnetic prisms

Amikam Aharoni[a)]
Department of Electronics, Weizmann Institute of Science, 76100 Rehovoth, Israel
JOURNAL OF APPLIED PHYSICS
VOLUME 83, NUMBER 6
15 MARCH 1998

$$N_{//} = 0.06$$
$$N_{\perp} = 0.80$$

$$\gamma \approx 2.1$$

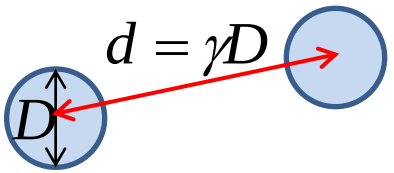

F.H. Sánchez

Estimation of γ from FG density and mass concentration of Fe oxide x, assuming a uniform distribution of NPs

$$x = \frac{m_{oFe}}{m_{FG}} \qquad \rho_{FG} = \frac{m_{FG}}{V_{FG}}$$

For FG 10_1

$$using \quad \begin{cases} \rho \approx 5.18 g/cm^3 \\ x = 0.157 \\ \rho_{FG} \approx 1.1 g/cm^3 \end{cases} \Rightarrow \quad \gamma \approx 2.5$$

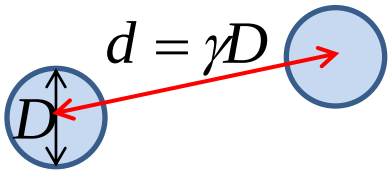

$\vec{\nabla} \cdot \vec{M} = 0$

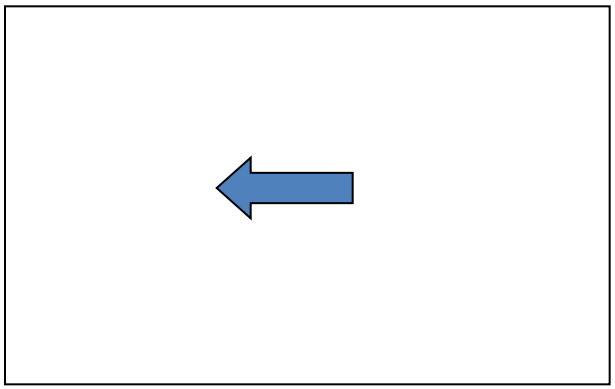

$\vec{\nabla} \cdot \vec{M} \neq 0$

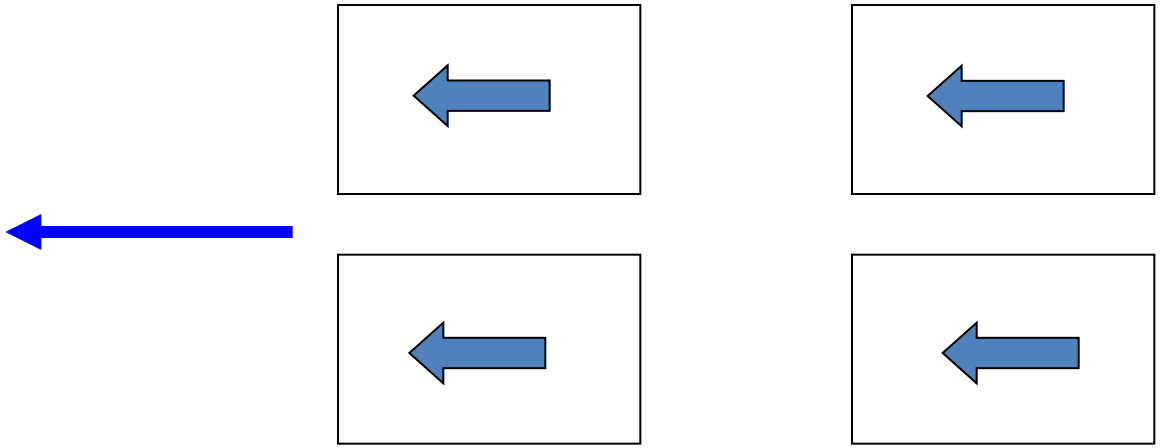

$\vec{H} = -N_D \vec{M}$

$\vec{\nabla} \cdot \vec{M} \neq 0$

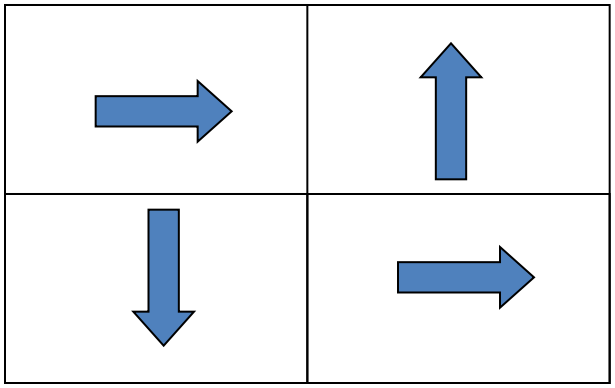

$\vec{\nabla} \cdot \vec{M} \neq 0$

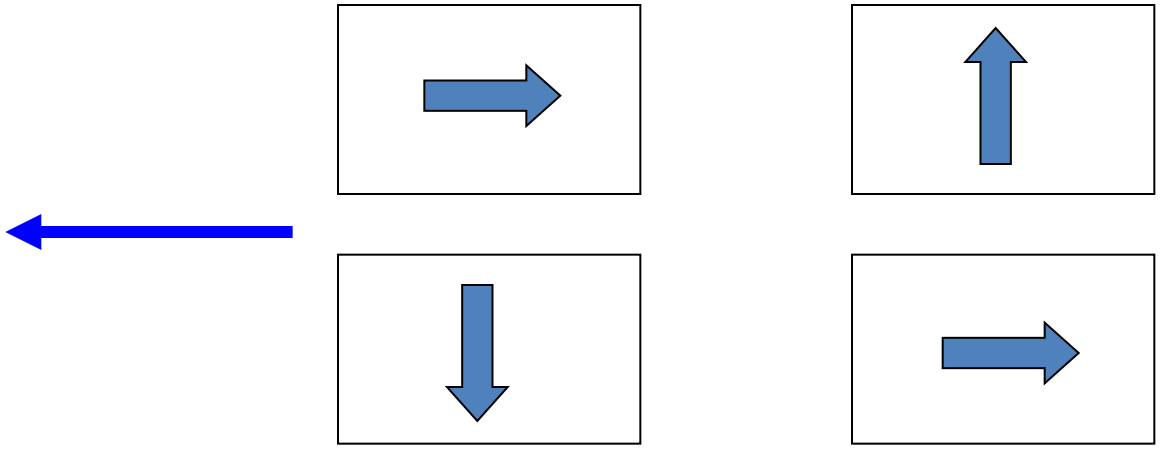

Class 2a

Understanding SAR and searching for high performance nanomaterials

zinc-doped magnetite nanoparticles and ferrofluids for hyperthermia applications

Citric Acid Coated Magnetite Nanoparticles for Magnetic Hyperthermia

In vitro experiments

Magnetic nanomaterials

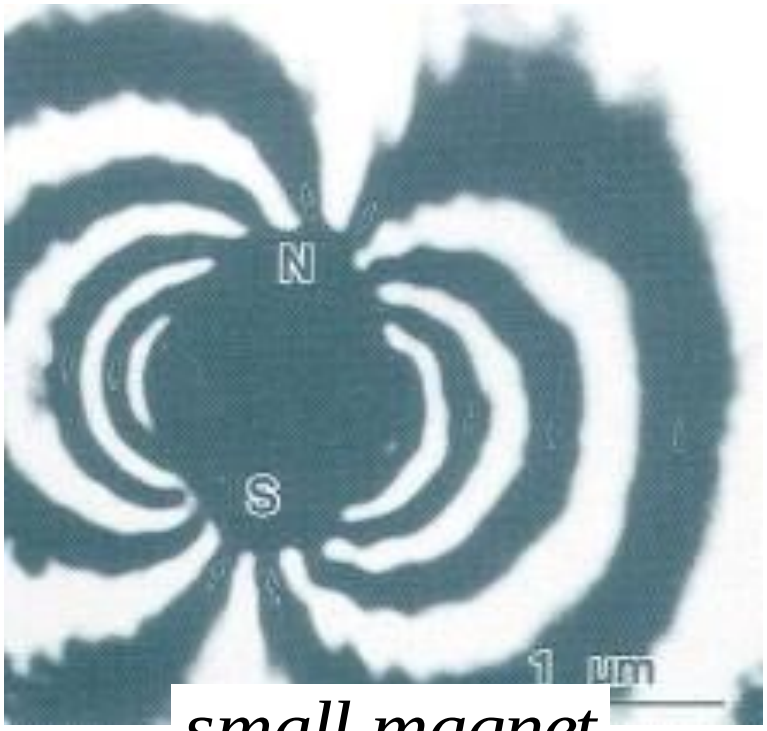

small magnet

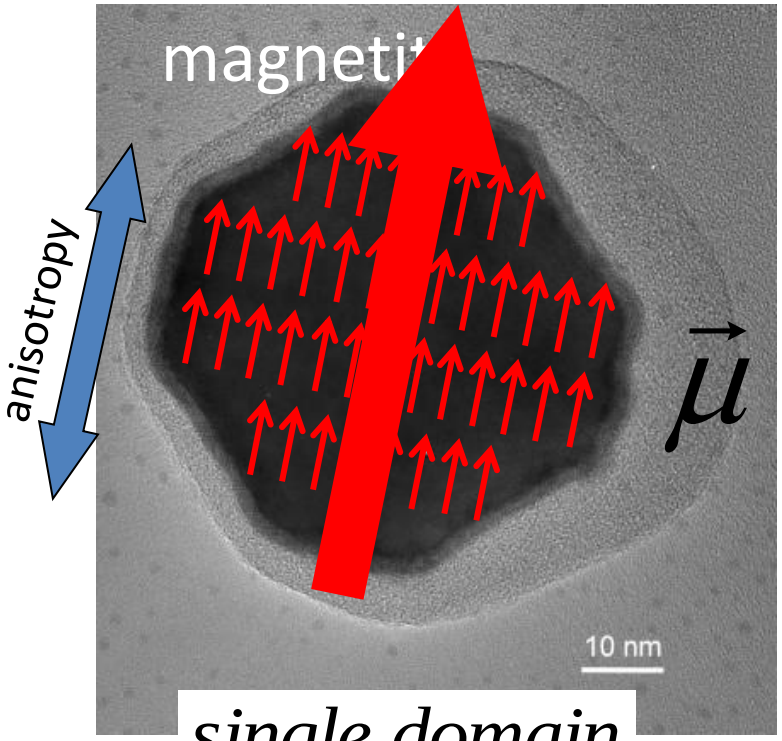

single domain

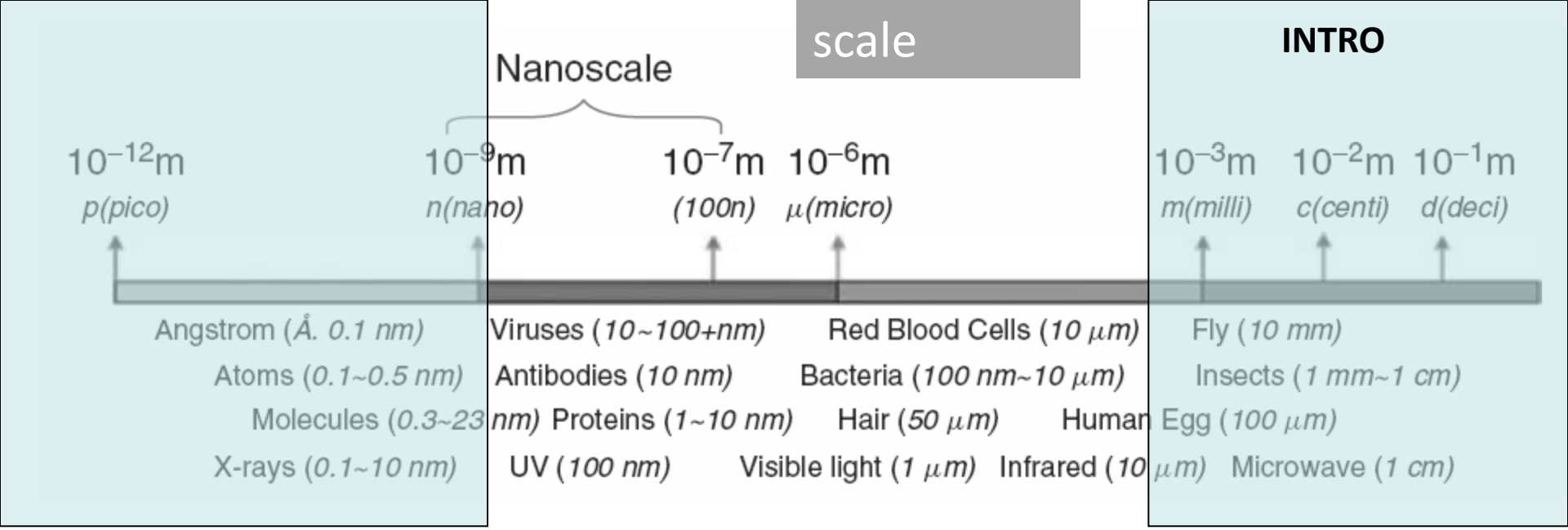

NANOMEDICINE

DESIGN AND APPLICATIONS OF MAGNETIC NANOMATERIALS, NANOSENSORS AND NANOSYSTEMS

Vijay K. Varadan, Linfeng Chen, Jining Xie

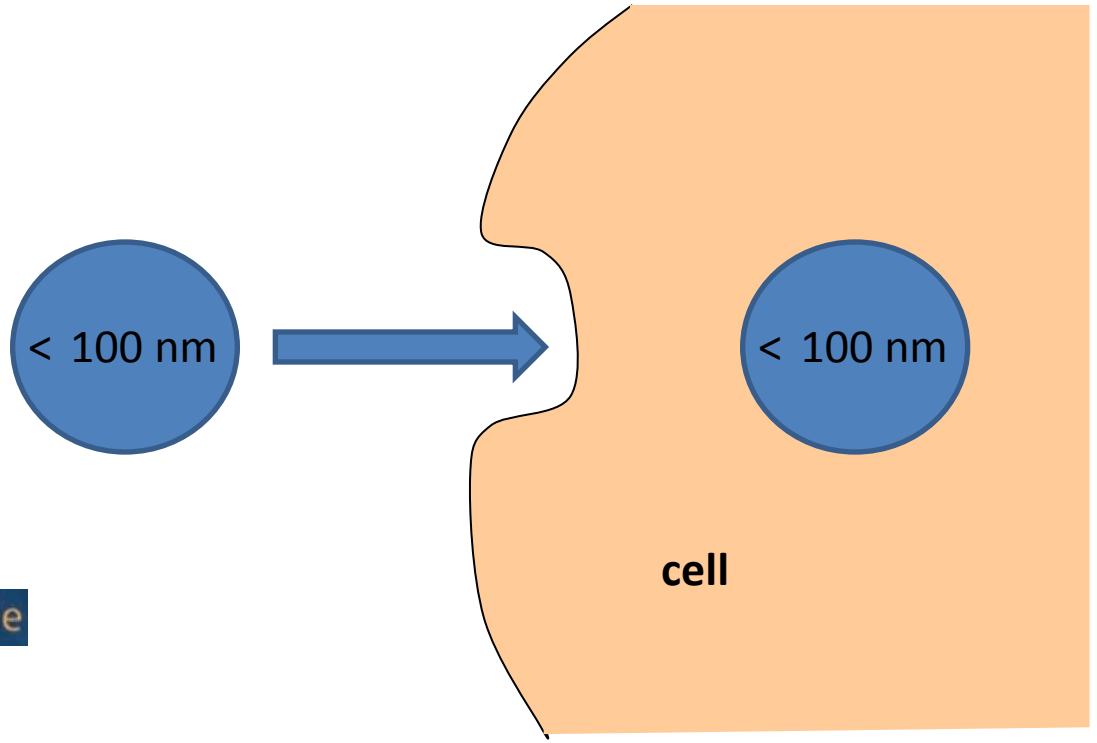

endocytosis

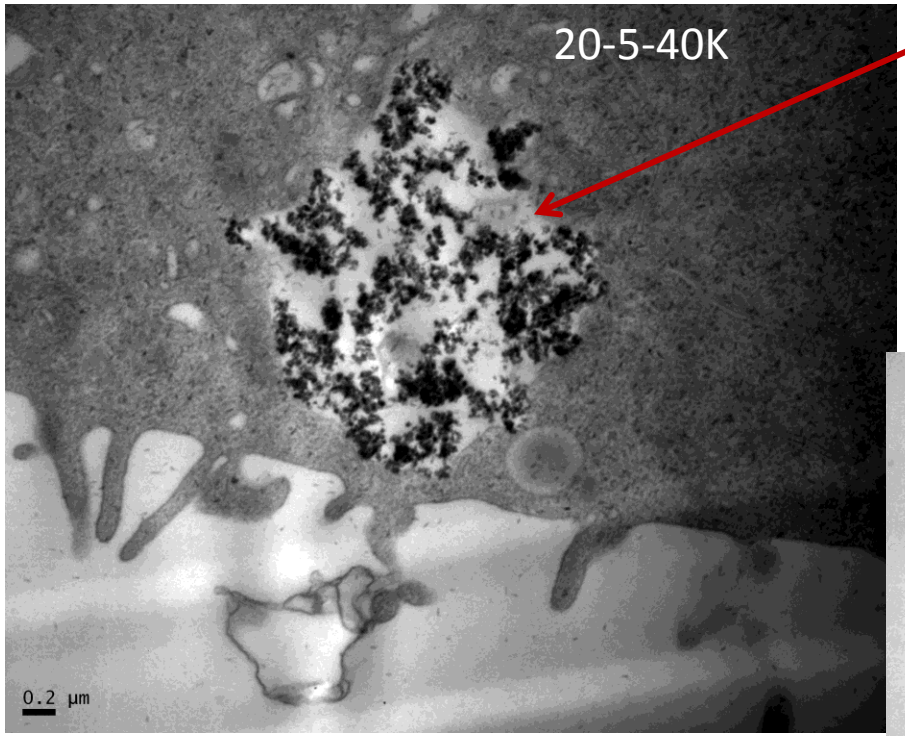

Cell endosome with MNP

endocytosis

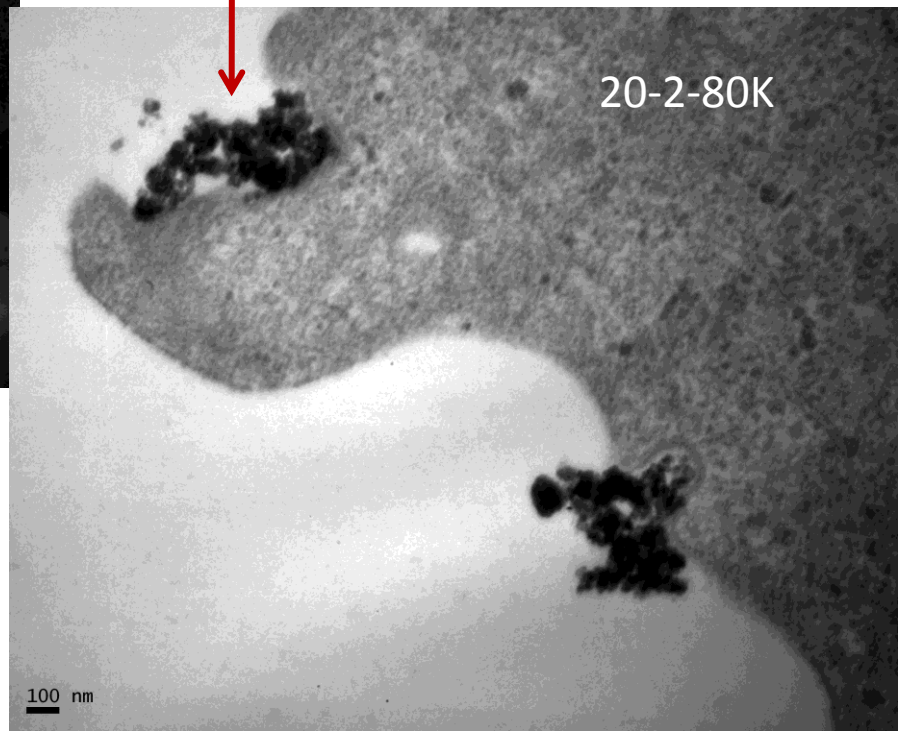

A549
Fe_3O_4
10 nm
20 μg/ml

Magnetic nanomaterials

Magnetic nanomaterials

MNP can be manipulated with static and dynamic magnetic fields and delivered to an specific place to perform a task

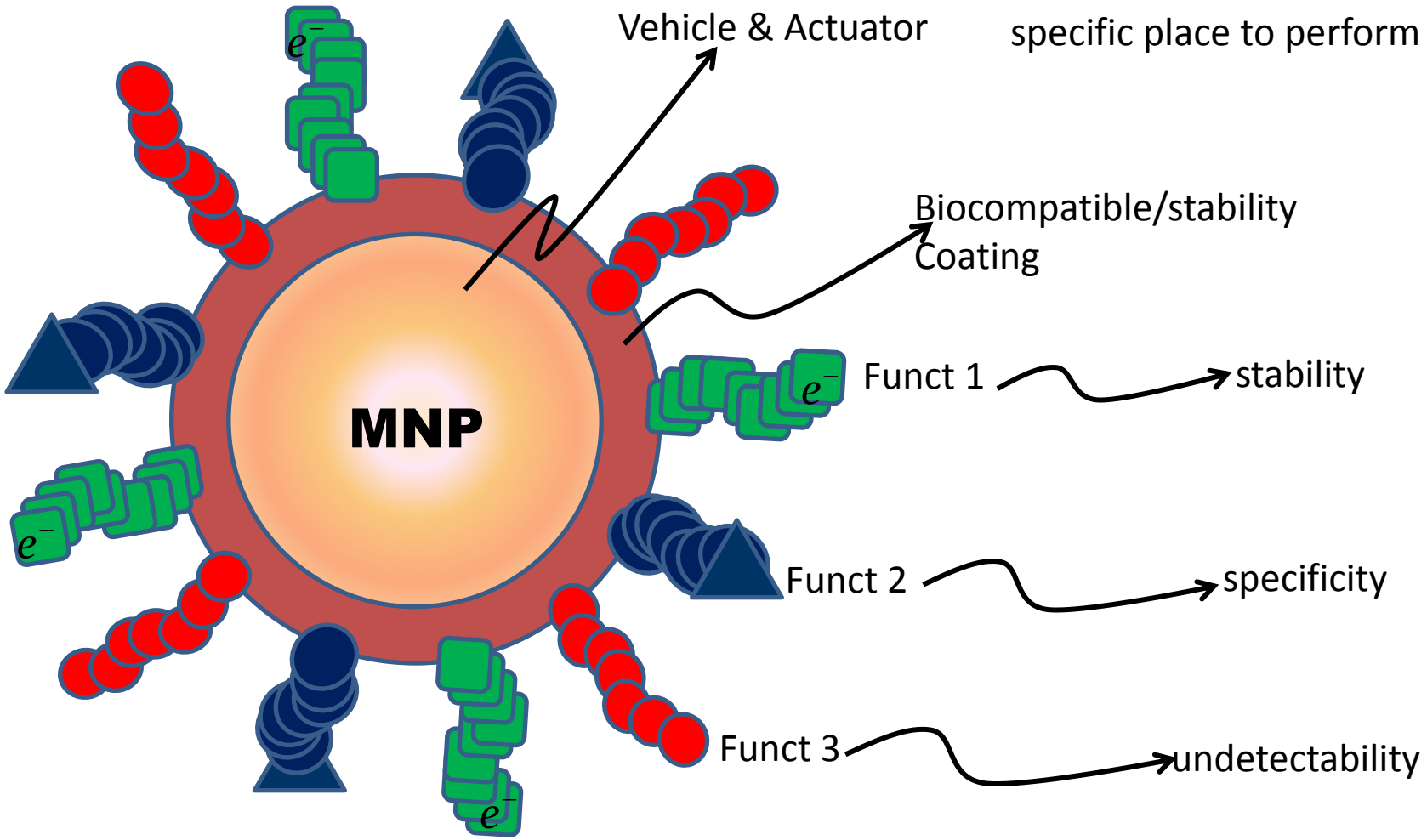

BioMag Nanomaterials

Magnetic nanomaterials

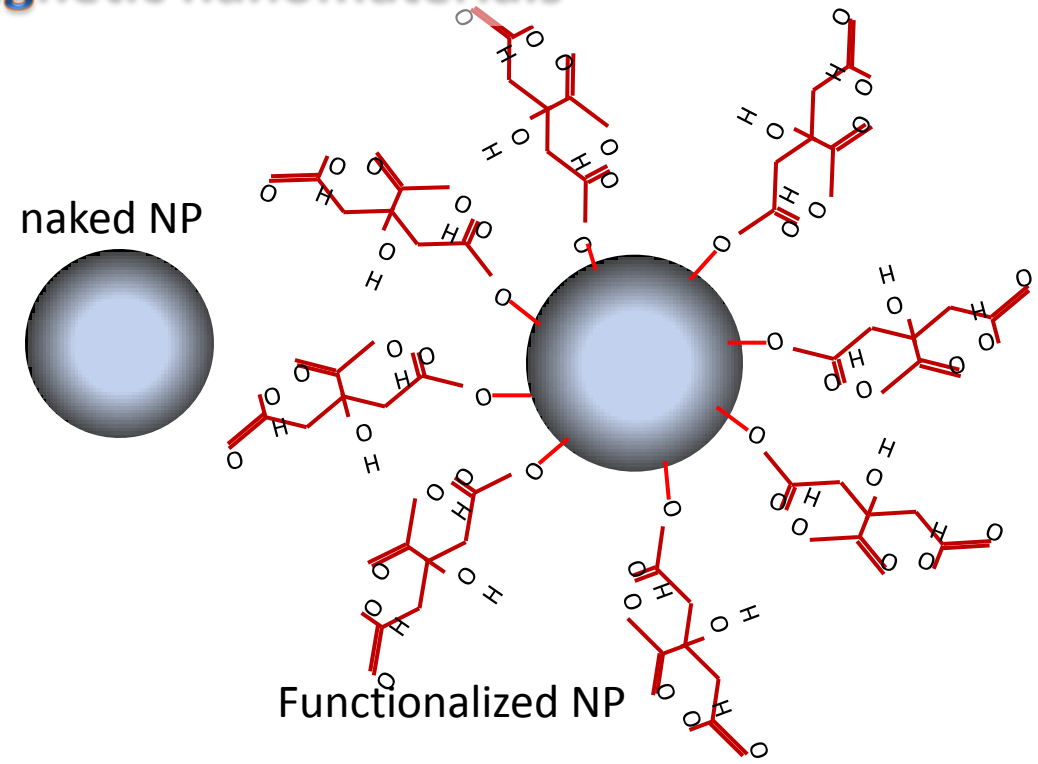

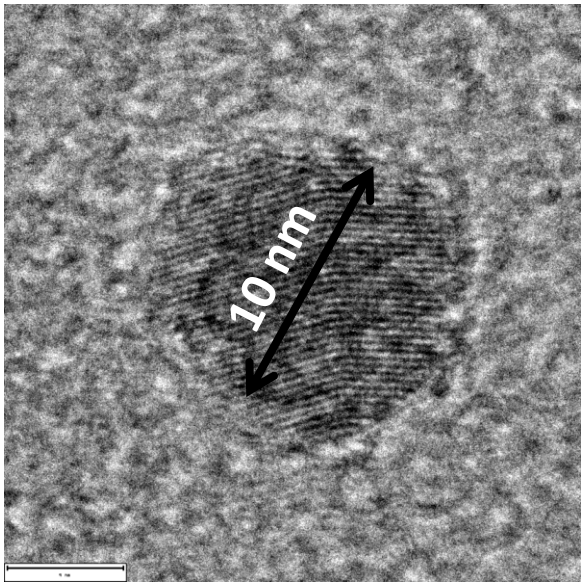

Citric Acid coated Magnetite

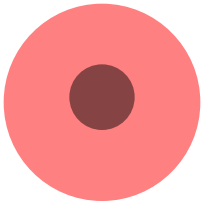

Core/Shell NP

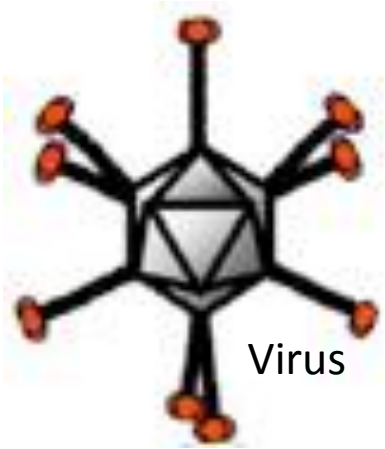

Virus

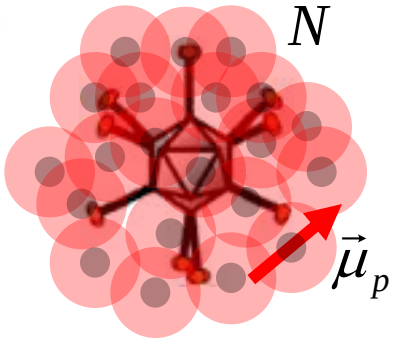

Complex
NP/Virus

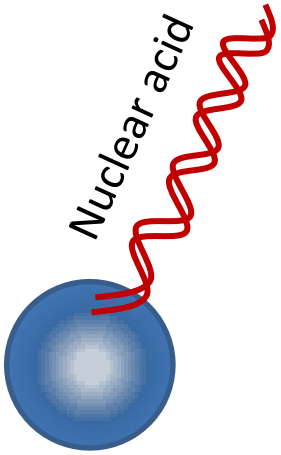

Composite
NP/hydrogel

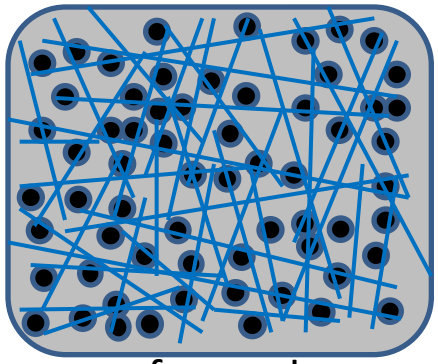

ferrogel

BioMag Nanomaterials

Some uses of Magnetic nanomaterials

Magnetic separation, magnetic delivery

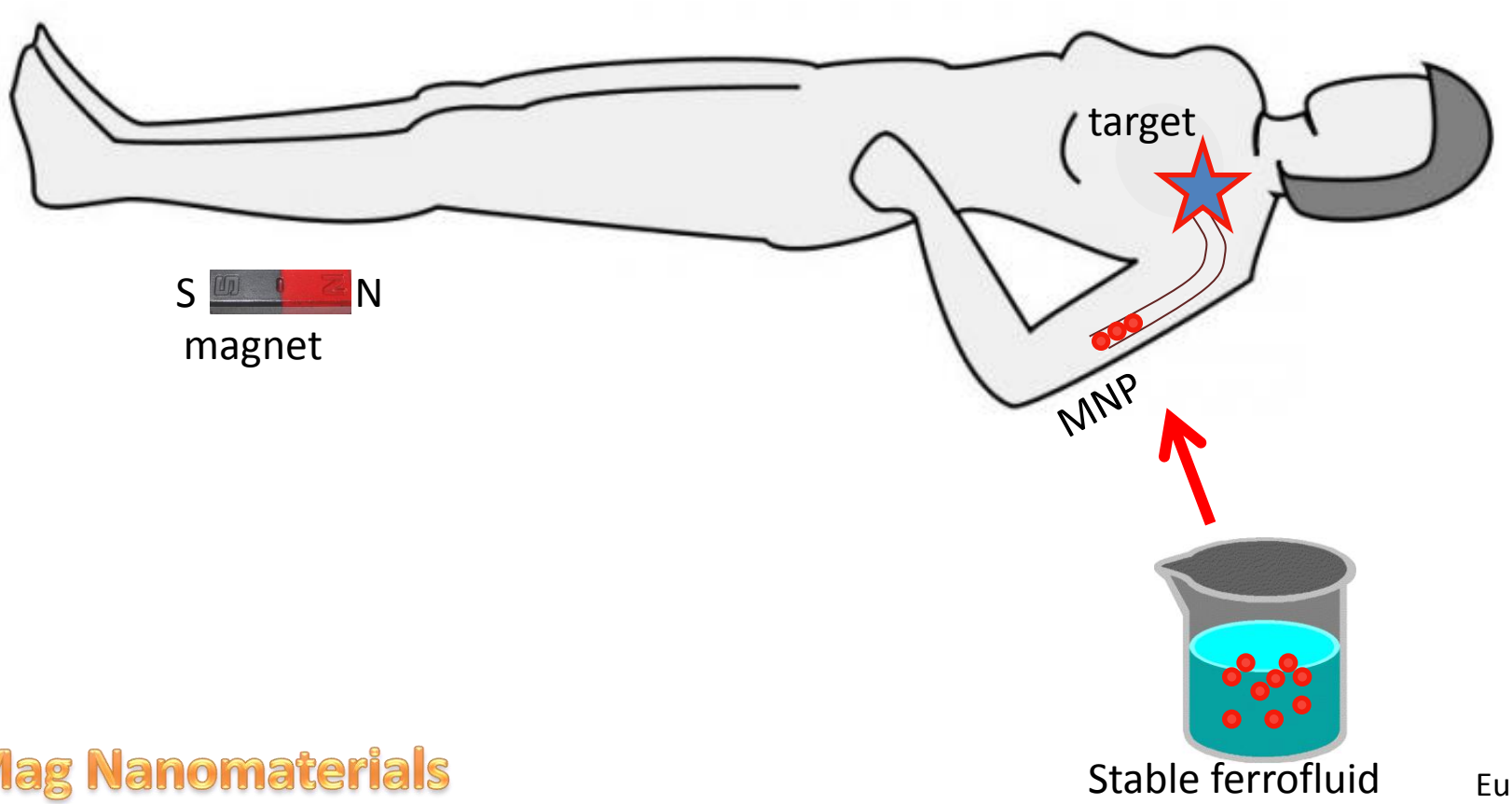

Magnetic separation, magnetic delivery

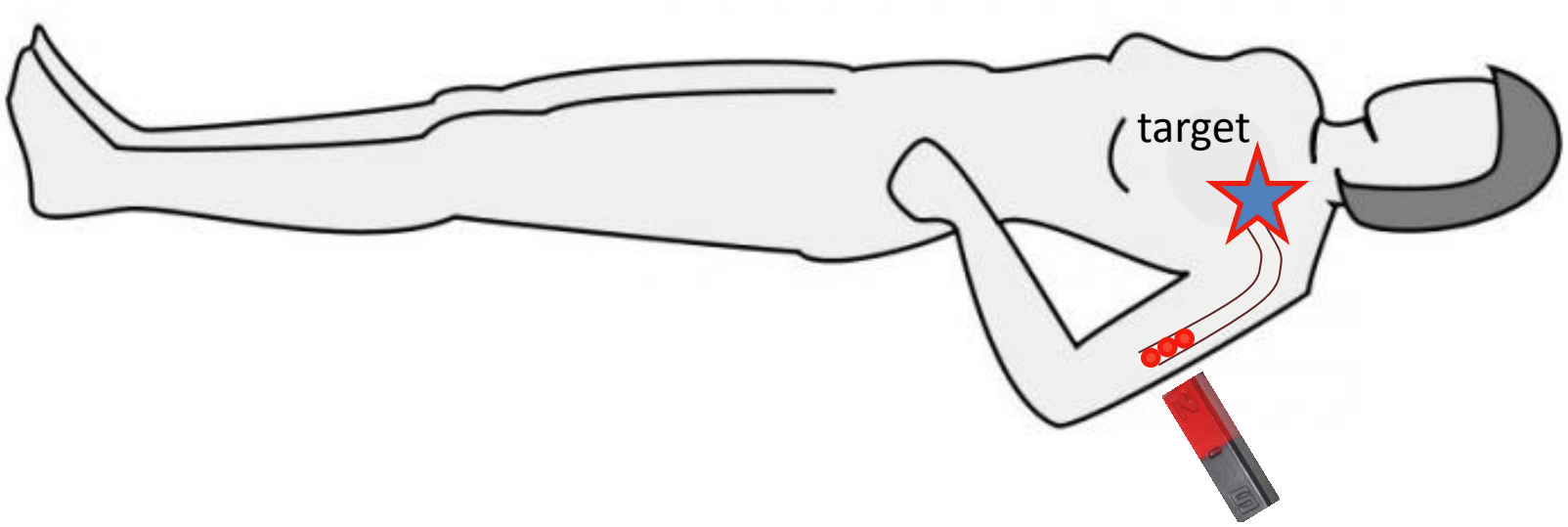

Magnetic separation, magnetic delivery

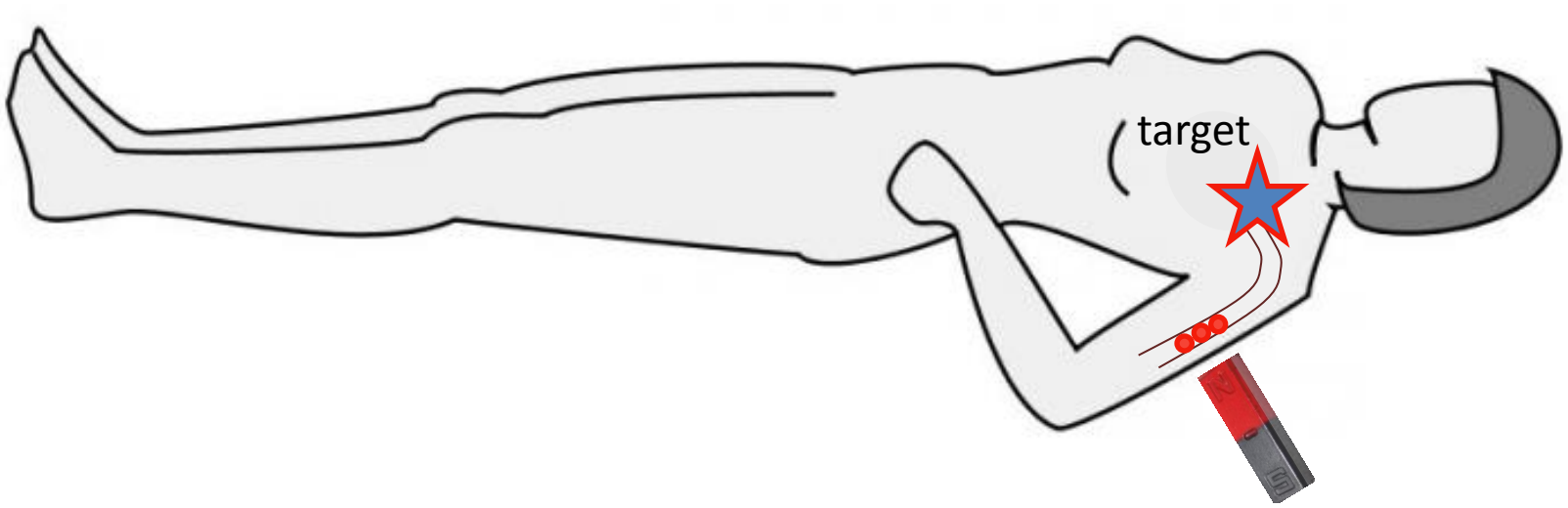

Magnetic separation, magnetic delivery

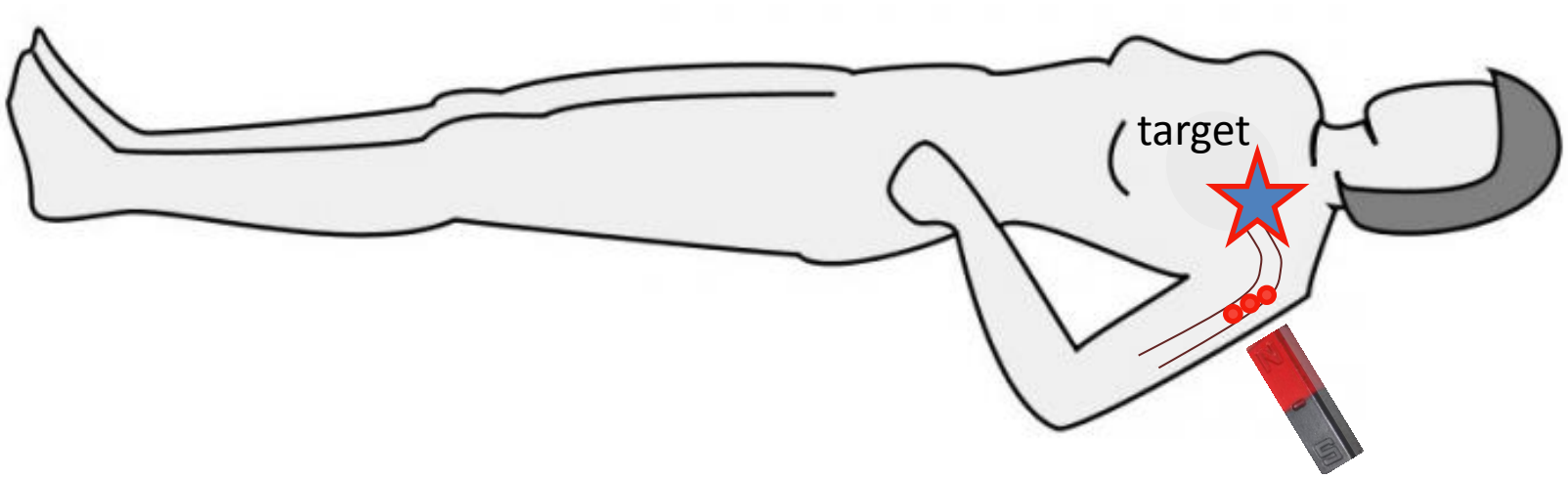

Magnetic separation, magnetic delivery

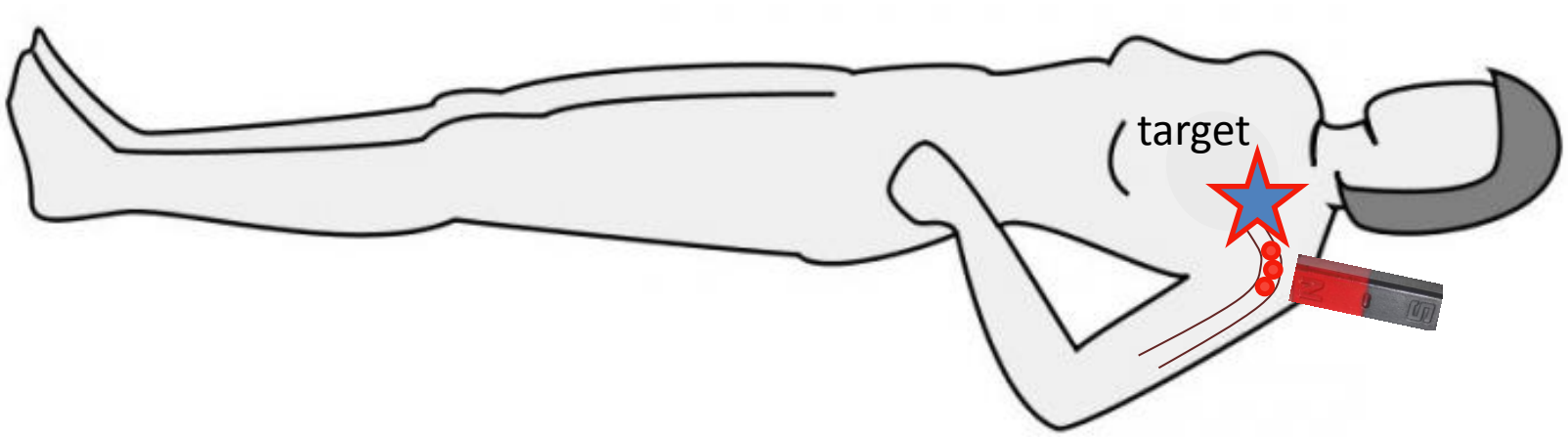

Magnetic separation, magnetic delivery

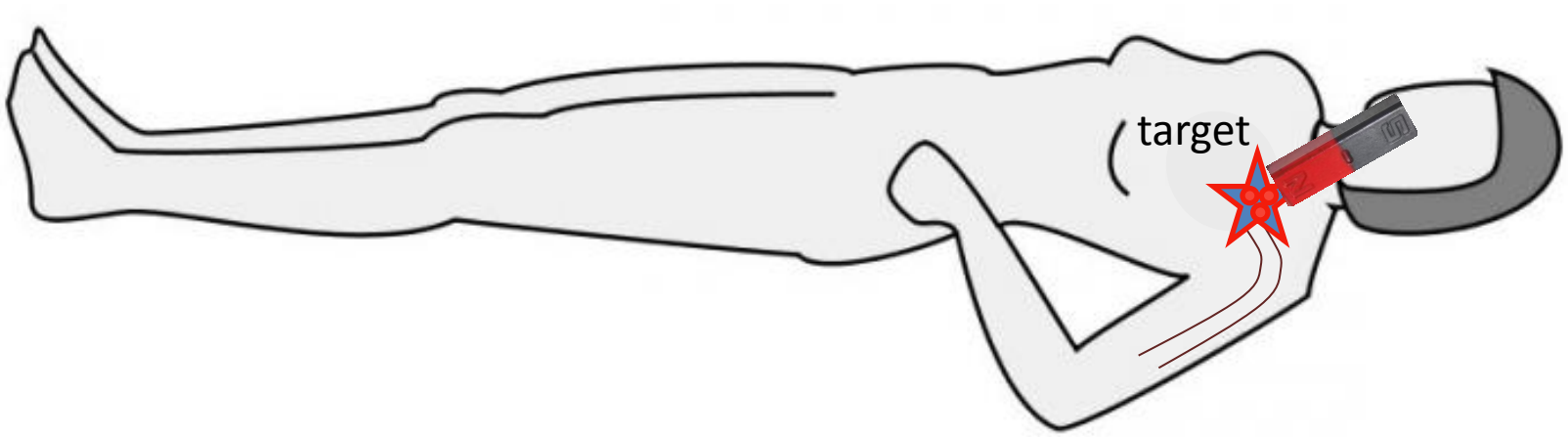

Magnetic separation, magnetic delivery

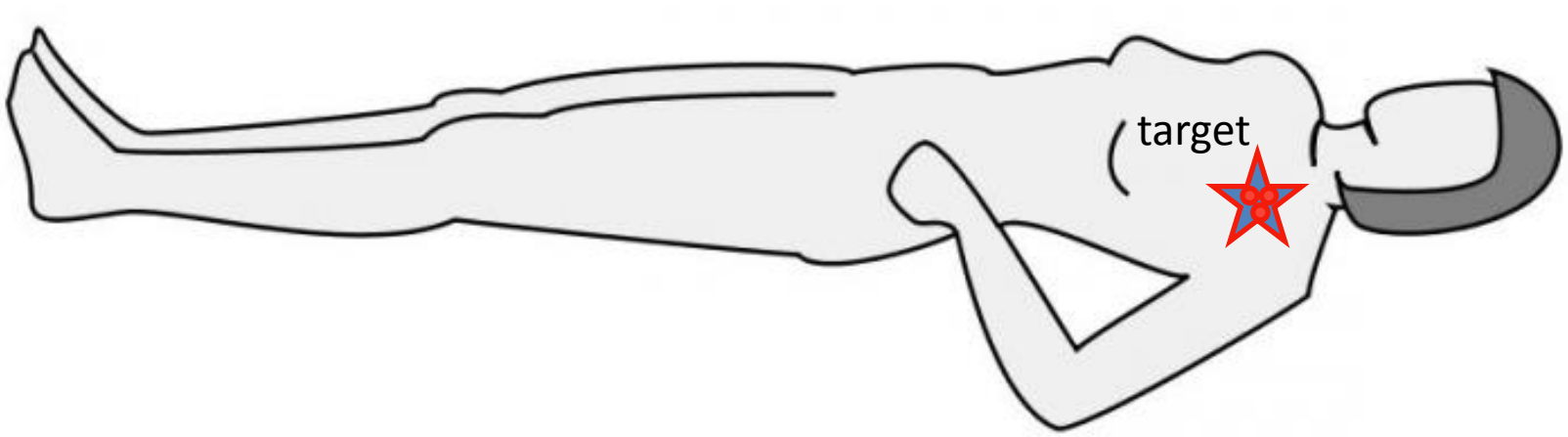

FORCES

Interactions among MNP

Mag dipolar

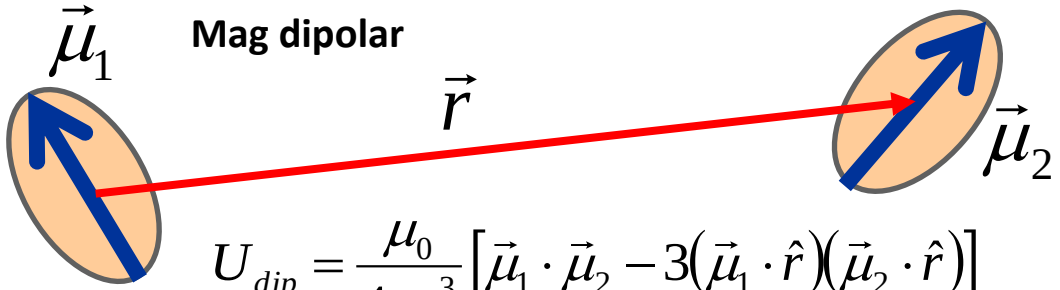

$$U_{dip} = \frac{\mu_0}{4\pi r^3}\left[\vec{\mu}_1 \cdot \vec{\mu}_2 - 3(\vec{\mu}_1 \cdot \hat{r})(\vec{\mu}_2 \cdot \hat{r})\right]$$

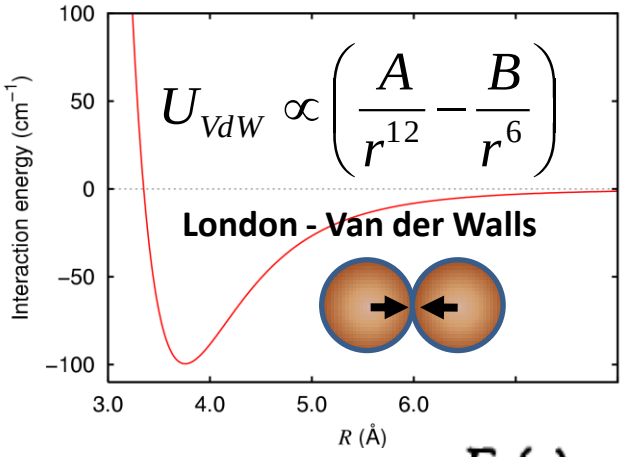

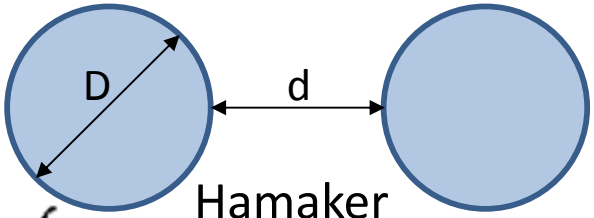

Hamaker

$$E_1(x) = \frac{1}{12}\left\{\frac{1}{x^2+2x} + \frac{1}{x^2+2x+1} + 2\,ln\,\frac{x^2+2x}{x^2+2x+1}\right\}$$

x=d/2D

electrostatic

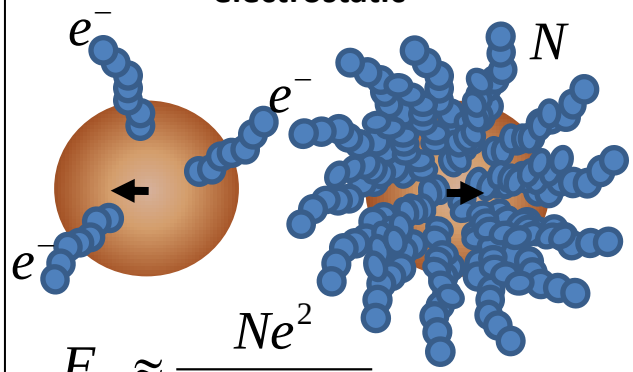

$$F_{el} \approx \frac{Ne^2}{4K\pi\varepsilon_0 r^2}$$

Magnetic field

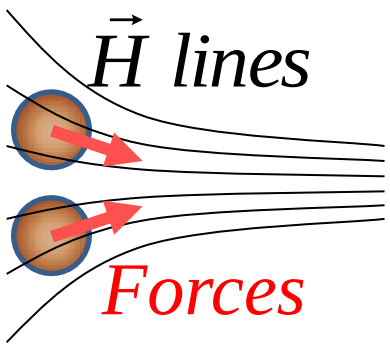

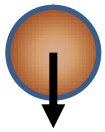

$$Fg = \frac{(\rho - \rho_S)\pi d_p^3 g}{6}$$

gravitational

viscous

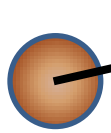

$$\vec{F}_\eta = 6\pi\eta R_v \vec{v}$$

MNP

Forces summary

interaction	value	comment
Dipolar magnetic	5e-3 nN	10 nm NP ~ in contact
Van der Waals - London	4e-1nN	10 nm NP ~ in contact
Gravitational	2e-11 nN	10 nm NP ~ in contact
Electrostatic	2e-3 to 5e3 nN	10 nm NP ~ in contact
viscous	6e-4 to 3e-2 nN	1cm/s < B_V < 100 cm/s
Magnetic field	2e-9 to 2e-7 nN	1 T^2/m <G_B <100 T^2/m**

**1e5 T^2/m would be required to compensate 1 cm/s viscous flow

Single Domain Magnetic Nanoparticle

Relaxation Mechanisms

fixed particle

Néel : moment oscillation

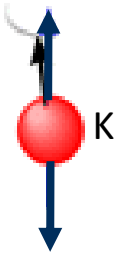

$$\tau_N = \tau_0 \exp\left(\frac{KV}{kT}\right)$$

anisotropy constant

particle volume

viscous media

Brown : particle rotation

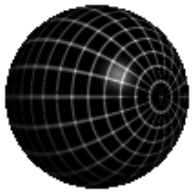

$$\tau_B = \frac{3\eta V}{kT}$$

viscosity

particle volume

volume?

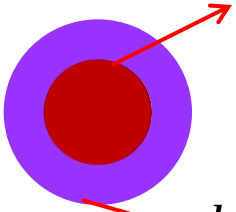

magnetic volume
Néel

hydrodinamic volume
Brown

$$\frac{1}{\tau} = \frac{1}{\tau_B} + \frac{1}{\tau_N}$$

SAR

MNP specific energy absorption rate from RF field

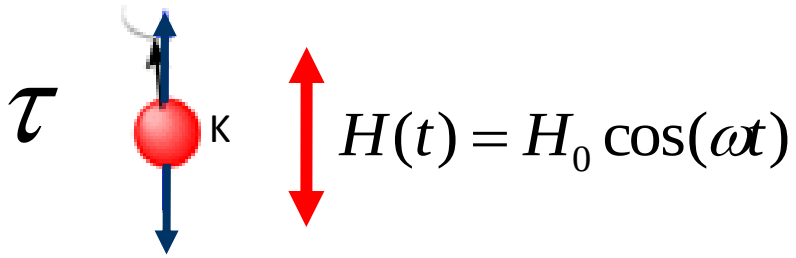

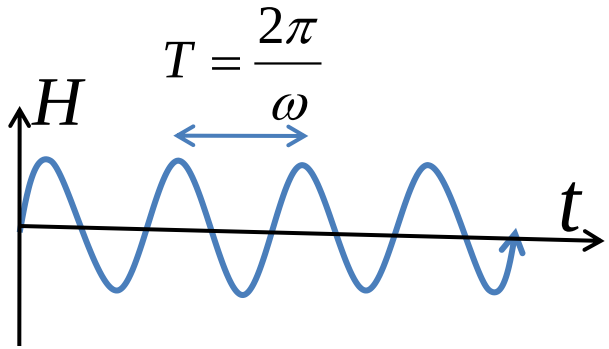

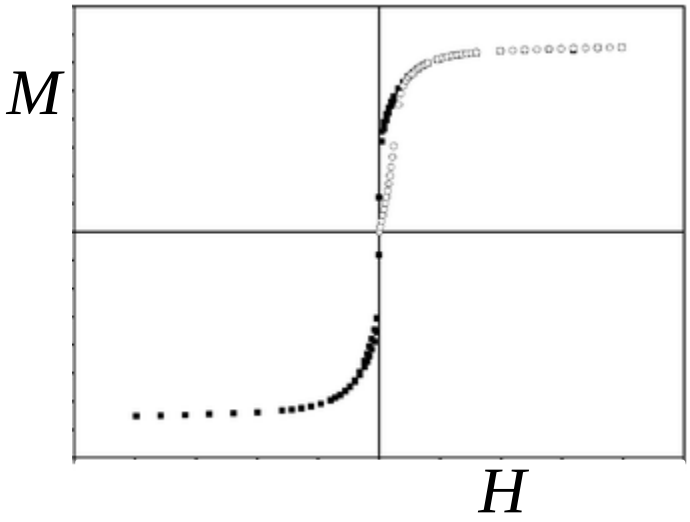

Linear response theory

$$SAR = f\varepsilon_{cycle} = -f\mu_0 \oint MdH = \mu_0 \pi \chi''_{MNP} f H_0^2$$

$$SAR = \frac{\pi \mu_0 H_0^2 f}{\rho} \frac{\mu_0 M_S^2 V \rho^2}{3kT} \frac{\omega\tau}{1+(\omega\tau)^2}$$

$$\tau = 1/\omega$$

energy absorption from a RF field (SAR)

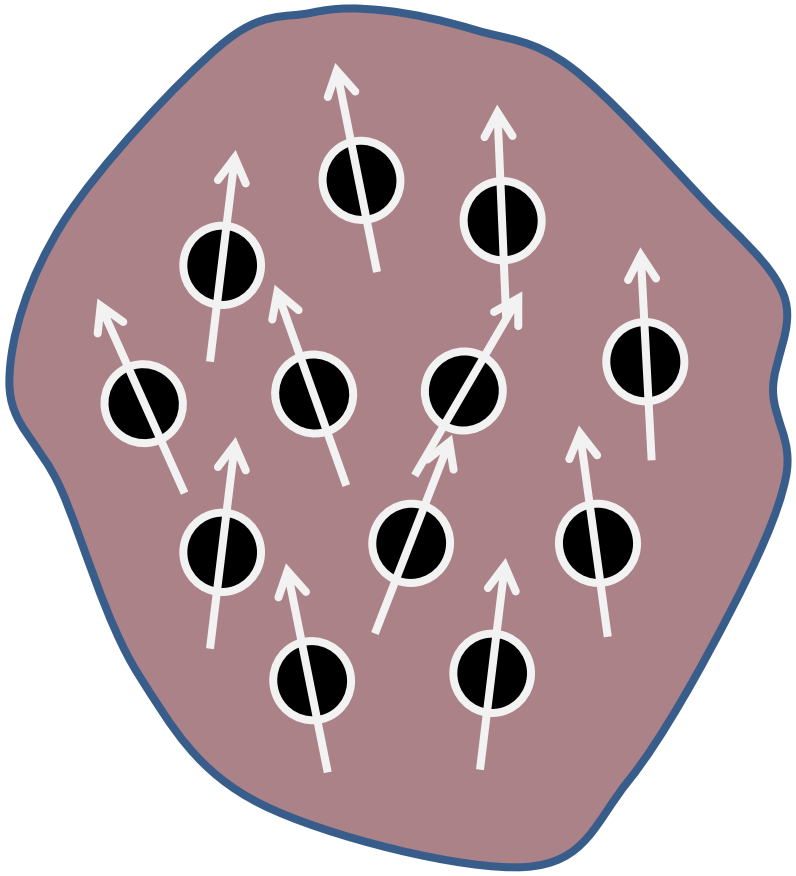

$$\tau \approx 1/\omega$$

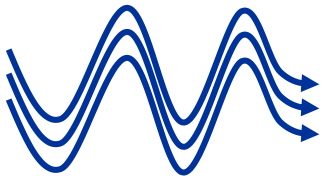

T 

energy absorption from a RF field (SAR)

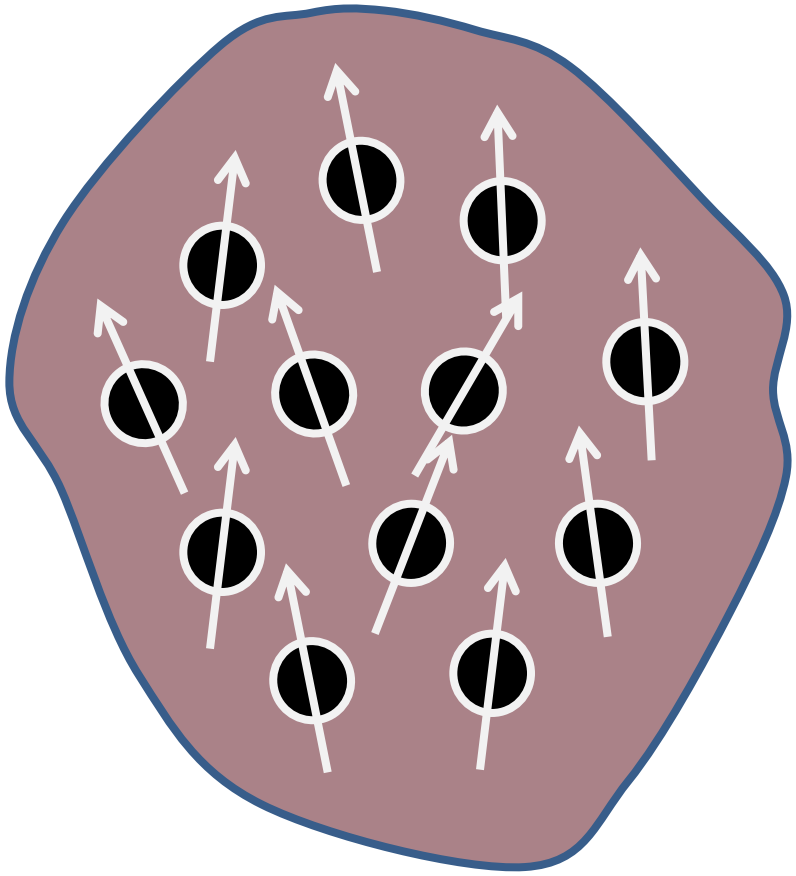

$$\tau \approx 1/\omega$$

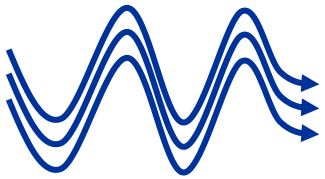

T 

energy absorption from a RF field (SAR)

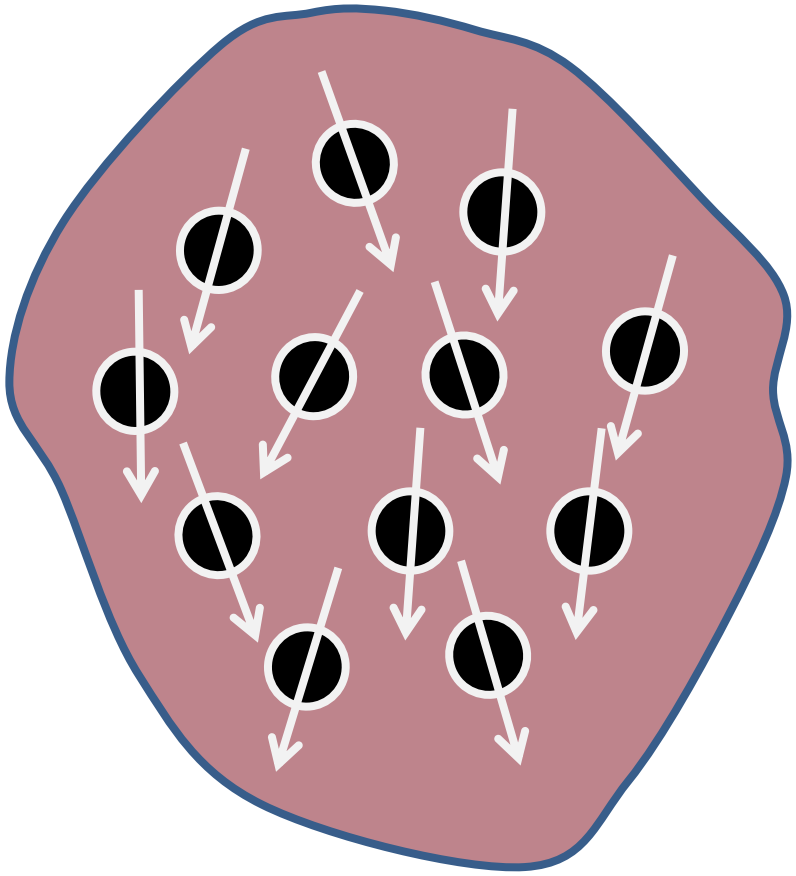

$$\tau \approx 1/\omega$$

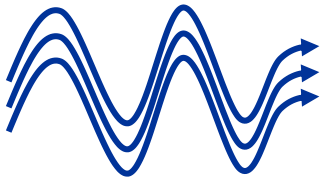

T 

energy absorption from a RF field (SAR)

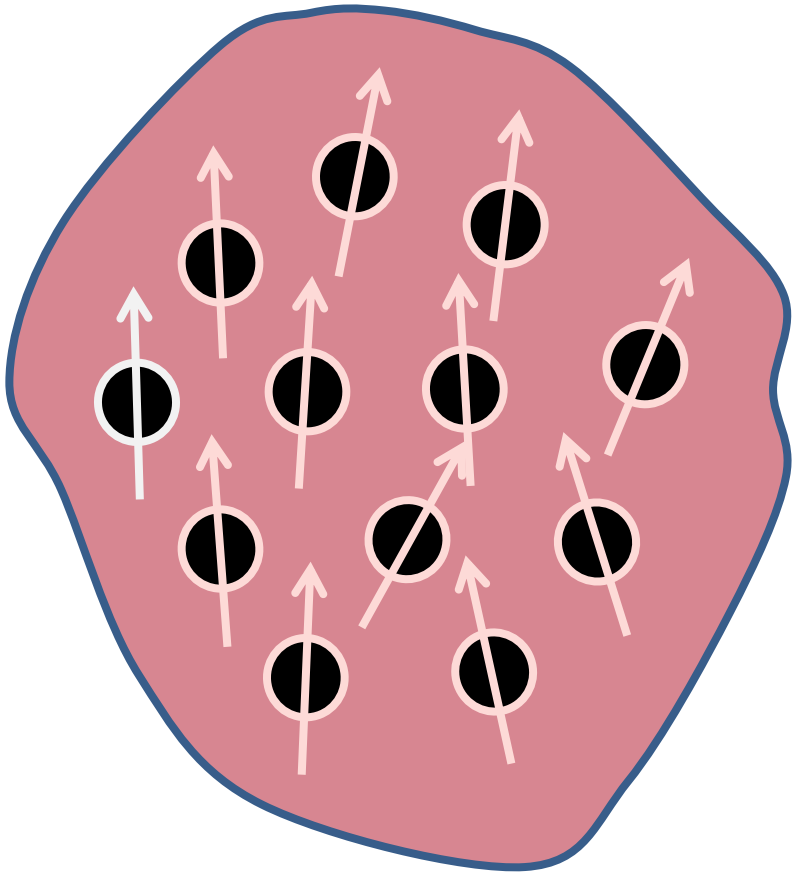

$$\tau \approx 1/\omega$$

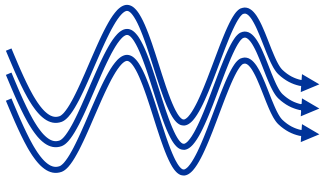

T 

energy absorption from a RF field (SAR)

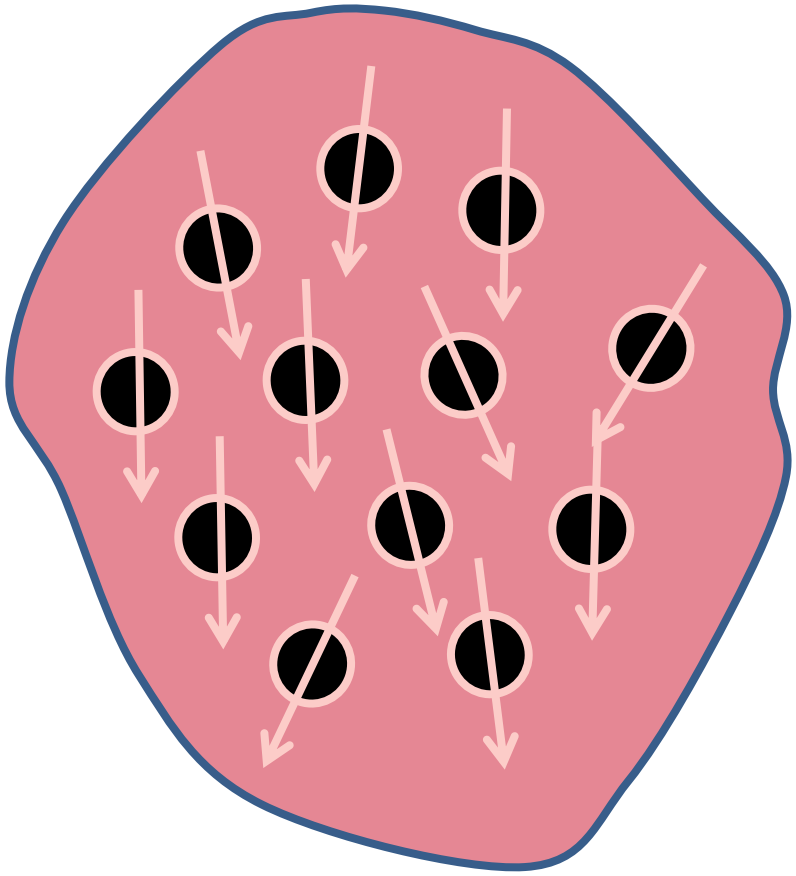

$$\tau \approx 1/\omega$$

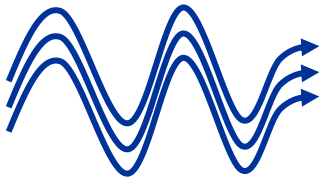

T

energy absorption from a RF field (SAR)

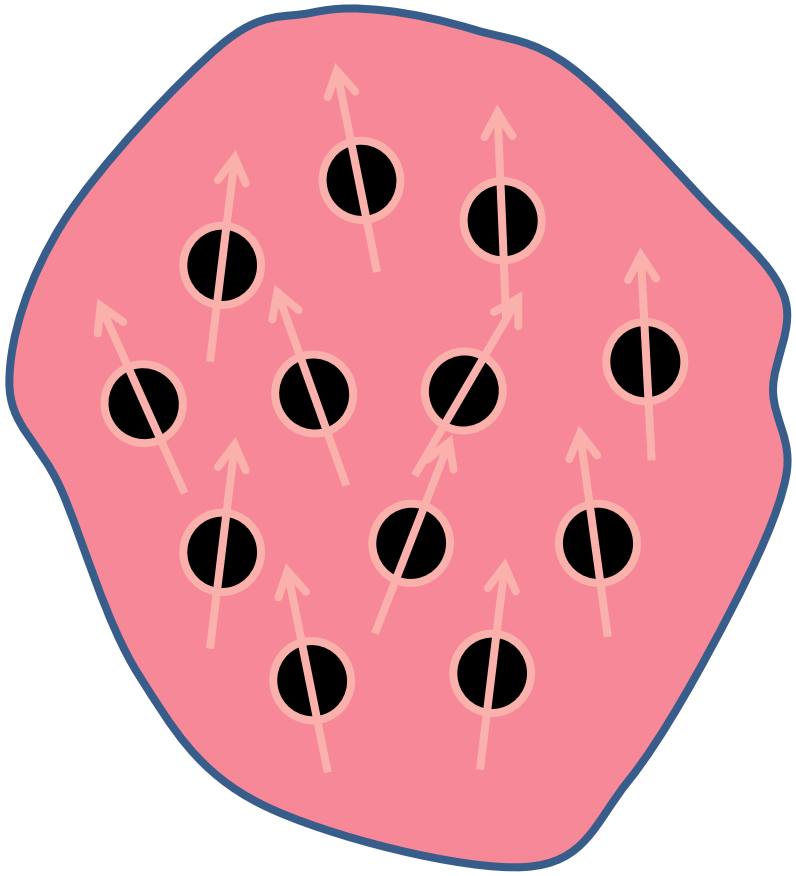

$$\tau \approx 1/\omega$$

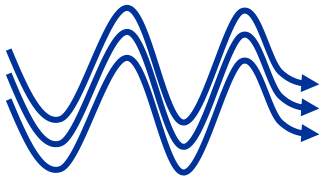

T

energy absorption from a RF field (SAR)

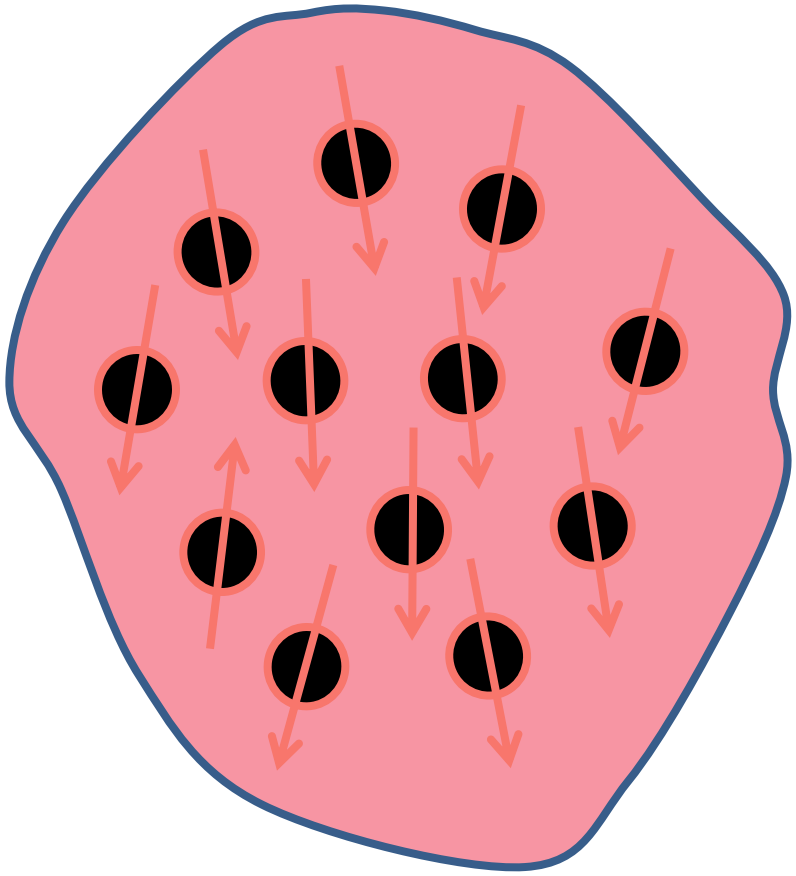

$$\tau \approx 1/\omega$$

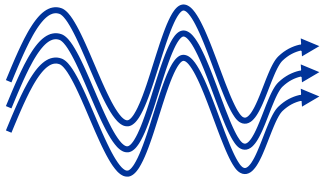

T

energy absorption from a RF field (SAR)

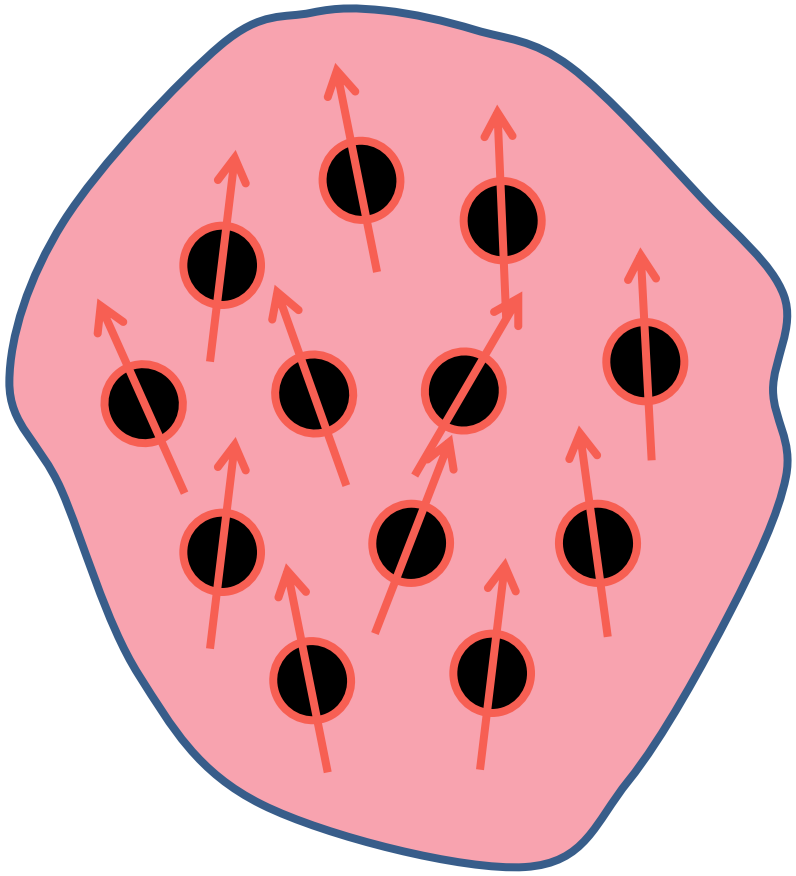

$$\tau \approx 1/\omega$$

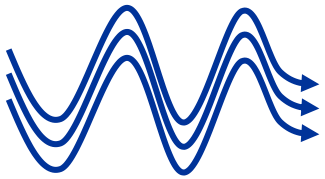

T

energy absorption from a RF field (SAR)

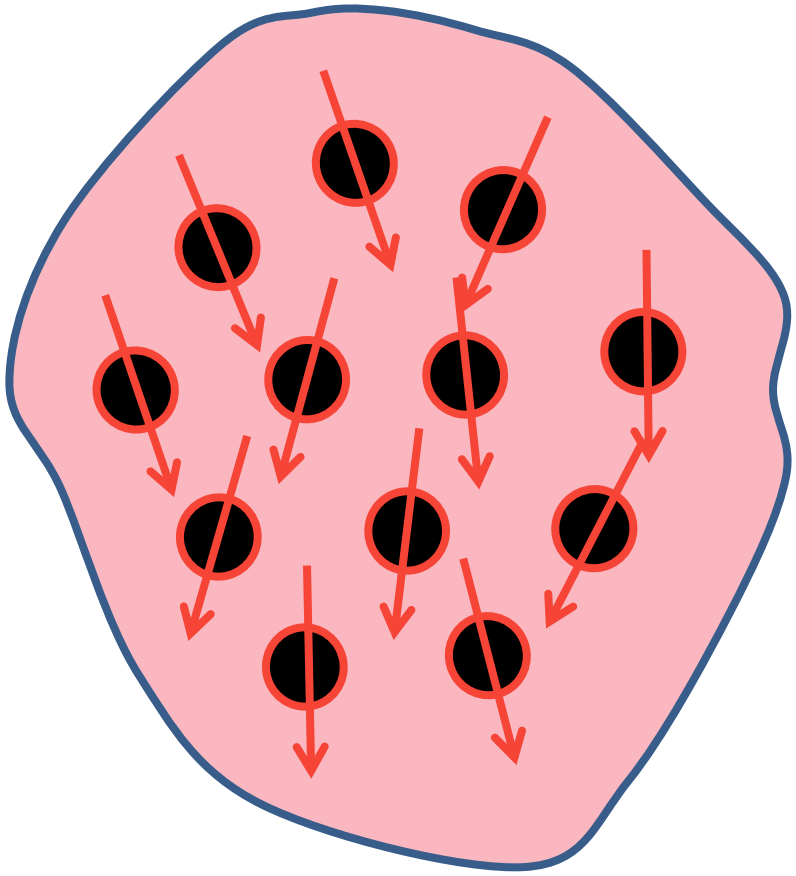

$$\tau \approx 1/\omega$$

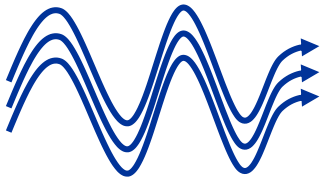

T

energy absorption from a RF field (SAR)

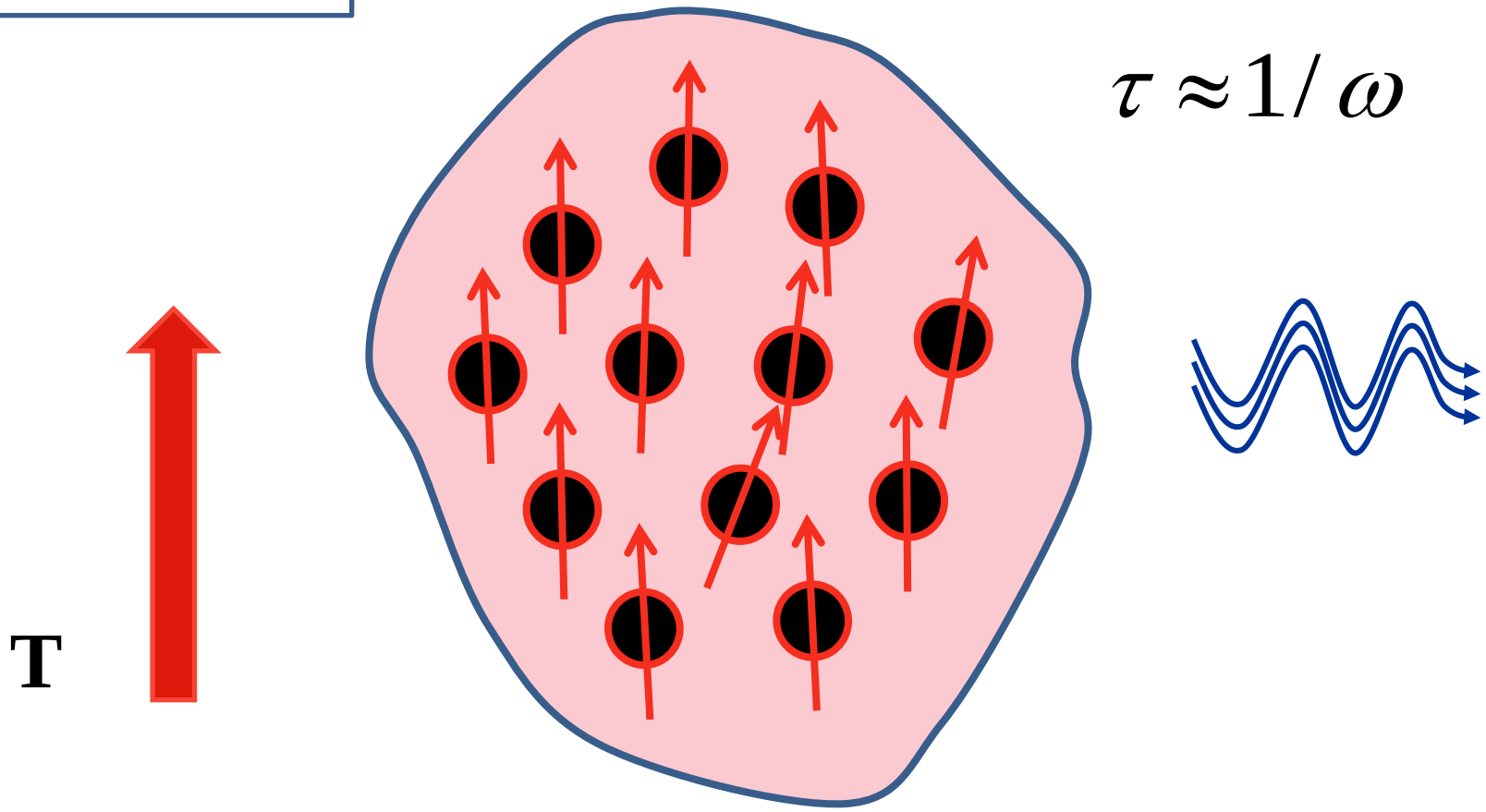

energy absorption from a RF field (SAR)

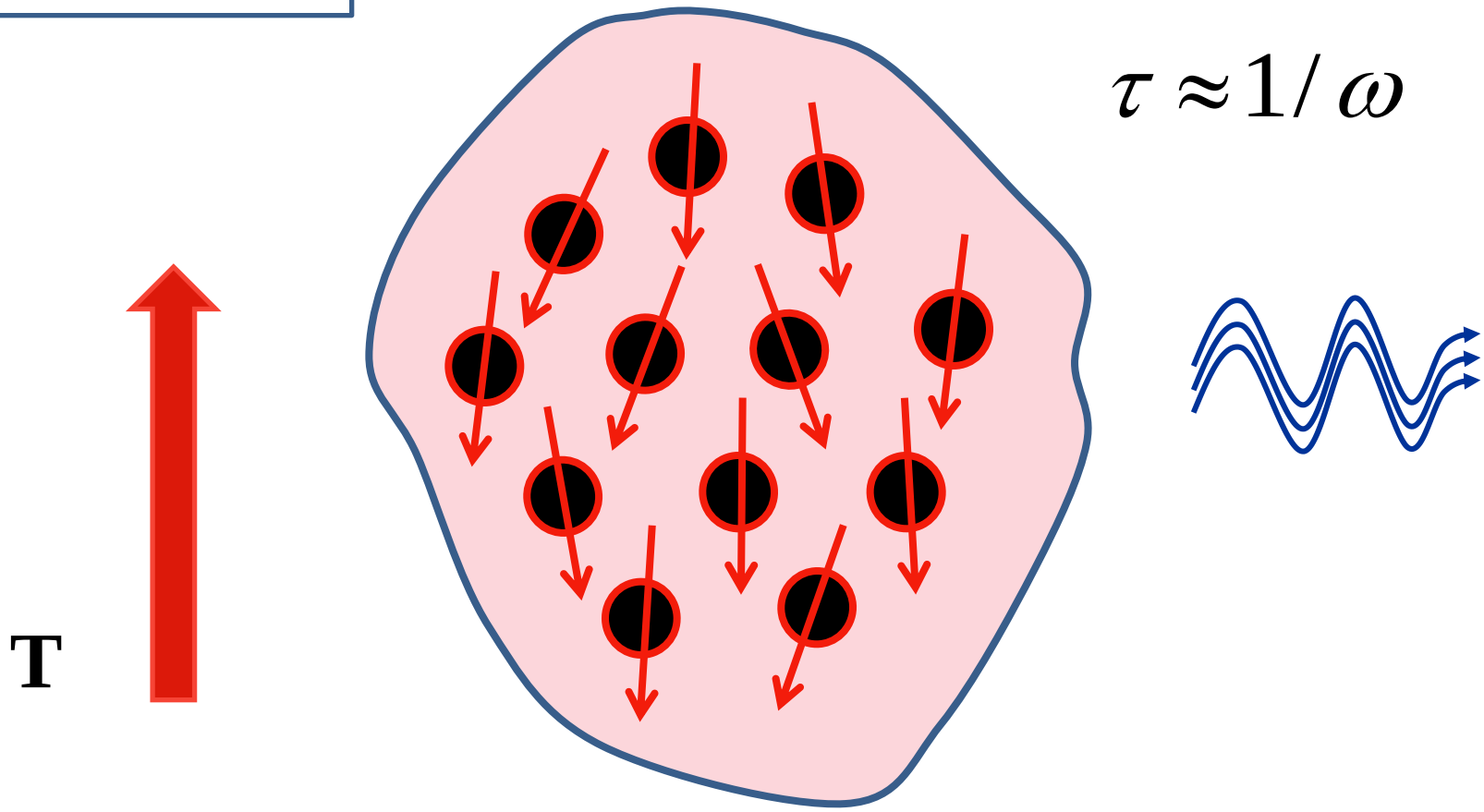

energy absorption from a RF field (SAR)

$\tau \approx 1/\omega$

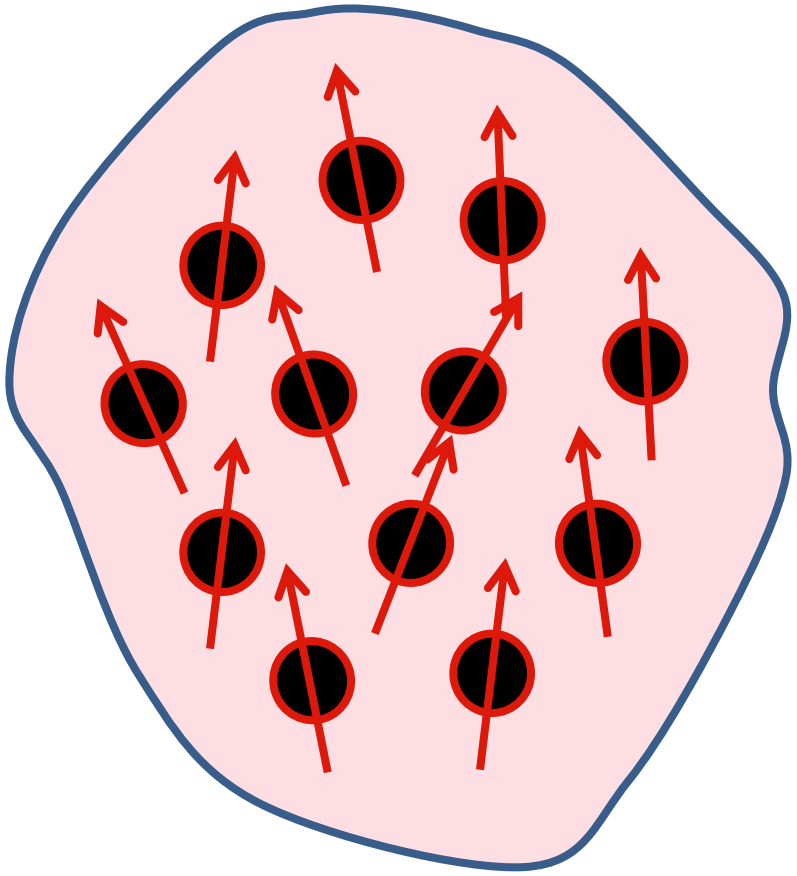

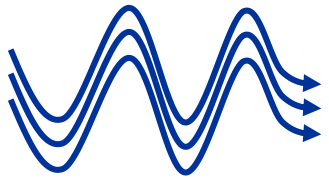

$$SAR \approx f\left(M_S, V_{MNP}, H_0, \omega, T\right)\frac{\omega\tau}{1+(\omega\tau)^2}; \quad need \ \ for \ 1kW/g$$

Smallest treatable tumor

Magnetic particle hyperthermia—biophysical limitations of a visionary tumour therapy

Rudolf Hergt*, Silvio Dutz

Journal of Magnetism and Magnetic Materials 311 (2007) 187–192

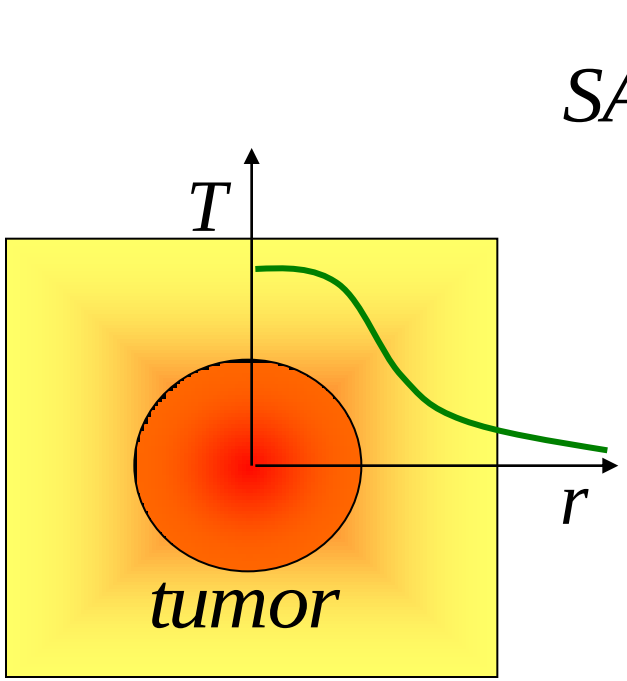

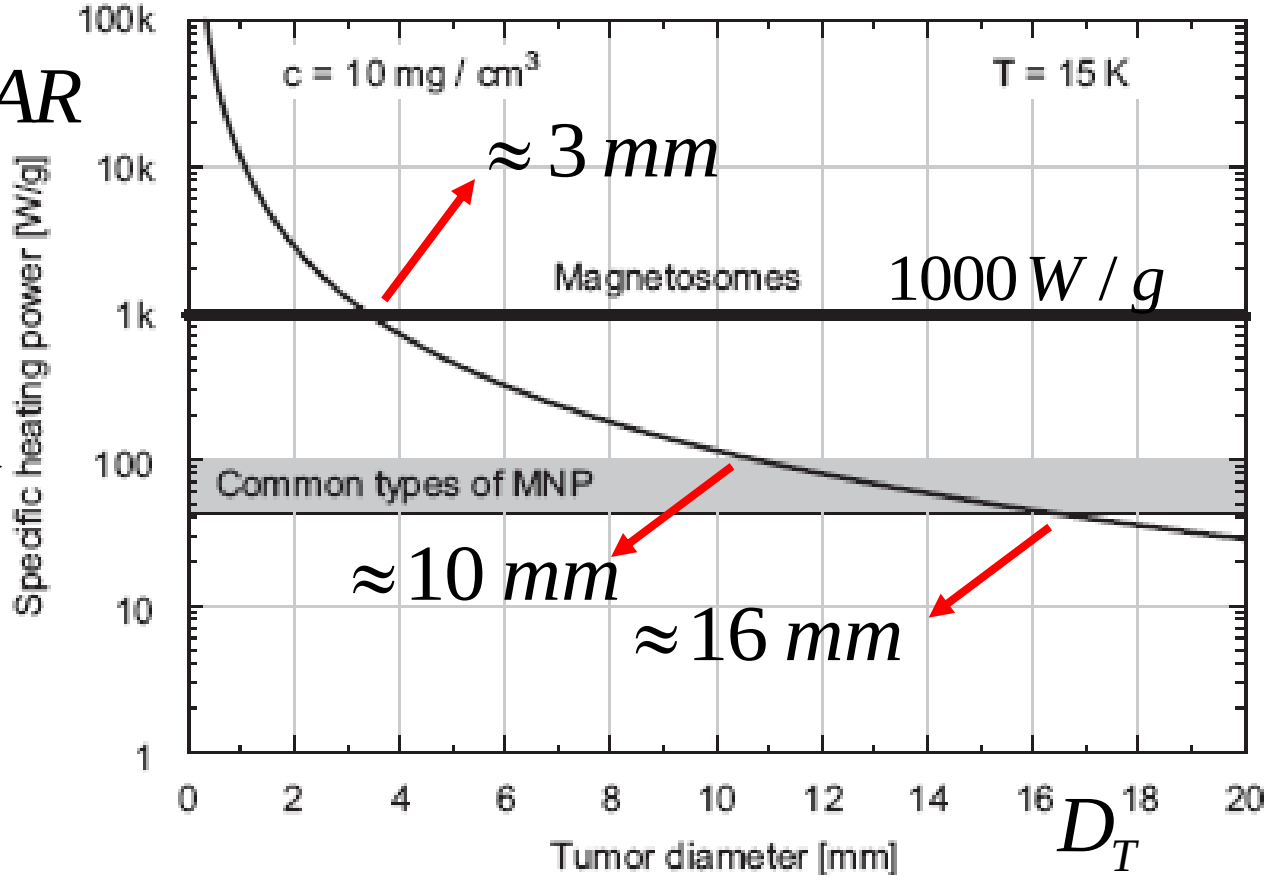

NP and FF for Magnetic Hyperthermia

Searching for high SAR nanomaterials

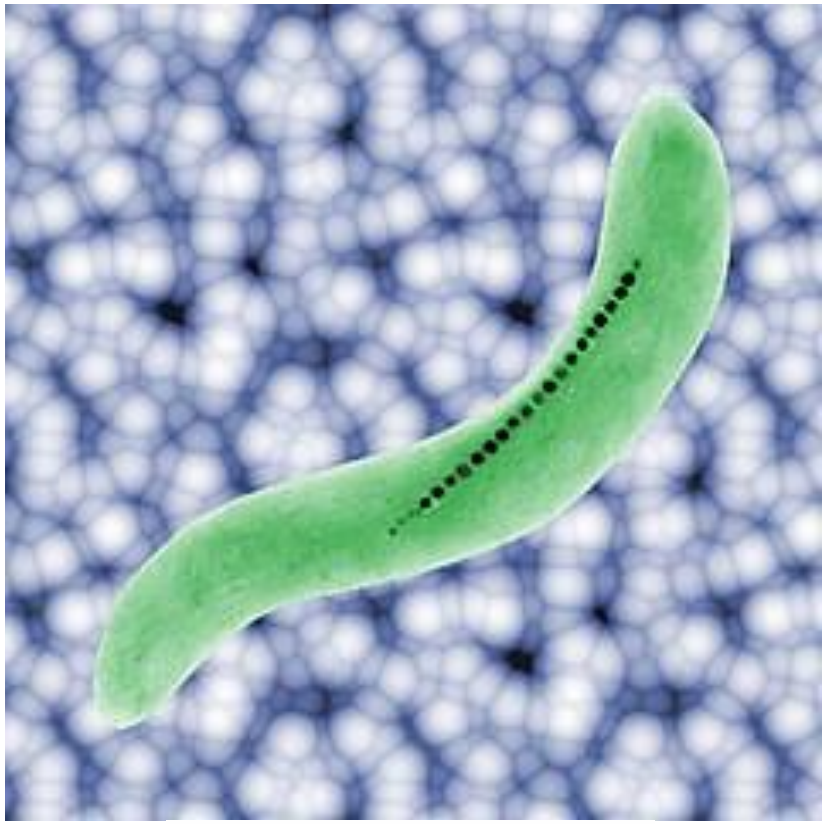

Magnetotactic bacteria

magnetosomes

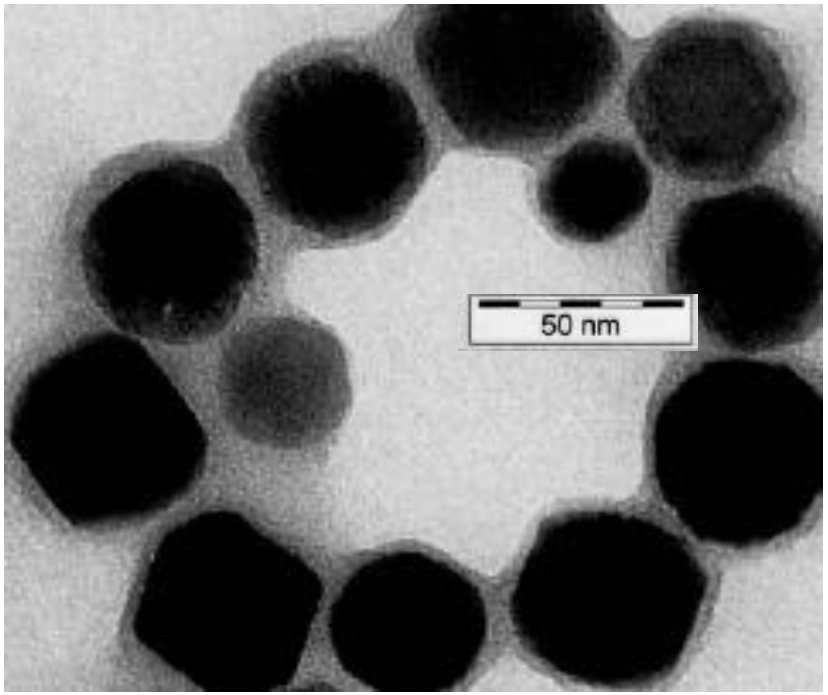

Journal of Magnetism and Magnetic Materials 293 (2005) 80–86
Hergt et al. 2005

$$SAR > 1 kW / g$$

Zn doped ferrites

Fe moment enhancement

$Zn_xFe_{3-x}O_4 \quad (0 \le x \le 0.5)$

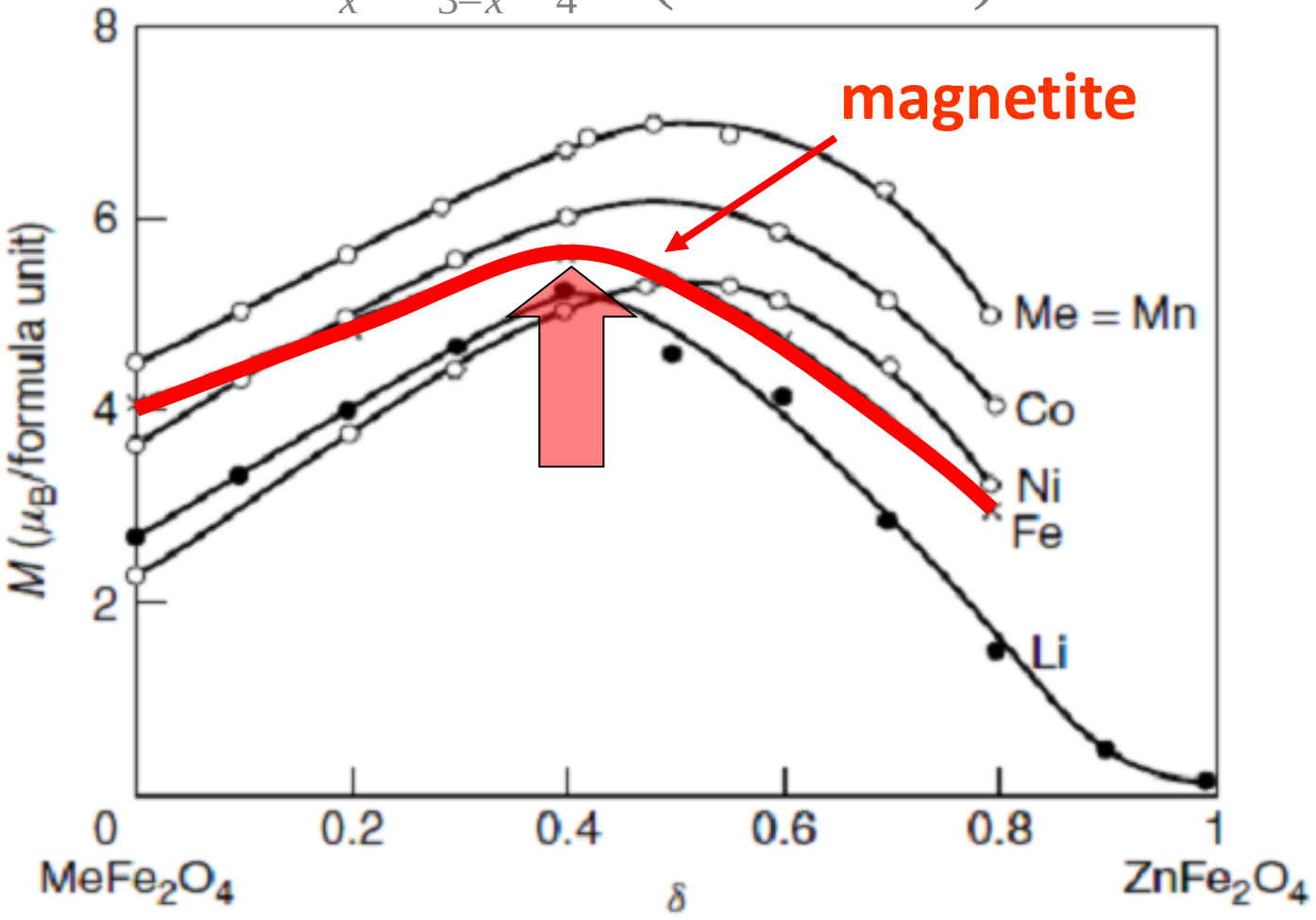

zinc-doped magnetite nanoparticles and ferrofluids for hyperthermia applications

P Mendoza Zélis, G A Pasquevich, S J Stewart, M B Fernández van Raap, J Aphesteguy, I J Bruvera, C Laborde, B Pianciola, S Jacobo and F H Sánchez

Structural and magnetic study of zinc-doped magnetite nanoparticles and ferrofluids for hyperthermia applications, ***J. Phys. D: Appl. Phys.*** *46, (**2013**), 125006 doi:10.1088/0022-3727/46/12/125006.*

NP preparation

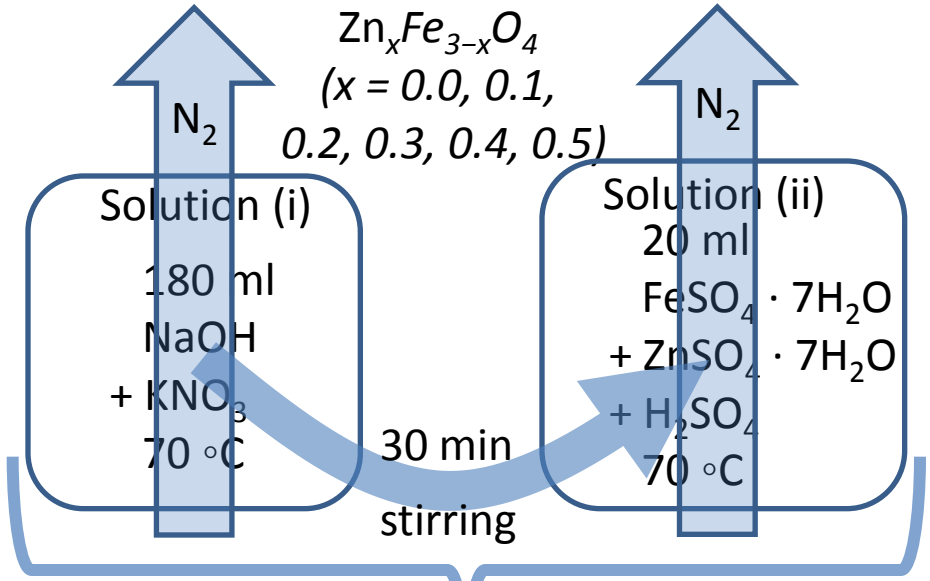

kept at 70 ◦C for 2 h

cooled down to RT

magnetic decantation

washed several times

centrifuged

Dried 40°C Vacuum 24 h

S1 NPs

FF preparation and purification

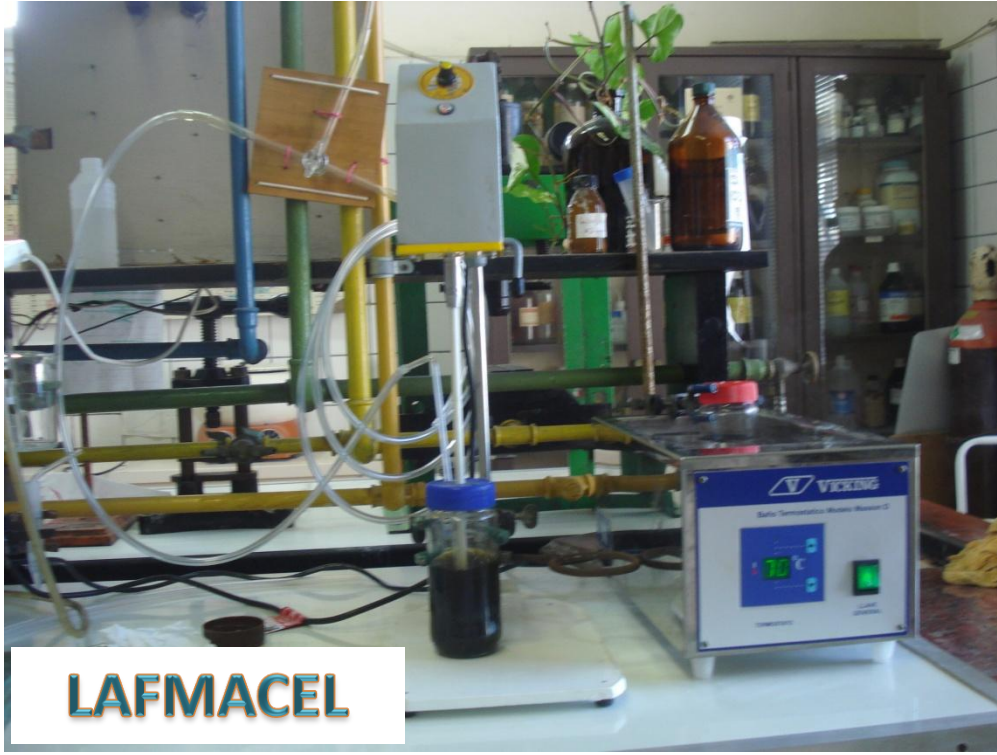

Washed NPs

2% chitosan + 1% acetic acid solution

Centrifugation 2500 rpm 10 min + 3500 rpm 15 min

resuspended in chitosan solution

stirred 6 h at RT

Sonicated 30 min

S1 FF

+ ethanol

S2 NPs & FF

XRD and TEM observation

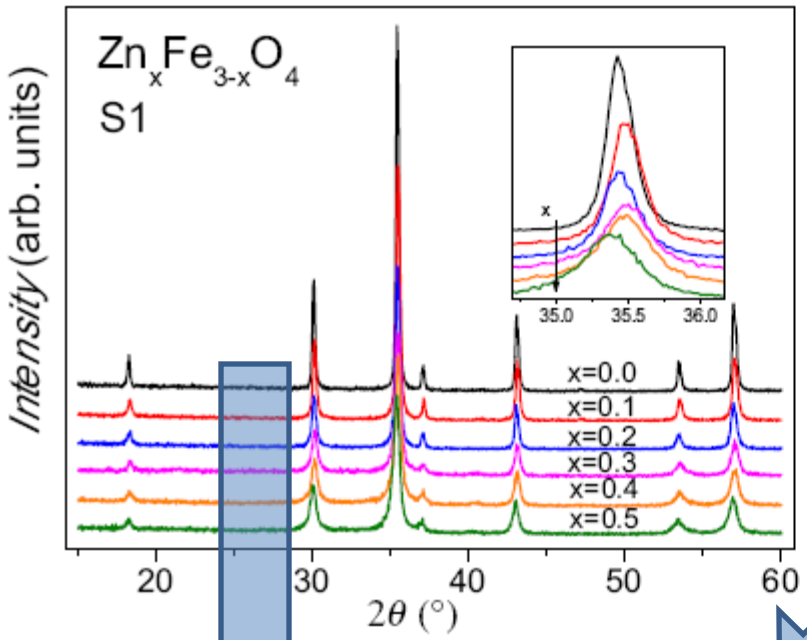

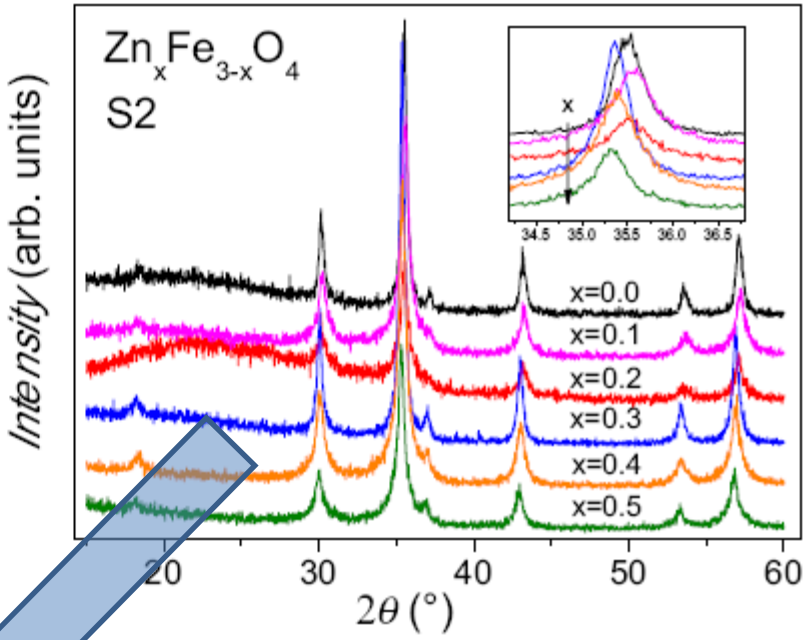

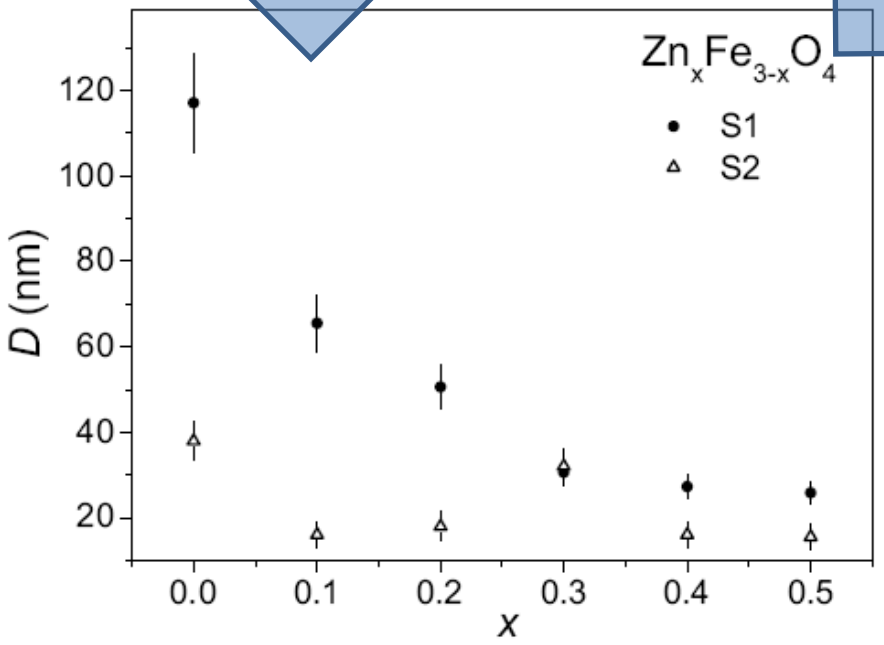

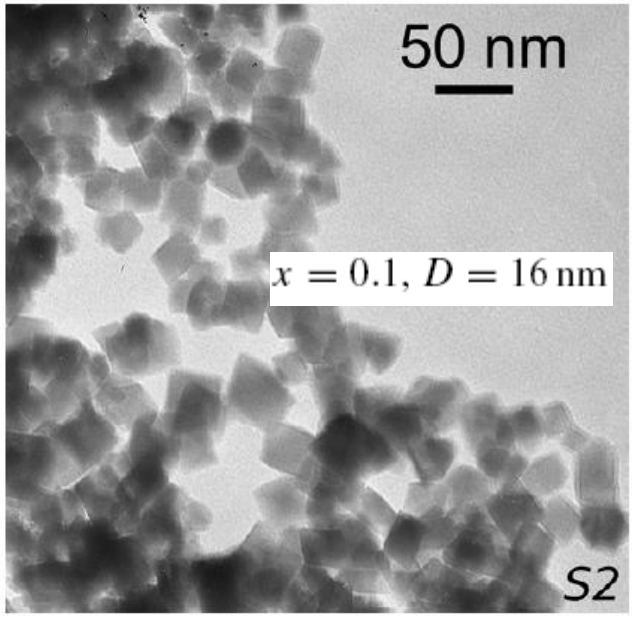

Mössbauer effect results

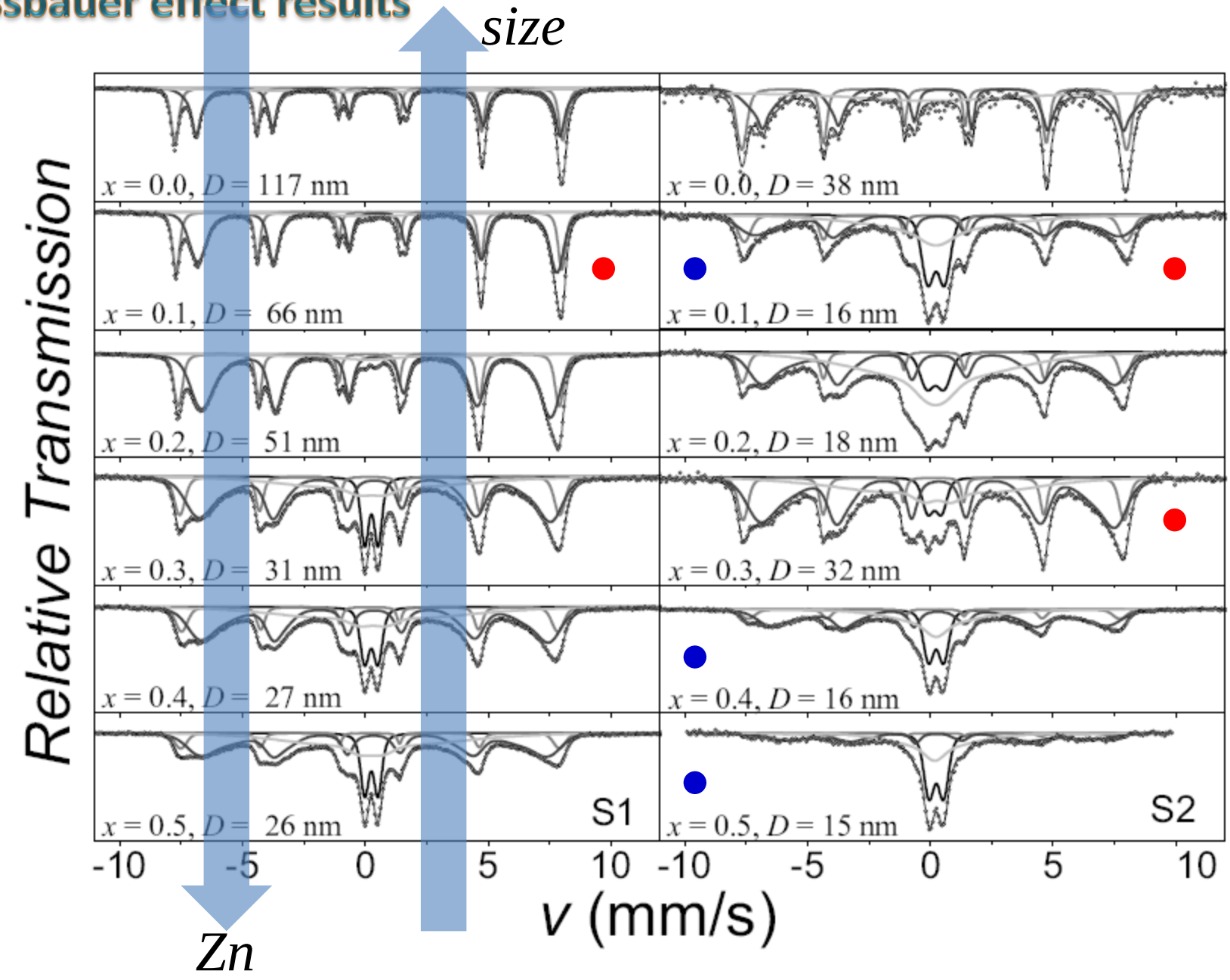

Mössbauer effect results

subspectra

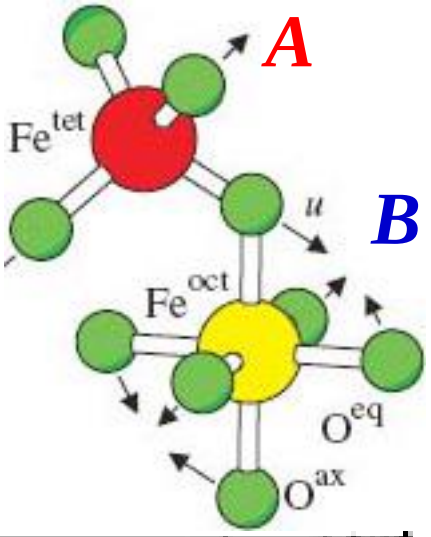

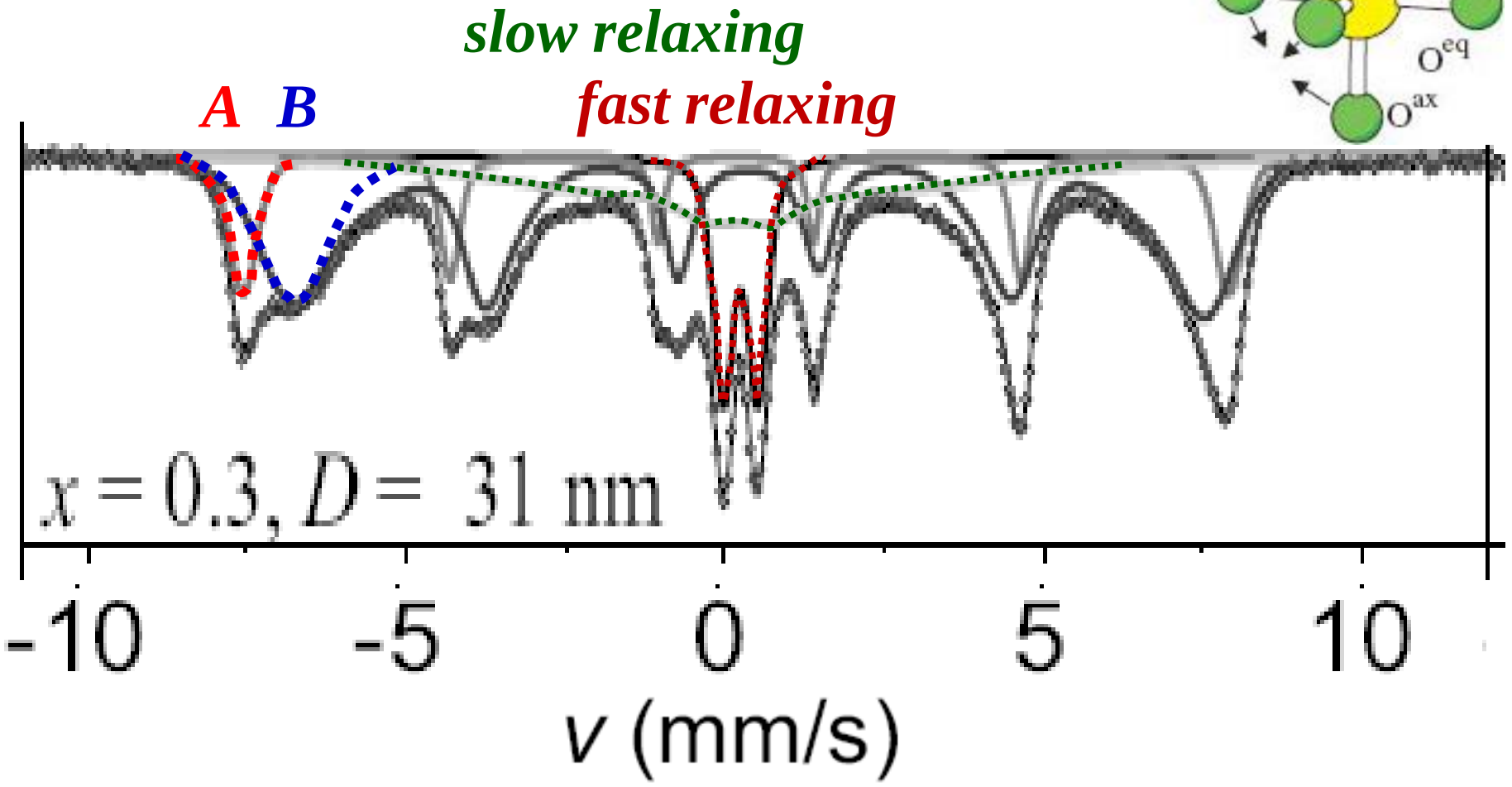

Mössbauer effect results

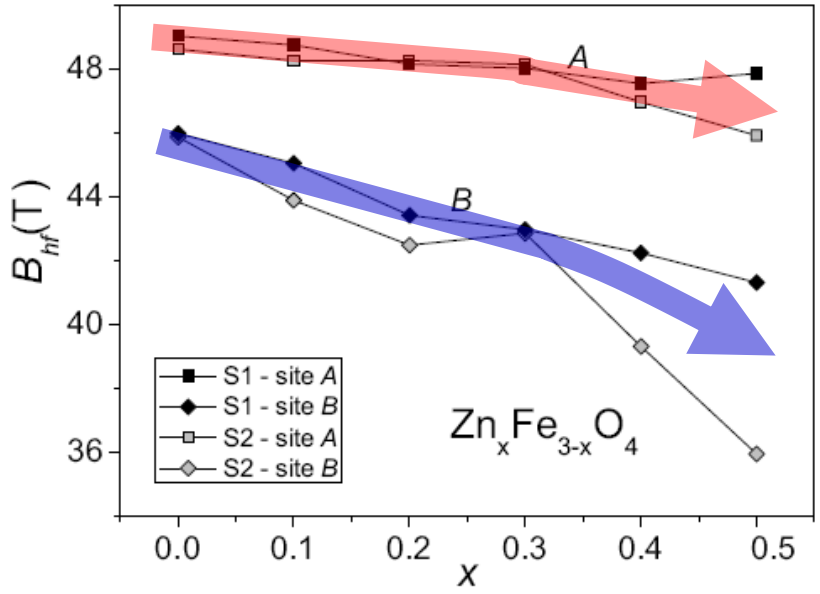

Hyperfine Field B

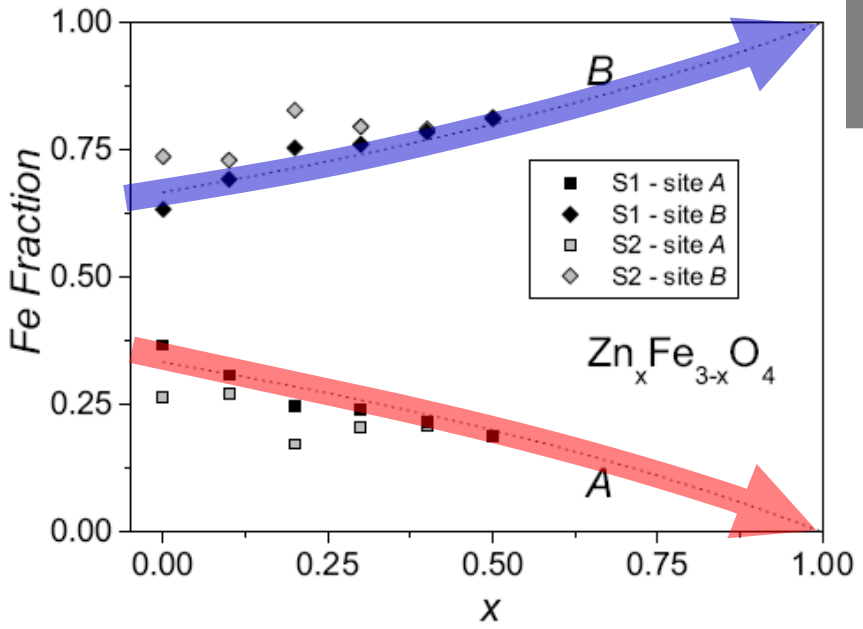

Fe site fraction

Zn

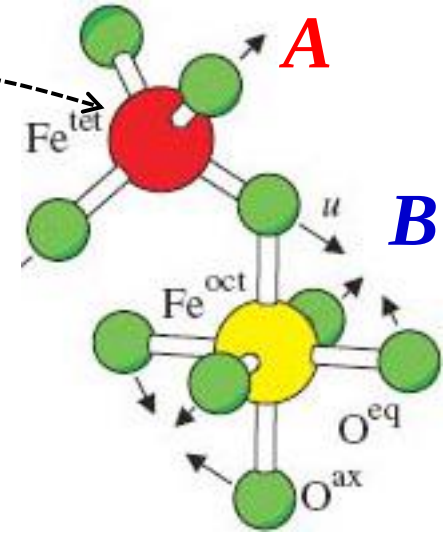

Mössbauer effect results

in magnetite:

$\tau_{Larmor} \approx 30\ ns$

Mössbauer spectra

$\tau < \tau_{Larmor} \Rightarrow$ *fast relaxing*

$\tau > \tau_{Larmor} \Rightarrow$ *non relaxing*

$\tau \approx \tau_{Larmor} \Rightarrow$ *slow relaxing*

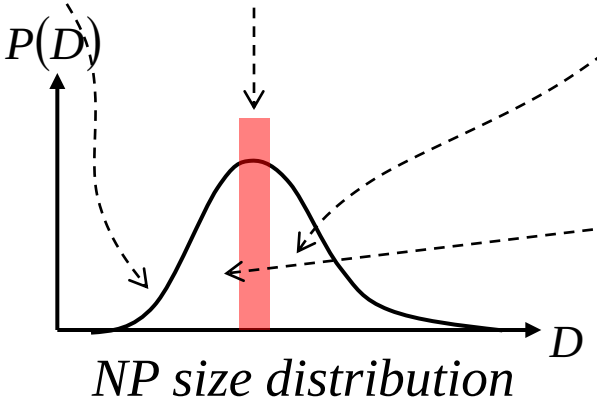

NP size distribution

Mössbauer blocking size at RT ~15 nm

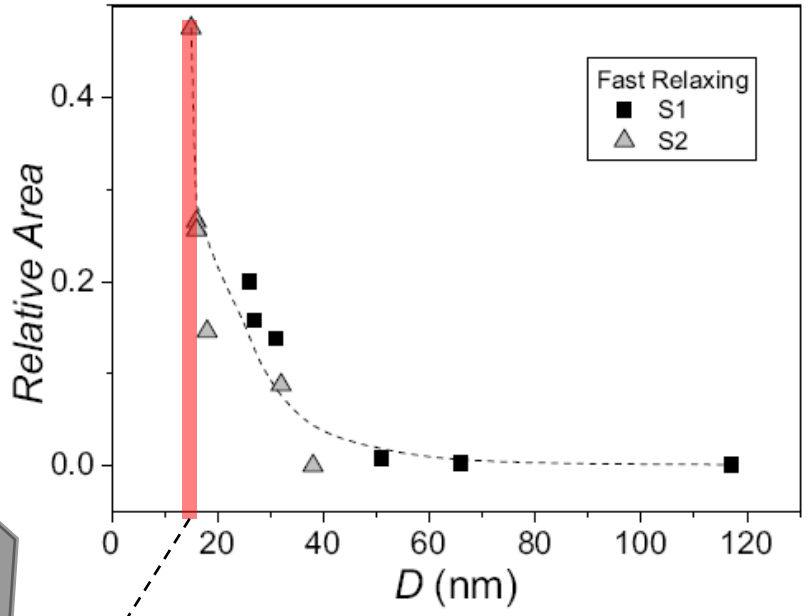

$$\tau_{Larmor} = \tau_0 e^{K_{eff} V / kT}$$

$V,\ \tau_{Larmor}$

$\tau_0 \sim 1\text{x}10^{-9}$ s

$K_{eff} \approx 1.9 \times 10^4\ J / m^3$

XAS observation

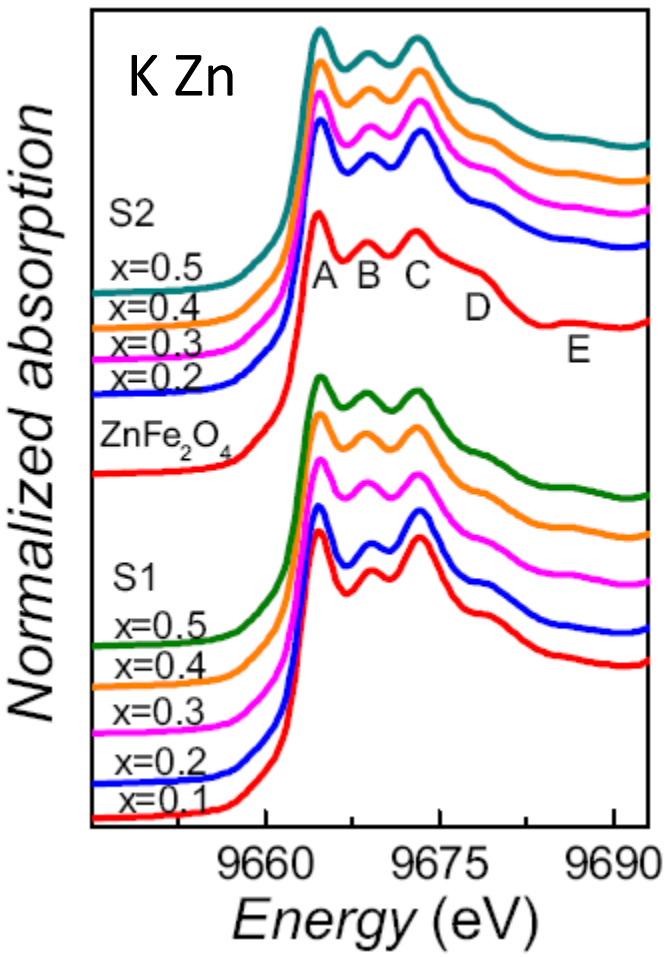

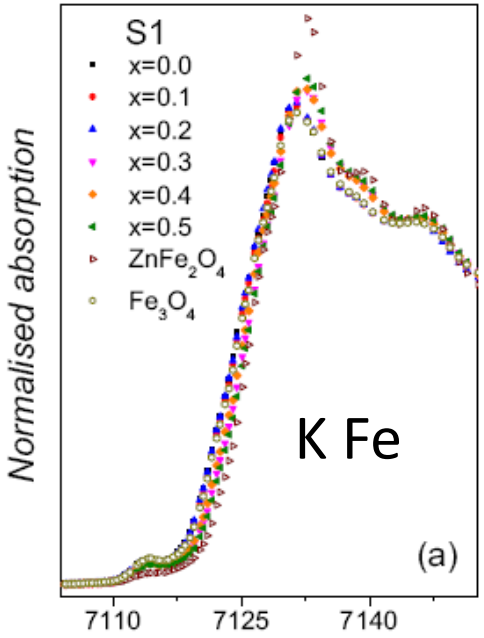

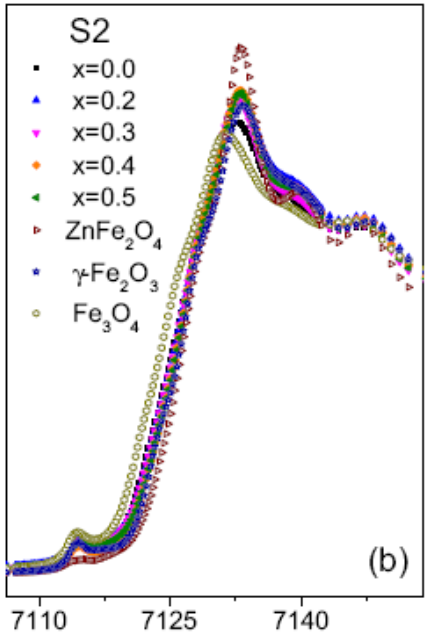

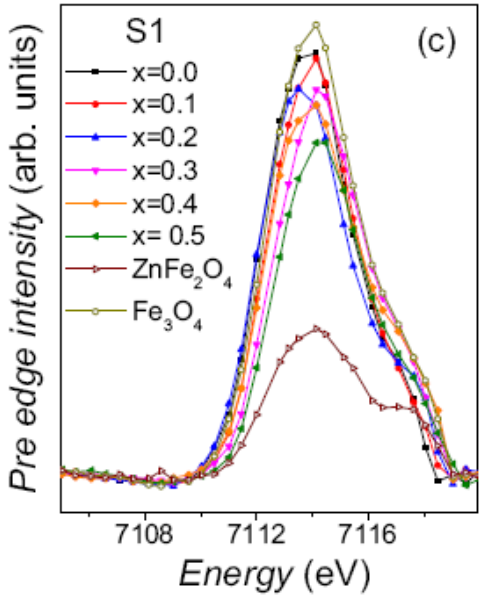

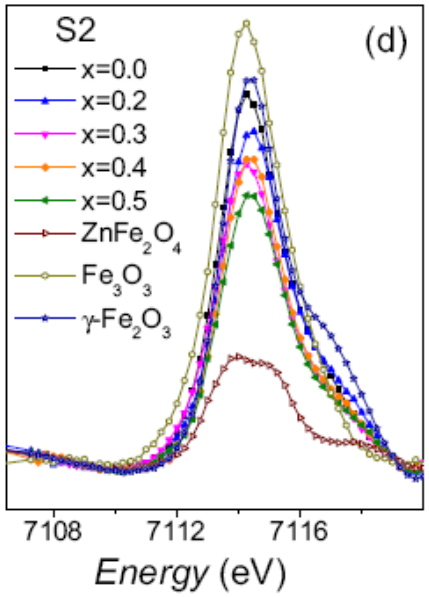

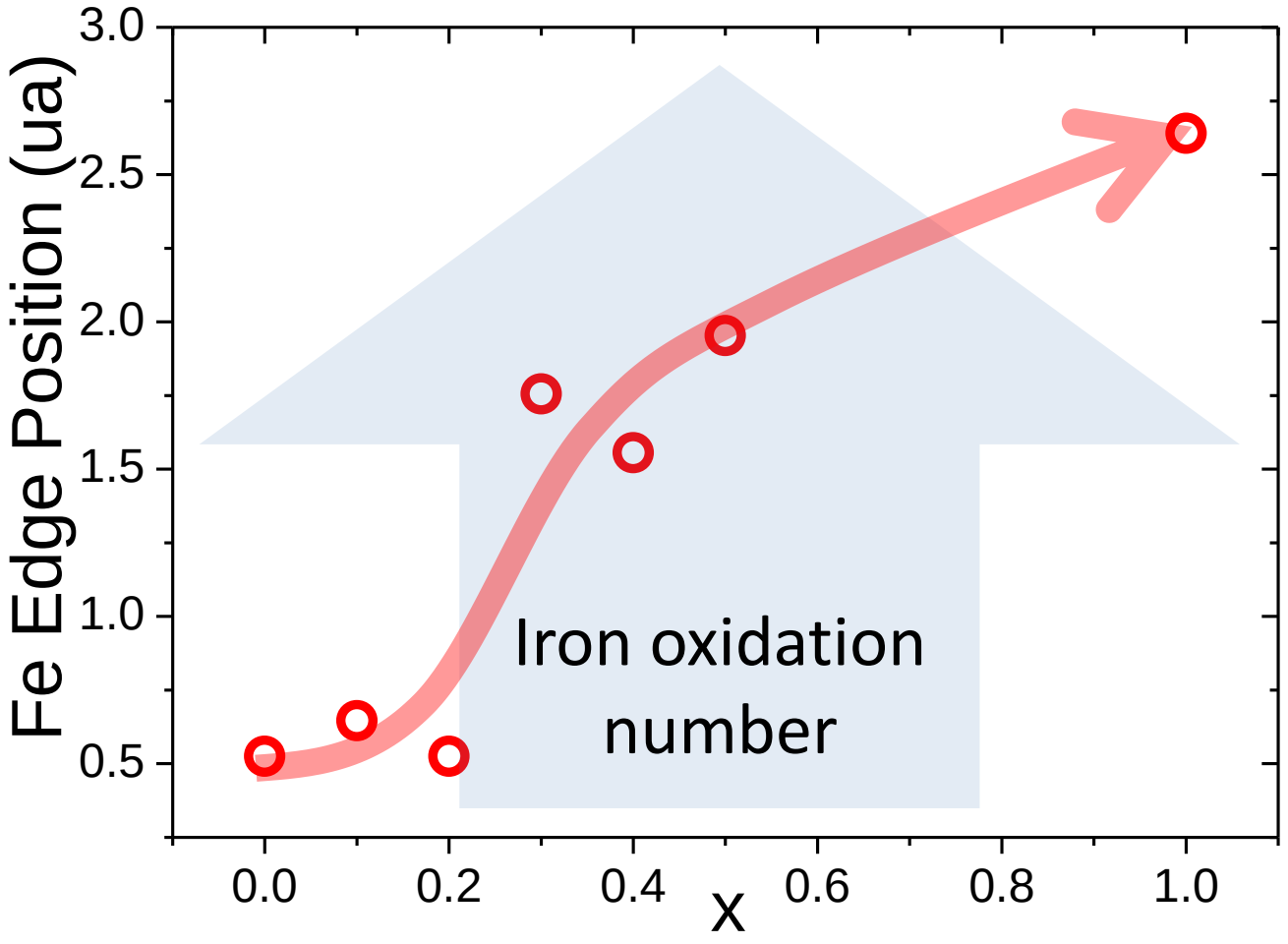
Fe Edge Position (ua)
3.0
2.5
2.0
1.5
1.0
0.5
0.0
0.2
0.4
0.6
0.8
1.0
X
Iron oxidation number

Magnetization results

$Zn_xFe_{3-x}O_4$

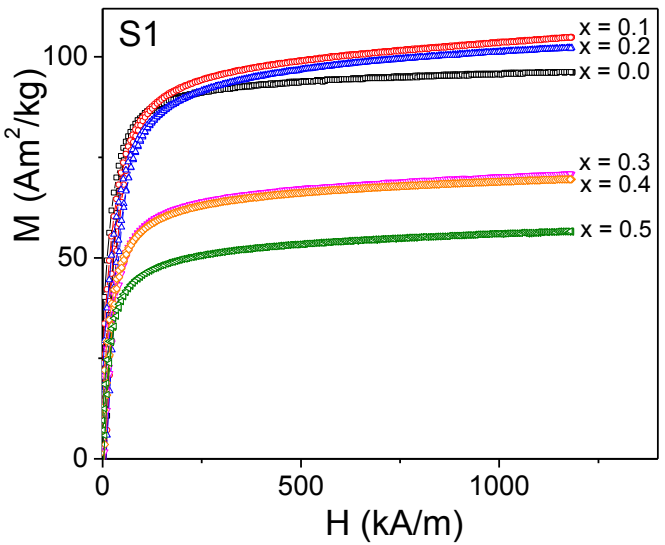

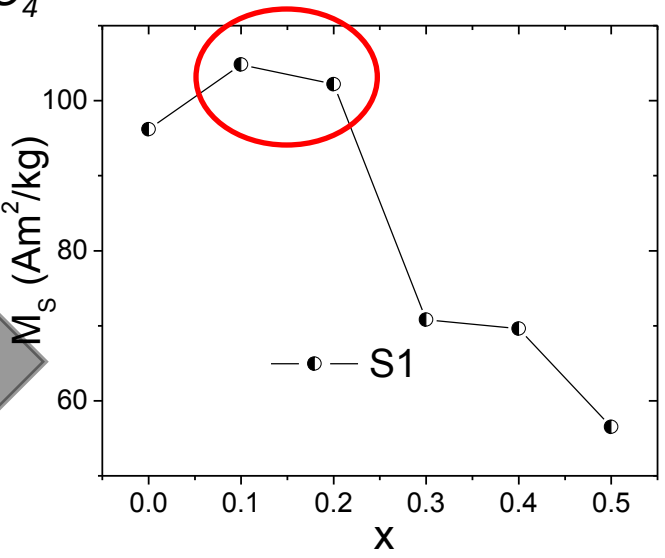

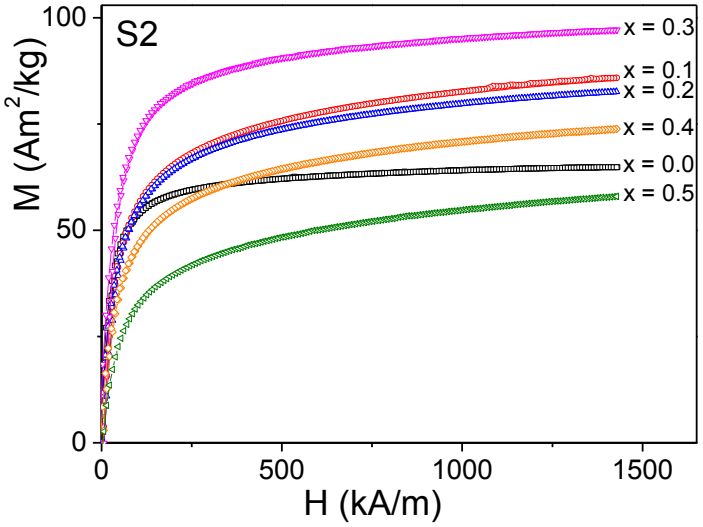

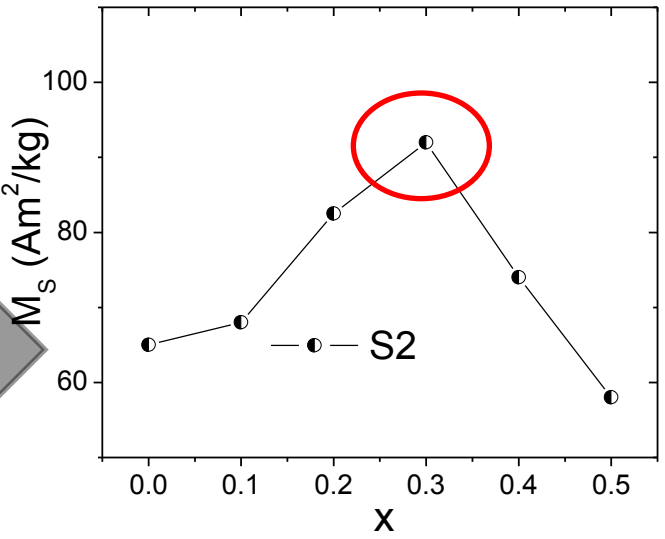

$\mu_{UF} \approx 4\mu_B$ $\quad Zn \Rightarrow A\ site$ $\quad \mu_{UF} \approx 10\mu_B$

SAR experiments

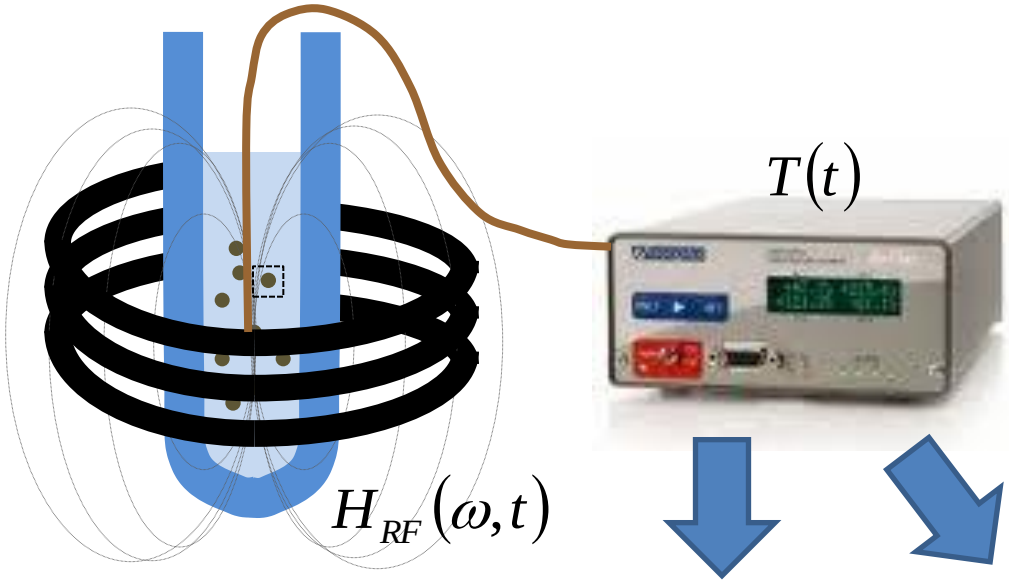

$$H_{RF}(\omega,t)$$

$$H_0 \le 57.7\ kA/m$$

$$\omega = 2\pi f$$

$$f = 260\ kHz$$

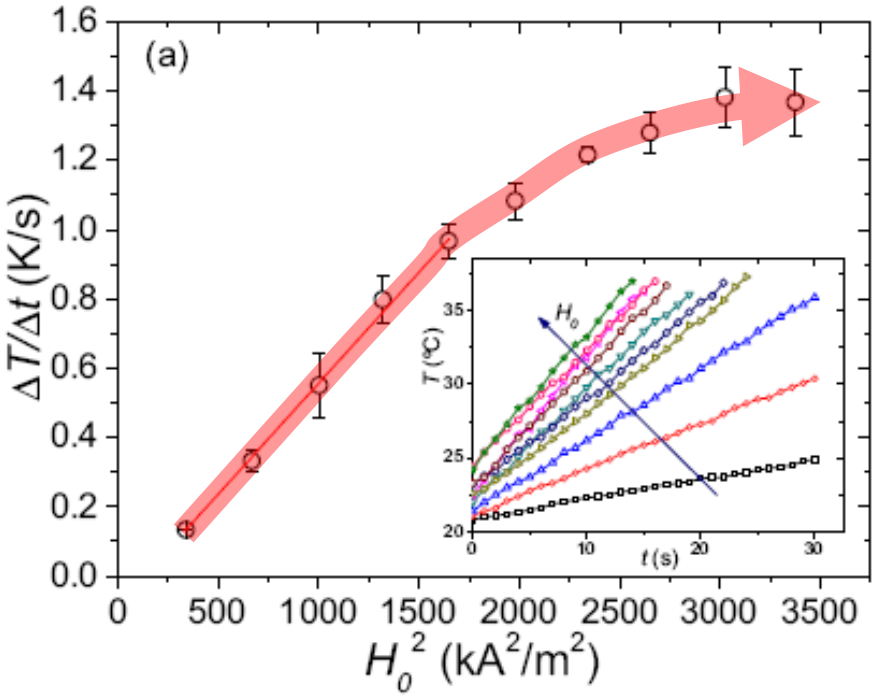

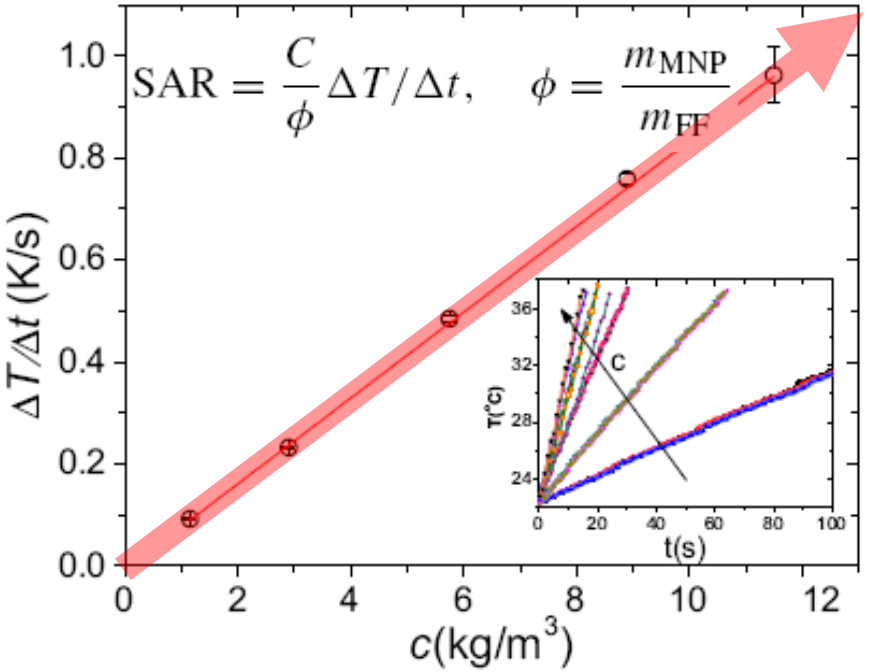

SAR results

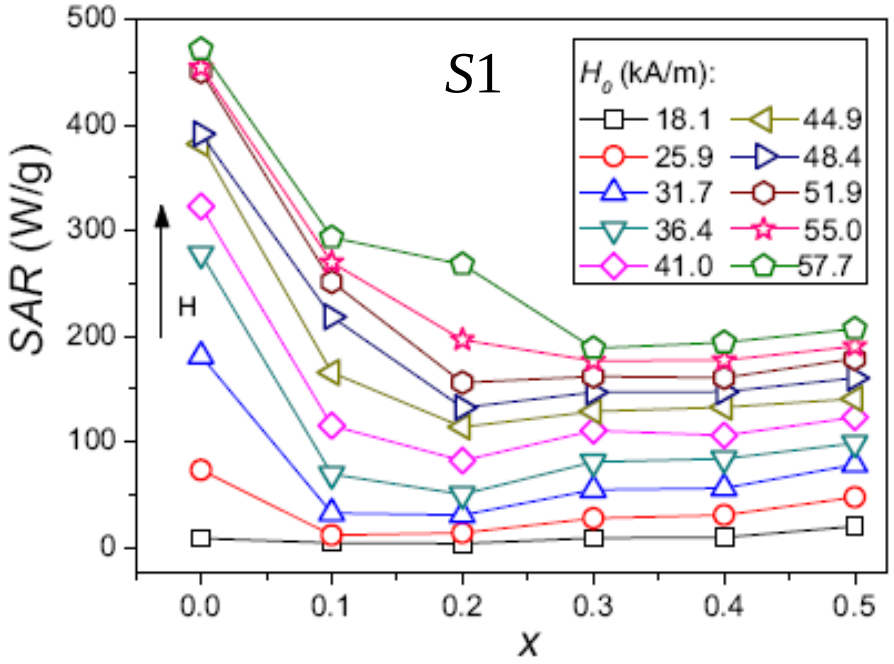

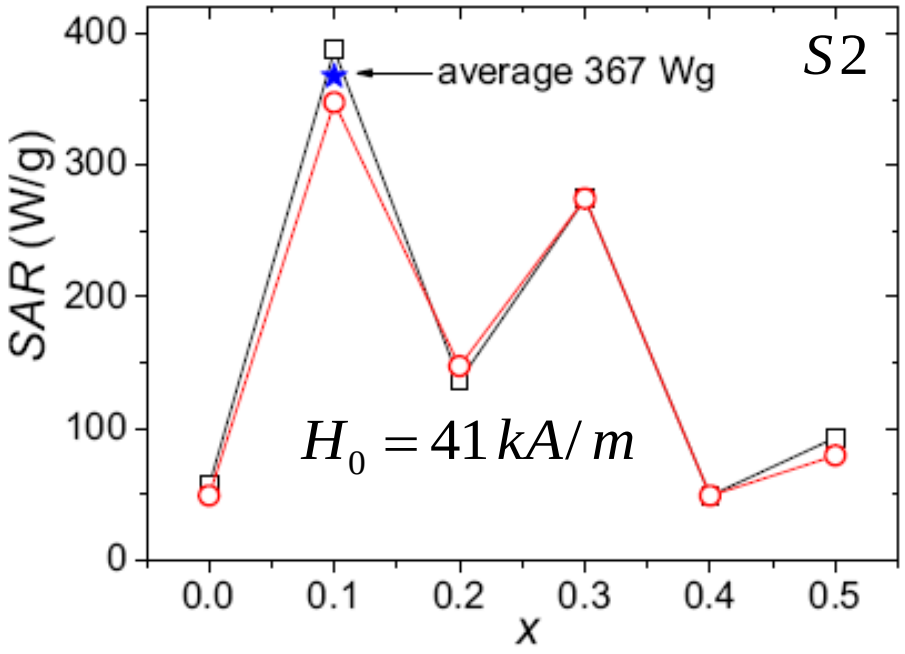

$$SAR = \frac{\pi\mu_0 H_0^2 f}{\rho}\,\frac{\mu_0 M_S^2 V\rho^2}{3kT}\,\frac{\omega\tau}{1+(\omega\tau)^2}$$

Normalizing all SAR data by H_0, M_S and V

$$\frac{SAR}{H_0^2 M_S^2 V} = \frac{\pi\mu_0^2 f\rho}{3kT}\,\frac{\omega\tau}{1+(\omega\tau)^2} = C\,\frac{\omega\tau}{1+(\omega\tau)^2}$$

SAR results – Relaxation time

$$\frac{SAR}{CH_0^2 M_S^2 V} = \frac{\omega\tau}{1+(\omega\tau)^2}$$

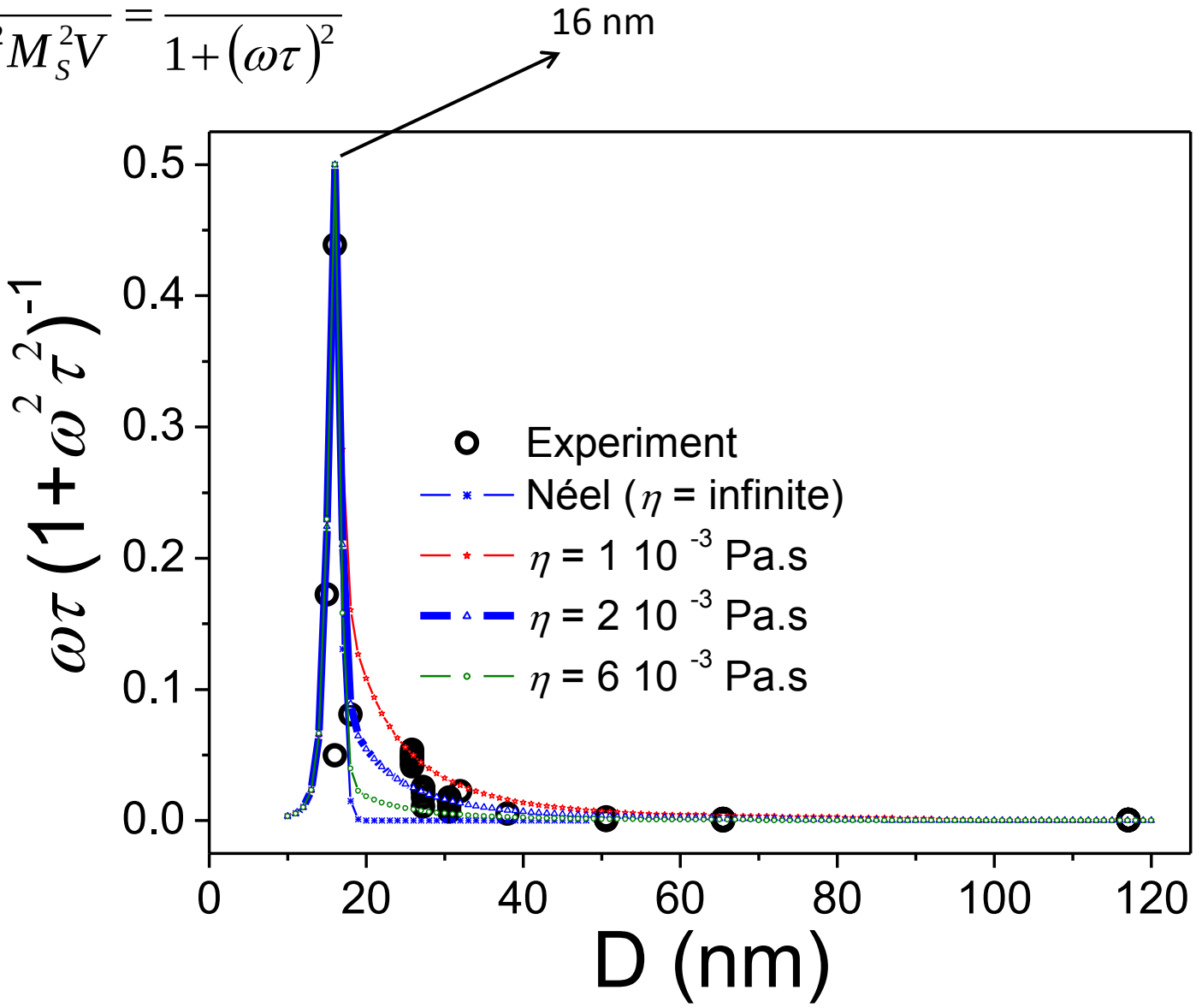

SAR results – Relaxation time

P Mendoza Zélis *et al*

$$\frac{\omega\tau}{1+(\omega\tau)^2} \Rightarrow \tau$$

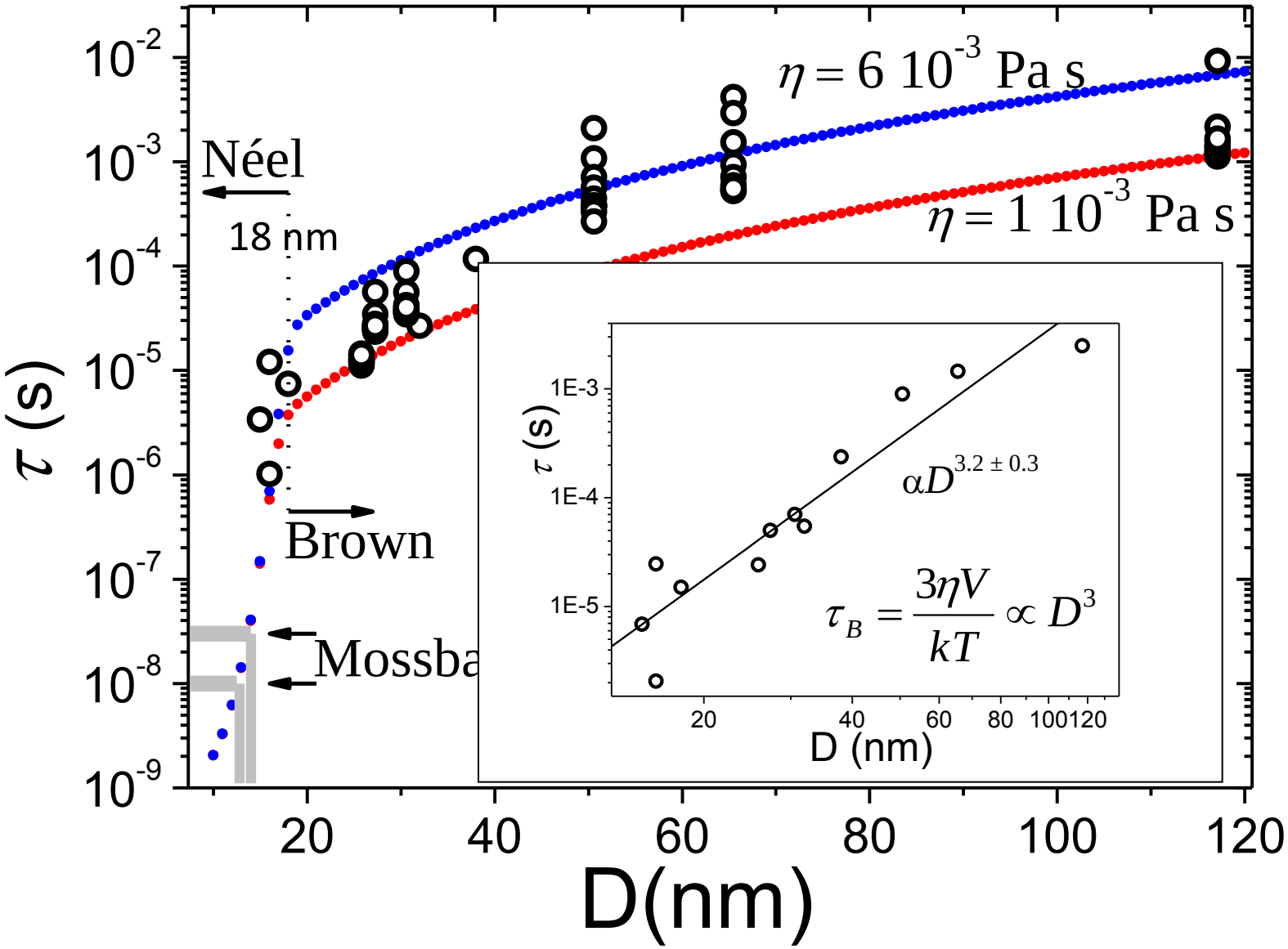

Conclusions II

Ms increases with Zn low doping of magnetite (x = 0.1-0.3)

High SARs of almost 400 W/g can be obtained

At 260 kHz crossover from Néel to Brown relaxation is at 18 nm

At 260 kHz frequency factor is maximum at 16 nm

SAR can be improved further by increasing Ms of 16 nm NPs and reducing polydistersity

Citric Acid Coated Magnetite Nanoparticles for Magnetic Hyperthermia

M. Elisa de Sousa*, *Marcela B. Fernández van Raap, *Patricia C. Rivas, Pedro Mendoza Zélis, Pablo Girardin, Gustavo A. Pasquevich, Jose L. Alessandrini, Diego Muraca, and Francisco H. Sánchez*

Stability and relaxation mechanisms of citric acid coated magnetite nanoparticles for magnetic hyperthermia, ***J. Phys. Chem. C****, (****2013****), 117 (10), pp 5436–5445. DOI: 10.1021/jp311556b.*

Modified Masart Method

Chemical coprecipitation from ferric chloride and ferrous chloride in the presence of excess ammonia NH4OH solution (AS) → magnetite NPs.

Magnetite cores were negatively charged by Citric Acid (CA) adsorption over its surfaces. Both steps, co-precipitation and CA adsorption, were carried out under a N2 reflux at 60 °C.

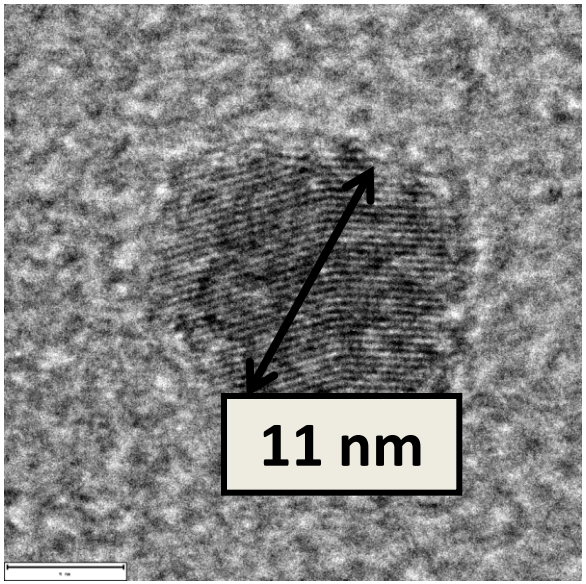

uncoated

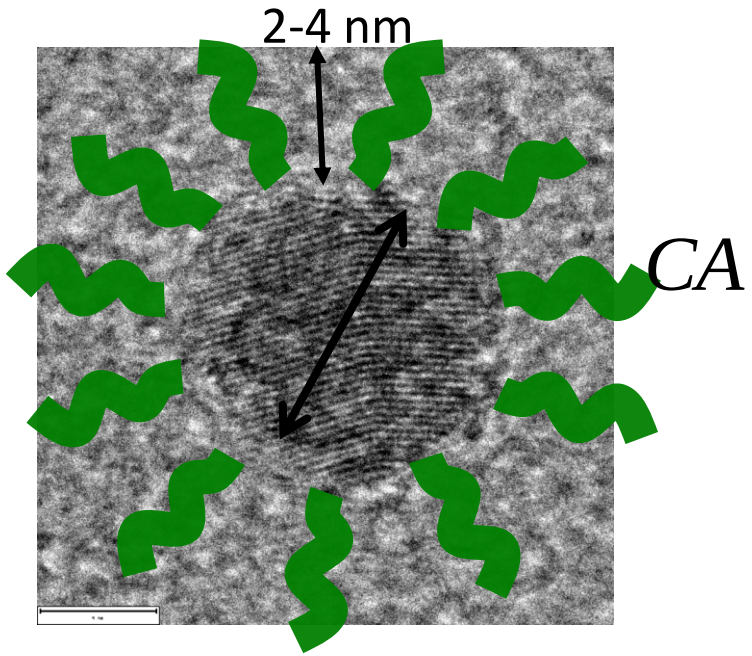

CA coated

preparation

The pH at which CA was adsorbed to the MNP surface (pH_{ad}) was varied from 4.58 to 7.08. AS (0.25% w/w) was used to adjust the suspension pH to pH_{sus} close to 7.

The suspensions were placed on a permanent magnet during 600 s. By this way six colloids C_i were obtained.

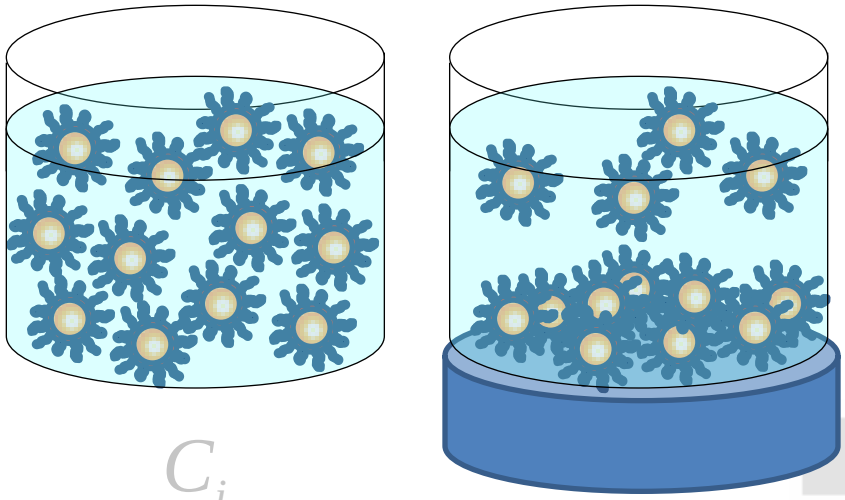

$$f = \frac{[CS_i]}{[C_i]}$$

CA adsorption efficiency and long term stability parameter

	[X] (g/L)	$pH_{ads} \pm 0.01$	$pH_{sus} \pm 0.01$
CS_1	13.4	4.58	7.44
CS_2	10.7	4.91	7.34
CS_3	18.3	5.50	6.97
CS_4	13.1	6.25	7.22
CS_5	5.6	6.88	7.10
CS_6	7.4	7.08	7.22

Structural studies

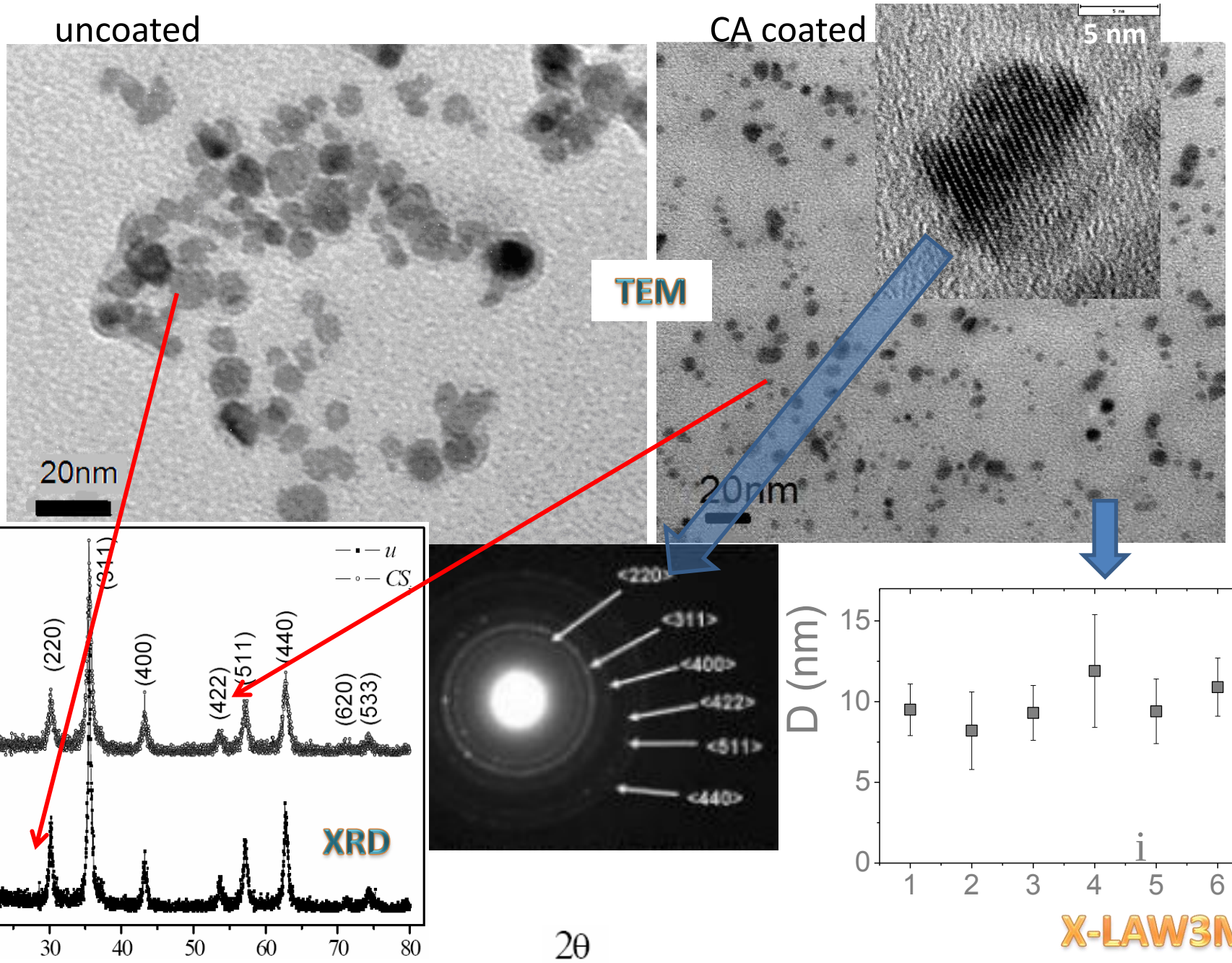

Thermal stability, TG-DTA

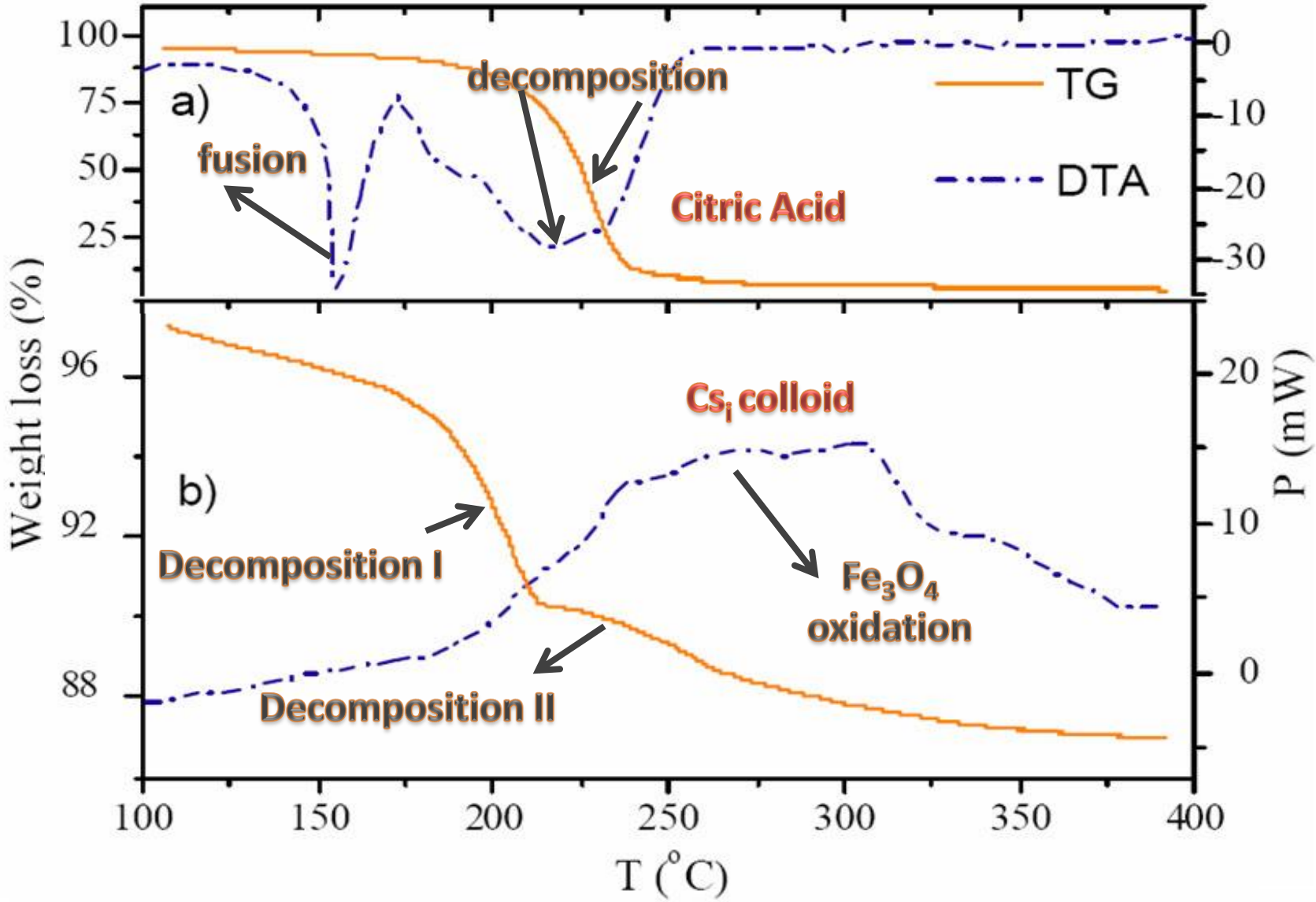

FF stability vs adsorption pH

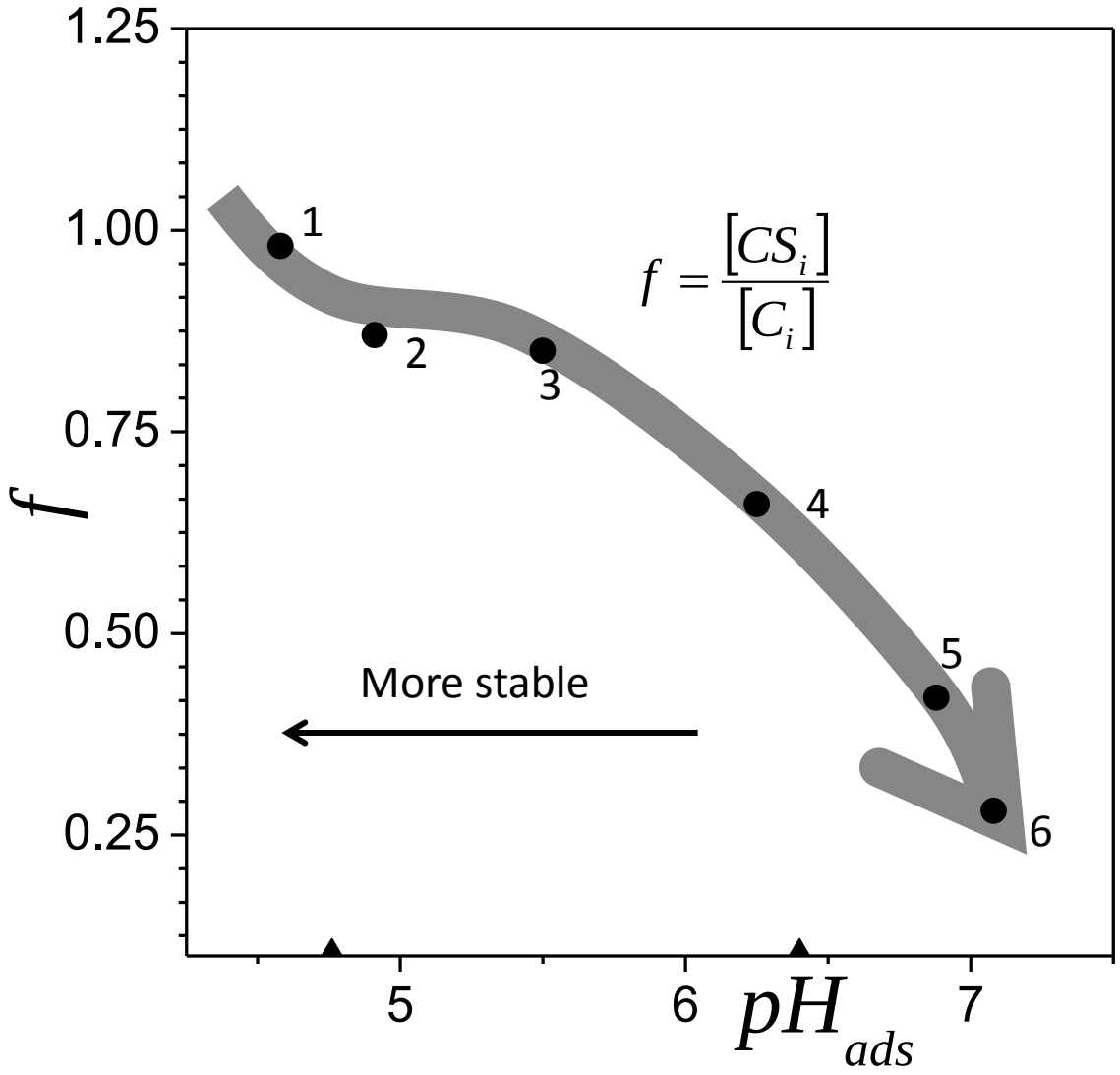

Z potential, surface charge

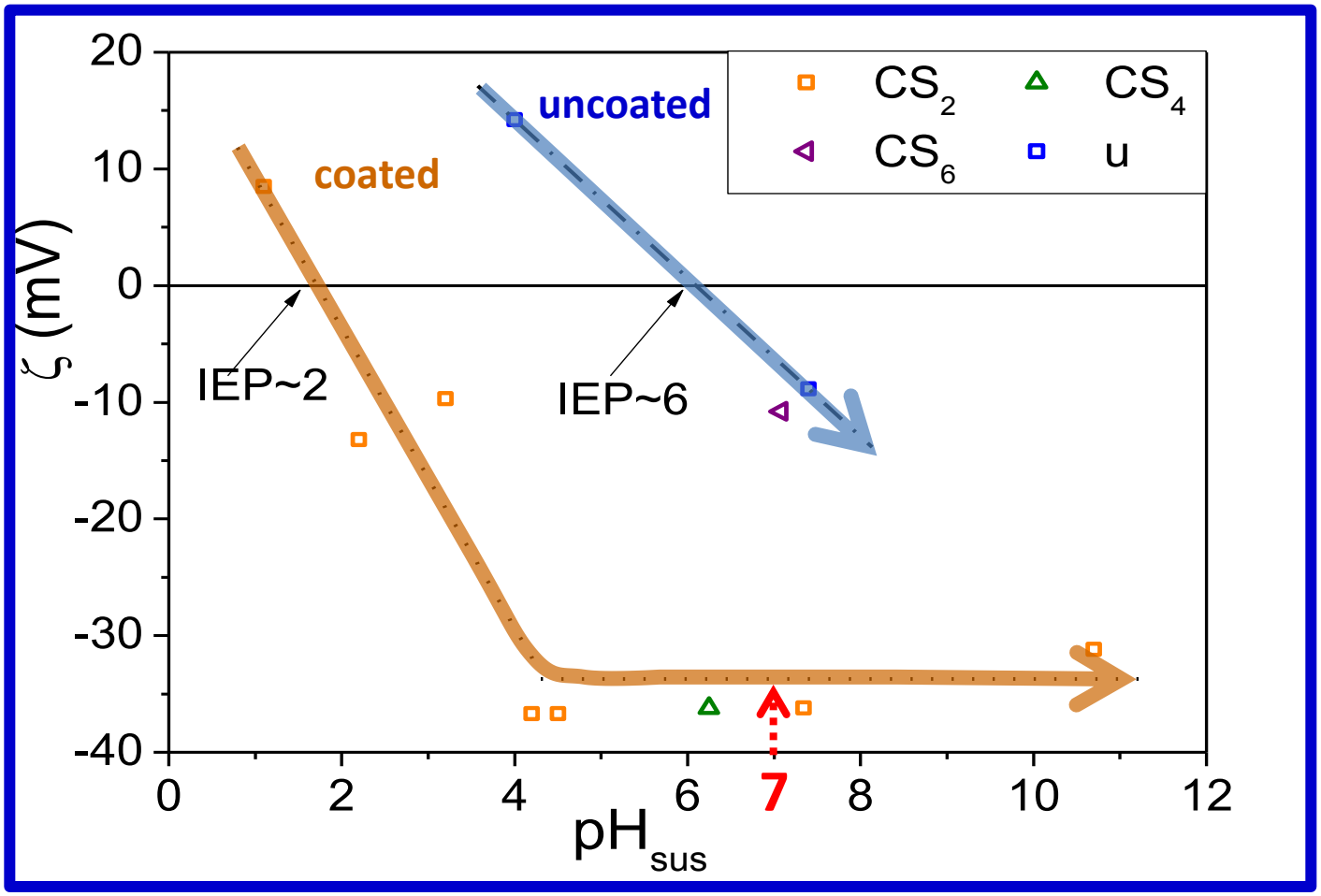

M vs H on frozen FF, stability – dead layer

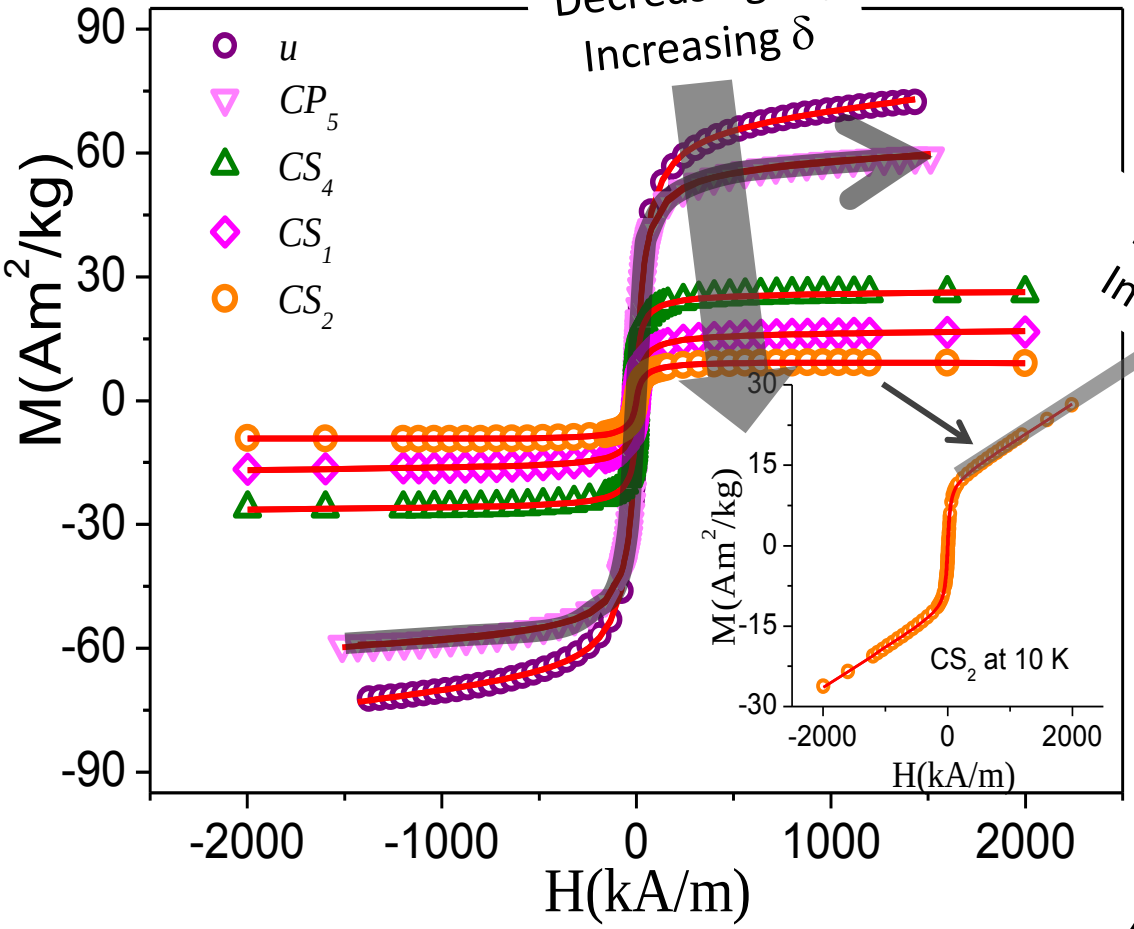

$$d = d_m + \delta$$

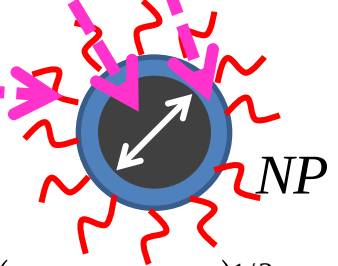

$$\delta = \frac{d_m\left(\left(M_S^{bulk}/M_S\right)^{1/3}-1\right)}{2}$$

M_S, d_m

$$M(T,H) = N\int_0^{\infty} \mu L\left(\frac{\mu_0 \mu H}{kT}\right) f(\mu)d\mu + \chi H$$

μ vs T, from M vs H curves on frozen FF, dipolar interactions

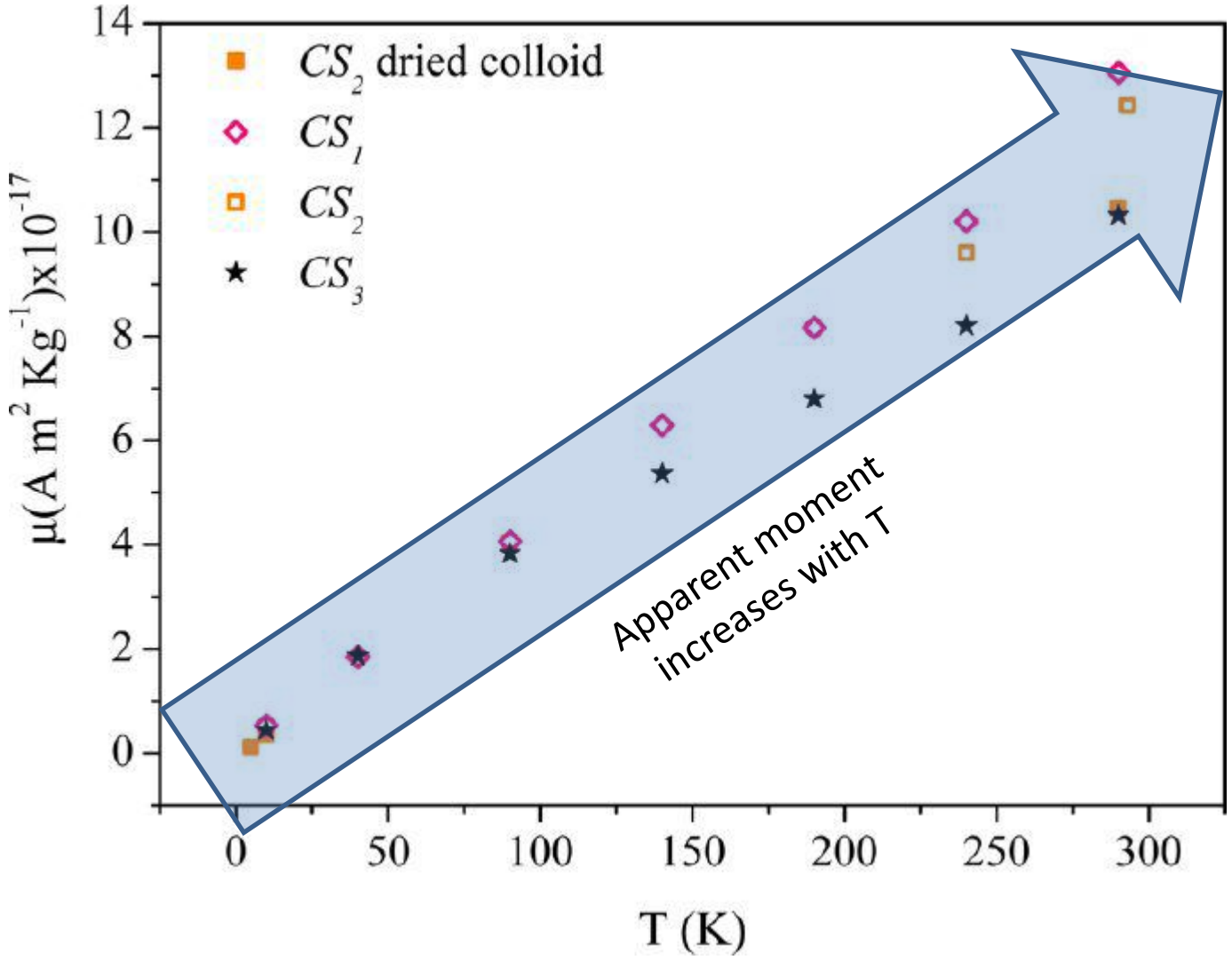

Allia et al., Phys. Rev. B 2001, 64 (14), 1–12.

M vs T on frozen FF, ZCF-FC, dipolar interactions

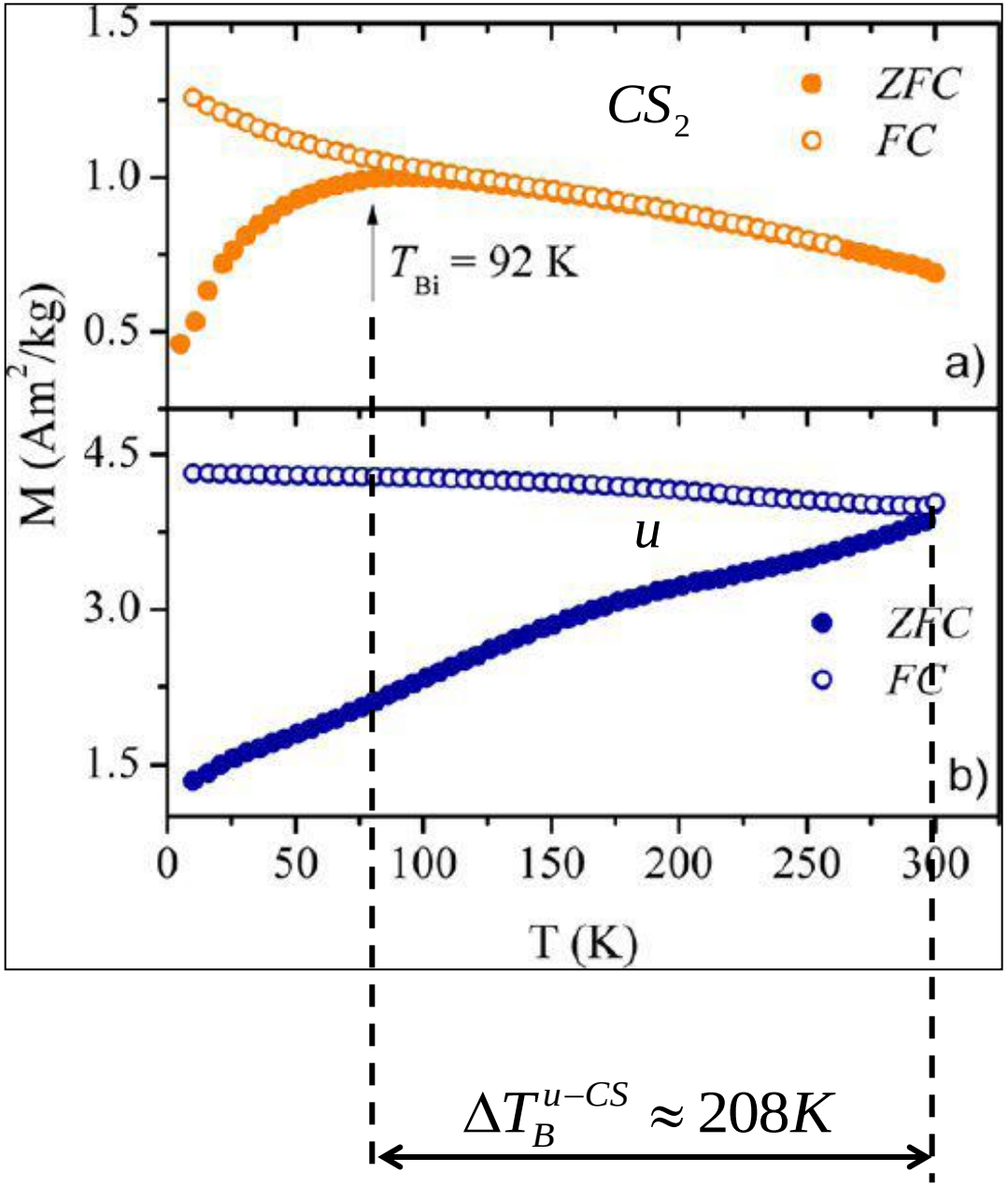

$$E_b \approx K_{eff} V + \varepsilon$$

Dormann et al., Advances in Chemical Physics 98; Wiley: New York, 2007.

M vs T on frozen FF, ZCF-FC, dipolar interactions

$$K_{eff} = K + \frac{6}{d} K_S$$

$$K_S = K_S^0 \tanh(d/\lambda)$$

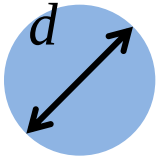

$$K_S^0 \approx 2\times10^{-5}\, J/m^2$$

$$\lambda \approx 4.1\times10^{-9}\, m$$

Gilmore *et al.* J. Appl. Phys. **97**, 10B301 (2005)

bulk $K = 1\times10^4\, J/m^3$

$$K_{eff} \approx 2\times10^4\, J/m^3$$

$$T_B^{ni}(d) \approx \frac{K_{eff}(d)V}{25.6k}$$

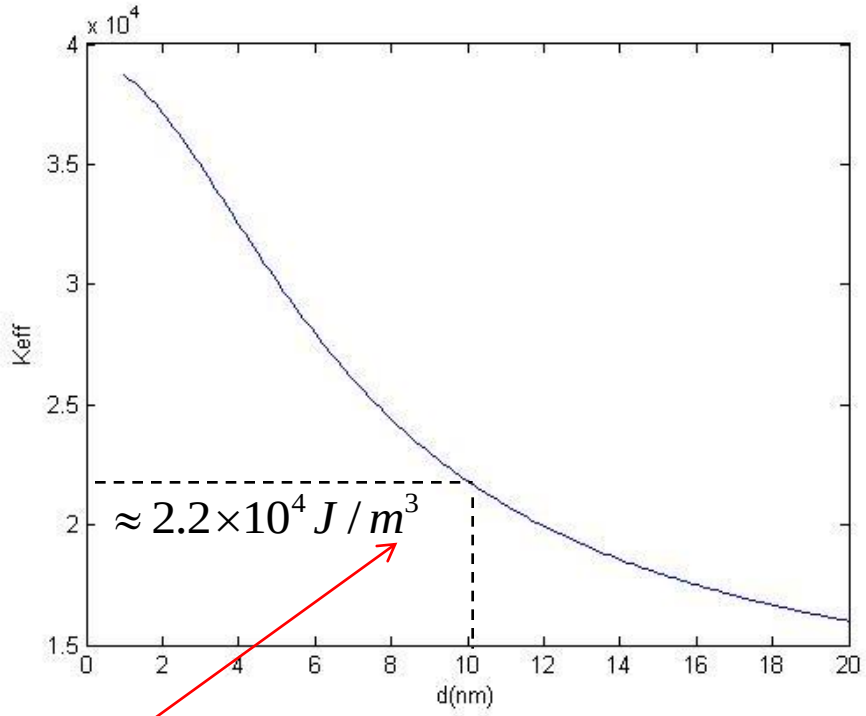

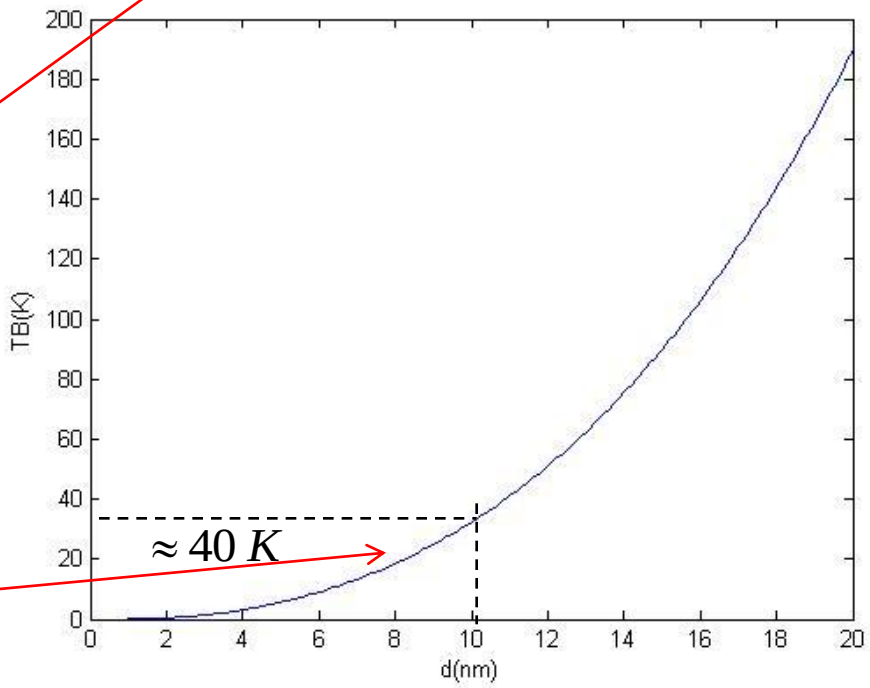

M vs T on frozen FF, ZCF-FC, dipolar interactions

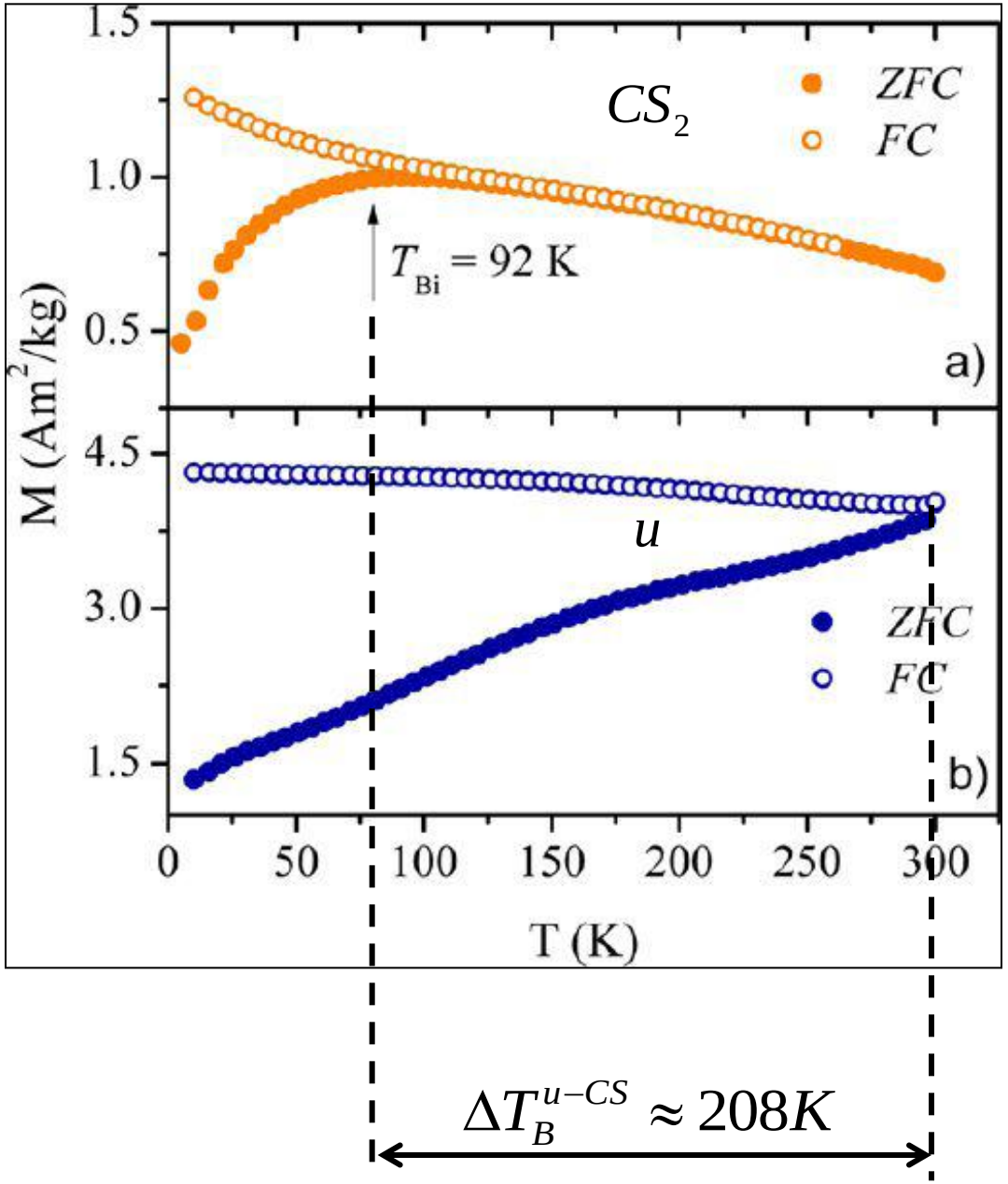

$$\varepsilon \approx k\Delta T_B$$

$$\varepsilon_{CS_2} \approx 0.7\times10^{-21} J / NP$$

$$\varepsilon_u \approx 3.6\times10^{-21} J / NP$$

at RT

$$kT \approx 4.1\times10^{-21} J$$

NP sizes

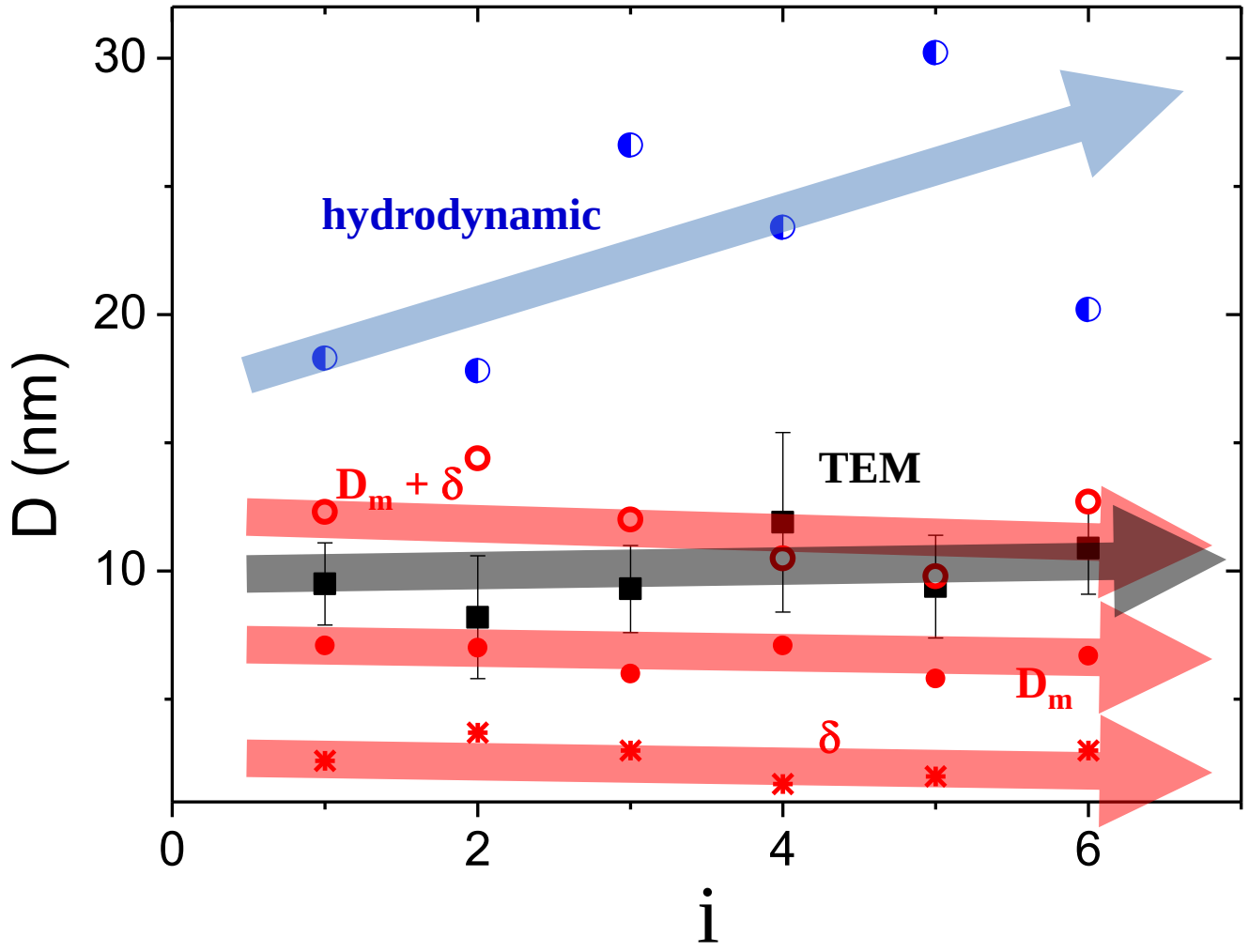

SAR, experimental

SAR, experimental

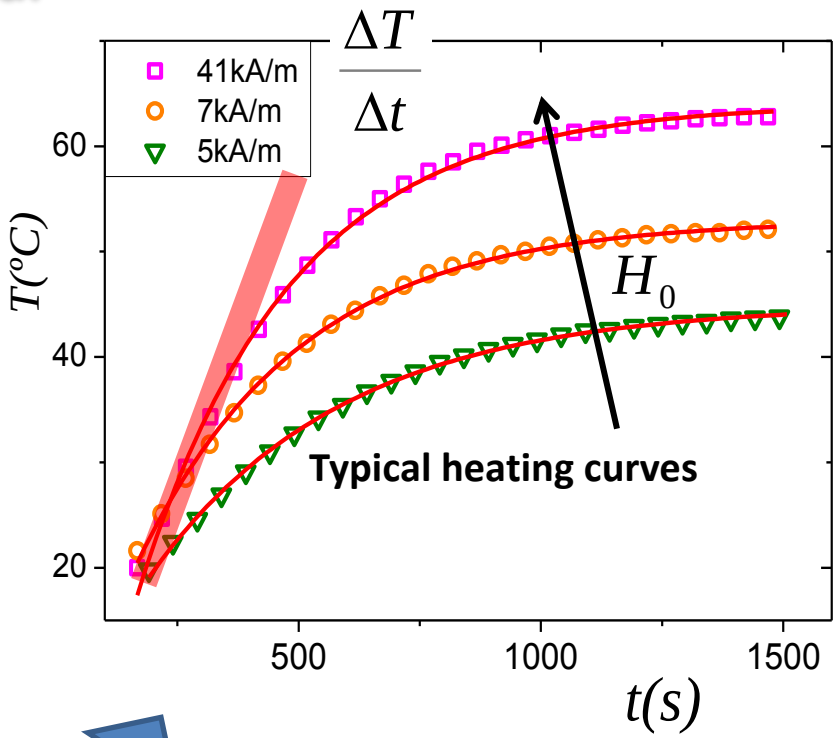

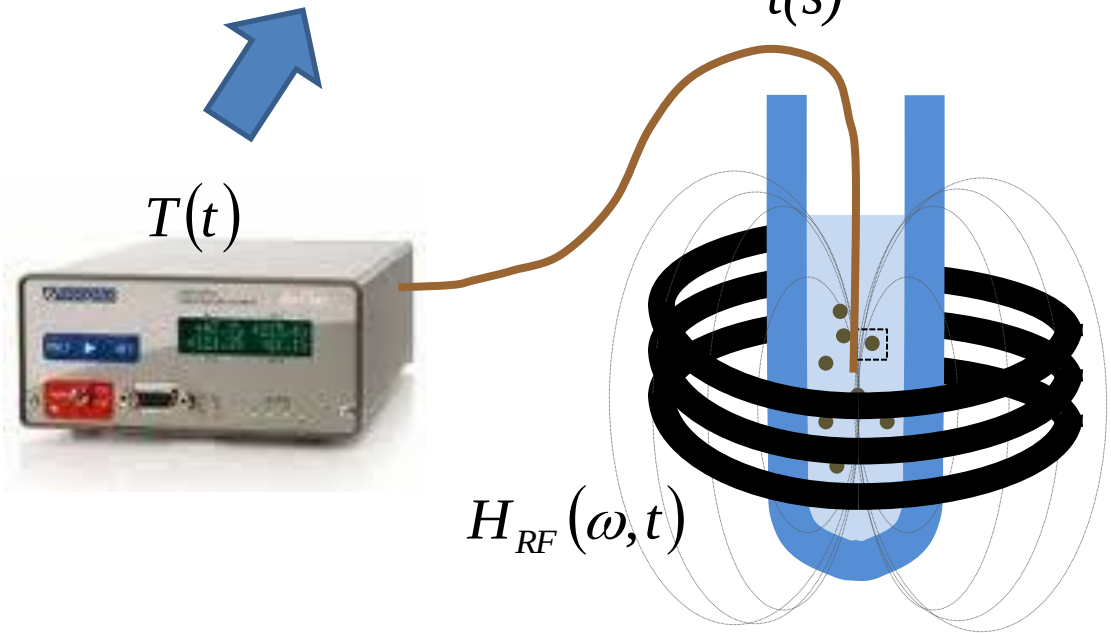

SAR, Ms dependence

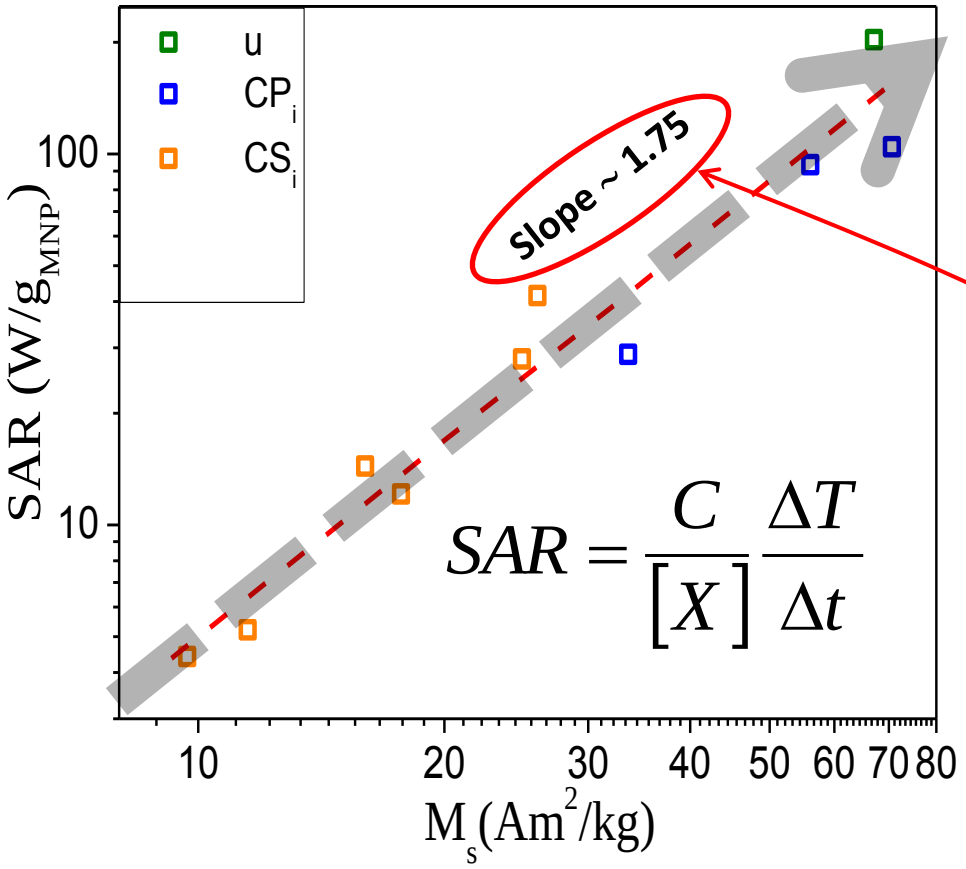

$$SAR = \frac{\pi \mu_0 H_0^2 f_{RF}}{\rho} \int_0^\infty \chi''(\tau(d)) f(d) \mathrm{d}d$$

$$\chi''(\omega) = \chi_0 \frac{\omega\tau}{1+(\omega\tau)^2}$$

$$\chi_0 \approx \frac{\mu_0 \rho^2 M_S^2 V}{3kT}$$

SAR, moment relaxation mechanism

$$SAR \propto \chi''(\omega) = \chi_0 \frac{\omega\tau}{1+(\omega\tau)^2}$$

$$\tau = \begin{cases} \tau_N \approx \tau_0 e^{\sigma}, \quad \sigma = E_b / kT \\ \tau_B \approx 3\eta V_H / kT \end{cases}$$

$$\tau^{-1} = \tau_N^{-1} + \tau_B^{-1}$$

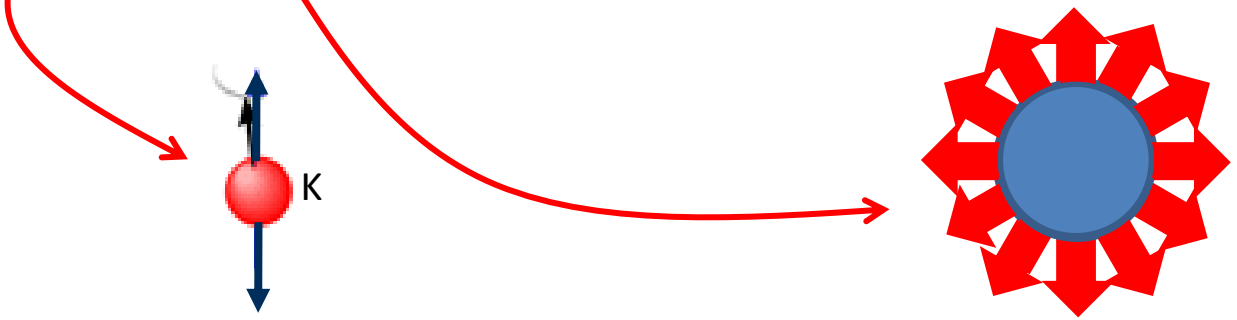

Néel *Brown*

Conclusions I

Citric accid coating: highly stable FFs

High influence of coating on dead layer thickness and Ms

High influence of dipolar interactions on SAR

In vitro experiments – A549

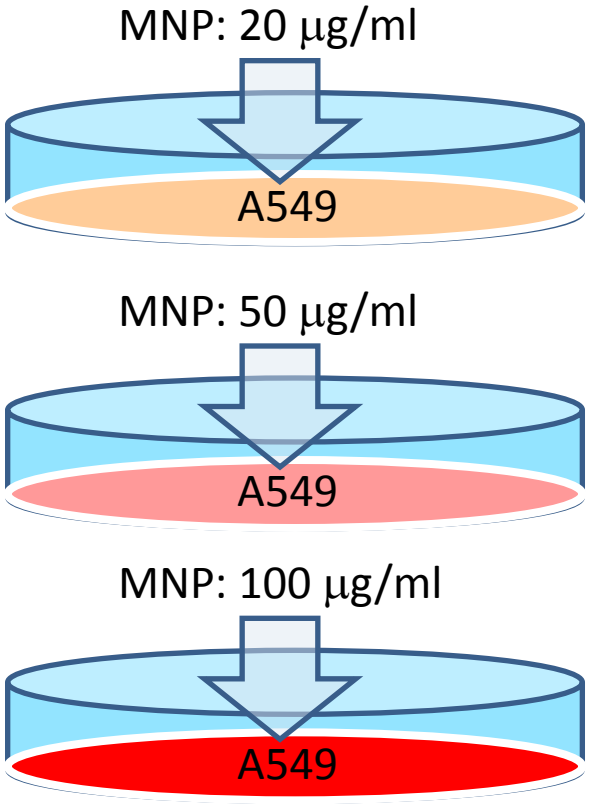

$$t \approx 12\ h$$

In vitro experiments – A549

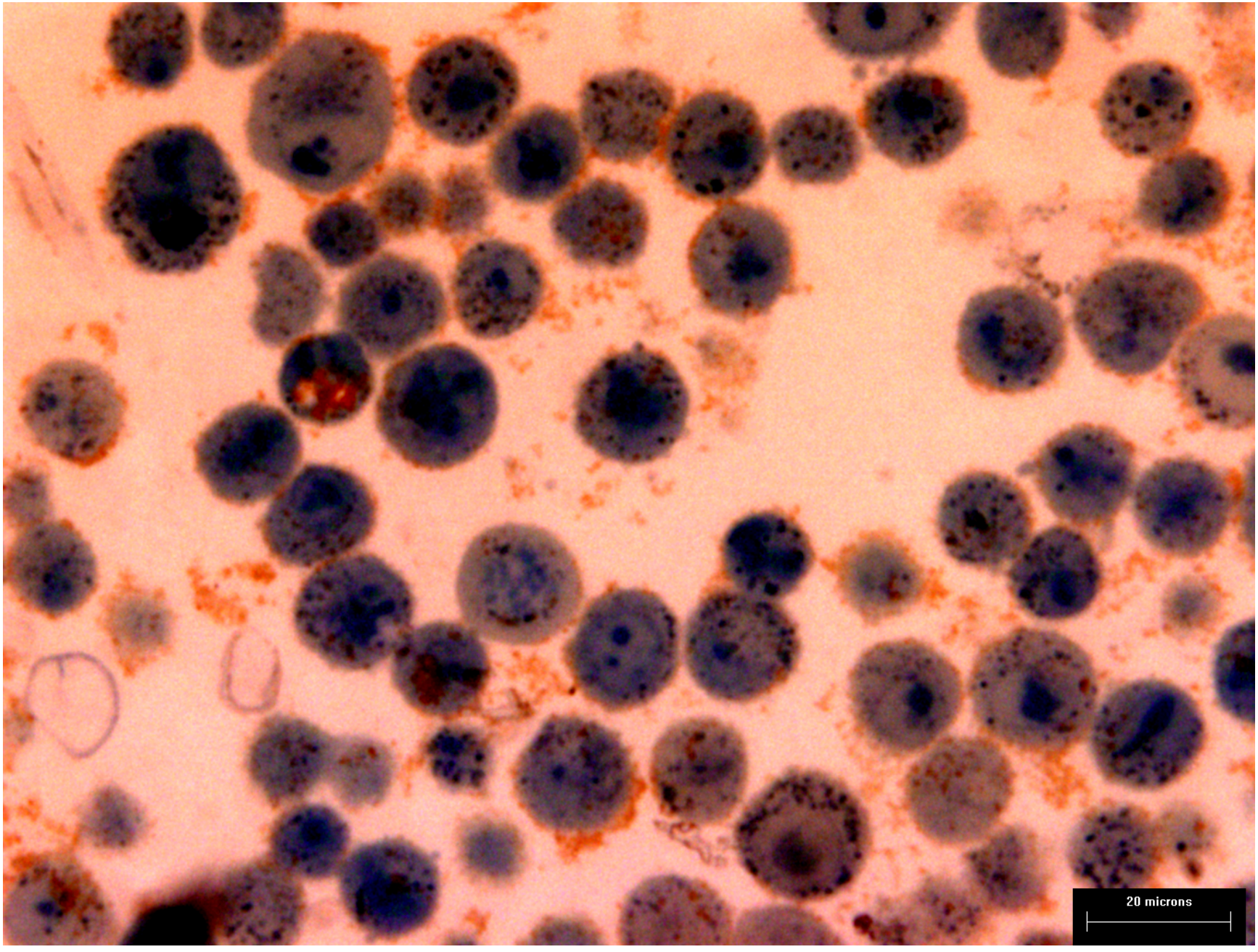

In vitro experiments – A549

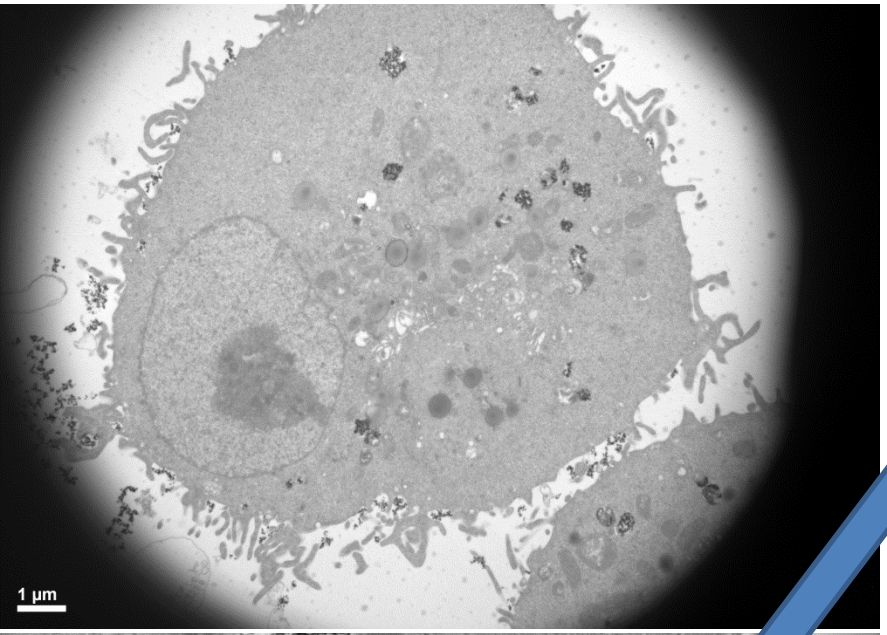

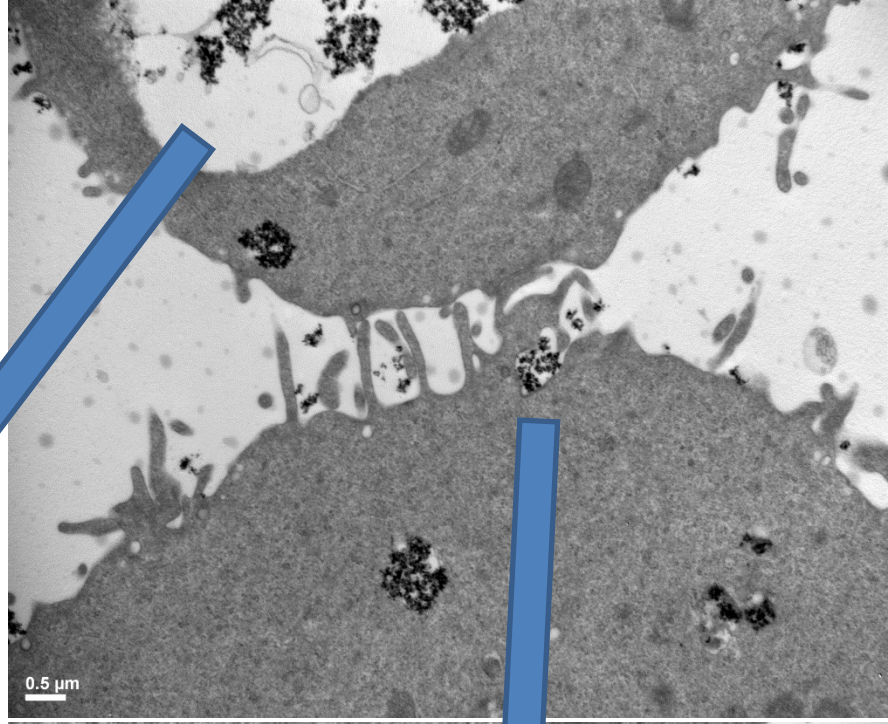

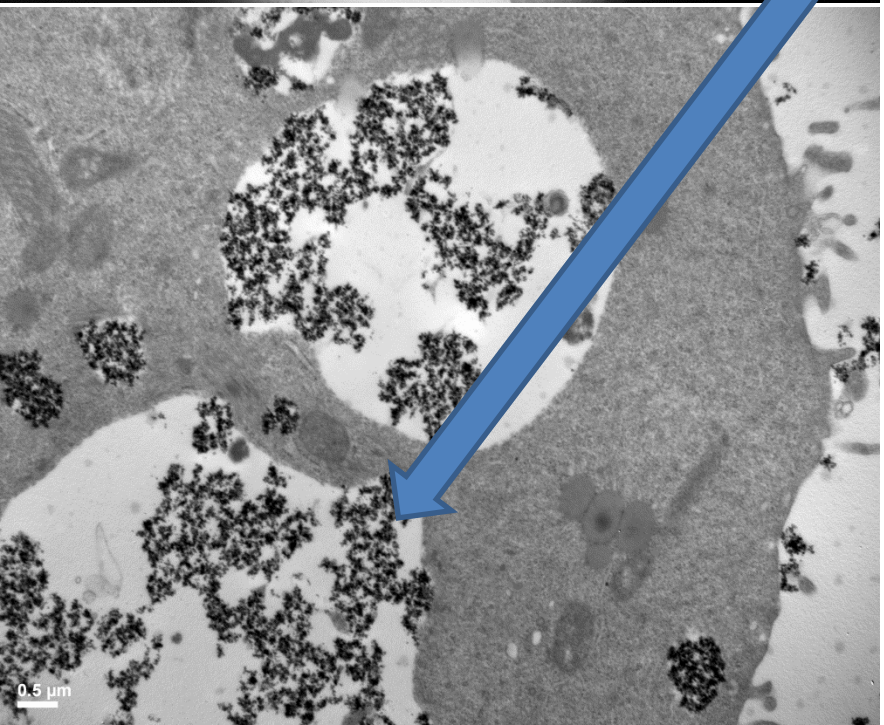

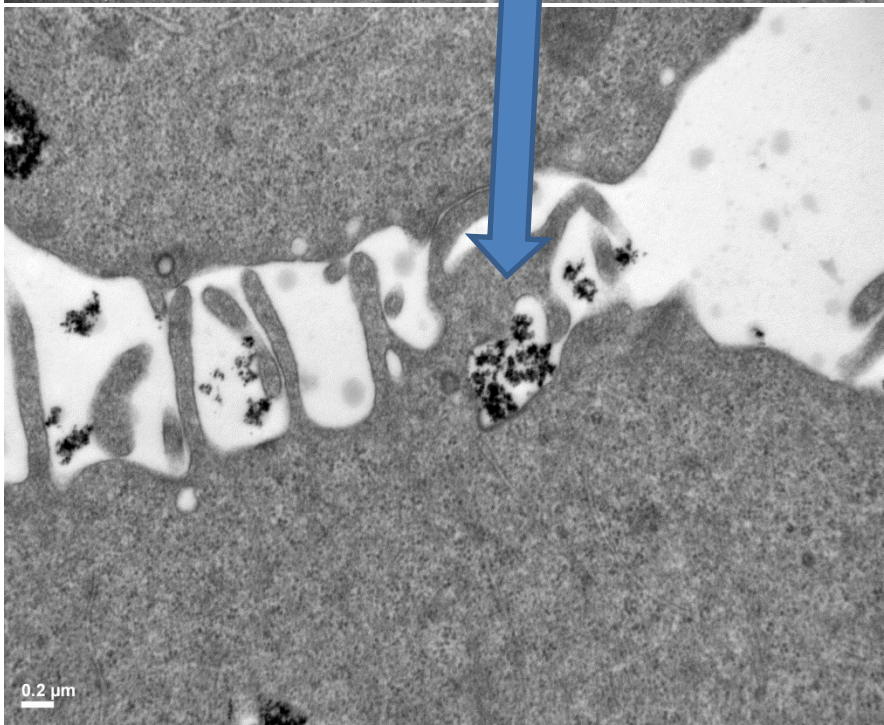


0.2 µm

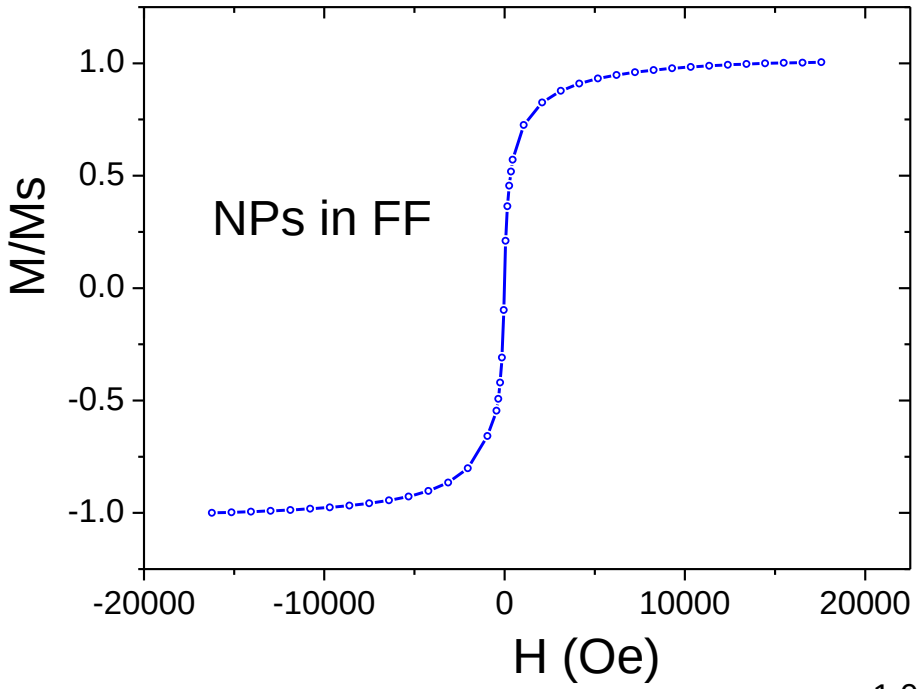
NPs in FF
M/Ms
H (Oe)
1.0
0.5
0.0
-0.5
-1.0
-20000
-10000
0
10000
20000

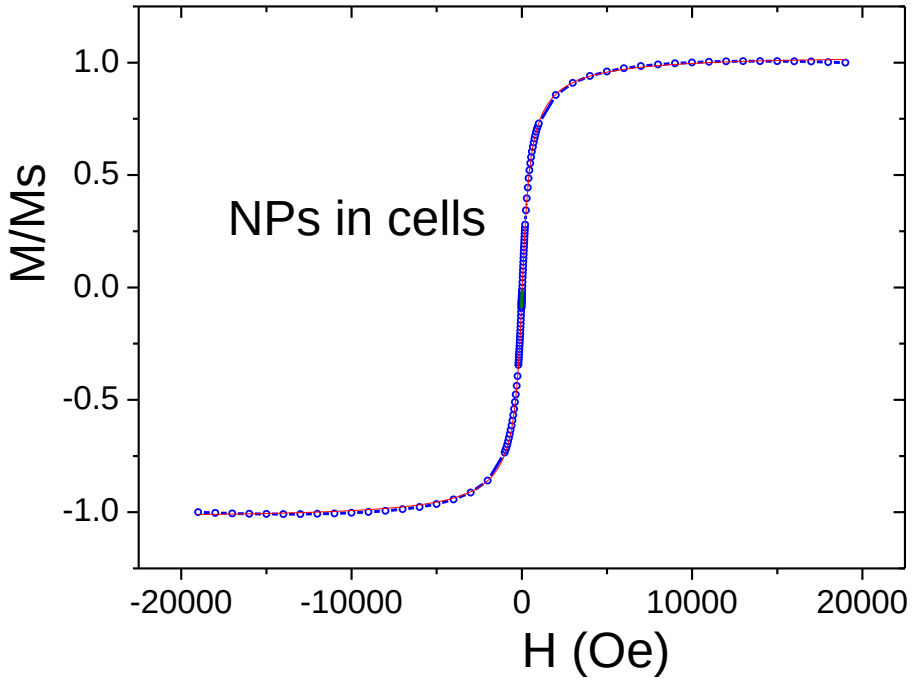
NPs in cells
M/Ms
H (Oe)
1.0
0.5
0.0
-0.5
-1.0
-20000
-10000
0
10000
20000

Internalization efficiency of NPM in cell cultures

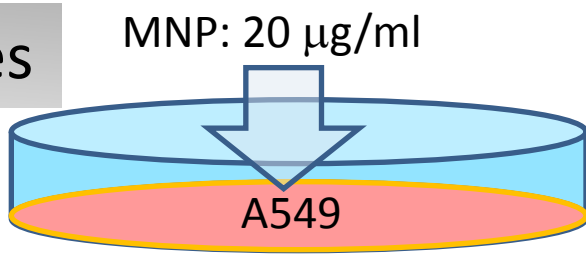

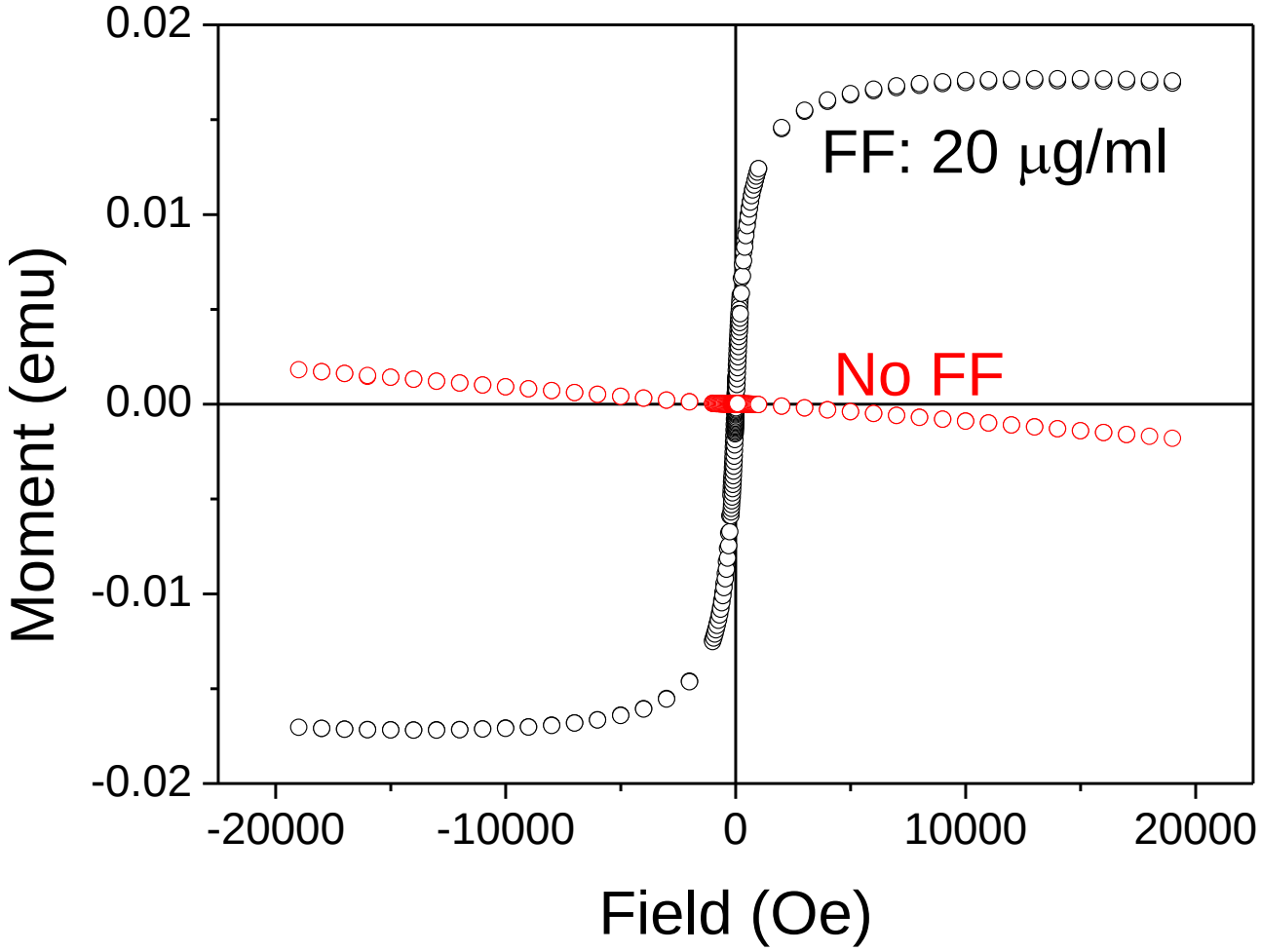

15 x 10^6 cells

29 pg_{mag}/cell

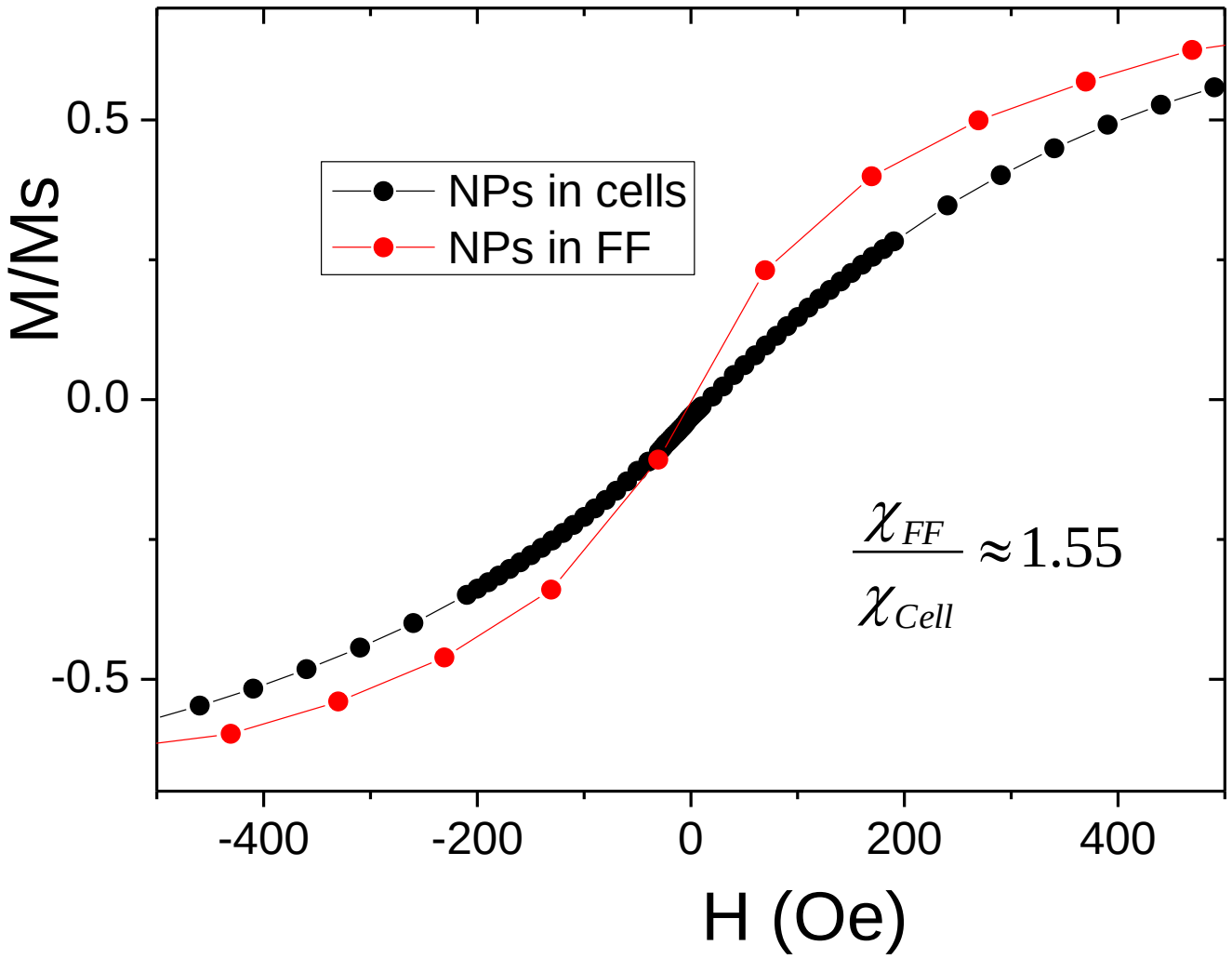
0.5
0.0
-0.5
M/Ms
-400
-200
0
200
400
H (Oe)
NPs in cells
NPs in FF
$\frac{\chi_{FF}}{\chi_{Cell}} \approx 1.55$

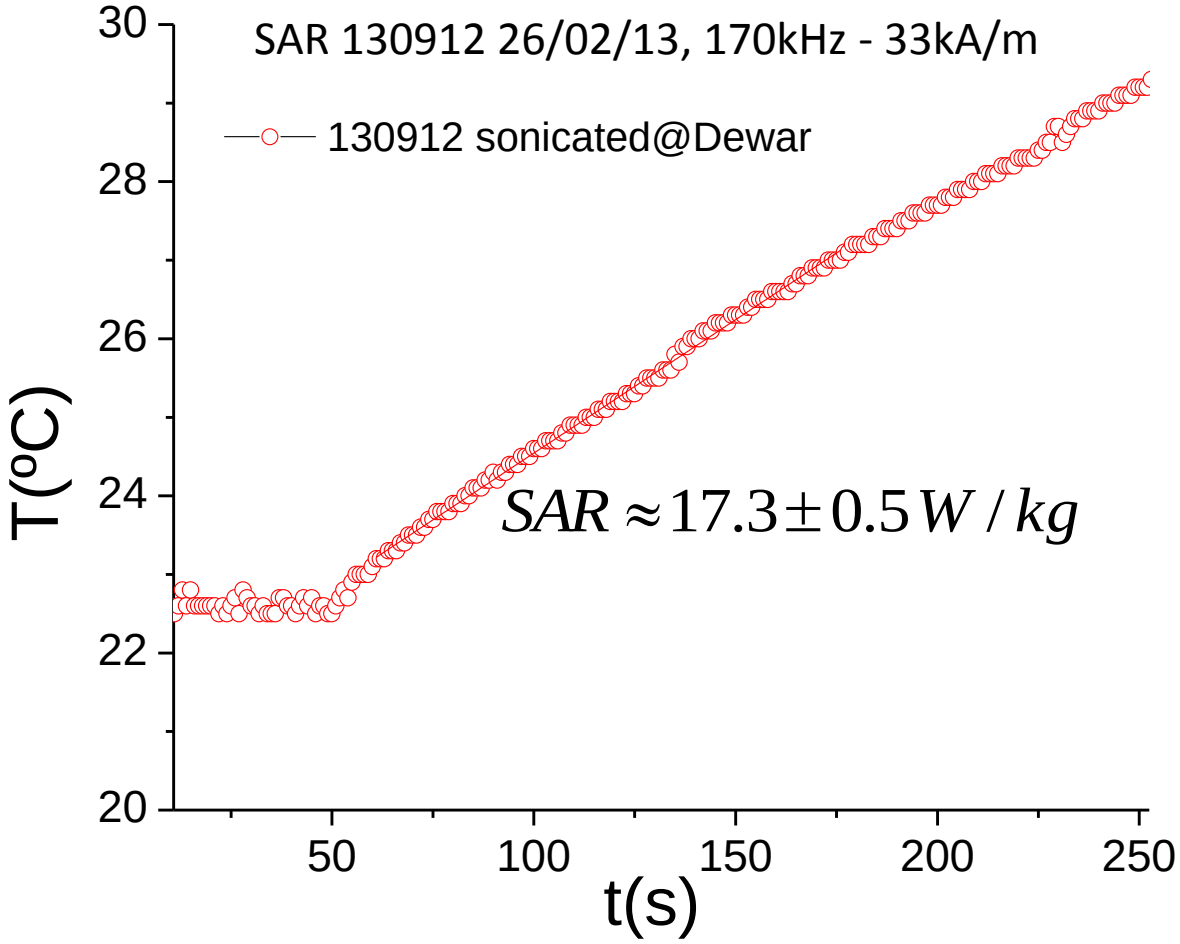
SAR 130912 26/02/13, 170kHz - 33kA/m
130912 sonicated@Dewar
$SAR \approx 17.3 \pm 0.5\, W/kg$
T(ºC)
t(s)
30
28
26
24
22
20
50
100
150
200
250

SAR 130912 (170kHz , 33 kA/m), 15 – 17 W/g

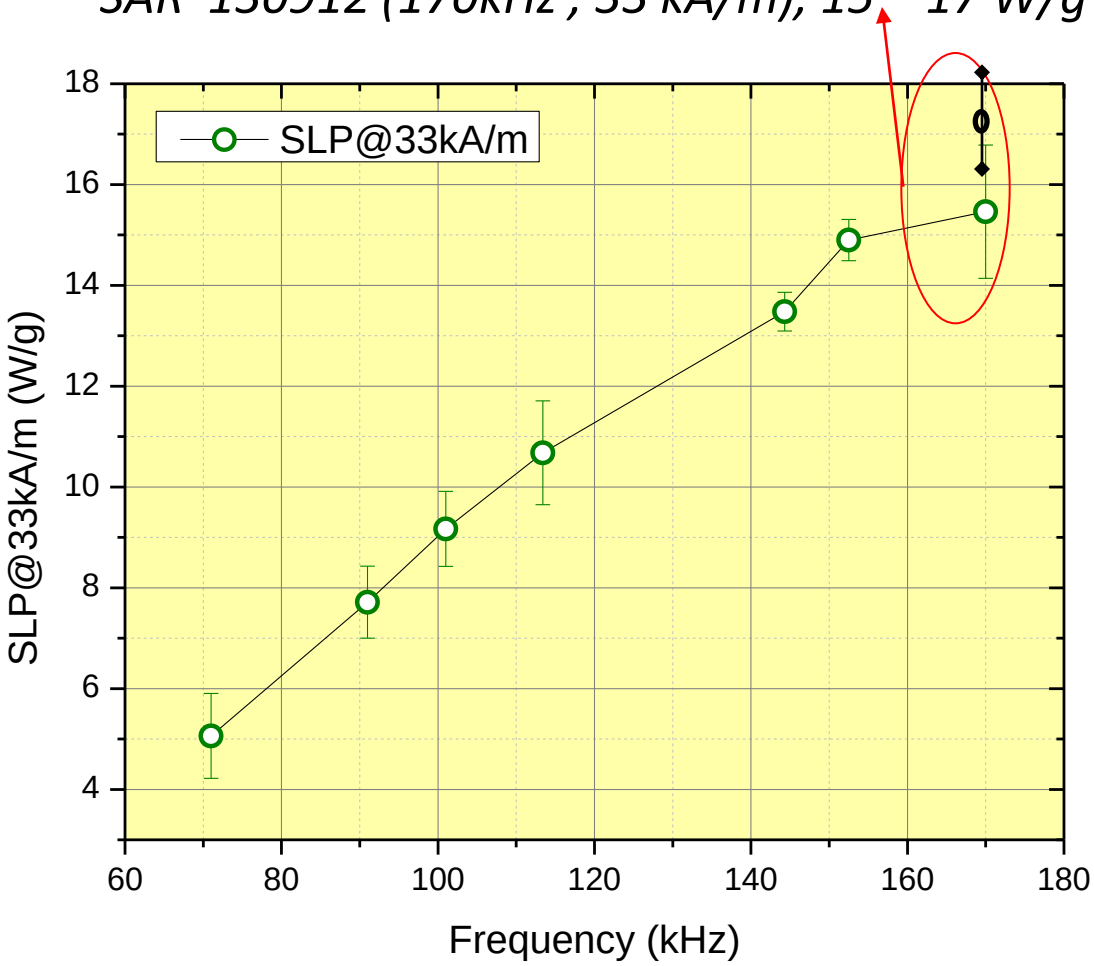

Sample	[X](mg/ml)	Suspension pH	Z Potencial	MS (emu/g)	SAR(W/g) F= 170kHz H=33kA/m
130912pt	8.3	7.44	-13.1mV	27.9	15-17 W/g

Cellular Thermometer for hyperthermia

Lentivectors encoding GFP under the human HSP70b promoter

HSP: Same cell line A549 infected with a lentiviral vector containing an inducible promotor (under stress) named HSP60B. It leads to the expression of GFP.

CMV: Same cell line A549 infected with a lentiviral vector containing a constitutive promotor named CMV. Always expreses GFP.

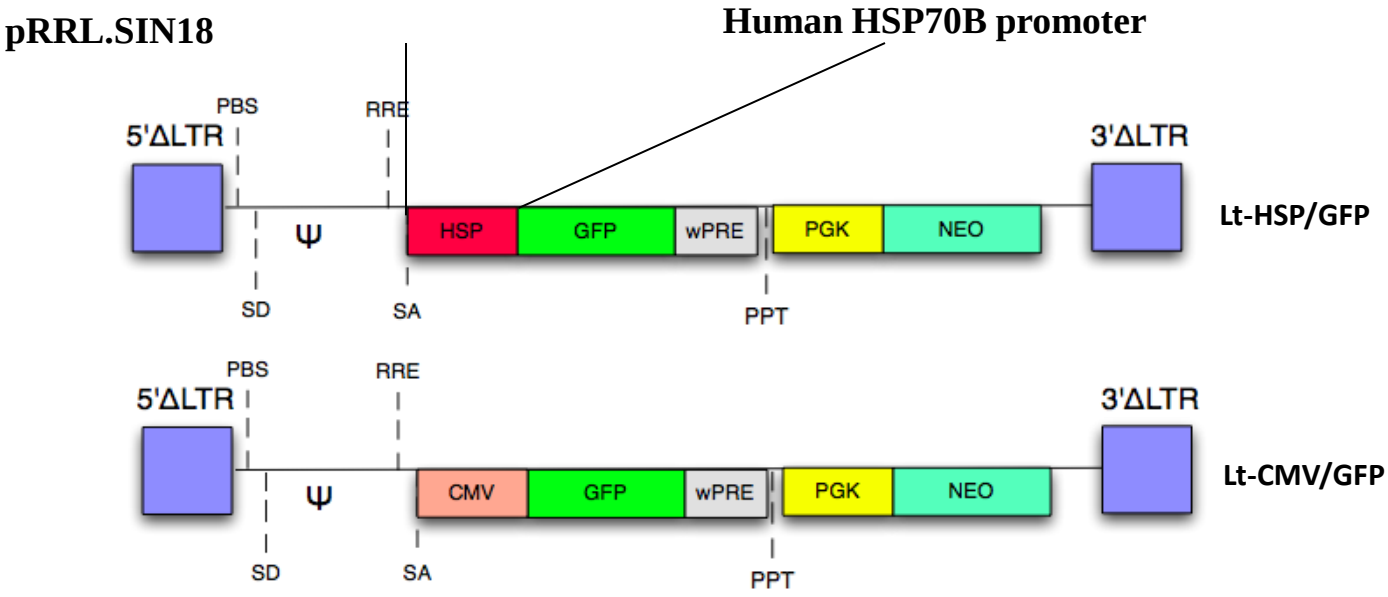

In vitro Inducibility properties of HSP70b promoter by hyperthermia

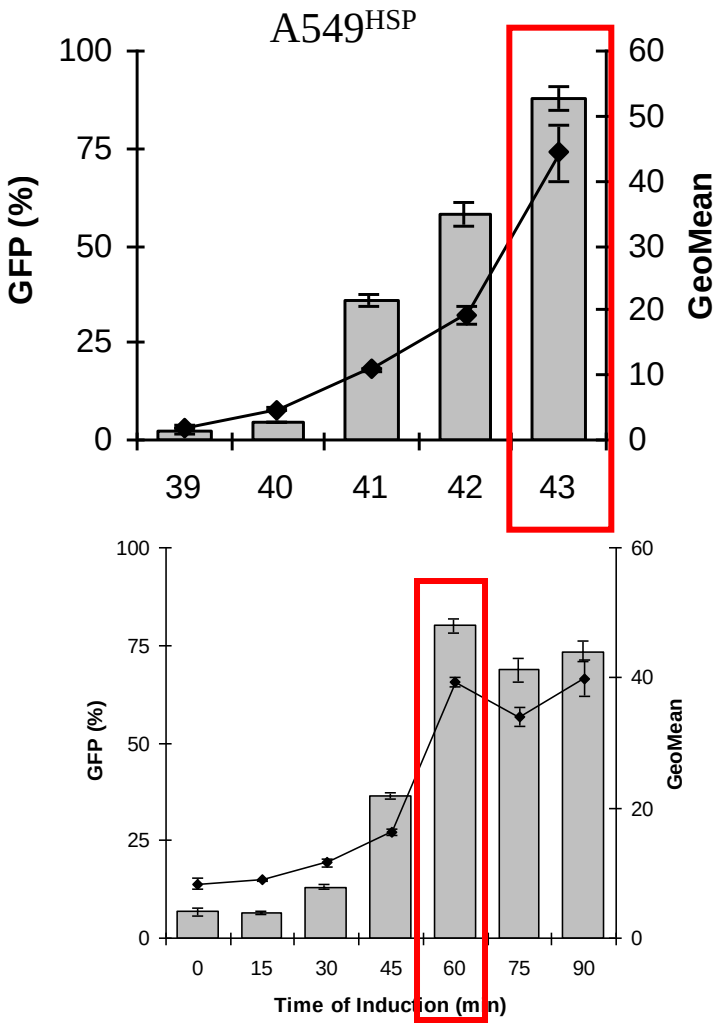

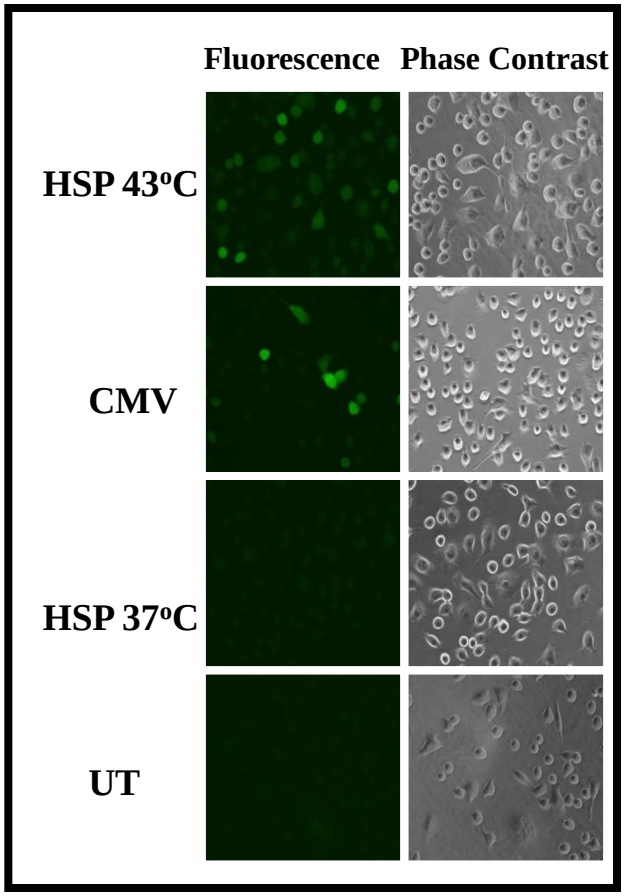

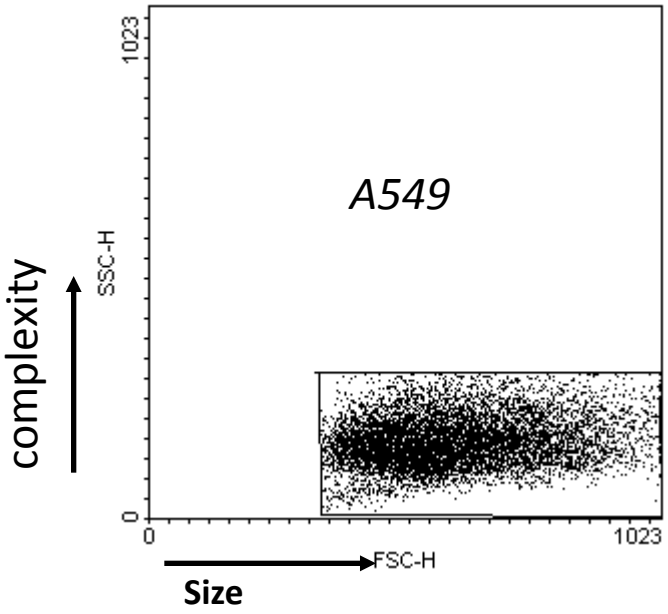
A549
complexity
SSC-H
1023
0
0
1023
FSC-H
Size

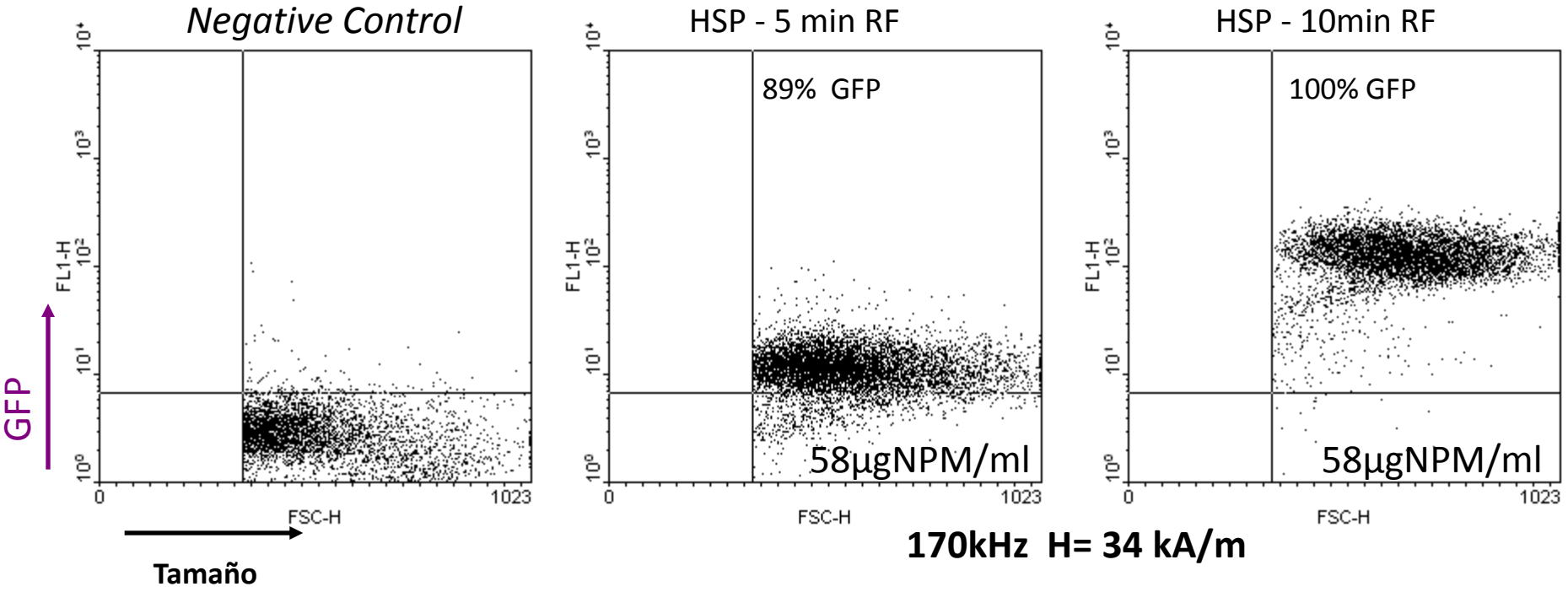
Negative Control
HSP - 5 min RF
HSP - 10min RF
89% GFP
100% GFP
58µgNPM/ml
58µgNPM/ml
GFP
FL1-H
FSC-H
Tamaño
170kHz H= 34 kA/m

HSP(58µgNPM/ml)
y 60 min de RF

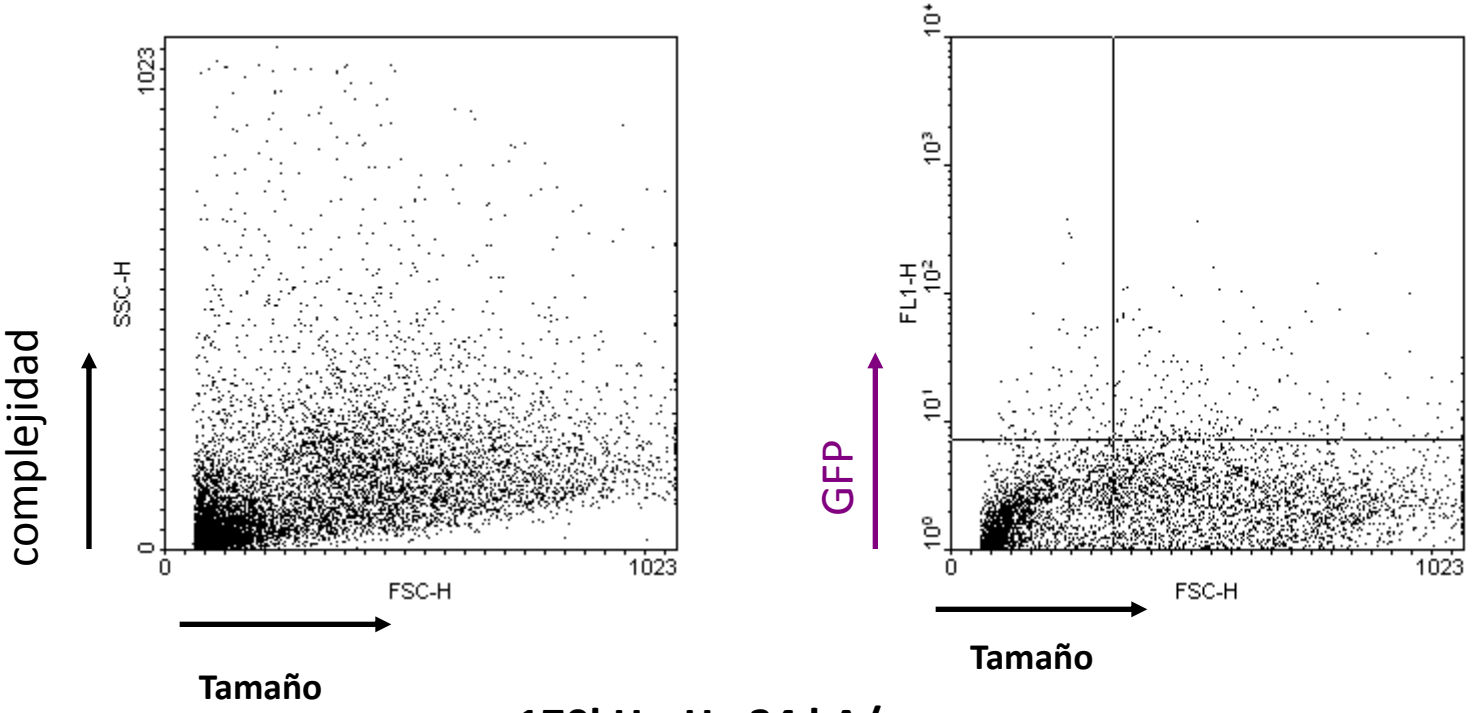

170kHz H= 34 kA/m

Se observa que la expresión de GFP bajo mucho ya que, como se ve en el grafico de la izquierda, estas células están muy dañadas y al lisarse la membrana se pierde la GFP.

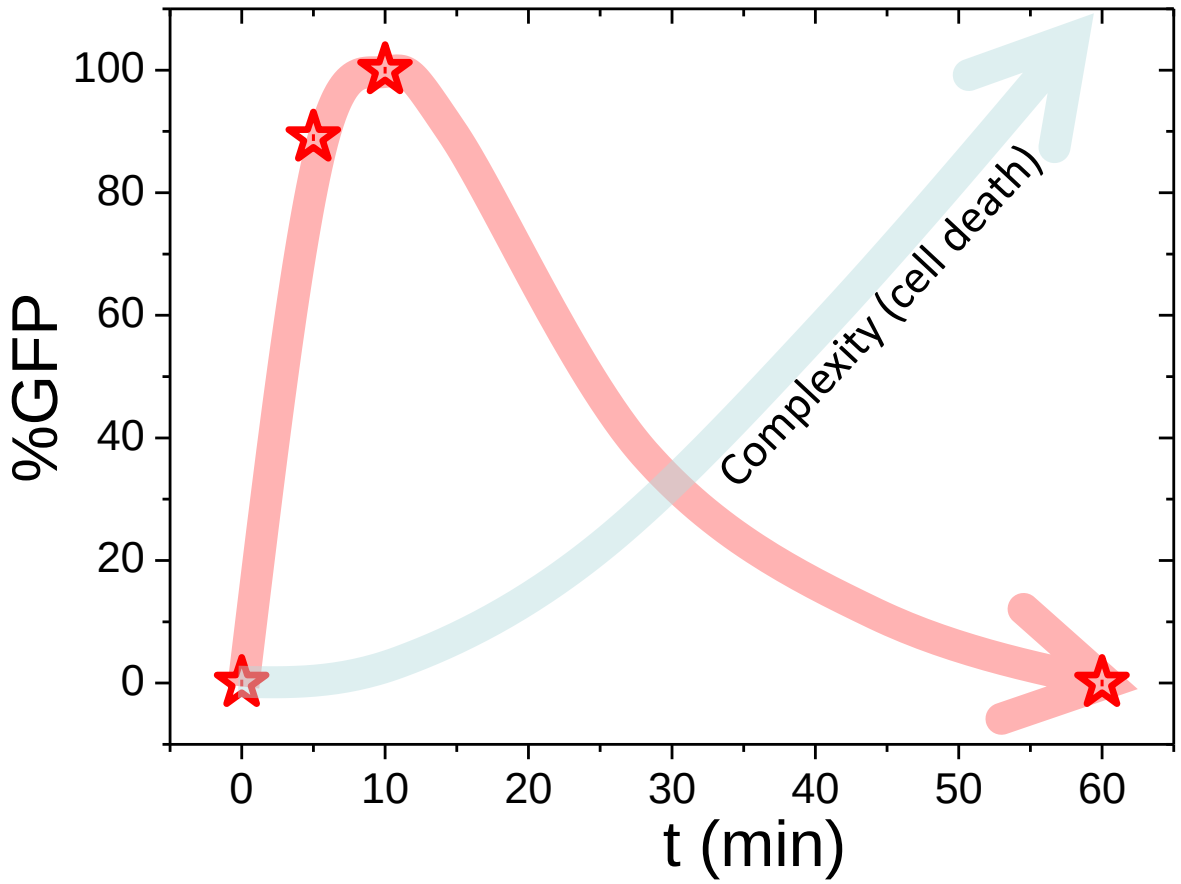
%GFP
100
80
60
40
20
0
0
10
20
30
40
50
60
t (min)
Complexity (cell death)

Class 2b

In Vitro Magnetofection: Magnetic Force Influence

Ferrogels PVA/Fe oxide

In Vitro Magnetofection: Magnetic Force Influence

Arciniegas L, Pardo J, Pasquevich GA, Goya RG,
Mykhaylik O, Sánchez FH

Magnetofection is a simple and highly efficient transfection method that uses magnetic fields to concentrate particles containing nucleic acid into target cells

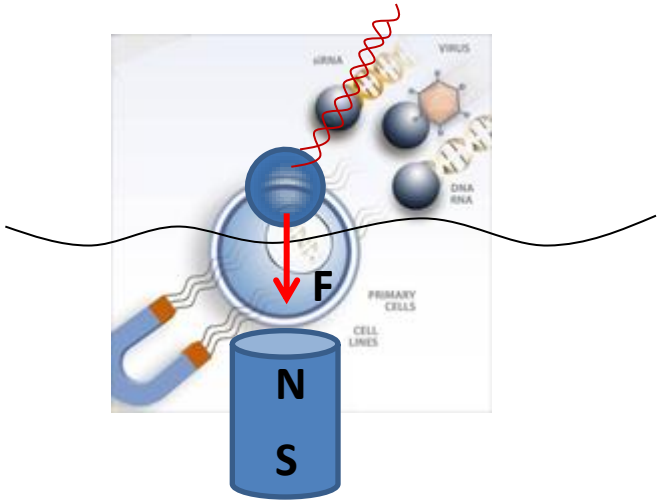

PEI-Mag2 Nanoparticles

Fe(II) + Fe(III) salts solution
oxygen-free atmosphere

precipitation of Fe(II)/Fe(III) hydroxide

fluorinated surfactant ZONYL FSA (lithium 3-[2-(perfluoroalkyl)ethylthio]propionate) + 25-kDa branched polyethylenimine (PEI-25Br)

PEI-Mag2 NPs

Dialyzed against ddH2O

+

sterilized using ^{60}Co gamma irradiation at 25 kGy

Olga Mykhaylyk, TUM, Munich

PEI-Mag2 RAd-GFP Complex

RAd-GFP

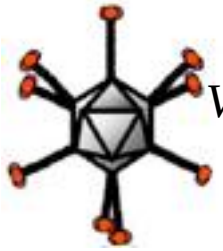

Virus (PVP, thickness $D_V \sim 80$ nm)

Rad-GFP: Adenovector which expresses GFP gen (Aequorea victoria) under citomegalovirus murino (mCMV) promotor control.

PEI-Mag2

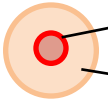

Magnetic core (thickness $D_m \sim 9$nm)

Polimeric coating (thickness $t_{pol} \sim 35$ nm)

PEI-Mag2 NPs

PEI-Mag2 RAd-GFP Complex

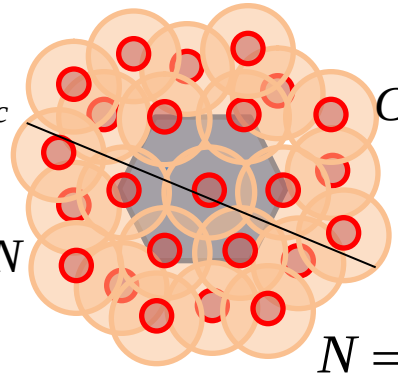

Complex PVP/NPs (volume V_c)

N NPs/ PVP

$N = 300 - 5000$

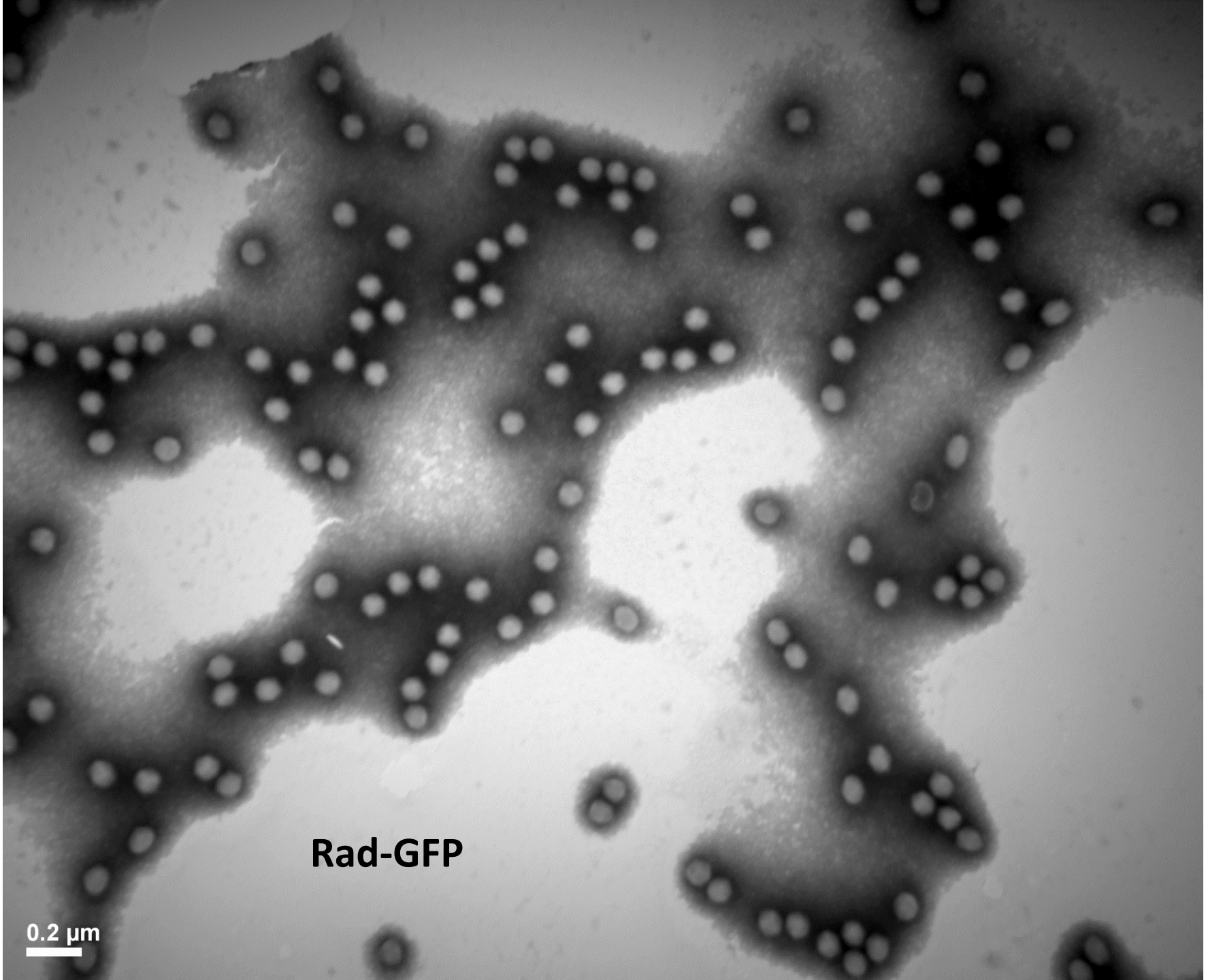
Rad-GFP
0.2 µm

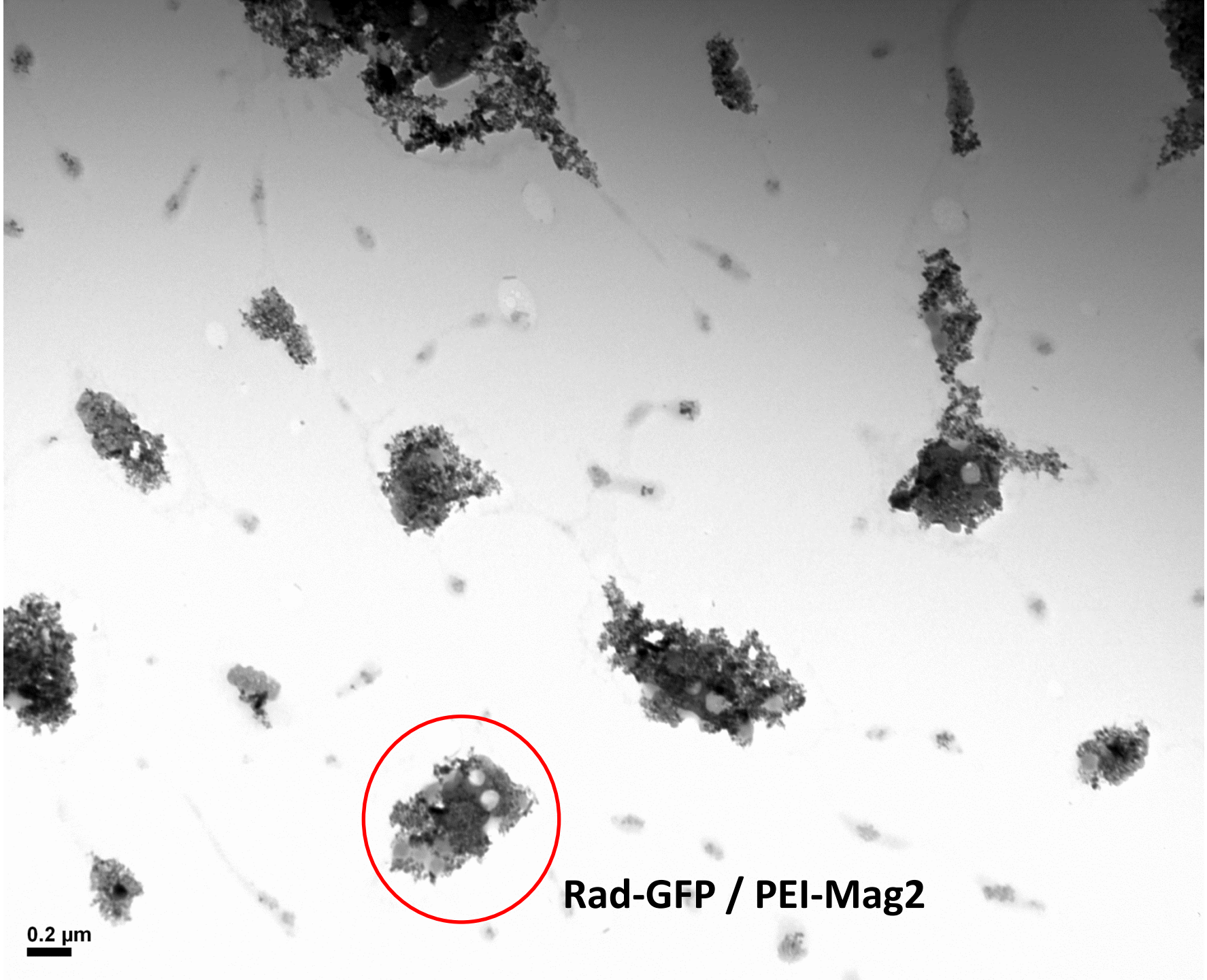
Rad-GFP / PEI-Mag2
0.2 µm

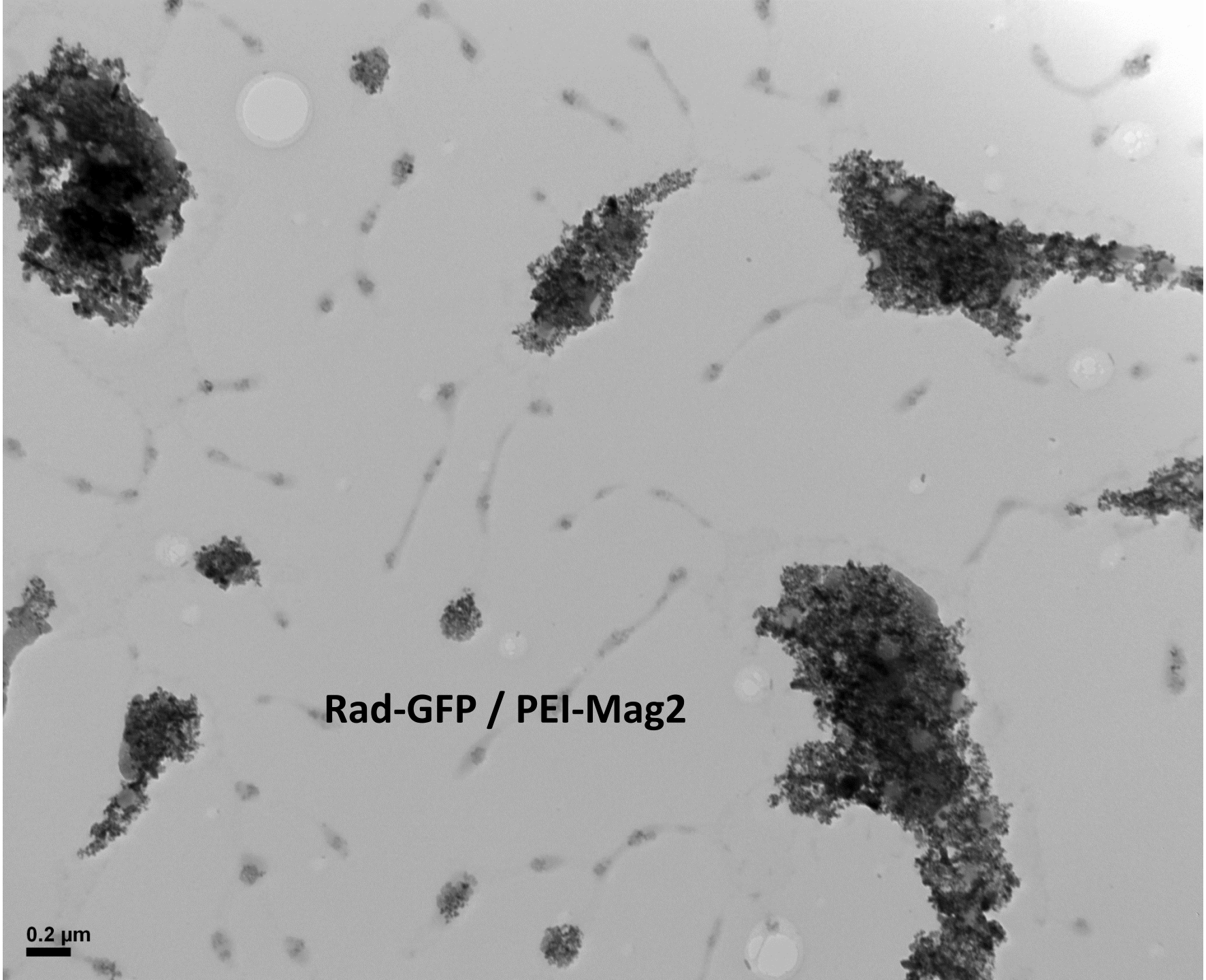
Rad-GFP / PEI-Mag2
0.2 µm

B92 cell culture conditions

B92 cells (mouse glial cell)
MEM (Minimum Essential Media),
10% FBS (Foetal Bovine Serum)
100 U de penicillin/ml
0,1 mg de streptomycin/ml
0,25 µg de anphotericin B/ml
5% CO_2 atmosphere
37 °C

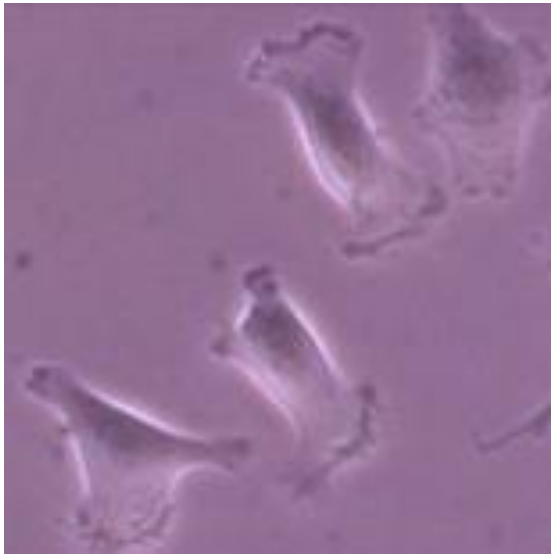

PEI-Mag2 RAd-GFP Complex / optimum ratio

Acta Bioquím Clín Latinoam 2013; 47 (2): 399-406

Joaquín Pardo[1a*], Yolanda Elena Sosa[2a*], Paula Cecilia Reggiani[3a],
Magda Lorena Arciniegas[4b], Francisco Homero Sánchez[5b], Rodolfo Gustavo Goya[6a]

Selected Ratio 0.5

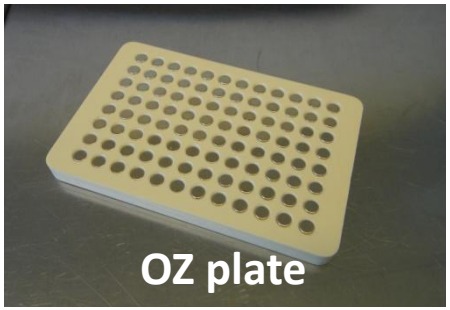

RELATIONSHIPS DETERMINATION

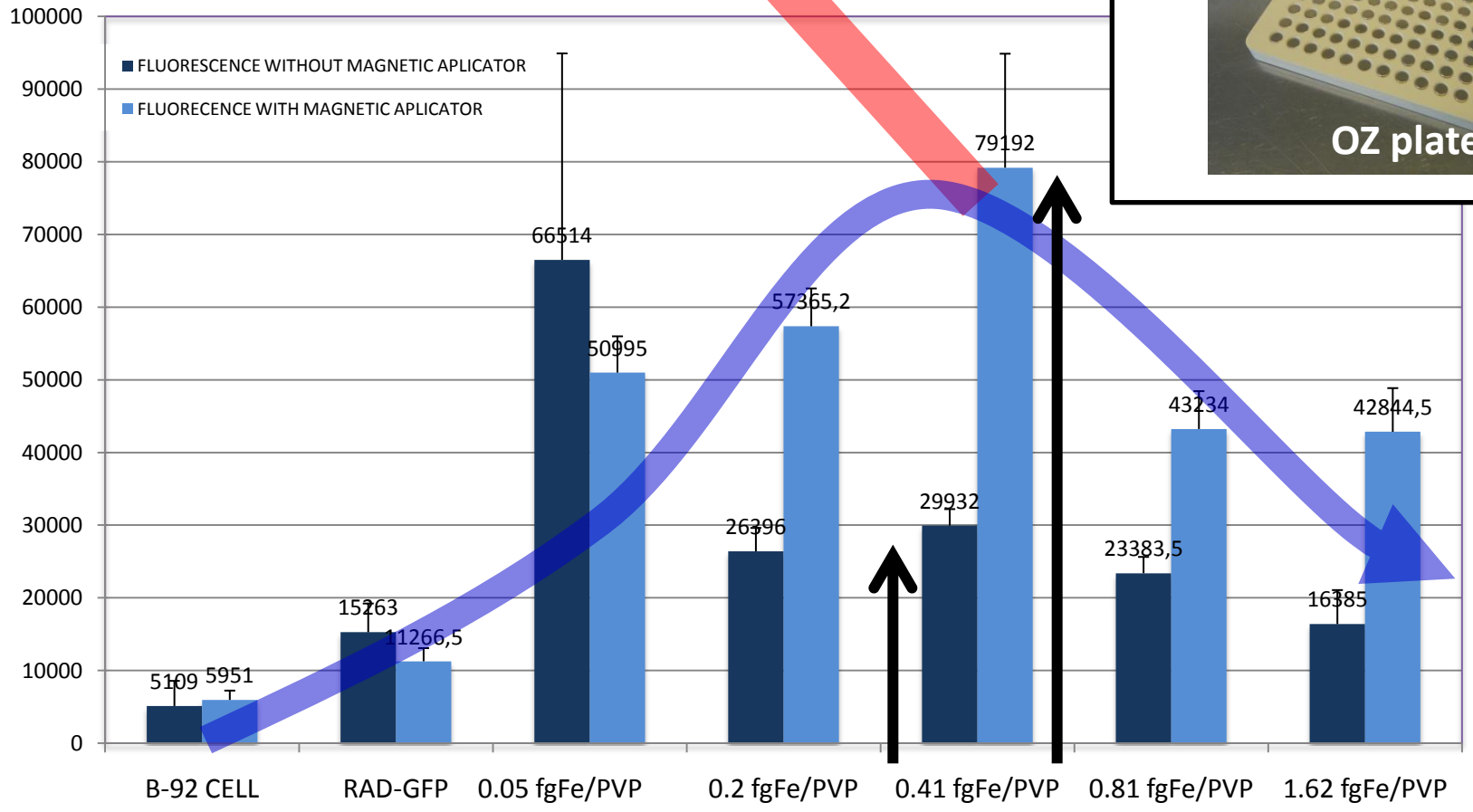

One word on magnetic applicators

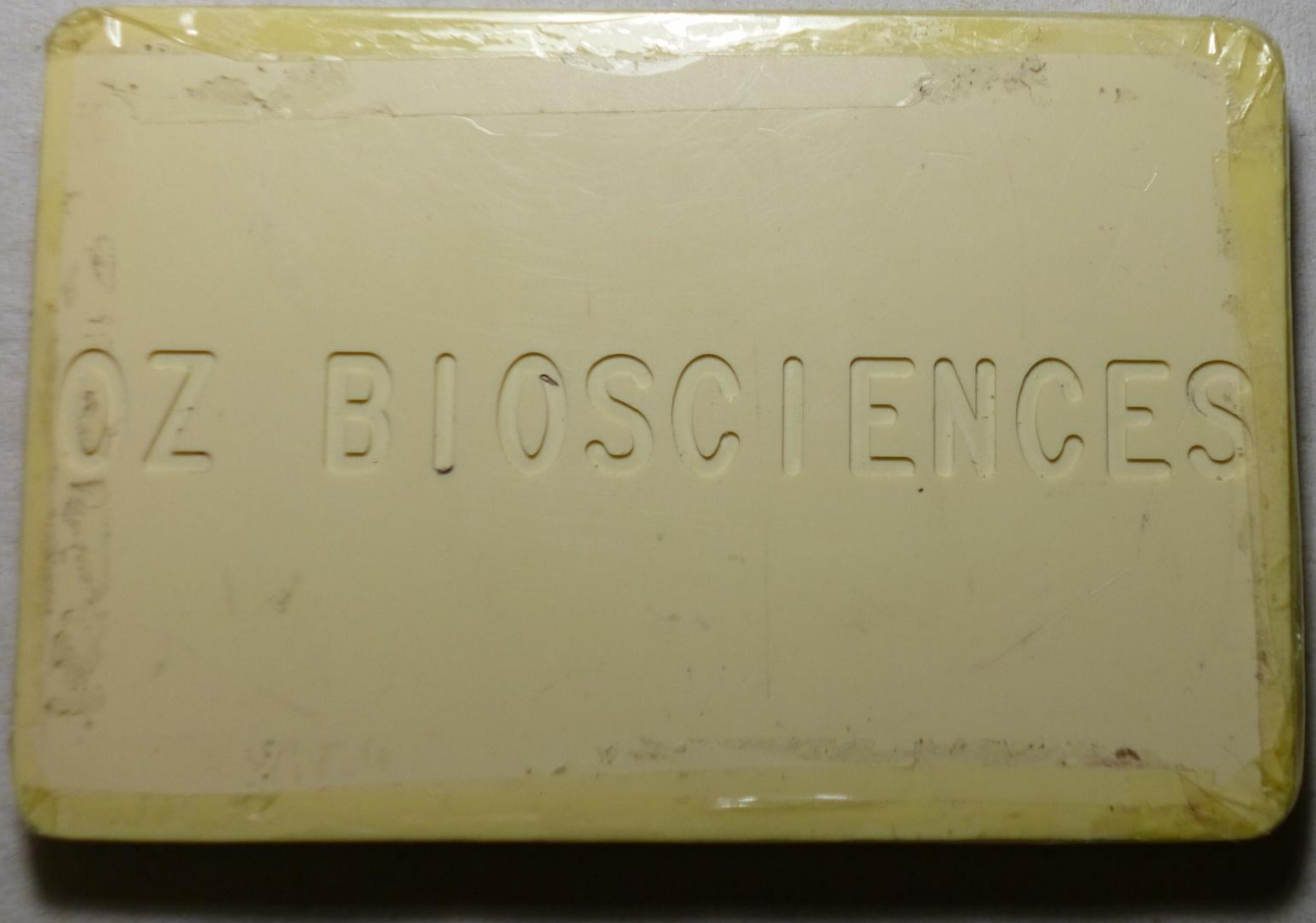

One word on magnetic applicators

One word on magnetic applicators

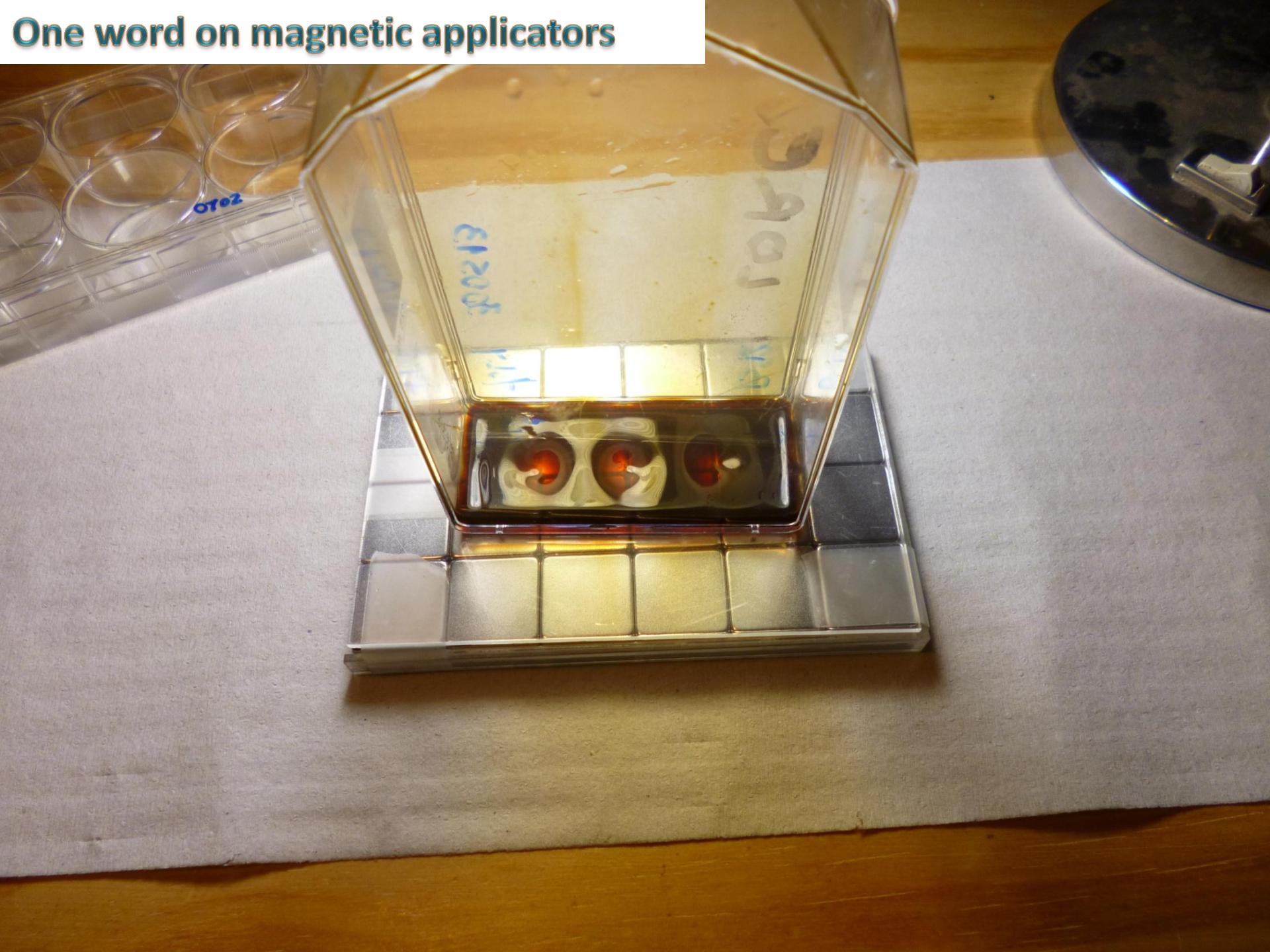

One word on magnetic applicators

One word on magnetic applicators

One word on magnetic applicators

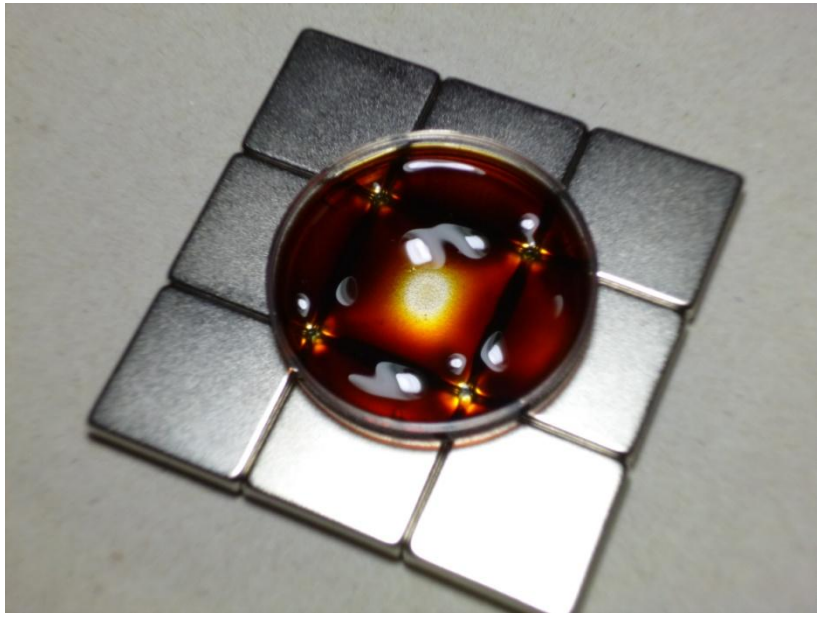

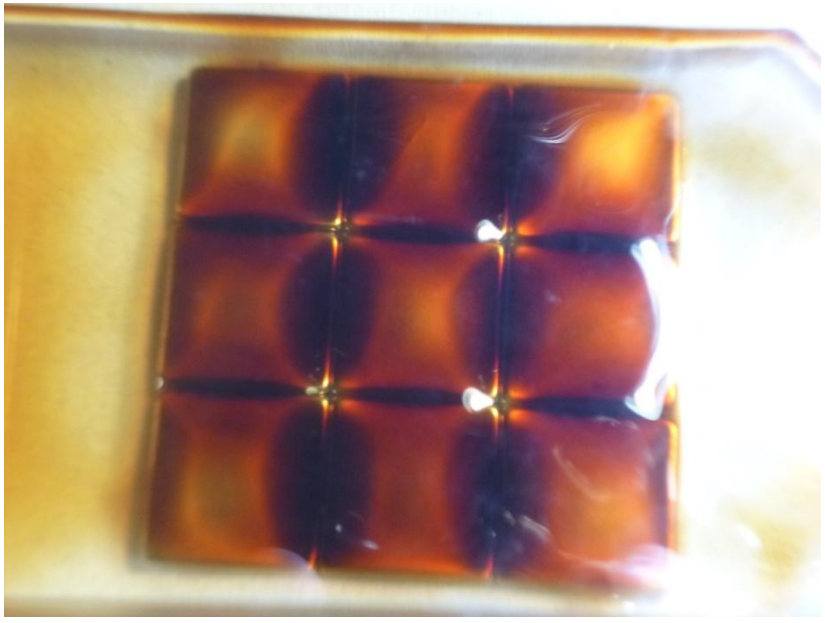

One word on magnetic applicators

PEI-Mag2 RAd-GFP Complex / magnetic response

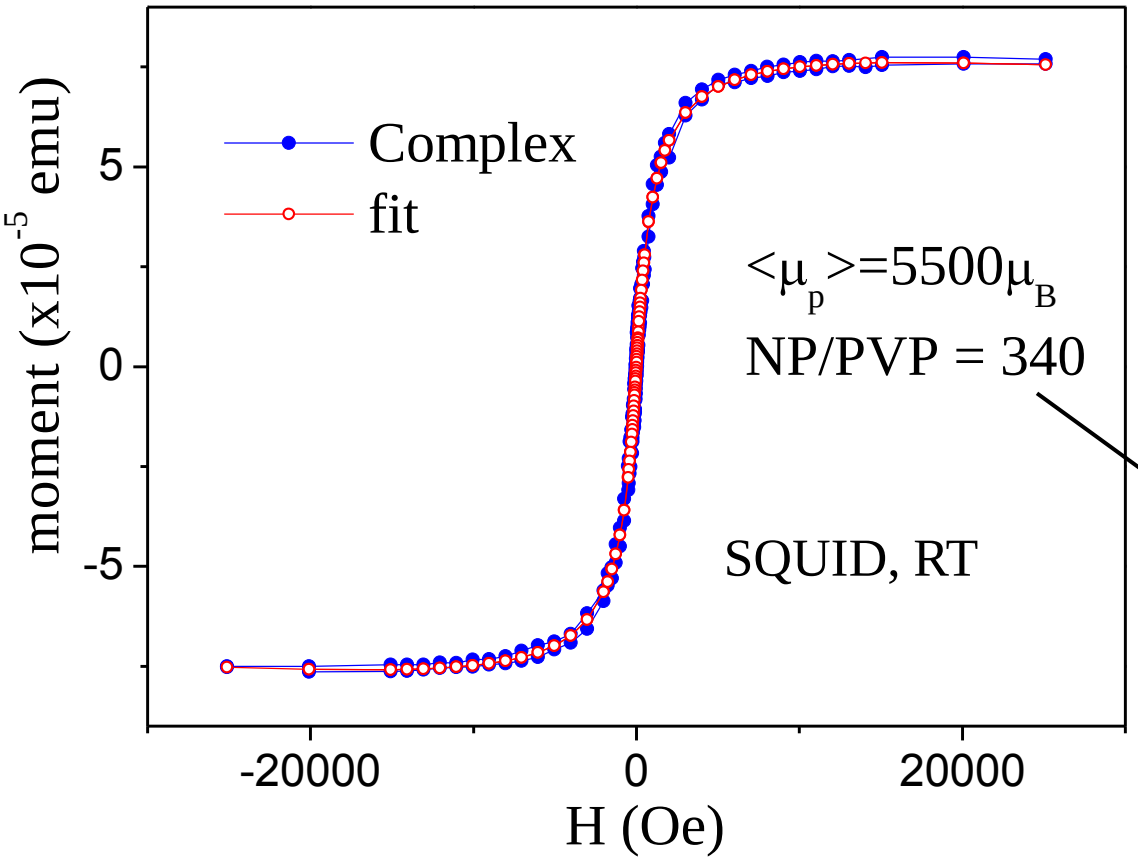

Consistent with selected 0.5 Ratio

Magnetofection experimental design

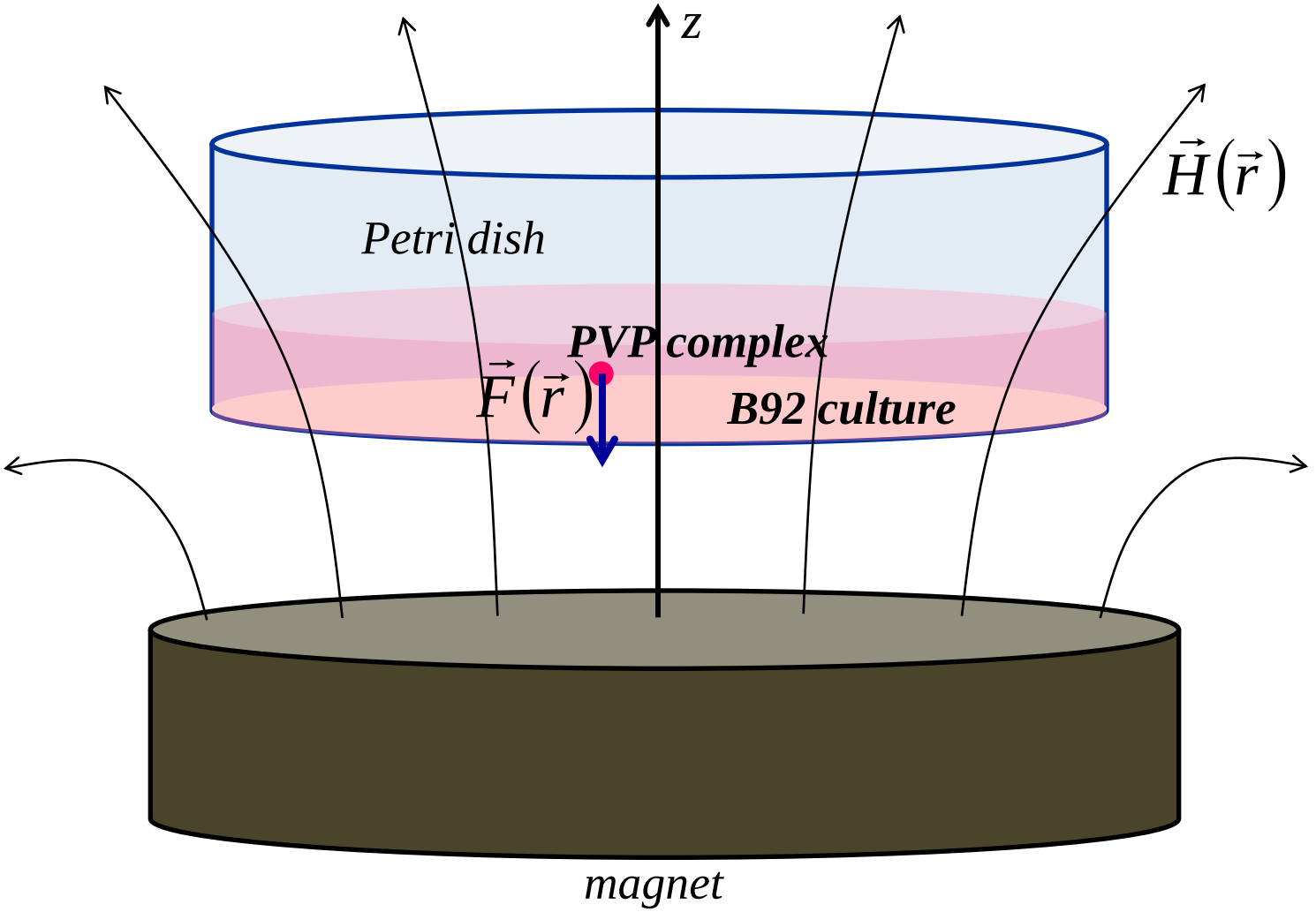

Magnetofection experimental design

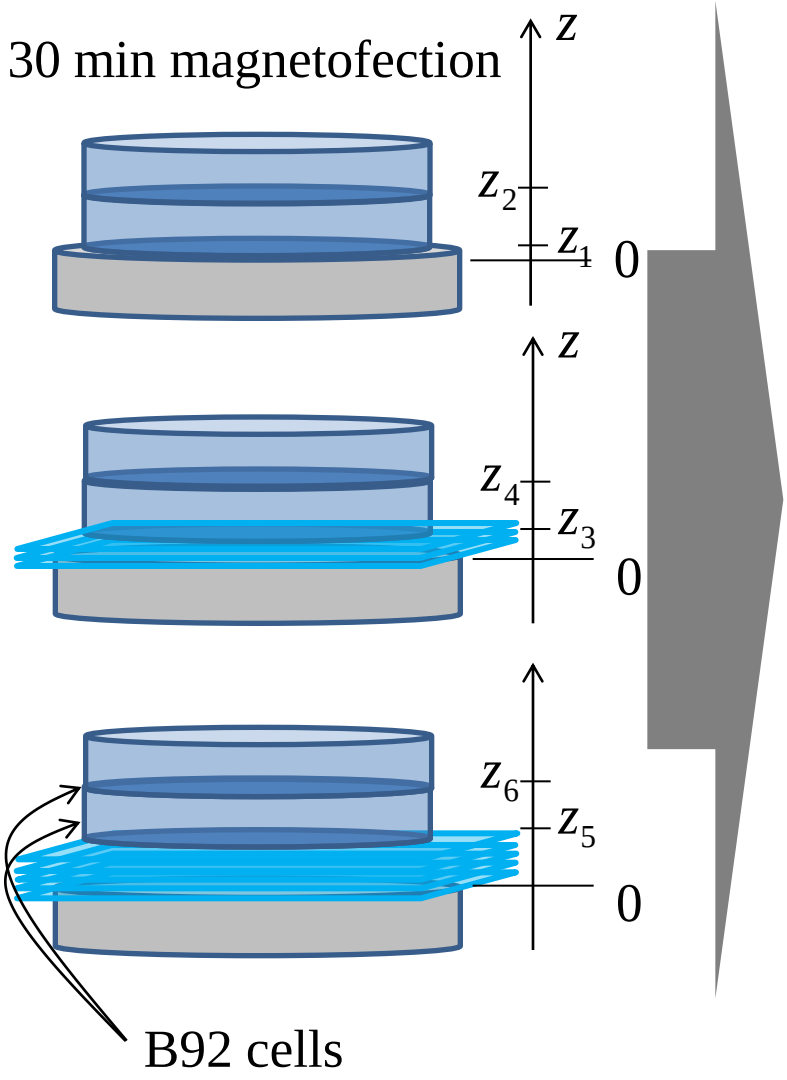

washing

72 h with MEM + FBS

Magnetofection fluorescence vs *z*

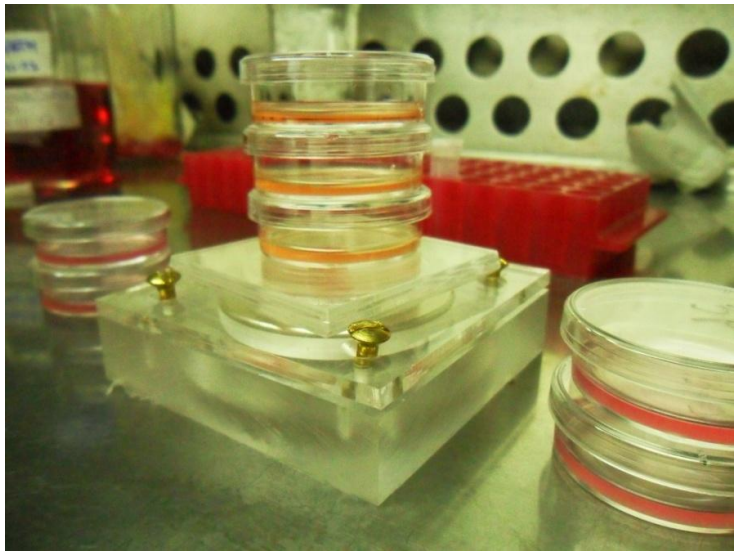

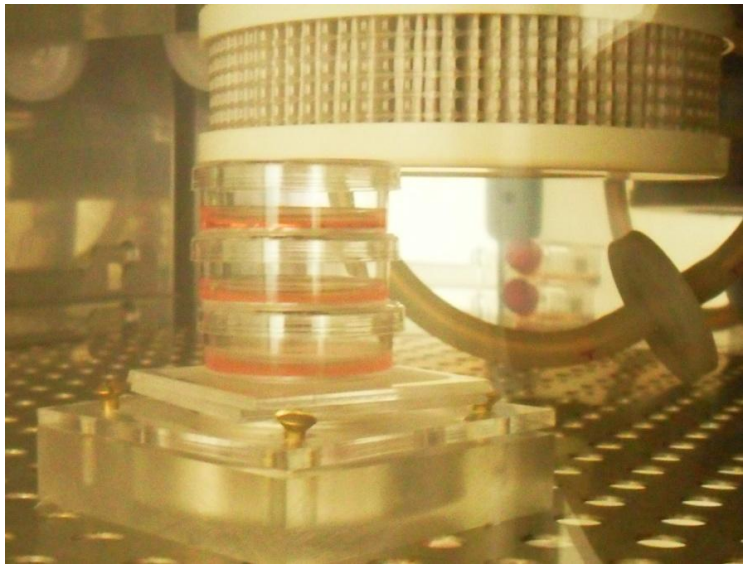

Magnetofection results – phase and fluorescence obs

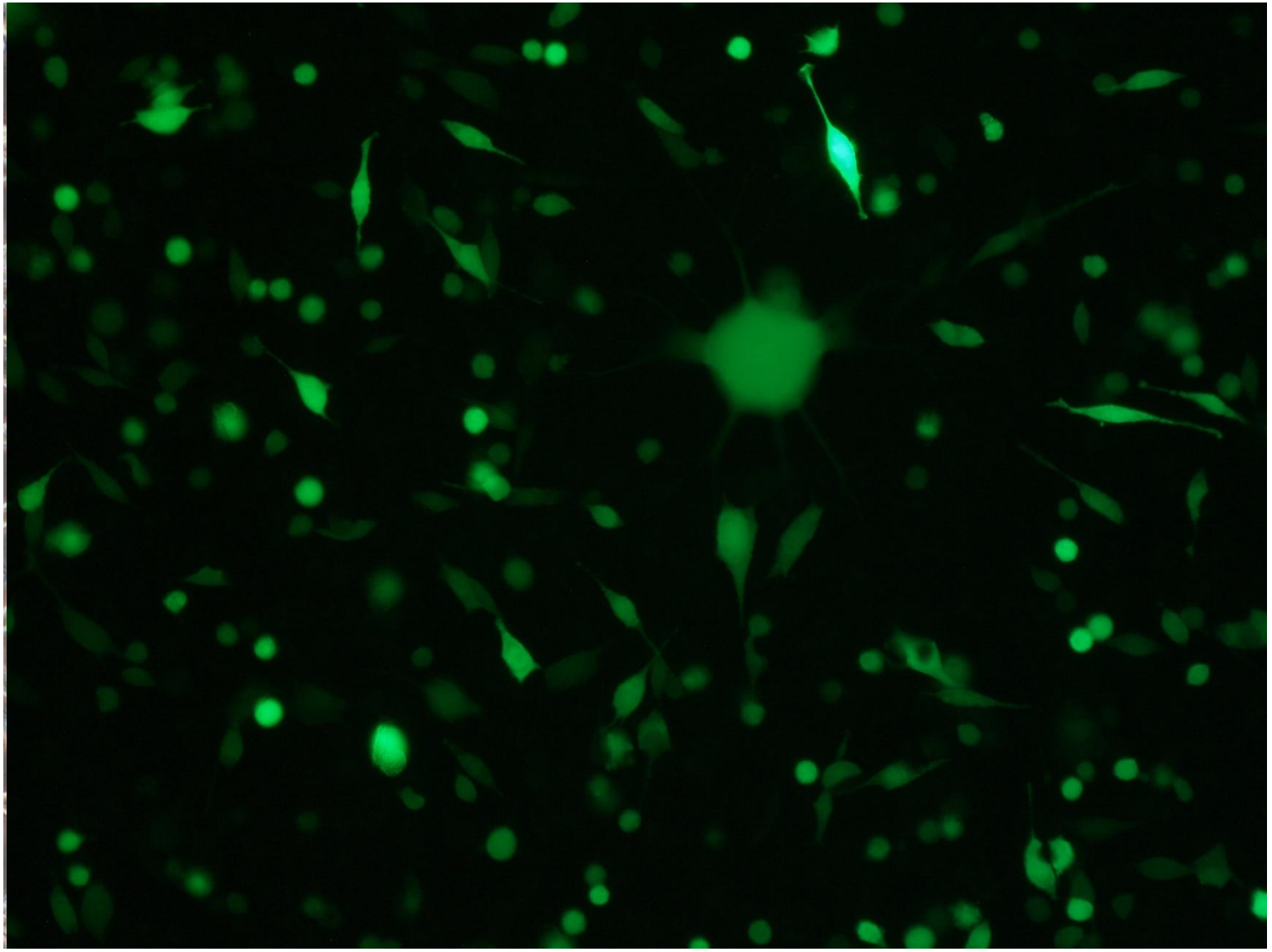

Magnetofection results – phase and fluorescence obs

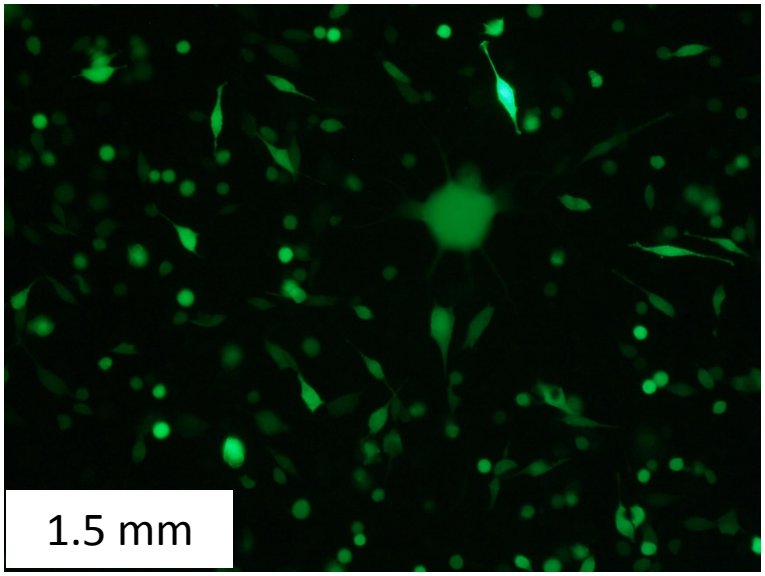

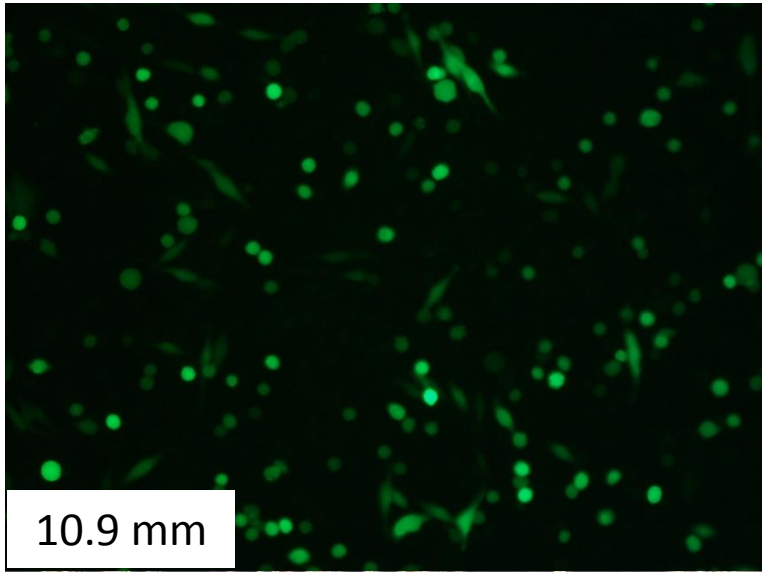

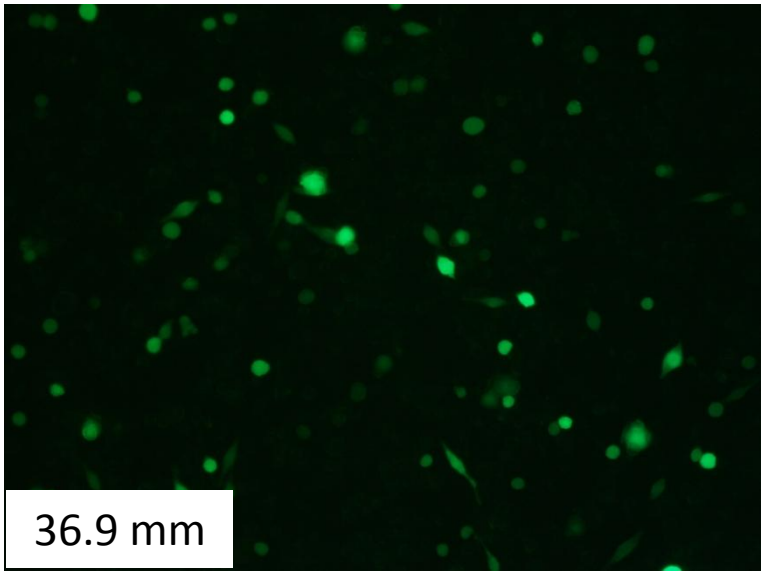

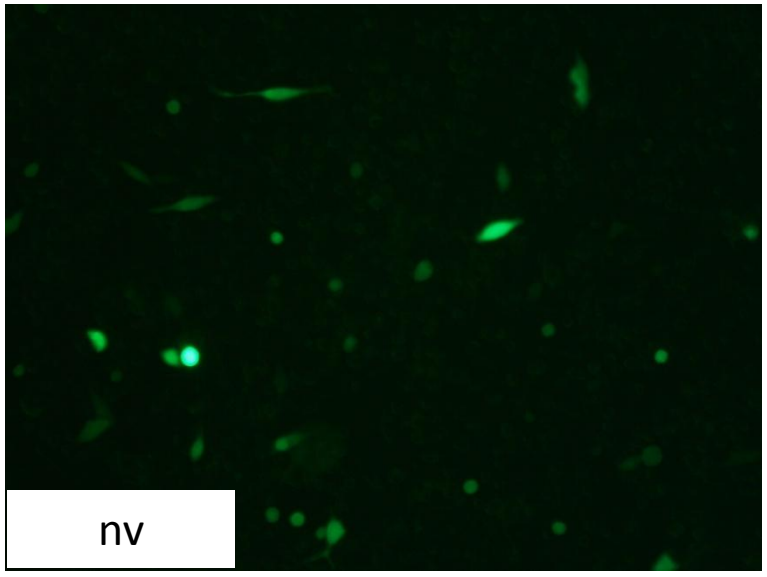

Magnetofection results – Elisa spectrometer

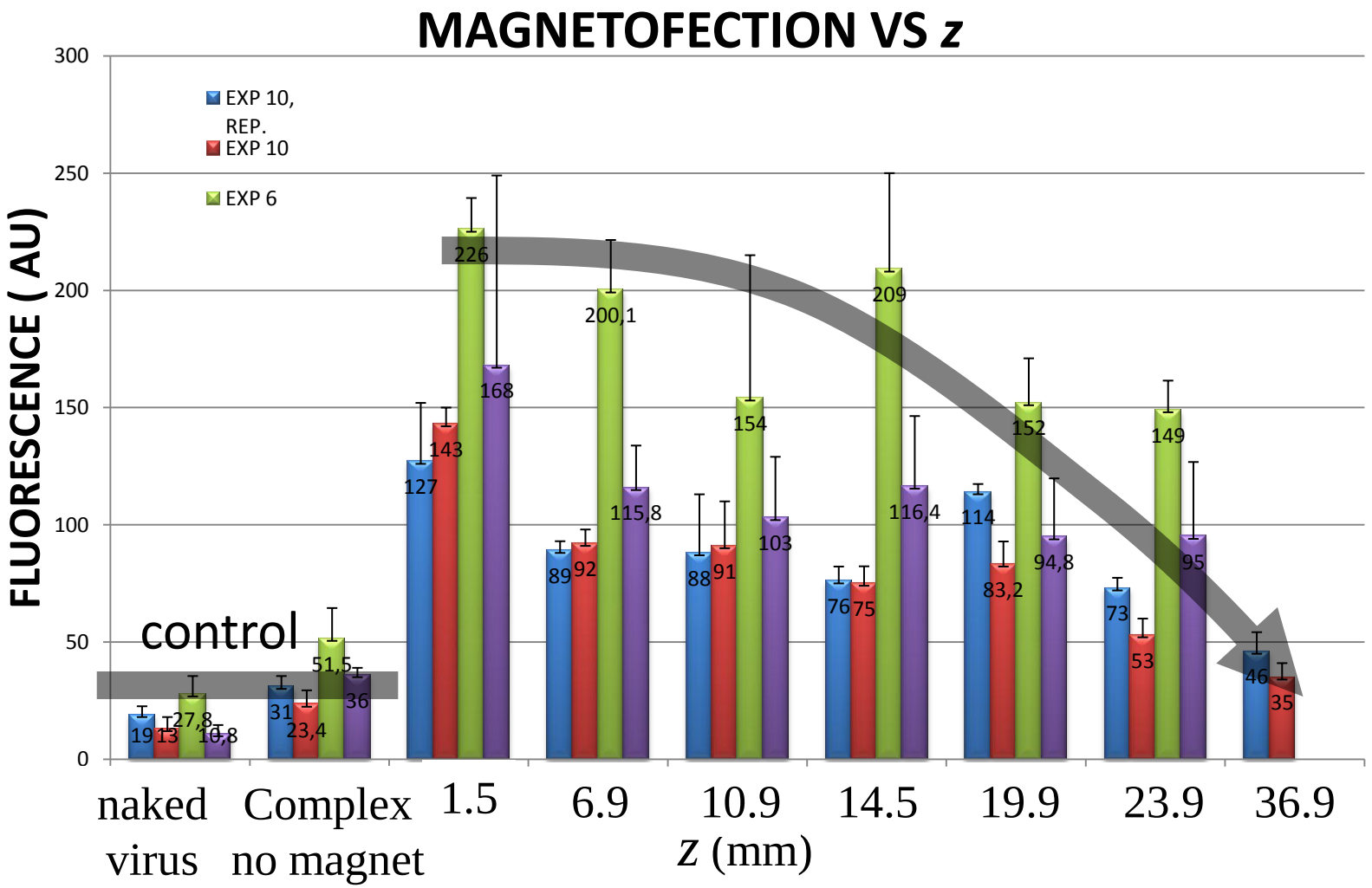

Magnetic Force analysis

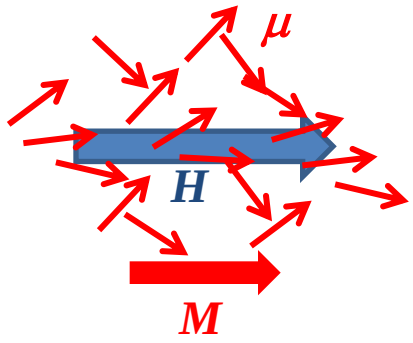

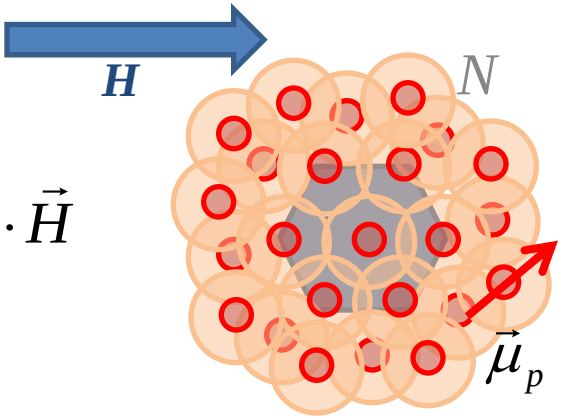

$$U_{\vec{B}} = -\sum \vec{\mu}_{pi} \cdot \vec{B} = -N\mu_0 \left\langle \vec{\mu}_p \right\rangle \cdot \vec{H}$$

$$\left\langle \vec{\mu}_p \right\rangle = V_p \vec{M}\left(\vec{H}\right) // \vec{H}$$

$$\vec{F} = -\vec{\nabla} U_{\vec{B}} = N\mu_0 V_p \vec{\nabla}\left(MH\right)$$

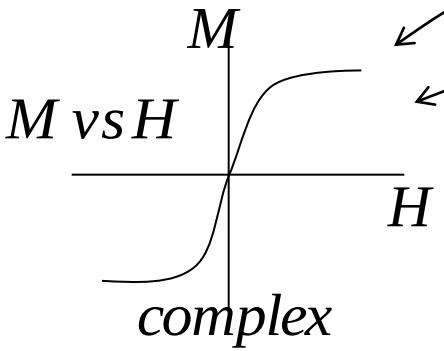

$$\boxed{\vec{F} = \mu_0 N V_p \left(H \frac{dM}{dH} + M(H) \right) \vec{\nabla} H}$$

magnets

H vs position

exp. data

Magnetic Force analysis, experimental

H(z) measurement

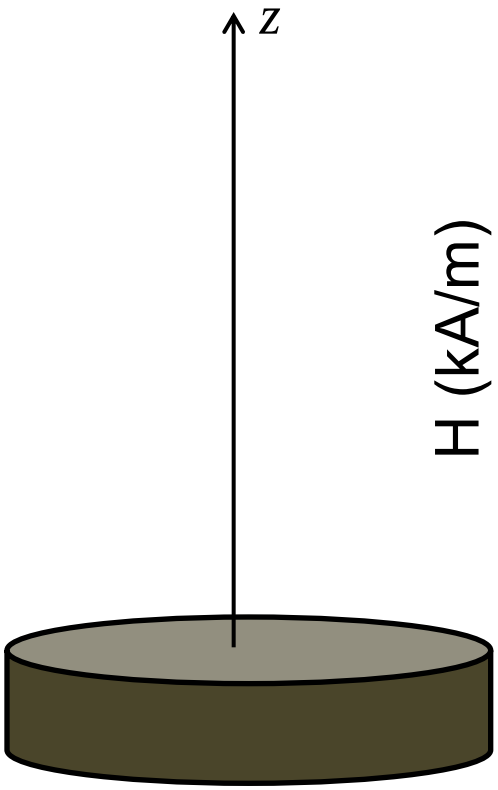

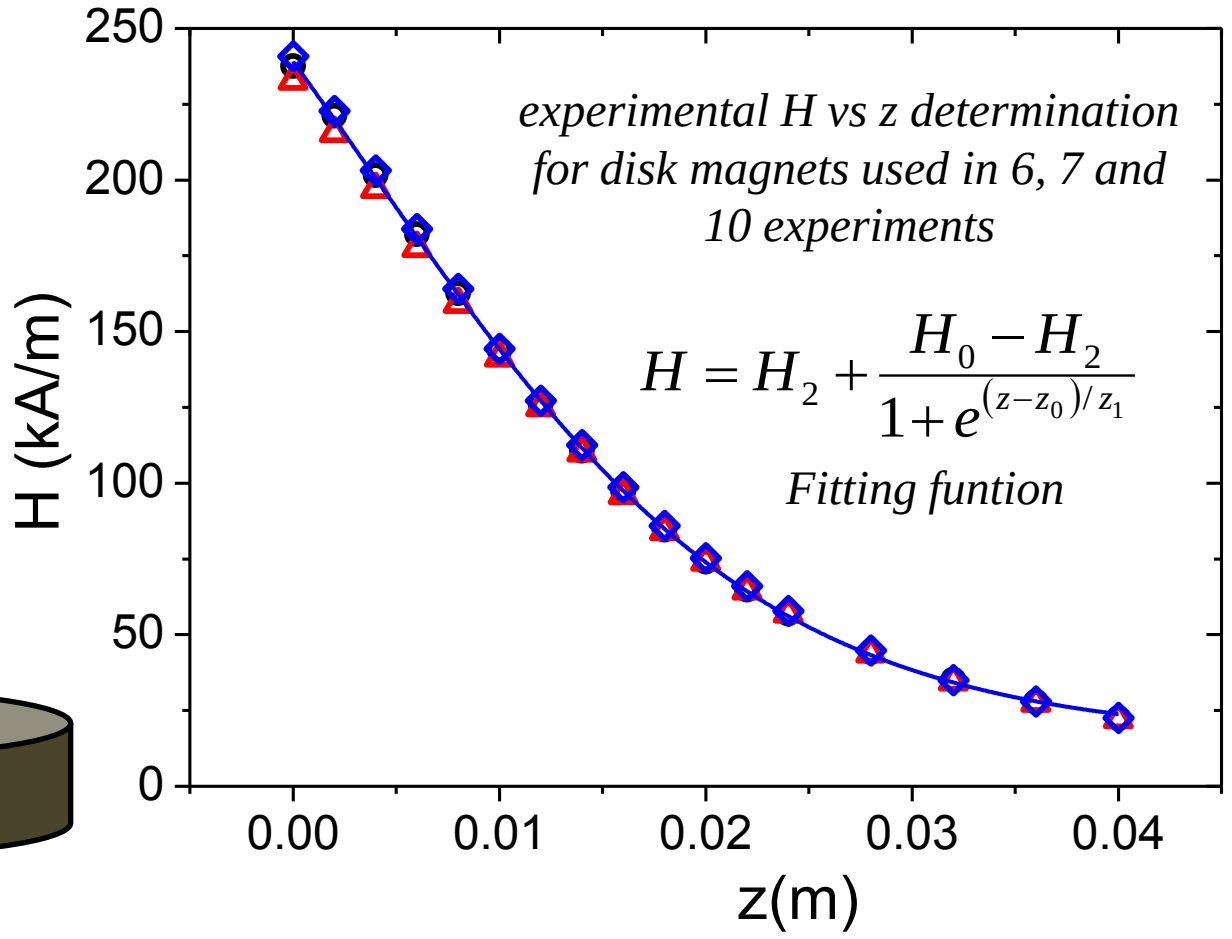

From M vs H

$\mu_p \approx 5500\ \mu_B$

$N \approx 350\ NP / PVP$

Magnetic Force analysis, experimental

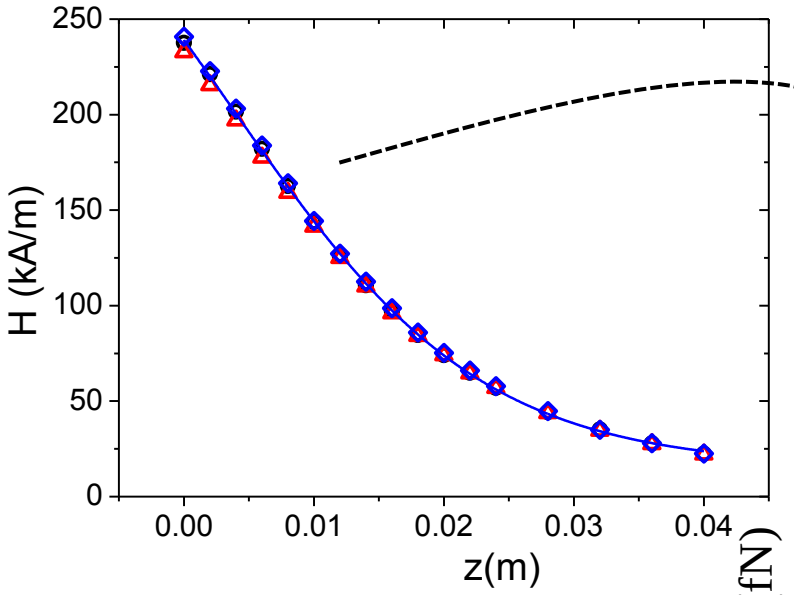

$H, \frac{dH}{dz}$

Max at ~4 mm

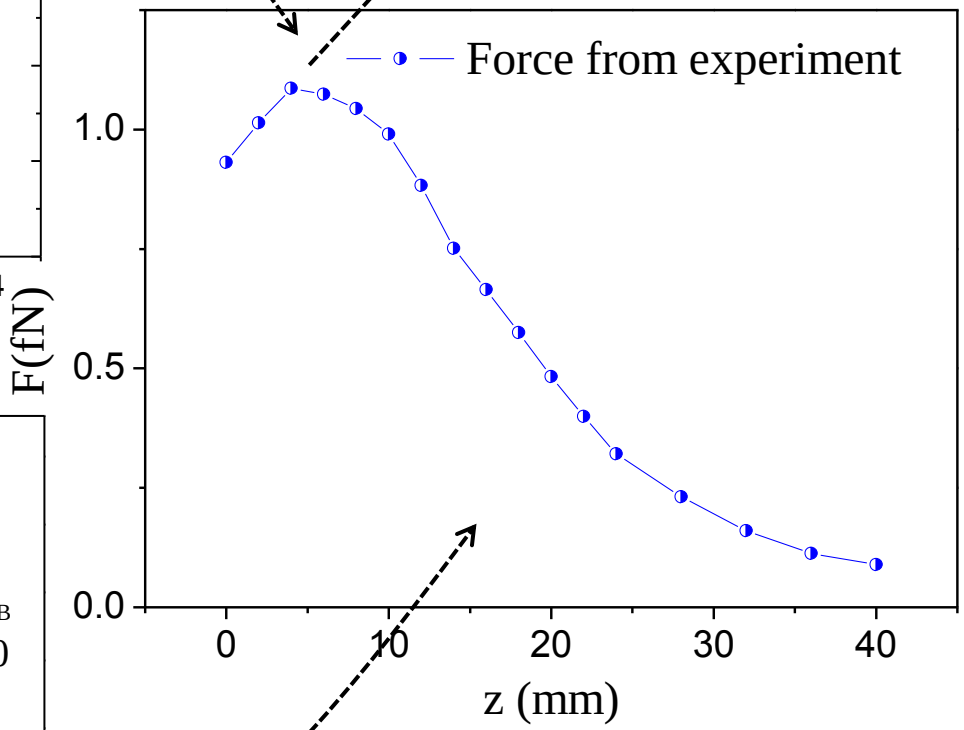

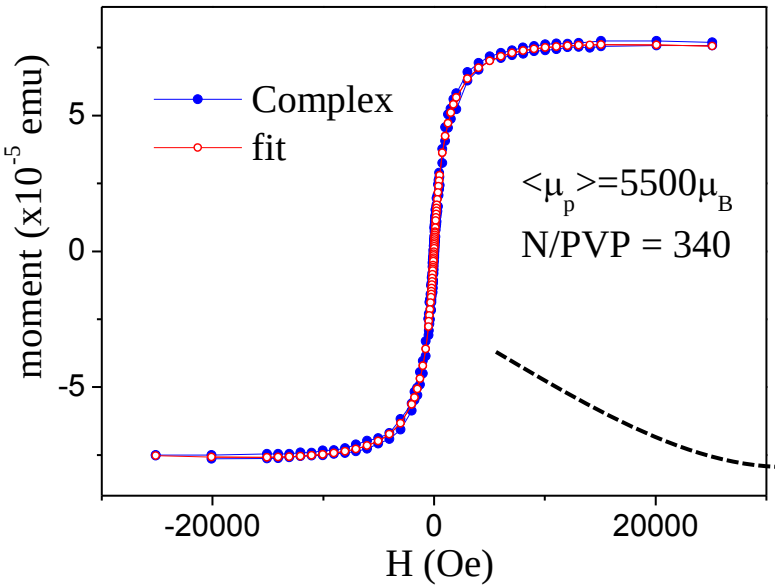

$M, \frac{dM}{dH}$

Magnetic Force analysis, what does it do?

It changes state of motion of complexes $v(z,t)$

It changes distribution of complexes in the fluid $c(z,t)$

Constant Force approximation: force variation within each PD can be neglected

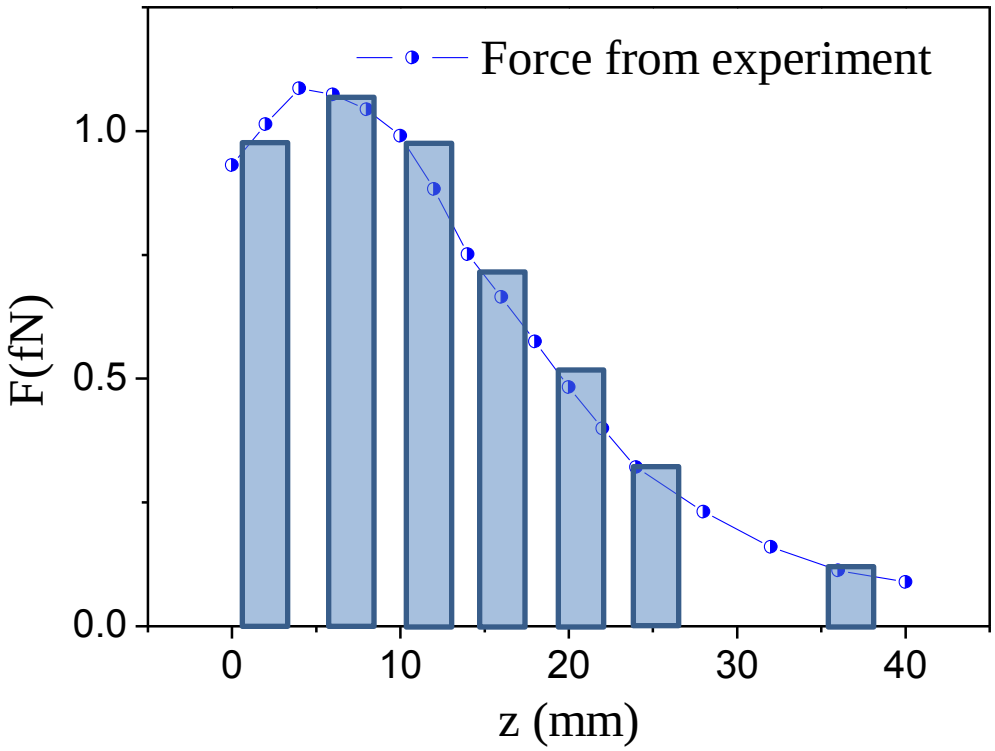

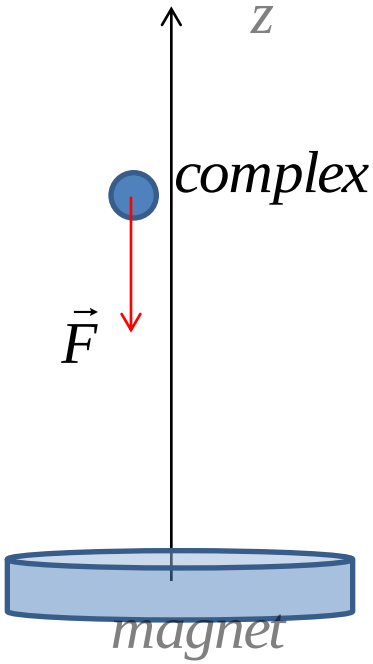

Magnetic Force analysis, dynamics

Complex dynamics

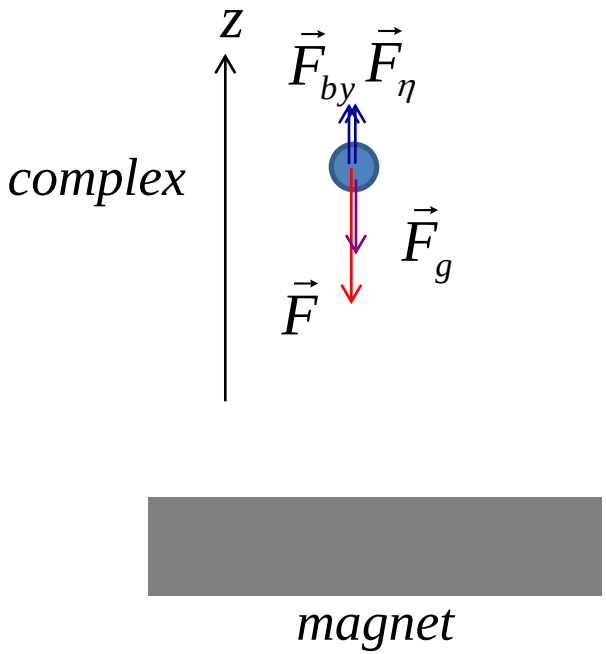

$$\vec{F}_{\eta} = 6\pi\eta D_C / 2$$

$$F^* = F_{by} - \left(F + F_g\right)$$

$$F_{by} = \rho_s V_c; \quad F_g = \rho_p V_c$$

solvent particle

Magnetic Force analysis, dynamics

Complex volume and mass

$$V_c \approx V_V + N\left(V_m + V_{pol}\right) \approx \frac{\pi}{6}\left(D_V^3 + N D_{pol}^3\right)$$

$$m_c \approx m_V + N\left(m_m + m_{pol}\right) \approx \frac{\pi}{6}\left(\rho_V D_V^3 + N\left(\rho_{pol}\left(D_{pol}^3 - D_m^3\right) + \rho_m D_m^3\right)\right)$$

$$\textit{USING} \quad \begin{cases} D_m \approx 9\ nm \\ D_{pol} \approx 70\ nm \\ D_V \approx 80\ nm \\ N \approx 350 \end{cases}$$

$$V_c \approx 1.3\times10^{-19} m^3 = 1.57\times10^{8} nm^3 \Rightarrow D_c \approx 600\, nm$$

$$m_c \approx 1.4\times10^{-16} kg = 0.14\, fg$$

$$P_c \approx 1.370\times10^{-15} N; \quad F_{by} \approx 1.27\times10^{-15} N$$

Magnetic Force analysis, space distribution of complexes

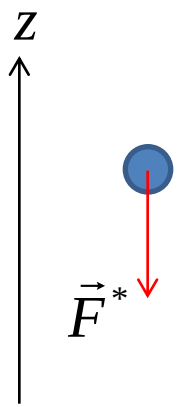

Energy U

$$U = F^* z$$

Equilibrium concentration c(z)

$$c(z)/c_0 = e^{-\frac{F^* z}{kT}}$$

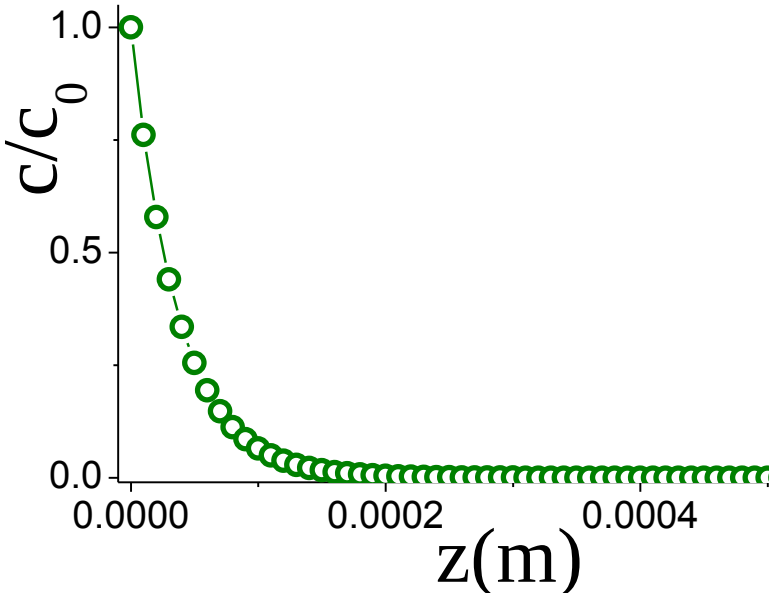

Magnetic Force analysis, space distribution of complexes

$h = 1\,mm$

z = 1.5 mm
z = 25 mm
z = 40 mm
z = inf

$$c(h)/c_0 = e^{-\frac{F^*(z)h}{kT}}$$

$h = 1\,mm$

c/c$_0$

1
0.1
0.01
1E-3
1E-4
1E-5
1E-6
1E-7
1E-8
1E-9
1E-10

0.0000
$200\,\mu m$
0.0005
0.0010

h(m)

Magnetic Force analysis, motion of complexes

complex motion dynamics

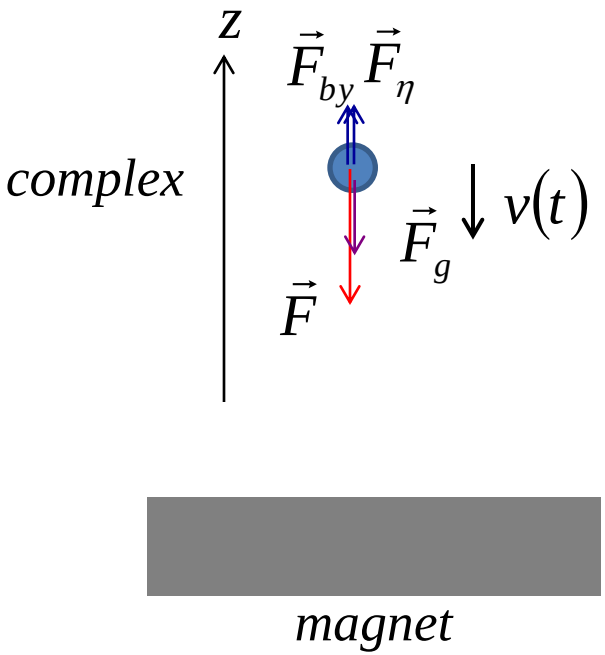

$$v(t) = \frac{F^*}{3\pi\eta D_c}\left(1 - e^{-\frac{3\pi\eta D_c}{m_p}t}\right)$$

complex speed

Magnetic Force analysis, theoretical

f_{30}: fraction of complexes reaching bottom of PD in 30 min (mf time t_{mf})

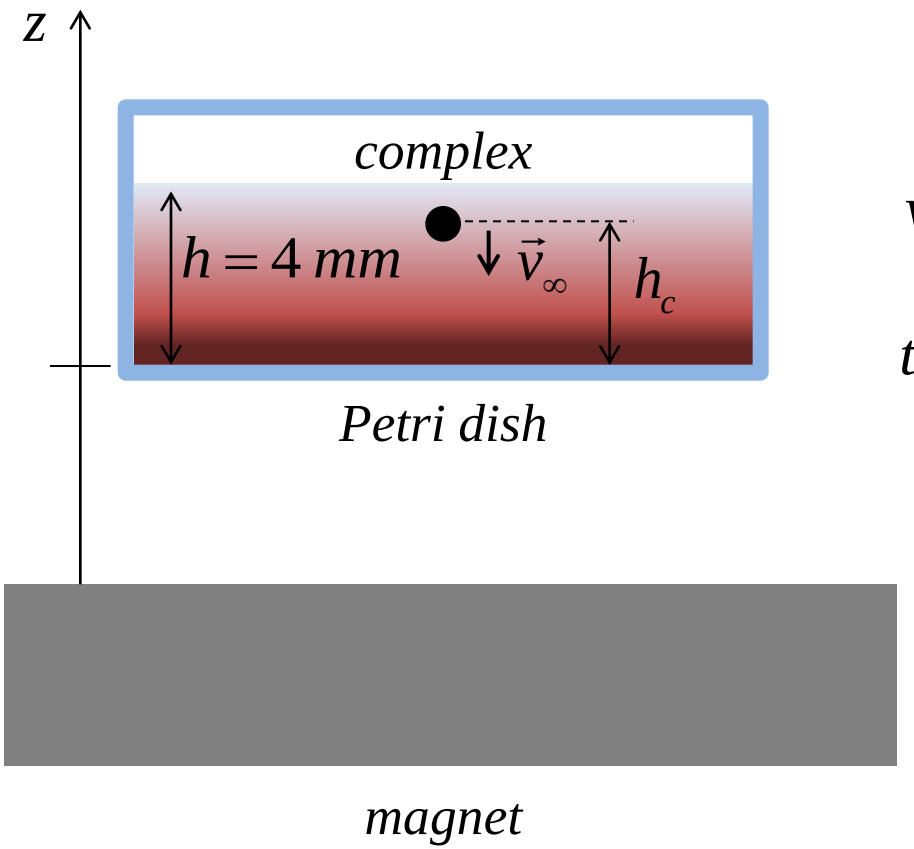

$$v_\infty = \frac{F^*}{6\pi\eta R}$$

$$t_{mf} = 30\ \text{min}$$

$$h_c = v_\infty t_{mf}$$

$$f_{30} = h_c / h$$

Comparison with experiment

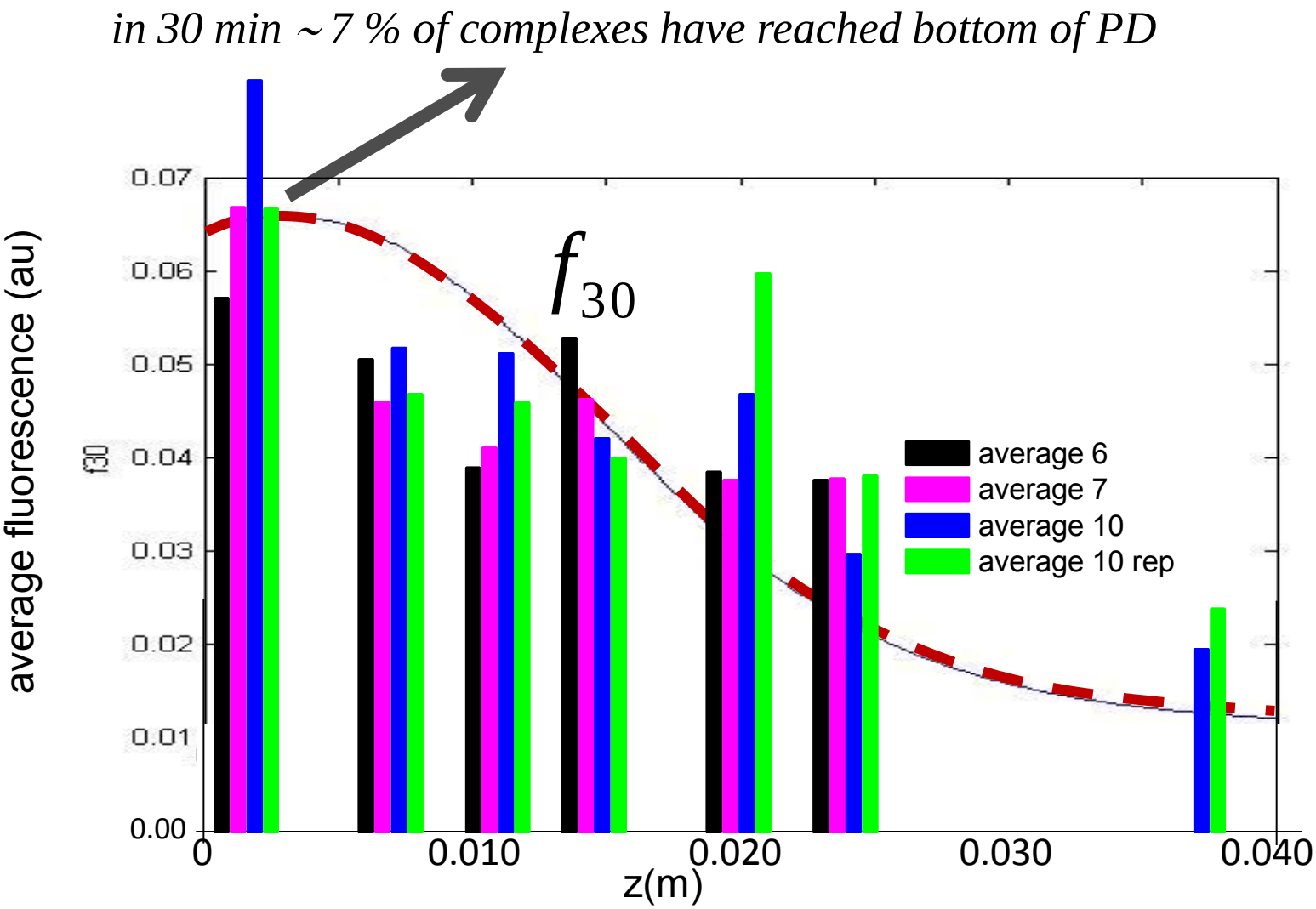

Magnetofection vs. time

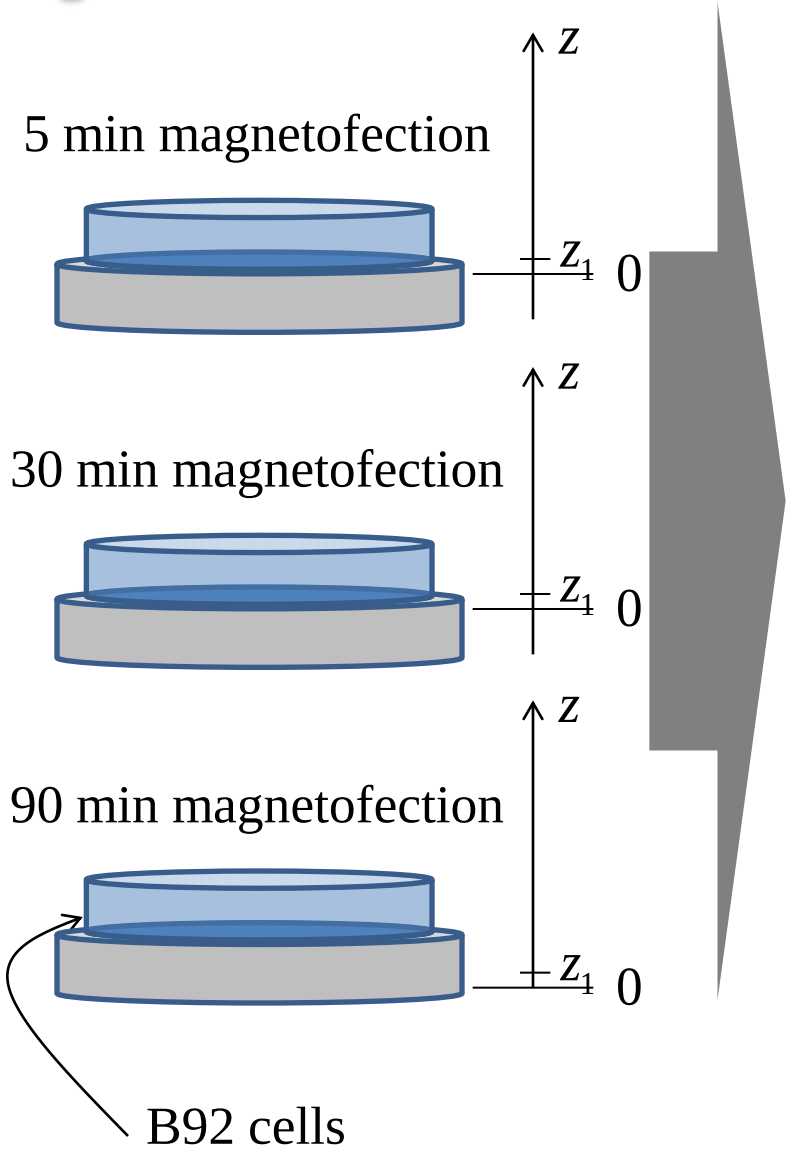

washing → 72 h with MEM + FBS → fluorescence vs *t*

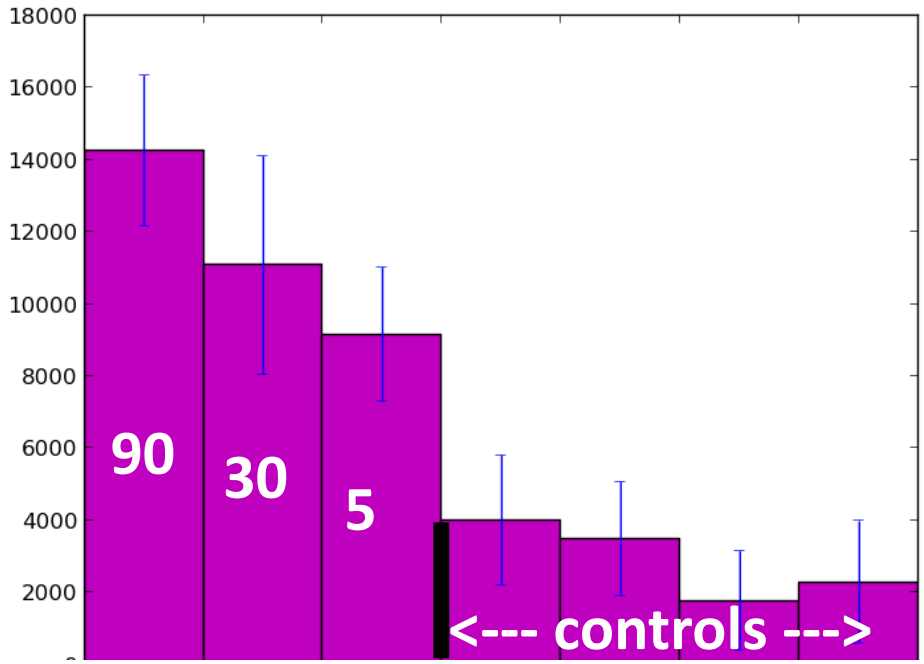

Conclusions III

Magnetic force analysis gives a fair semiquantitative account of experiments of magnetofection vs z

Field applicators can be designed to optimaze magnetic force for in vivo magnetofection at moderate depths

Longer times or **Stronger** magnetic force is needed in order to improve magnetofection effects.

Ferrogels PVA/Fe oxide

Arciniegas L, Pasquevich GA, Mendoza Zélis P,
González J., Álvarez V, Hoppe C, Sánchez FH

Ferrogeles: magnetic hydrogels with high hydration ability and strong magnetic response.

Hydrogels are constituted by crosslinked polymeric chains.
Physically crosslinked PVA hydrogels are soft biocompatible materials.
With nanometric aditions (nanocelulose, hidroxiapatite, iron oxide) produce composites with specific potential aplications in biomedicina:

Hydrogels

PVA

PVA hydrogel crosslinked by freezing – thawing cycling

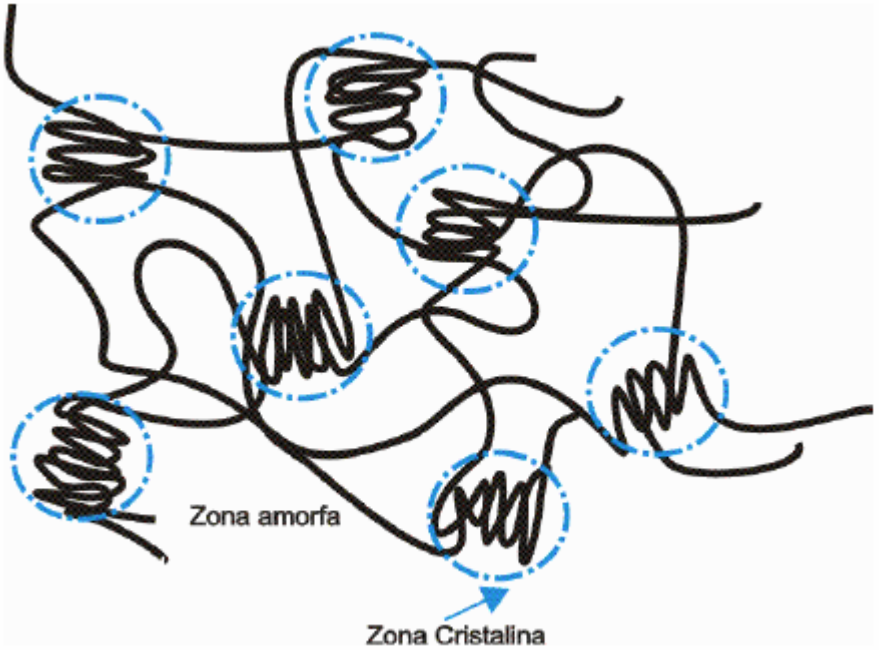

Hydrogels

PVA

- 5 % p/v
- 10 % p/v
- 15 % p/v

- 18.000 g/mol
- 41.000 g/mol
- 93.500 g/mol
- 155.000 g/mol

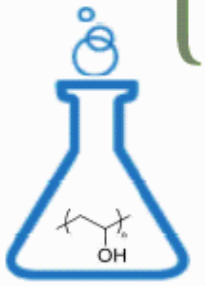

4h-85°C
Agitación Constante

→ Colado → Congelar -18°C → Descongelar 23°C → **CRIOGELES** → Tratamiento Térmico

- 100°C
- 110°C
- 120°C
- 130°C

Ciclos: 1,2,3 y 4

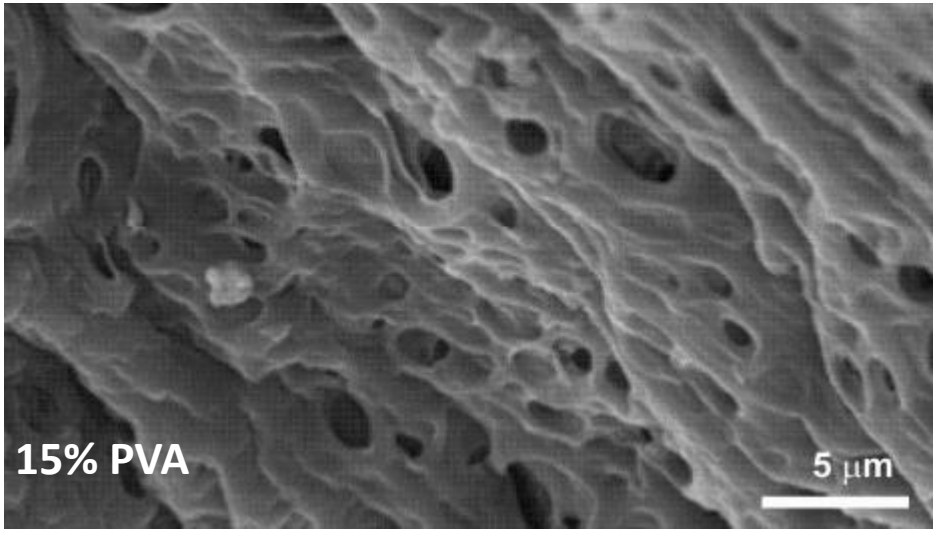

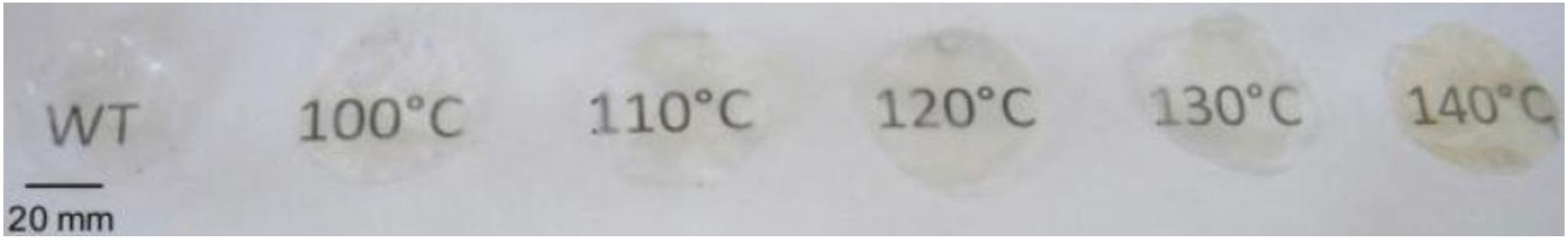

Ferrogels (one pot synthesis)

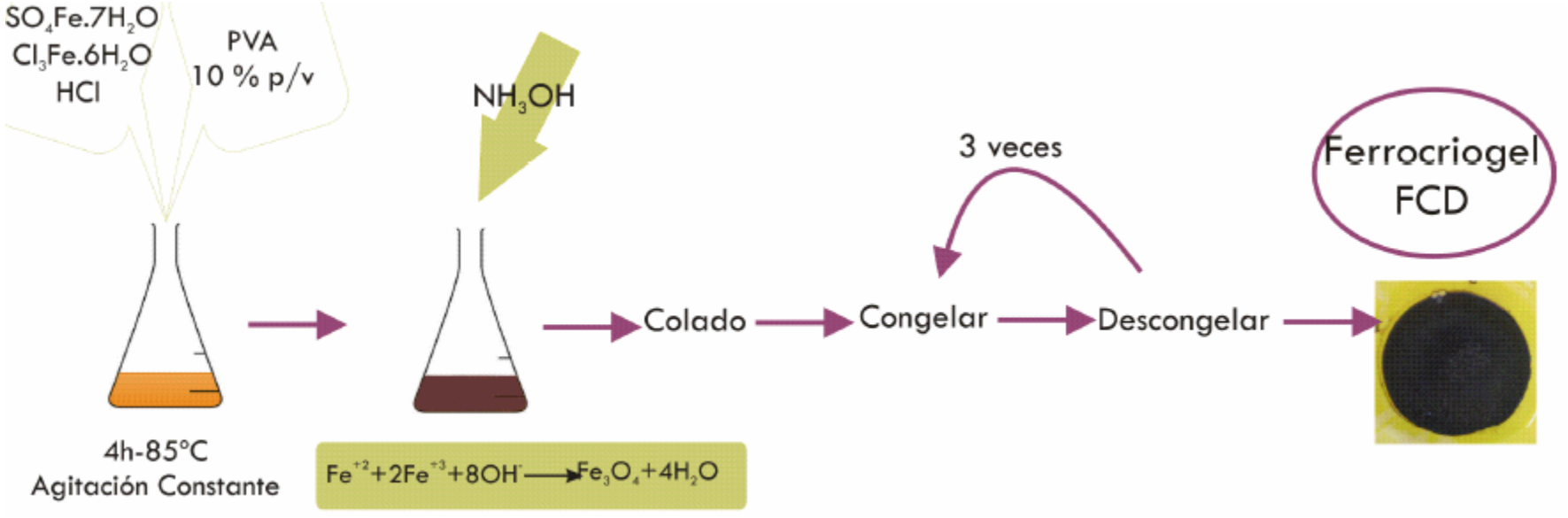

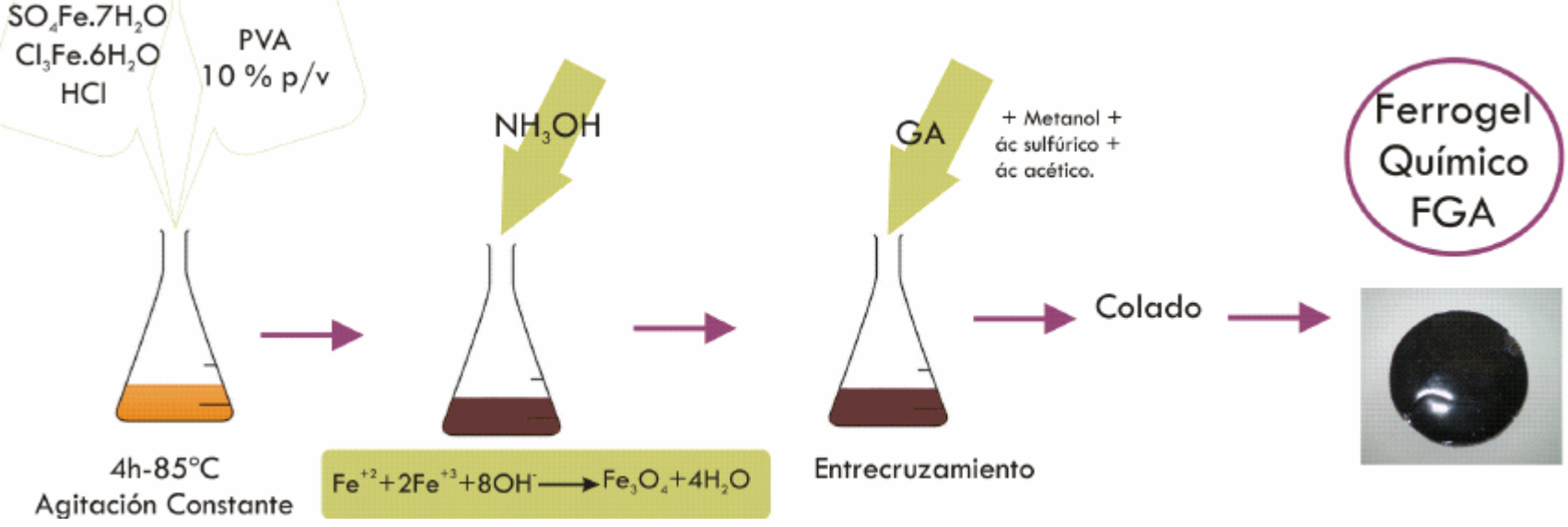

$$x_{FeO} \approx 0.06\,(mass\ ratio)$$

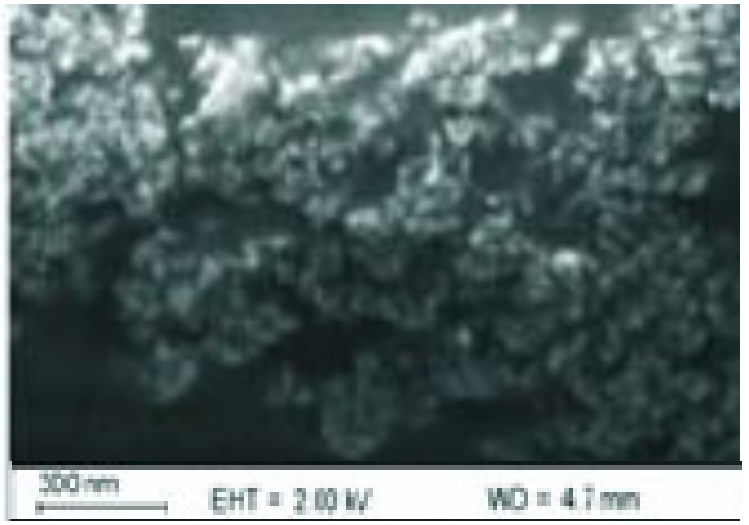

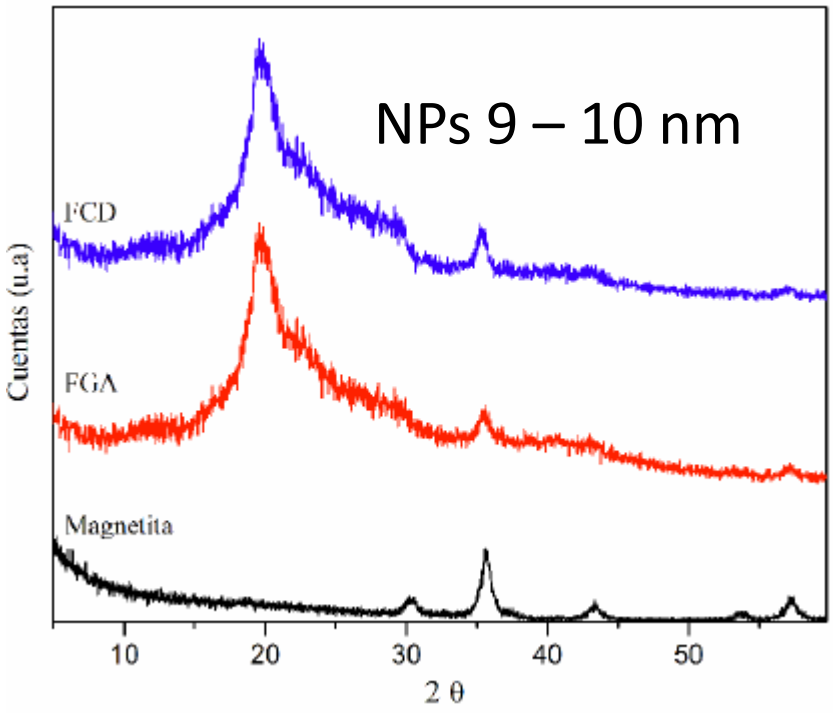

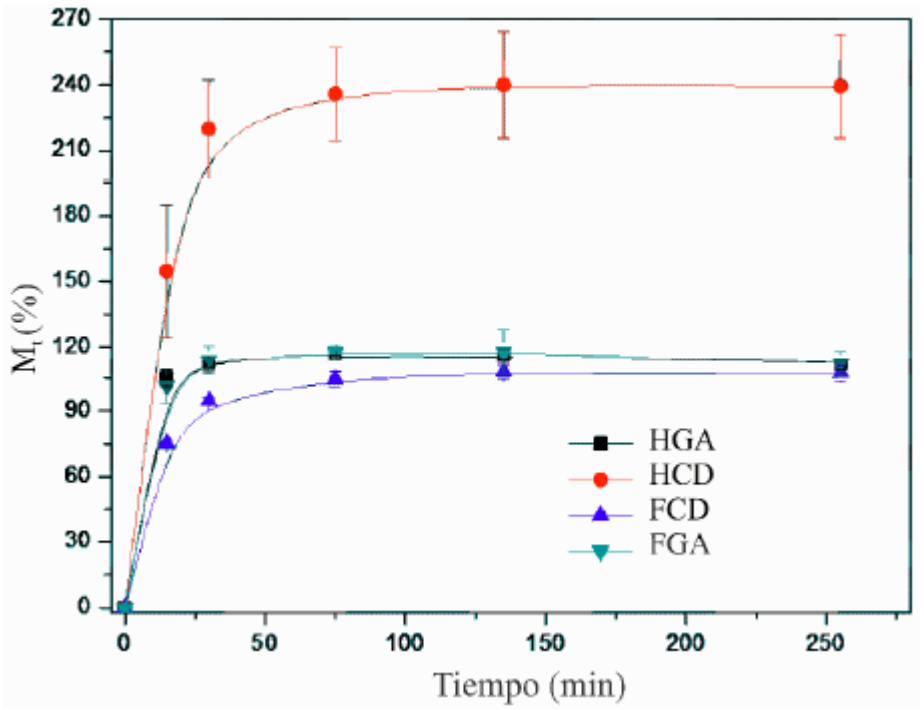

Synthesis and characterization of PVA ferrogels obtained through a one-pot freezing–thawing procedure

Jimena S. Gonzalez · Cristina E. Hoppe · Diego Muraca · Francisco H. Sánchez · Vera A. Alvarez

Colloid Polym Sci (2011) 289:1839–1846

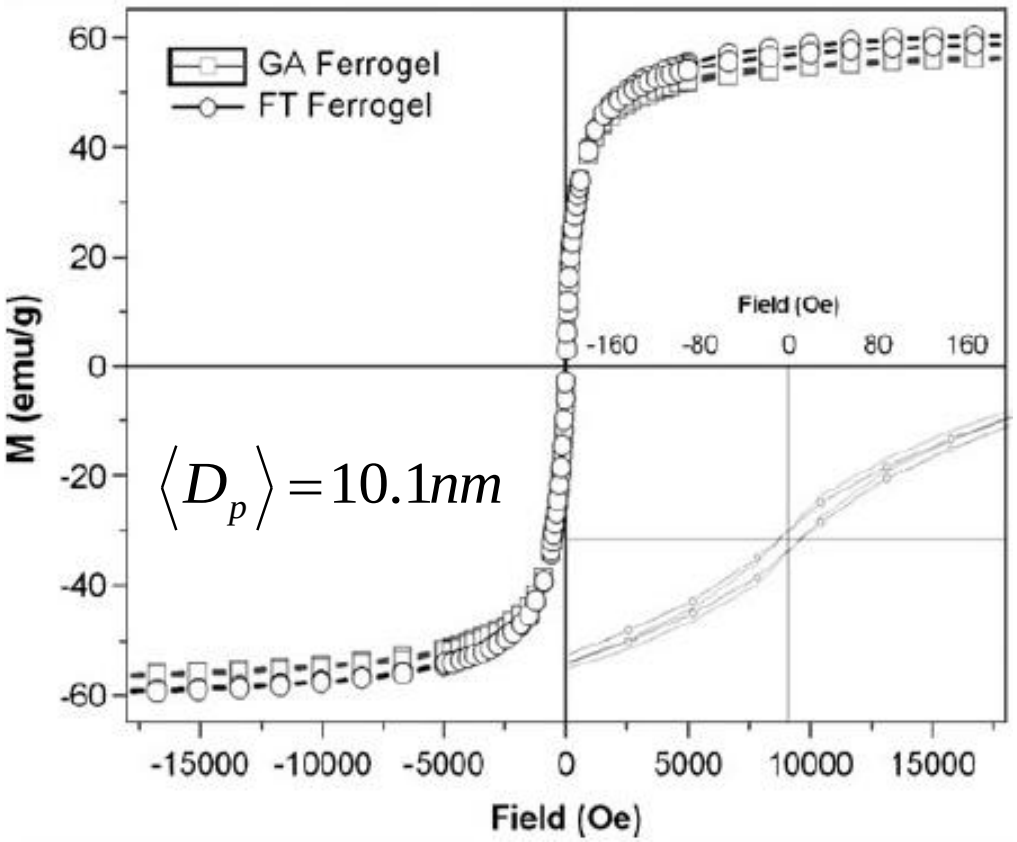

$$M = \frac{N\langle\mu\rangle \int_0^\infty \mu L(\alpha\mu) P(\mu) d\mu}{\int_0^\infty \mu P(\mu) d\mu} \qquad \alpha = B/kT,$$

Magnetic properties study of iron-oxide nanoparticles/PVA ferrogels with potential biomedical applications

P. Mendoza Zélis · D. Muraca · J. S. Gonzalez · G. A. Pasquevich · V. A. Alvarez · K. R. Pirota · F. H. Sánchez

J Nanopart Res (2013) 15:1613

Fe XANES

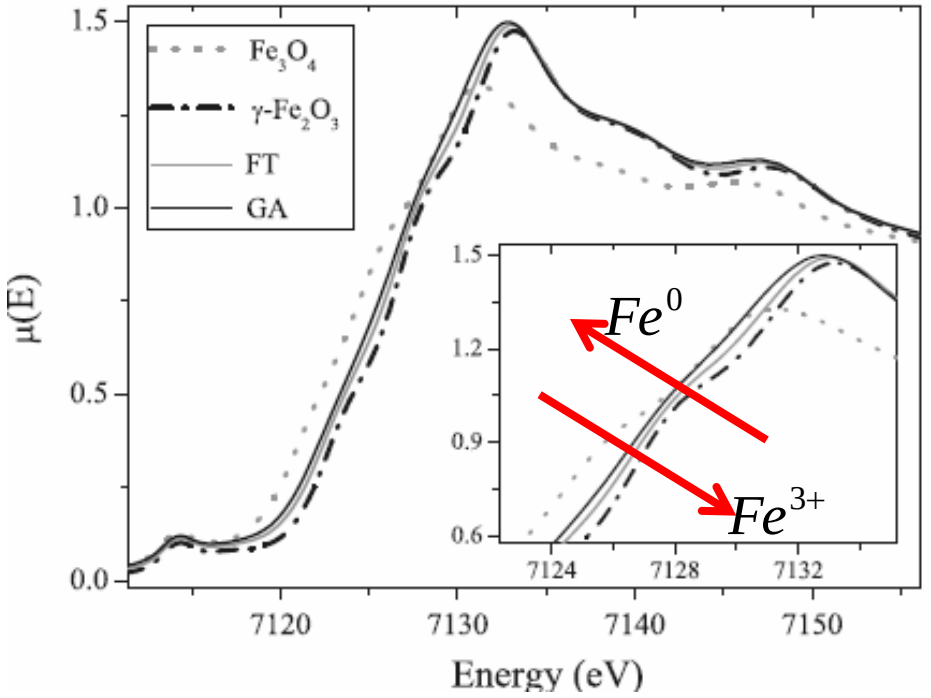

^{57}Fe Mössbauer

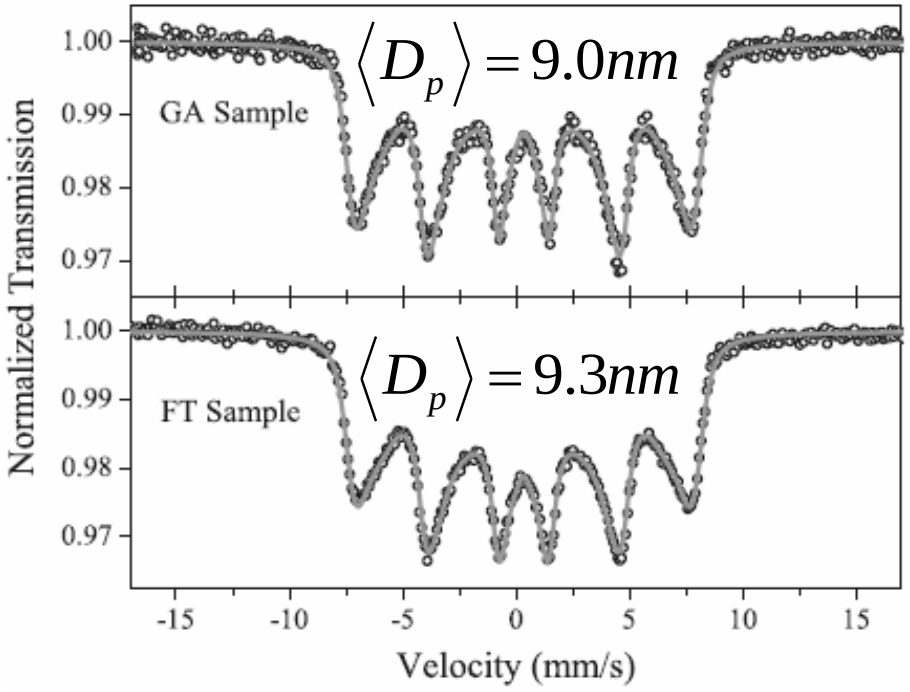

$$H_{hf}(V,T) \simeq H_{hf}(V=\infty,T)\left(1-\frac{k_B T}{2KV}\right)$$

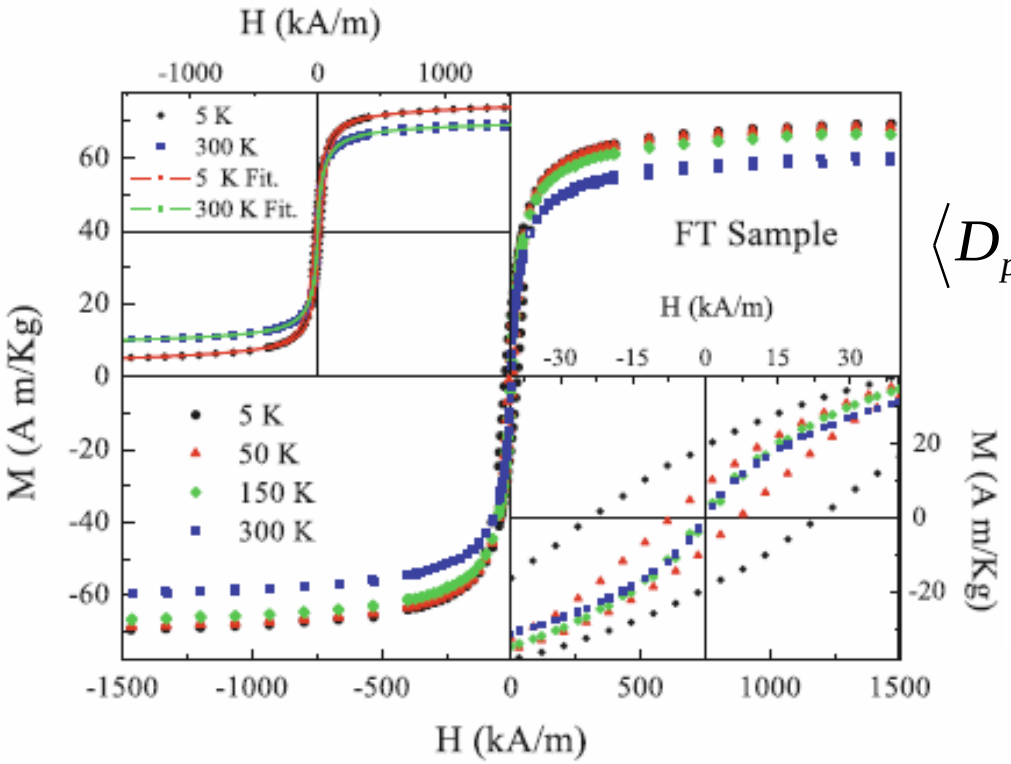

$$\langle D_p \rangle = 8.1nm$$

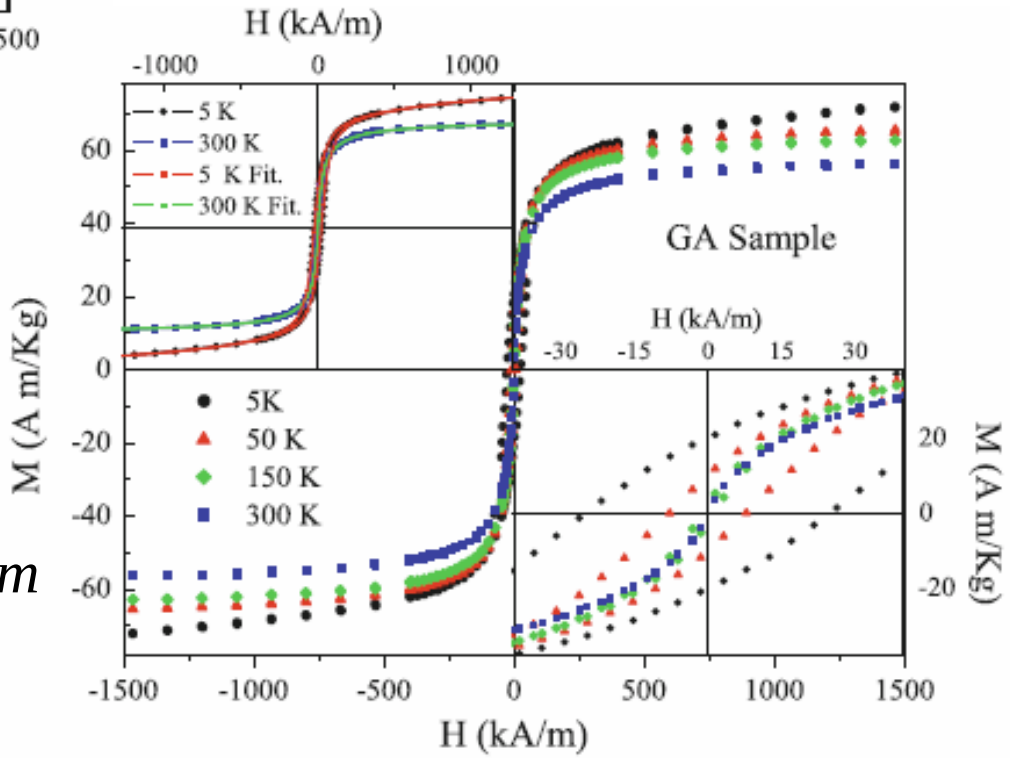

$$\langle D_p \rangle = 9.1nm$$

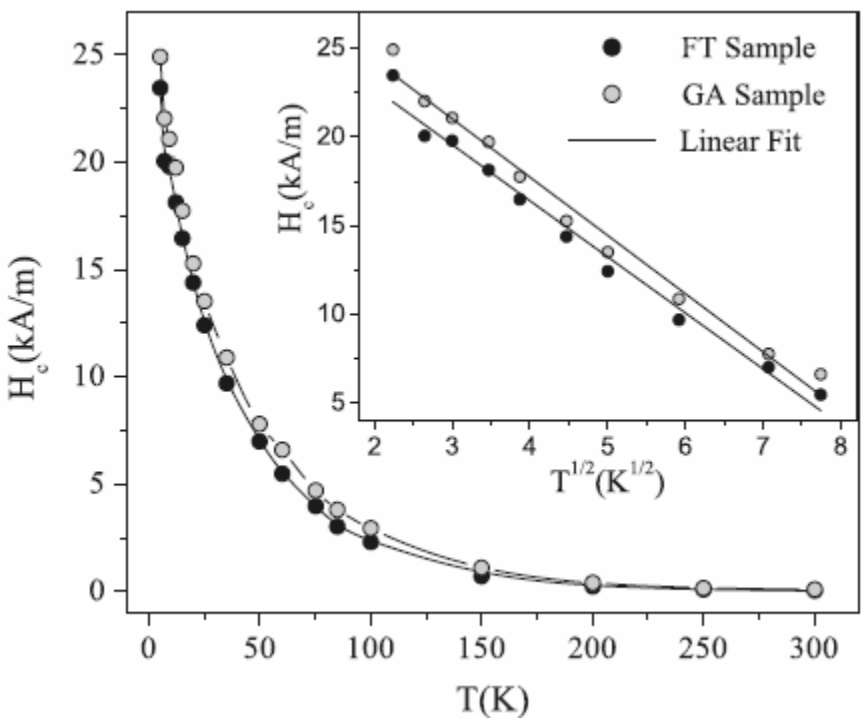

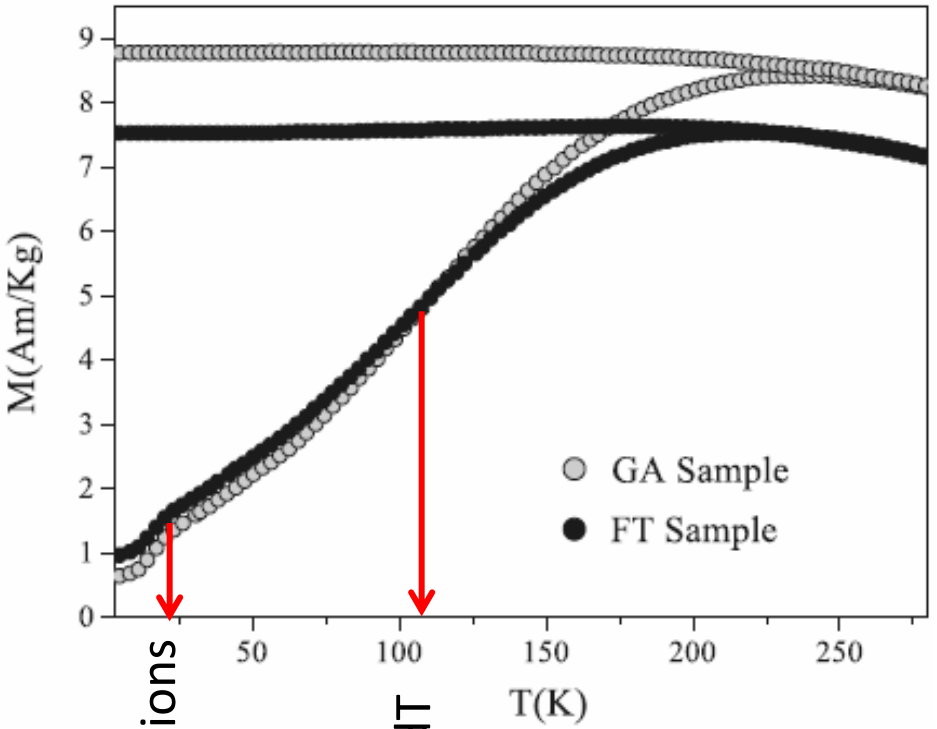

τ' - no interactions

τ - d(FC-ZFC)/dT

$$M(H,T)=\frac{N_a\langle\mu_a\rangle\int_0^\infty \mu_a L(b\mu_a)P(\mu_a)d\mu_a}{\int_0^\infty \mu_a P(\mu_a)d\mu_a} \qquad b=\mu_0 H/kT$$

$$M(H,T)=\frac{N\langle\mu\rangle\int_0^\infty \mu L(b^*\mu)P(\mu)d\mu}{\int_0^\infty \mu P(\mu)d\mu} \qquad b^*=\mu_0 H/k(T+T^*)$$

Allia et al.

$$\frac{\xi}{\chi}=\frac{3kN}{\mu_0}\left(\frac{T}{M_S^2}\right)+3\alpha$$

$$\xi=\frac{\langle\mu^2\rangle}{\langle\mu\rangle^2}=\frac{\langle\mu_a^2\rangle}{\langle\mu_a\rangle^2}$$

$$\varepsilon_d=\alpha\frac{\mu_0\mu^2}{d^3}$$

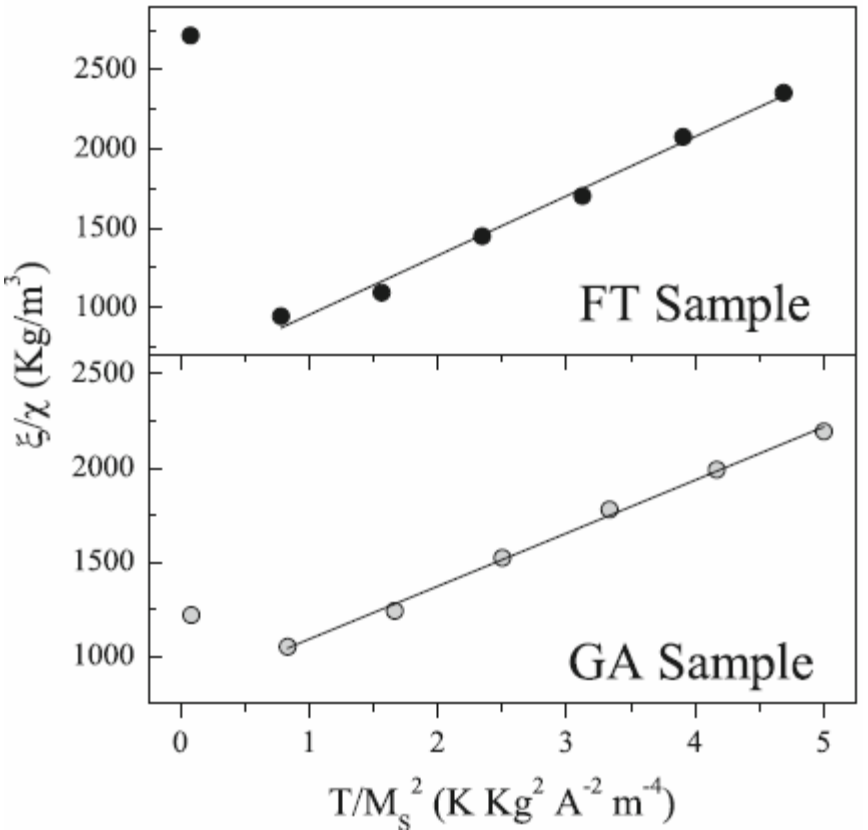

Ferrogels (impregnation synthesis)

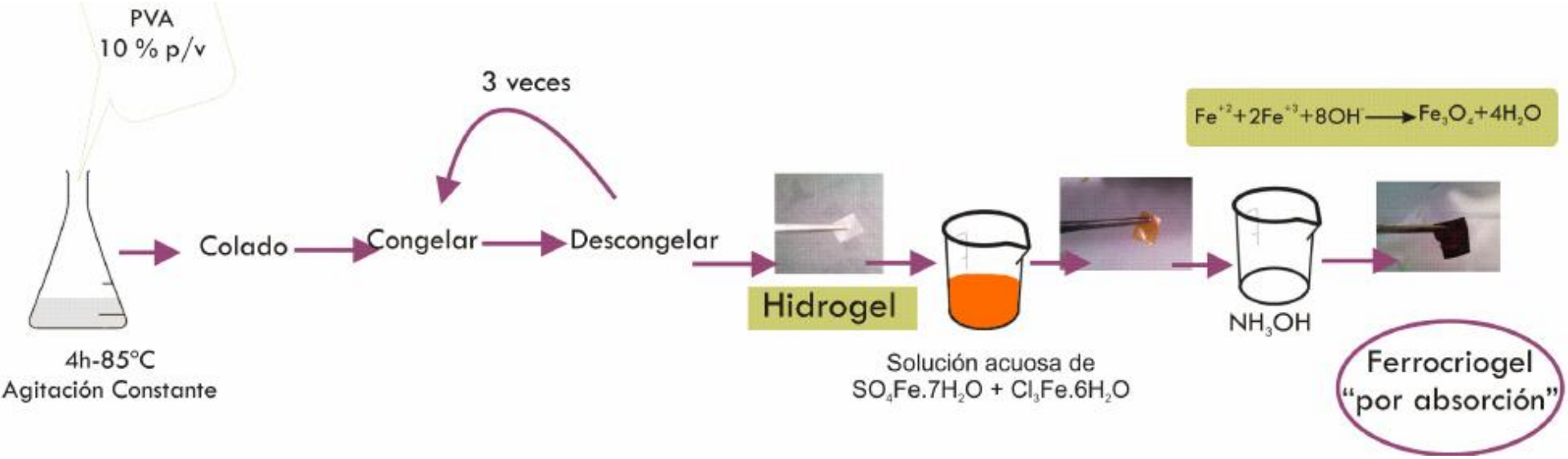

A SIMPLE AND EFFICIENT PROCEDURE FOR THE SYNTHESIS OF FERROGELS BASED ON PHYSICALLY CROSSLINKED PVA

Jimena S. Gonzalez[a*], Cristina E. Hoppe[a], Pedro Mendoza Zélis[b], Lorena Arciniegas[b], Gustavo A. Pasquevich[b], Francisco H. Sánchez[b] and Vera A. Alvarez[a]

Industrial & Engineering Chemistry Research (under evaluation)

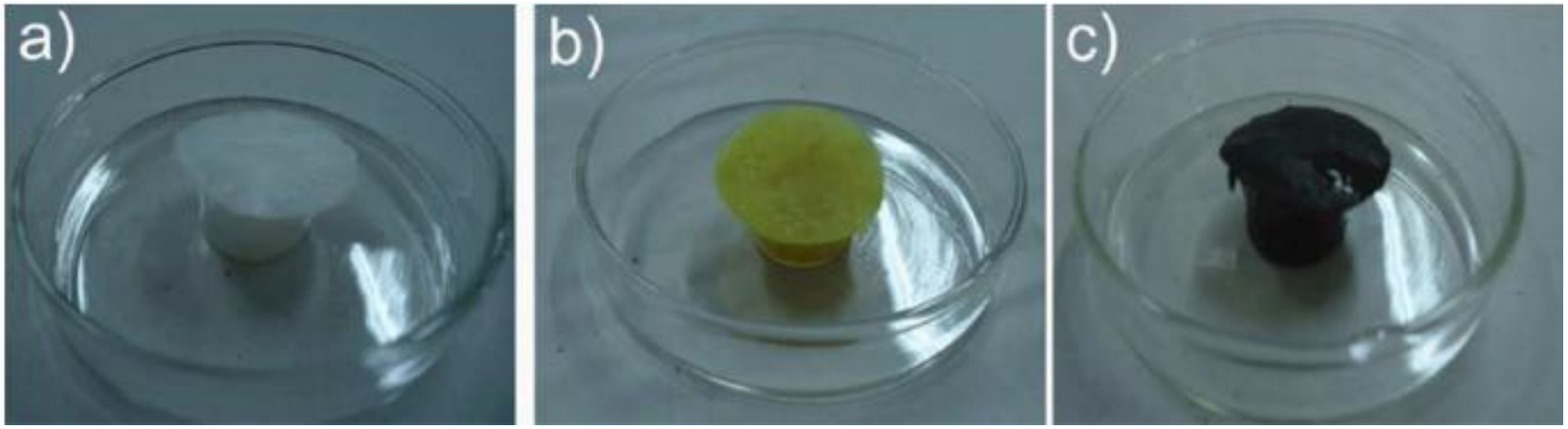

	T_m °C	X_{cr} %	T_p °C	w_t % Fe_2O_3
Hydrogel	220.5±0.3	31.80±3.2	284.3±5.3	0
Ferrogel	223.7±0.6	35.3±5.1	295.9±6.4	15.7±3.1

TEM

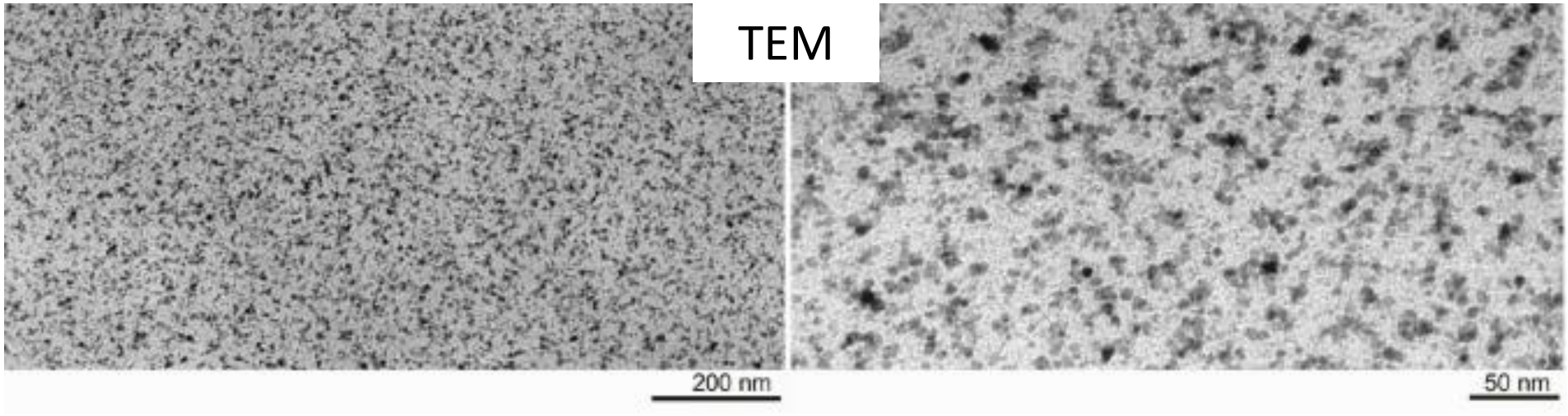

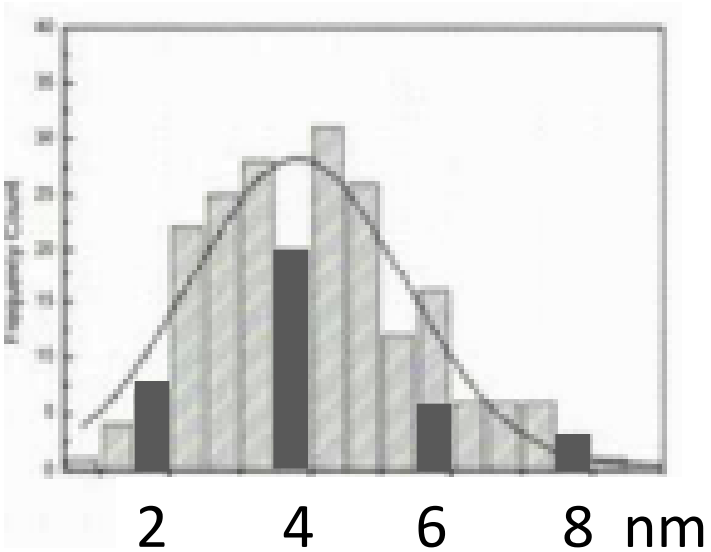

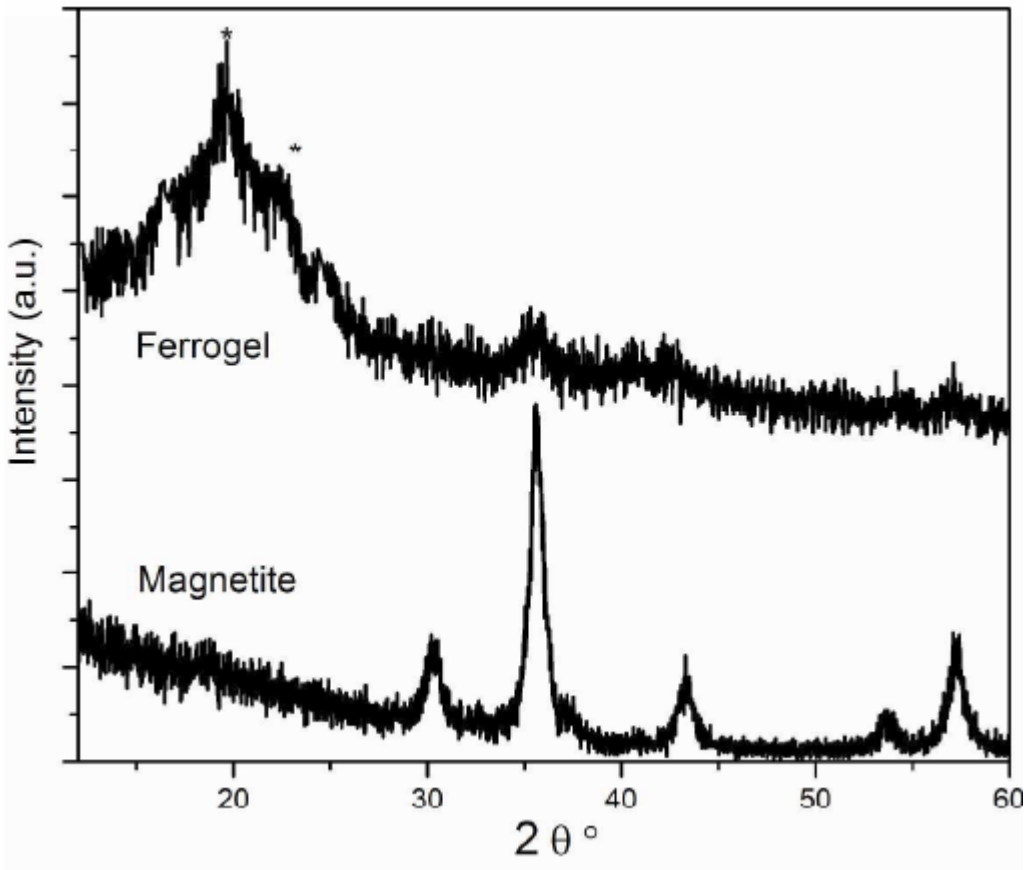
Intensity (a.u.)
Ferrogel
Magnetite
*
*
20
30
40
50
60
2 θ °

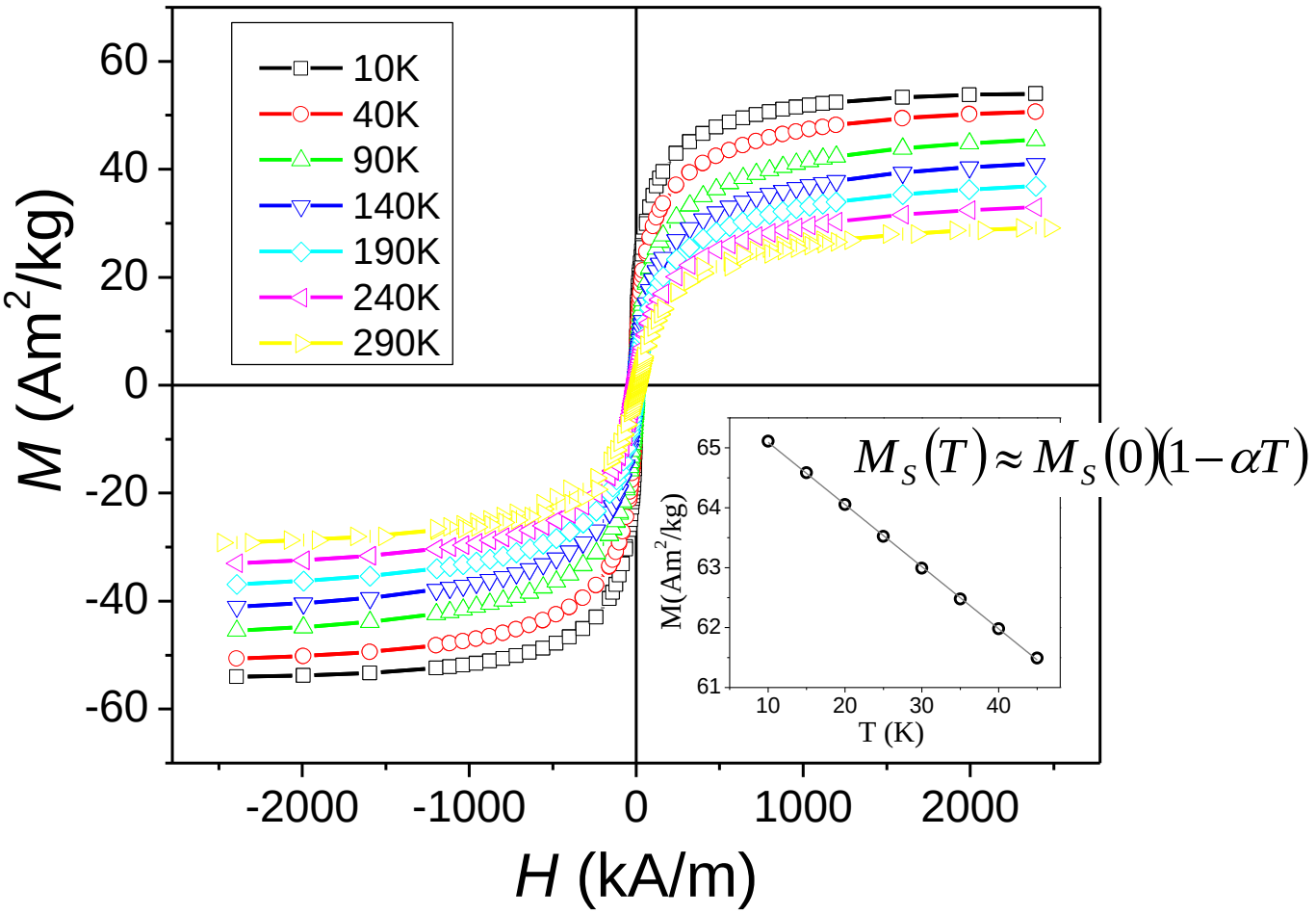

$$H_C = 0 \quad for \quad T \geq 40K$$

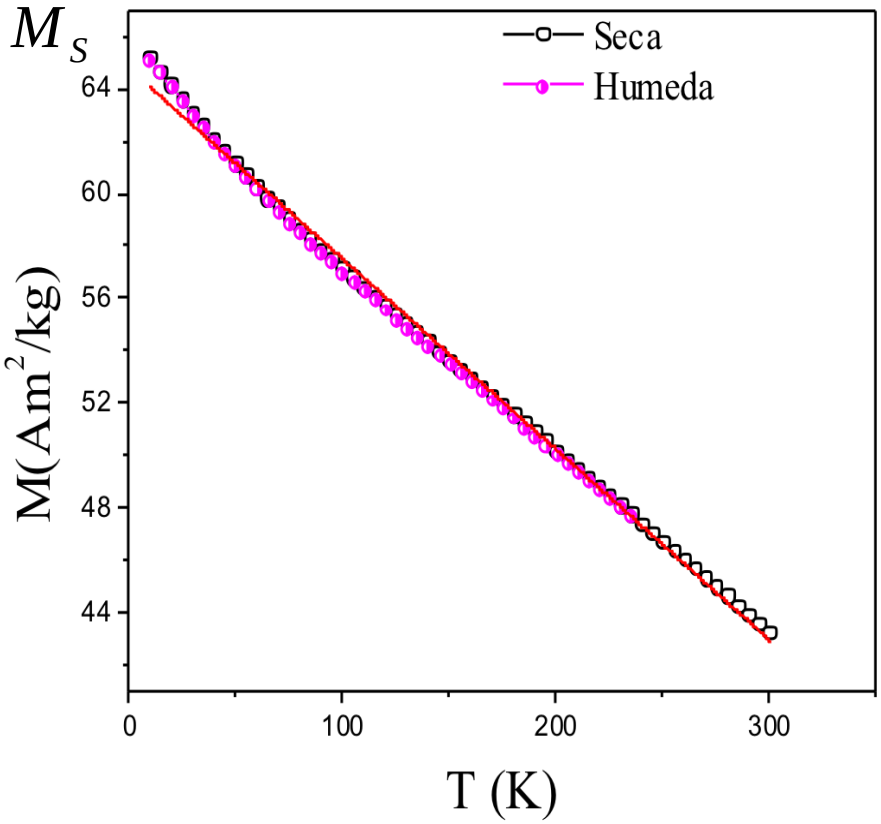

$$M_S(T) \approx M_S(0)(1-\alpha T)$$

$$\alpha \approx k/8(KV + E_{\text{int}})$$

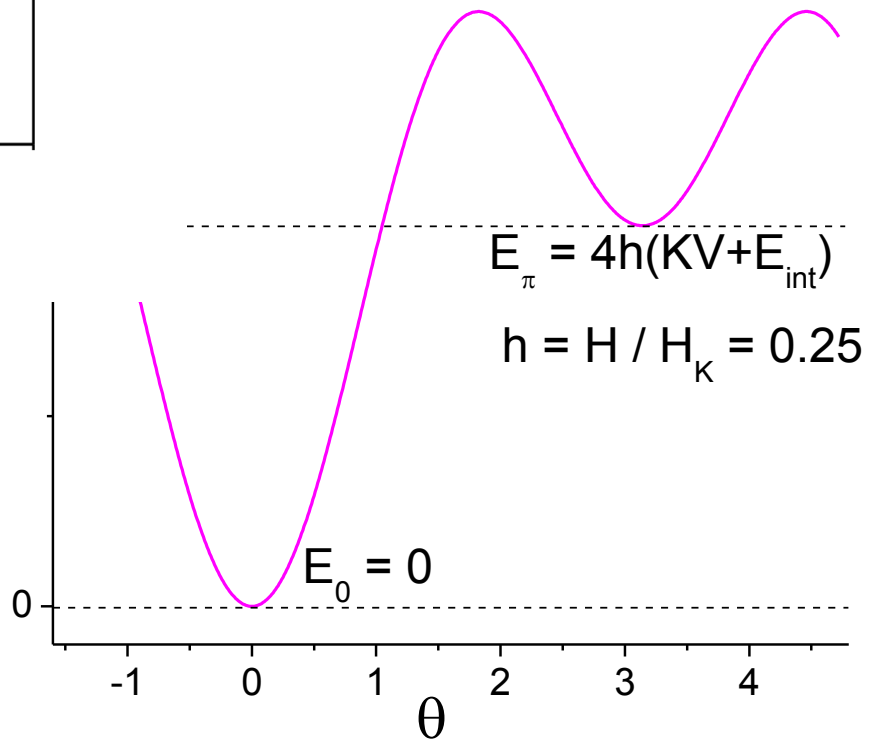

Ferrogel swelling

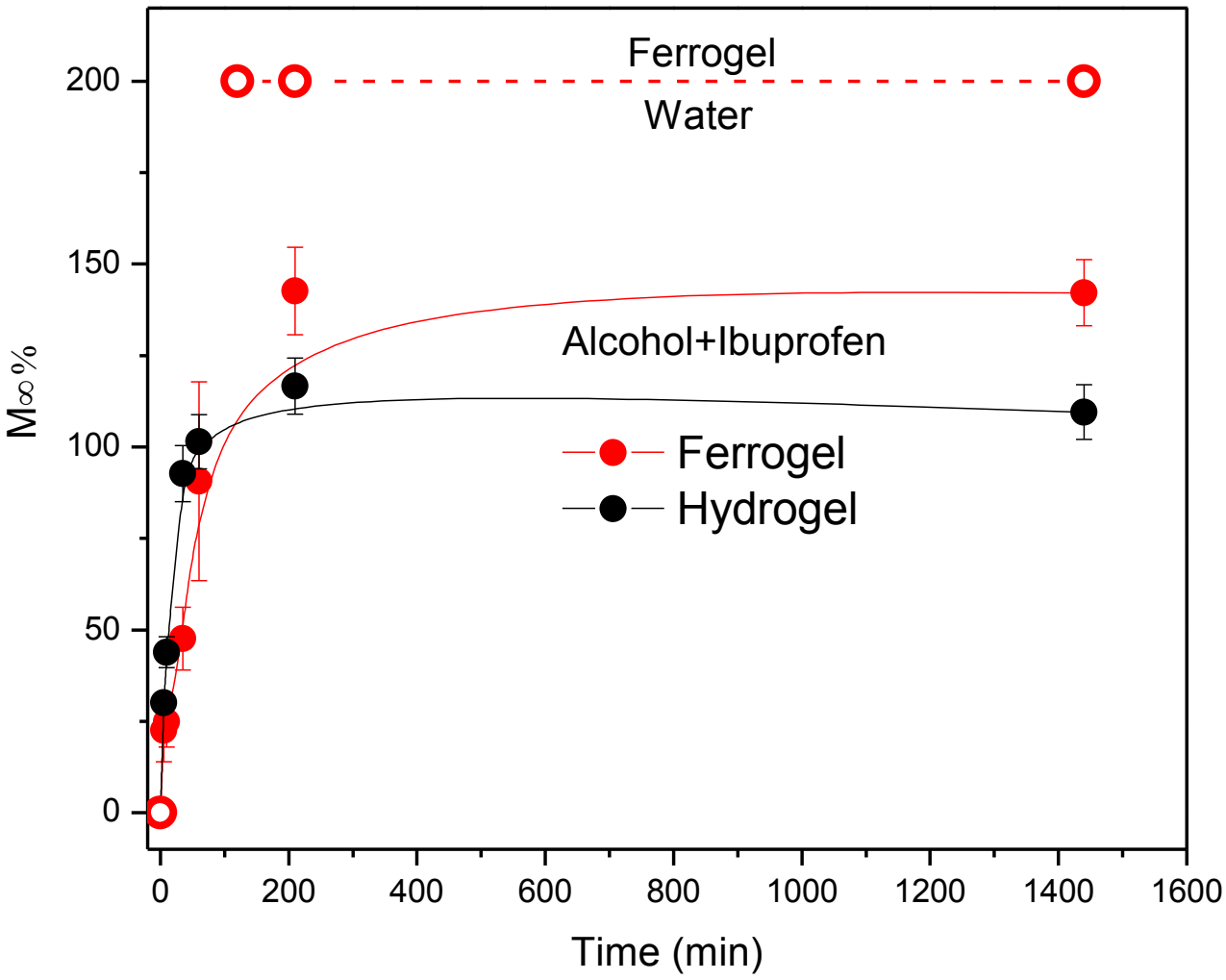

Ferrogel swelling

dry

hydrated

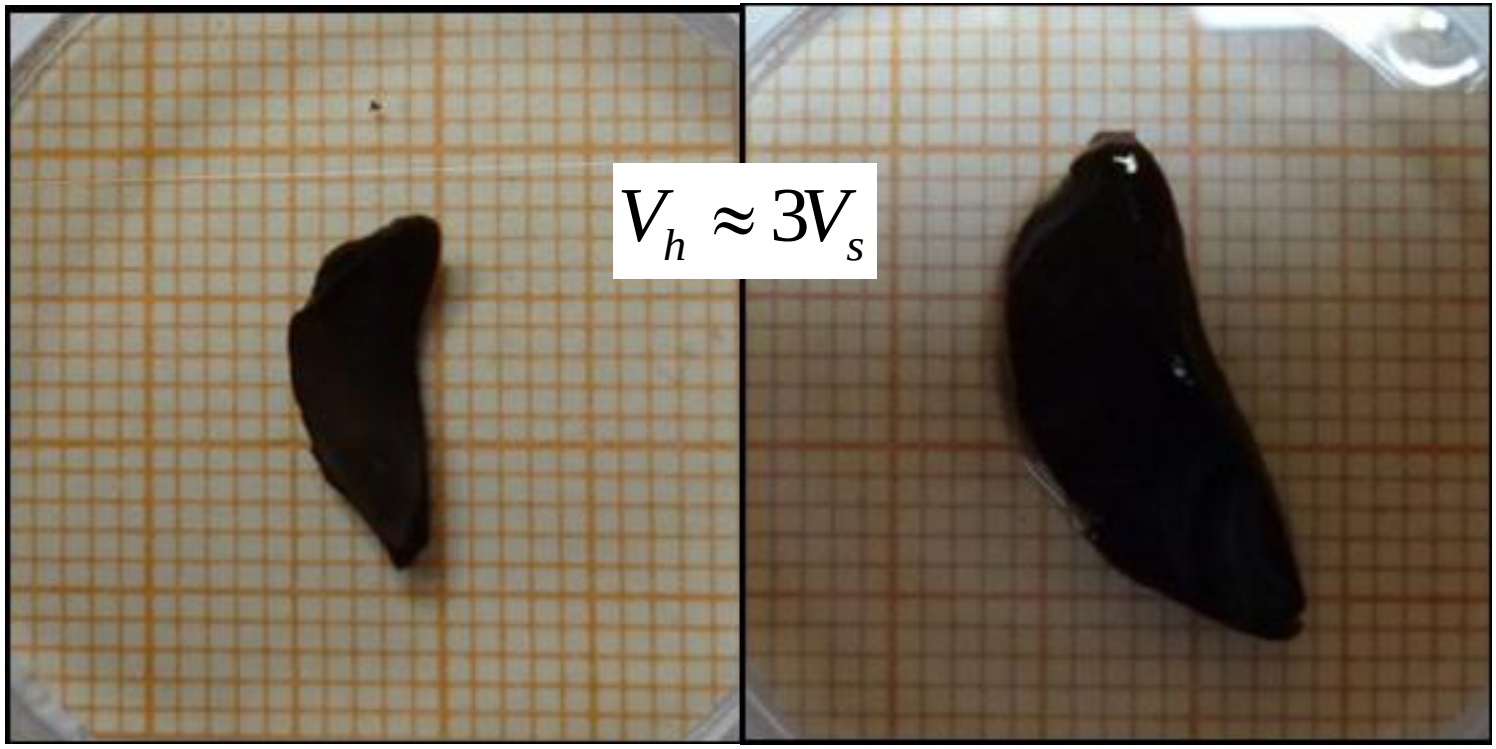

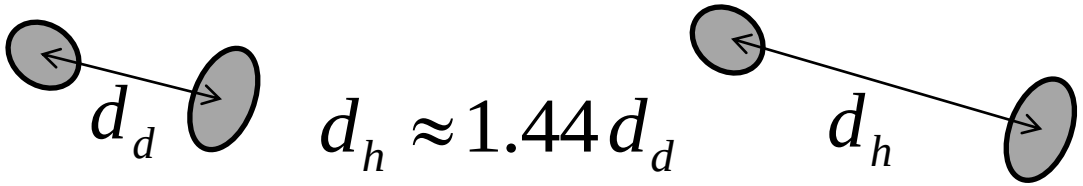

$$\tau_{seco} \approx \tau_0 e^{\left(KV + E_{\text{int}}^{seco}\right)/kT}$$

$$\tau_{hid} \approx \tau_0 e^{\left(KV + E_{\text{int}}^{hid}\right)/kT}$$

$$E_{\text{int}}^{seco} > E_{\text{int}}^{hid} \Rightarrow T_B^{seco} > T_B^{hid}$$

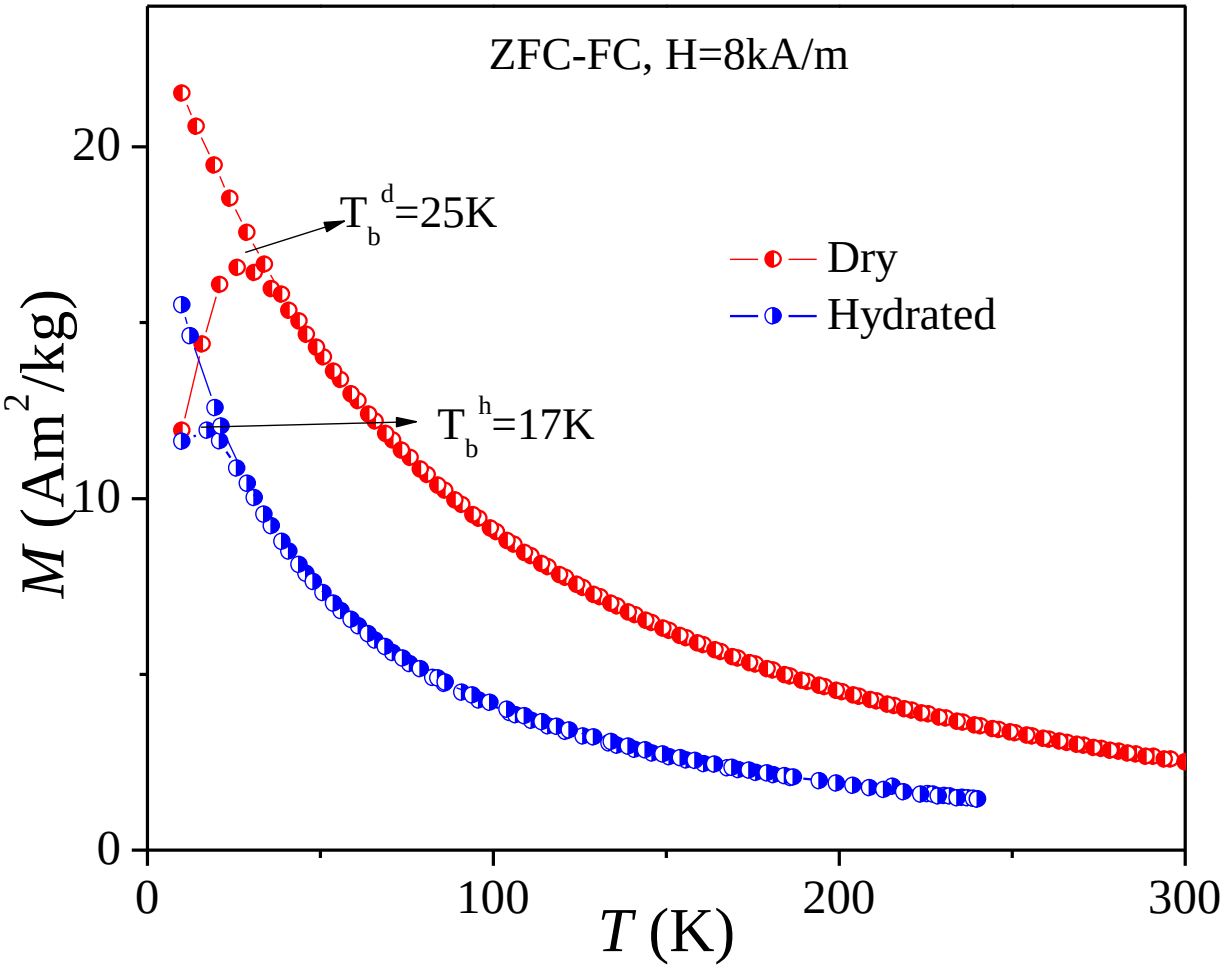

Shape Effects

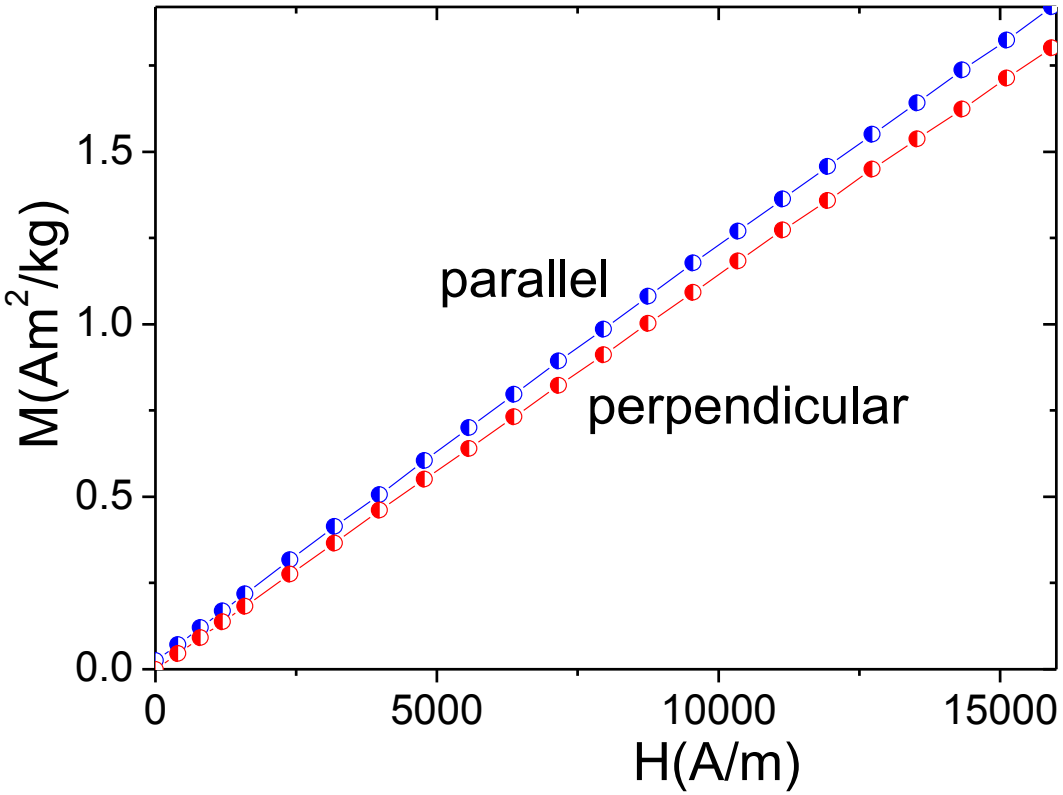

$\gamma \approx 2.1$

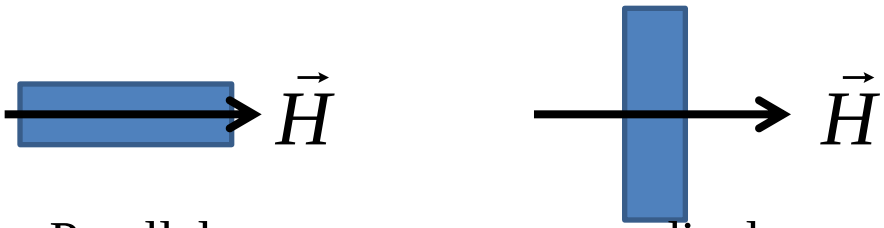

Parallel

perpendicular

Response to a Magnetic RF Field

Duty Coil

$$f = 260\ kHz$$

Response to a Magnetic RF Field

$$f = 260\,kHz$$

$$H_0 = 3.83\,\text{kA/m} - 58.2\,\text{kA/m}$$

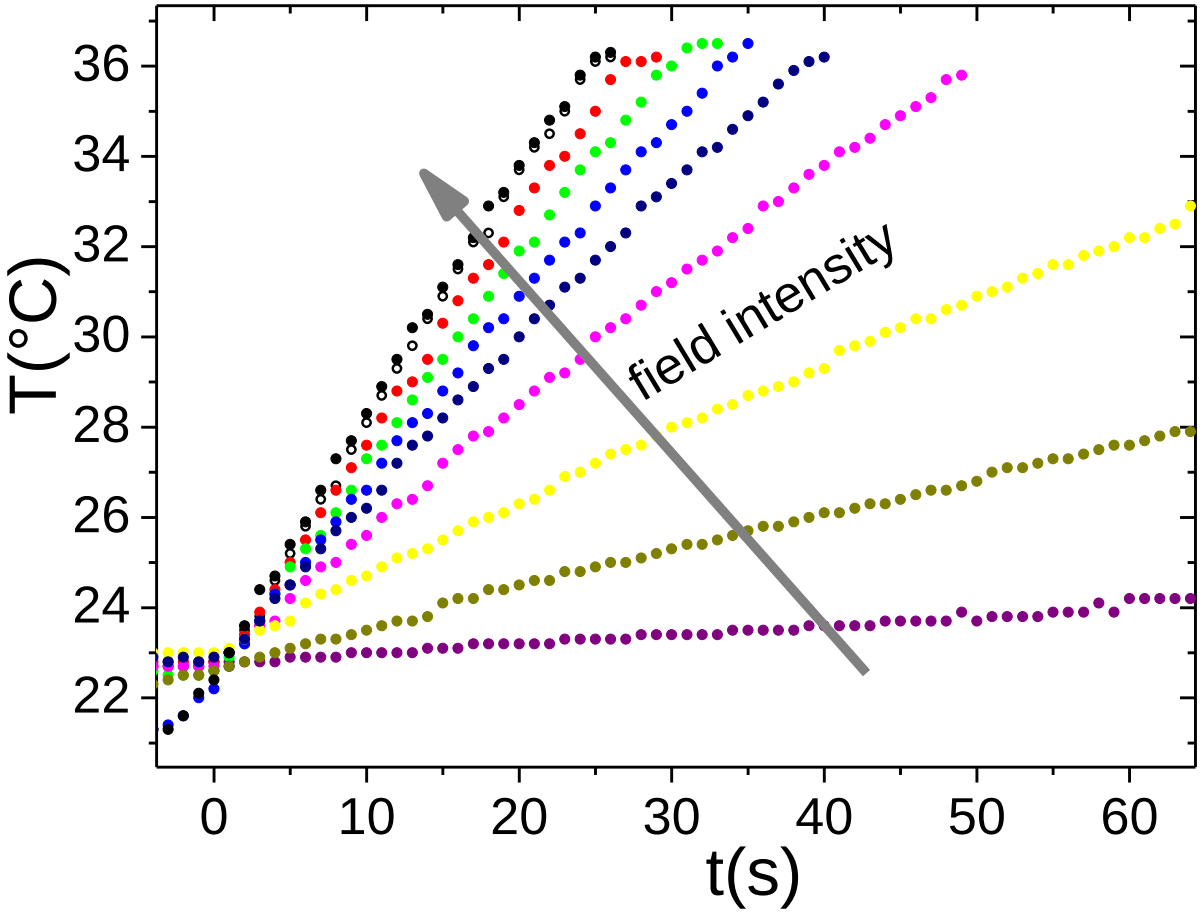

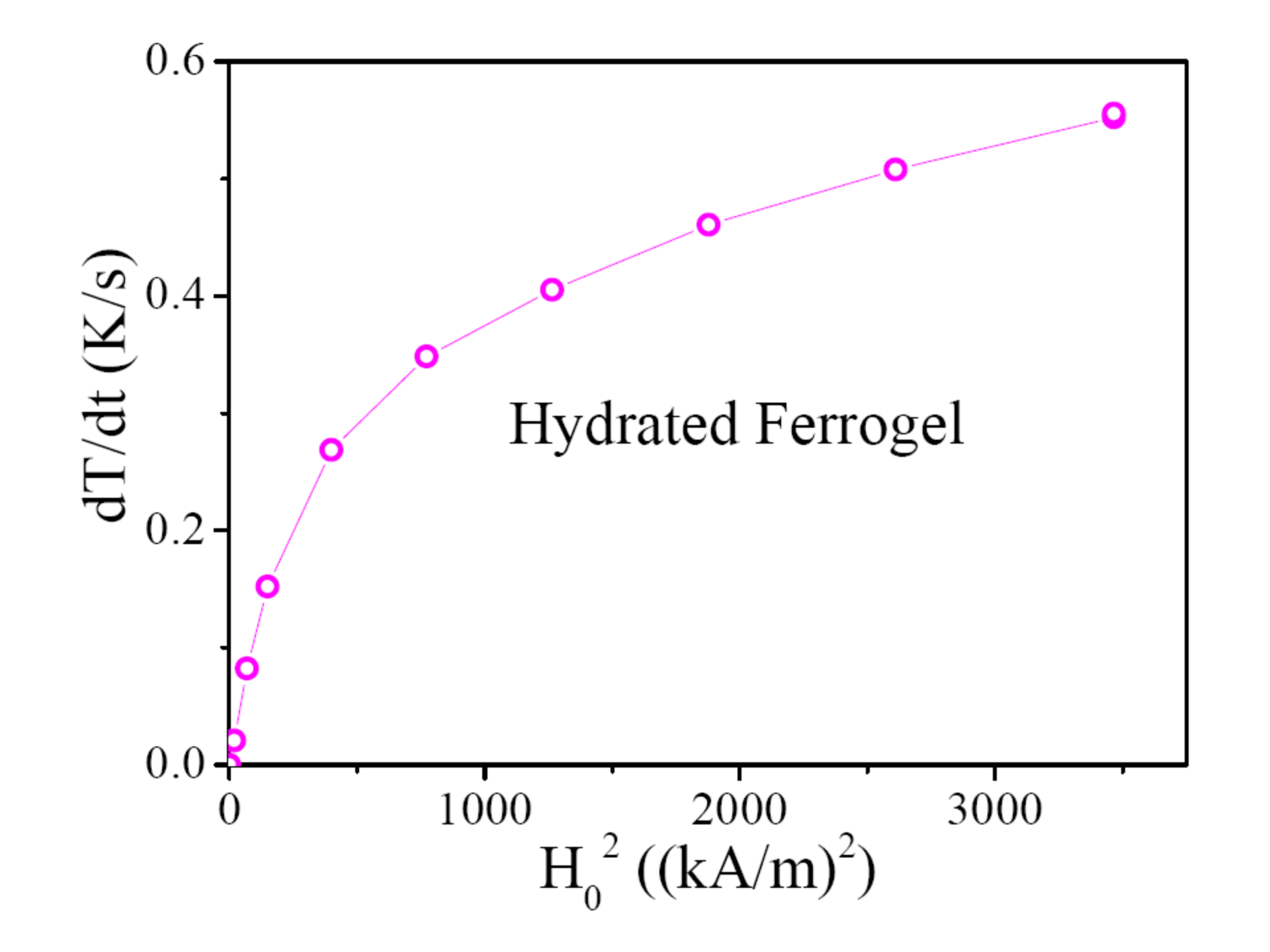
0.6
0.4
0.2
0.0
dT/dt (K/s)
Hydrated Ferrogel
0
1000
2000
3000
H0 2 ((kA/m)2)

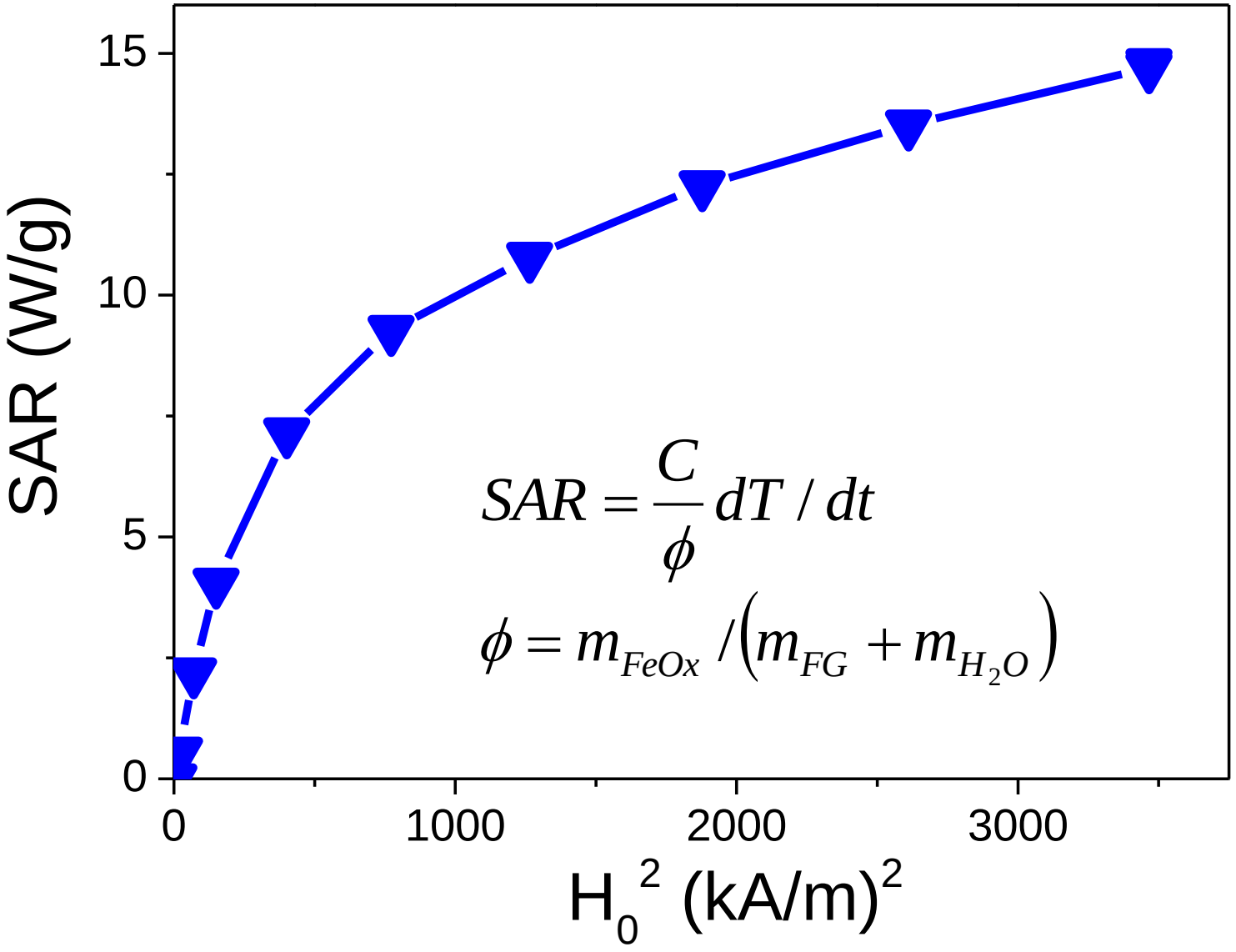
SAR (W/g)
15
10
5
0
0
1000
2000
3000
H0 2 (kA/m)2
SAR = C/ϕ dT / dt
ϕ = mFeOx /(mFG + mH2O)

Muito obrigado!

G3M

Marcela B. Fernández van Raap
Pedro Mendoza Zélis
Gustavo A. Pasquevich
Ignacio Bruvera
Elisa de Sousa
Diego Coral
Lorena Arciniegas

Francisco H. Sánchez

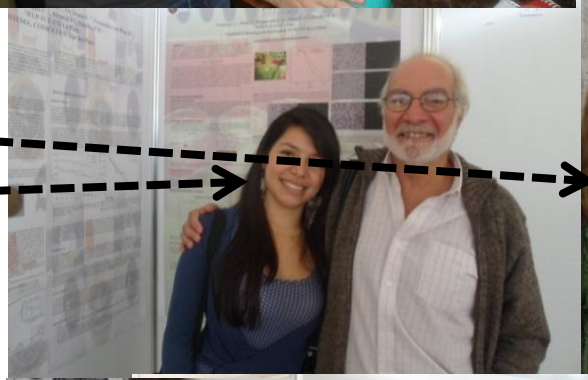

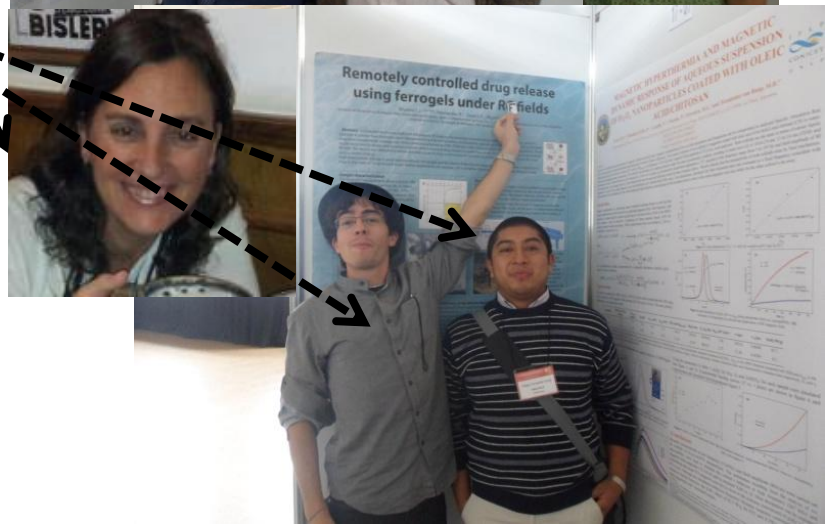

e-mail: sanchez@fisica.unlp.edu.ar

BioMag Nanomaterials

Subjects & People

In-vitro magnetofection

Olga Mykhailyc
Rodolfo Goya
Joaquín Pardo
Gustavo A. Pasquevich
Lorena Arciniegas

La-Mn-perovskites

Marcela B. Fernández
van Raap
Pedro Mendoza Zélis
Gustavo A. Pasquevich
Gabriela Leyva
Ignacio Bruvera
Cecilia Laborde

Zn-doped magnetites

Marcela B. Fernández
van Raap
Pedro Mendoza Zélis
Gustavo A. Pasquevich
Silvia Jacobo
Juan Aphesteguy
Ignacio Bruvera
Cecilia Laborde
Betiana Pianciola

Co-Ferrites

Marcela B. Fernández
van Raap
Pedro Mendoza Zélis
Gustavo A. Pasquevich
Gerardo Goya
Clara Marquina
Teo Torres
Diego Coral

Functionalized SDION cell internalization

Marcela B. Fernández
van Raap
Pedro Mendoza Zélis
Gustavo A. Pasquevich
Ricardo Dewey
Nolberto Martínez
Verónica Lasalle
Elisa de Sousa
Diego Coral
J.L. Alessandrini

PVA Ferrogels

Cristina Hoppe
Vera Alvarez
Jimena González
Pedro Mendoza Zélis
Gustavo Pasquevich
Lorena Aciniegas

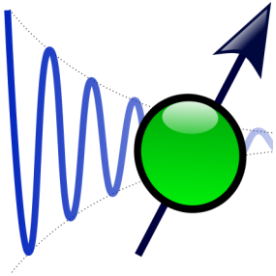

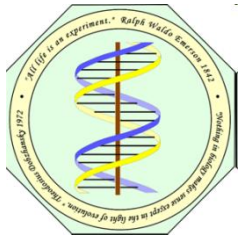

G3M

e-mail: sanchez@fisica.unlp.edu.ar

Recent related papers

•Synthesis and Characterization of PVA Ferrogels obtained through a One-pot Freezing-Thawing Procedure, *JS Gonzalez, CE Hoppe, D Muraca, FH Sánchez and VA Alvarez*, **COLLOID & POLYMER SCIENCE**, Volume 289, Numbers 17-18, 1839-1846, (**2011**), DOI: 10.1007/s00396-011-2501-1

•Ascorbic Acid Encapsulation in Hydrophobic Silica Xerogel, *MV Revuelta; MB Fernández van Raap; P Mendoza Zélis; FH Sánchez; GR Castro*, **Food Technol. Biotechnol**. 49 (3) 347–351 (**2011**)

•Self organization in oleic acid-coated CoFe2O4 colloids: a SAXS study, *MB Fernández van Raap Mendoza Zélis P, Coral, DF, TETorres, C Marquina, GF Goya, and FHSánchez*, **J Nanopart Res** (**2012**) 14:1072-1, 1072-5

•Magnetic field-assisted gene transfer: Studies in glial cells, **Acta Bioquímica Latinoamericana**, *Pardo J, Sosa YE, Reggiani PC, Arciniegas ML, Sánchez FH y Goya RG*; ISSN 1851-6114, 47, 399-406 (**2013)**.

•Structural and magnetic study of zinc-doped magnetite nanoparticles and ferrofluids for hyperthermia applications, *P Mendoza Zélis, GA Pasquevich, SJ Stewart, MB Fernández van Raap, J Aphesteguy, IJ Bruvera, C Laborde, B Pianciola, S Jacobo, FH Sánchez*, **J. Phys. D: Appl. Phys.** 46, (**2013**), 125006 doi:10.1088/0022-3727/46/12/125006.

•Stability and relaxation mechanisms of citric acid coated magnetite nanoparticles for magnetic hyperthermia, *de Sousa M, Fernandez van Raap M, Rivas P, Mendoza Zélis P, Girardin P, Pasquevich G, Alessandrini J, Muraca D, Sánchez FH*, **J. Phys. Chem. C**, (**2013**), 117 (10), pp 5436–5445. DOI: 10.1021/jp311556b.

•Magnetic properties study of PVA/iron oxide ferrogels with potential biomedical applications, *P Mendoza Zelis, D Muraca, JS Gonzalez, GA Pasquevich, VA Alvarez, KR Pirota, FH Sánchez*, **J Nanopart Res**, **(2013)** in the press.

THANKS!

Collaborations scheeme Hyperthermia

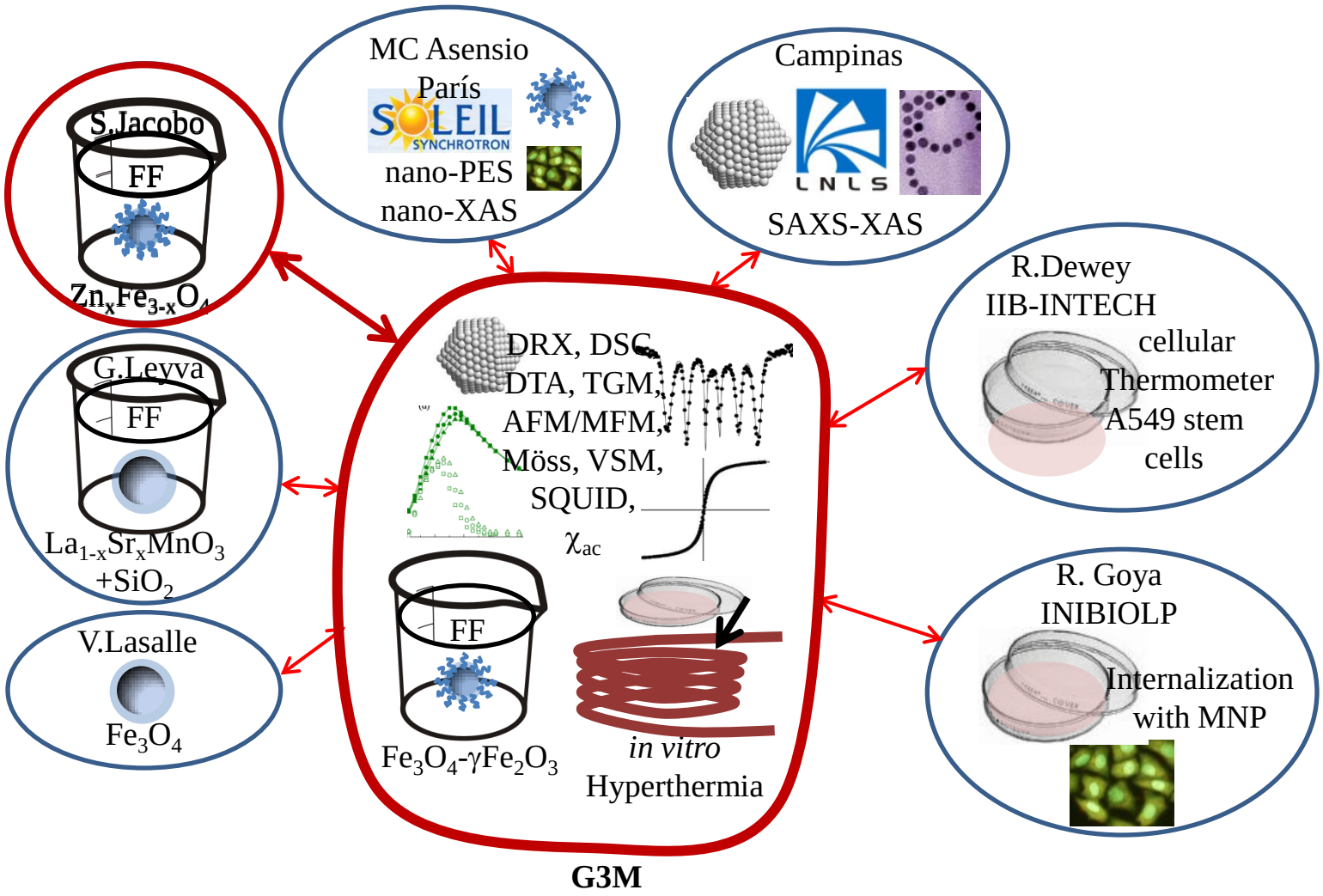

Collaborations scheeme Magnetofection

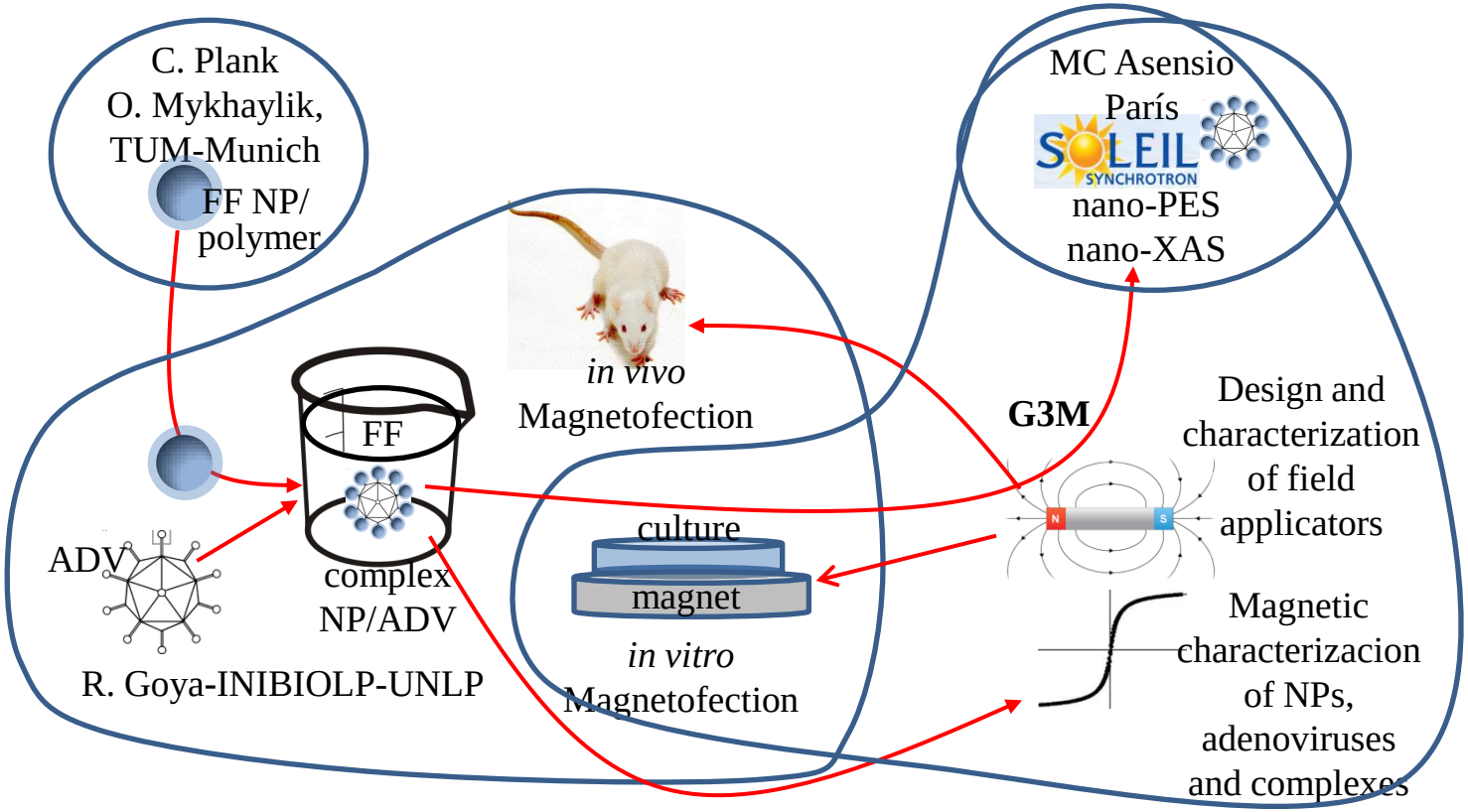

Collaborations scheeme Smart membranes

J. González, V. Alvarez,
C. Hoppe, INTEMA

Hydrogel+NP=Ferrogel

PVA+Fe_3O_4

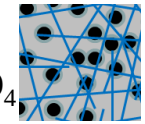

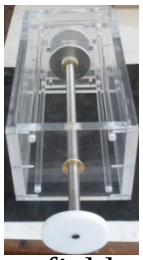

field
Applicator

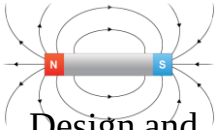

Design and characterization of field applicators

G3M

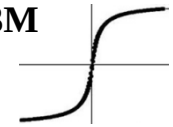

Magnetic characterization of dry and hydrated FG

Collaborations scheeme

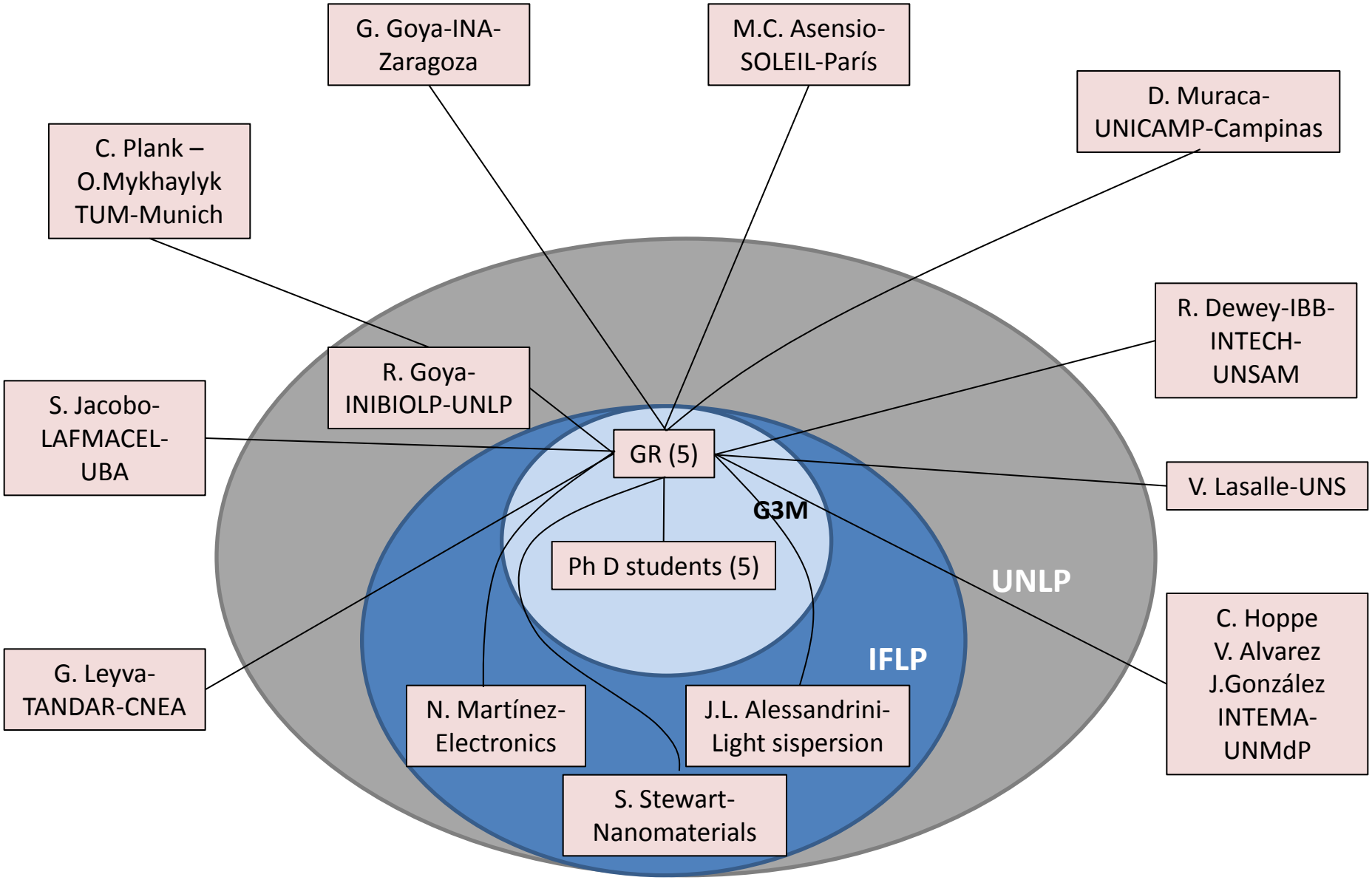

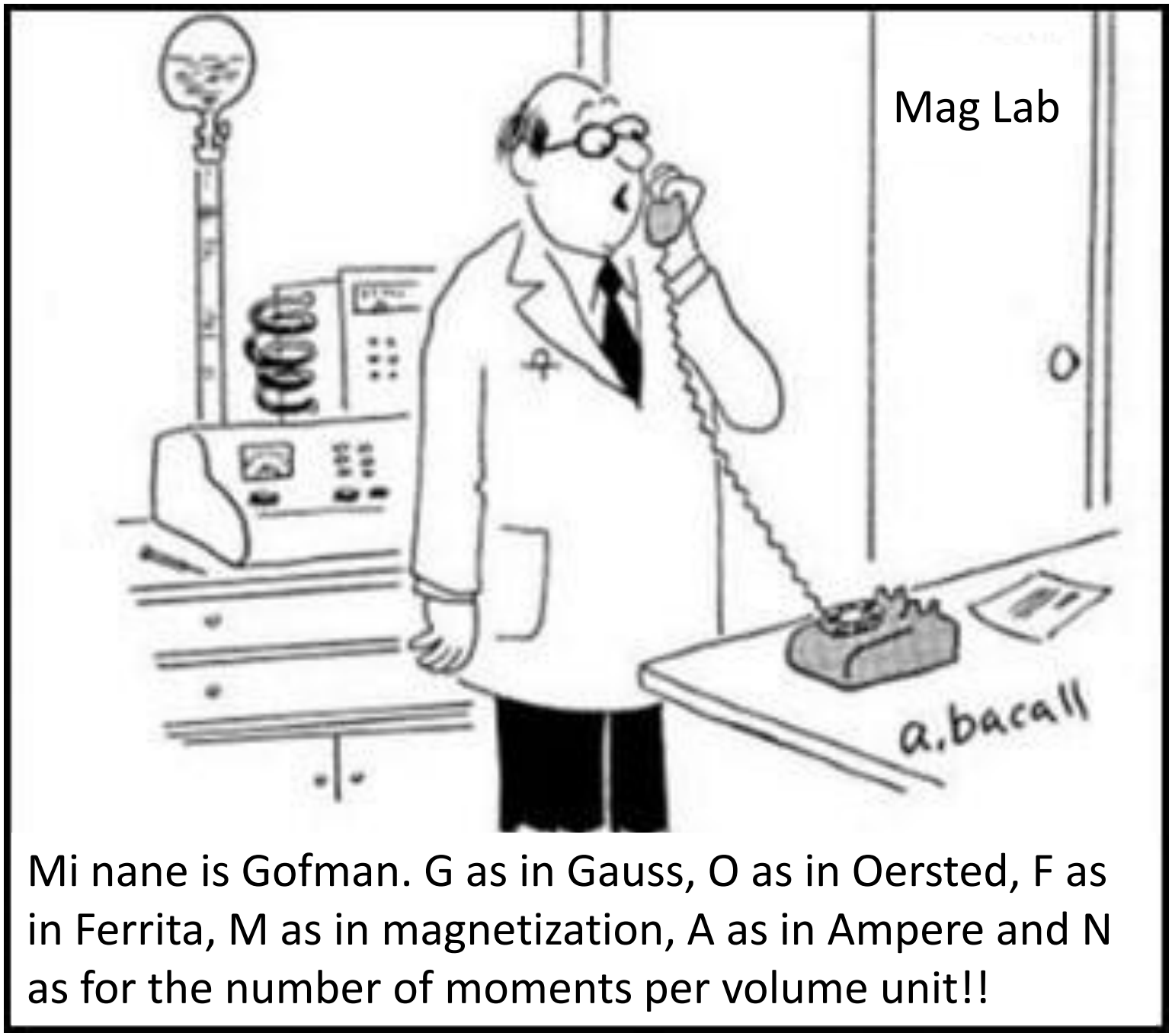

Mi nane is Gofman. G as in Gauss, O as in Oersted, F as in Ferrita, M as in magnetization, A as in Ampere and N as for the number of moments per volume unit!!

BULLETS GET ATTRACTED TO THE MAGNET AND MISS YOU COMPLETELY

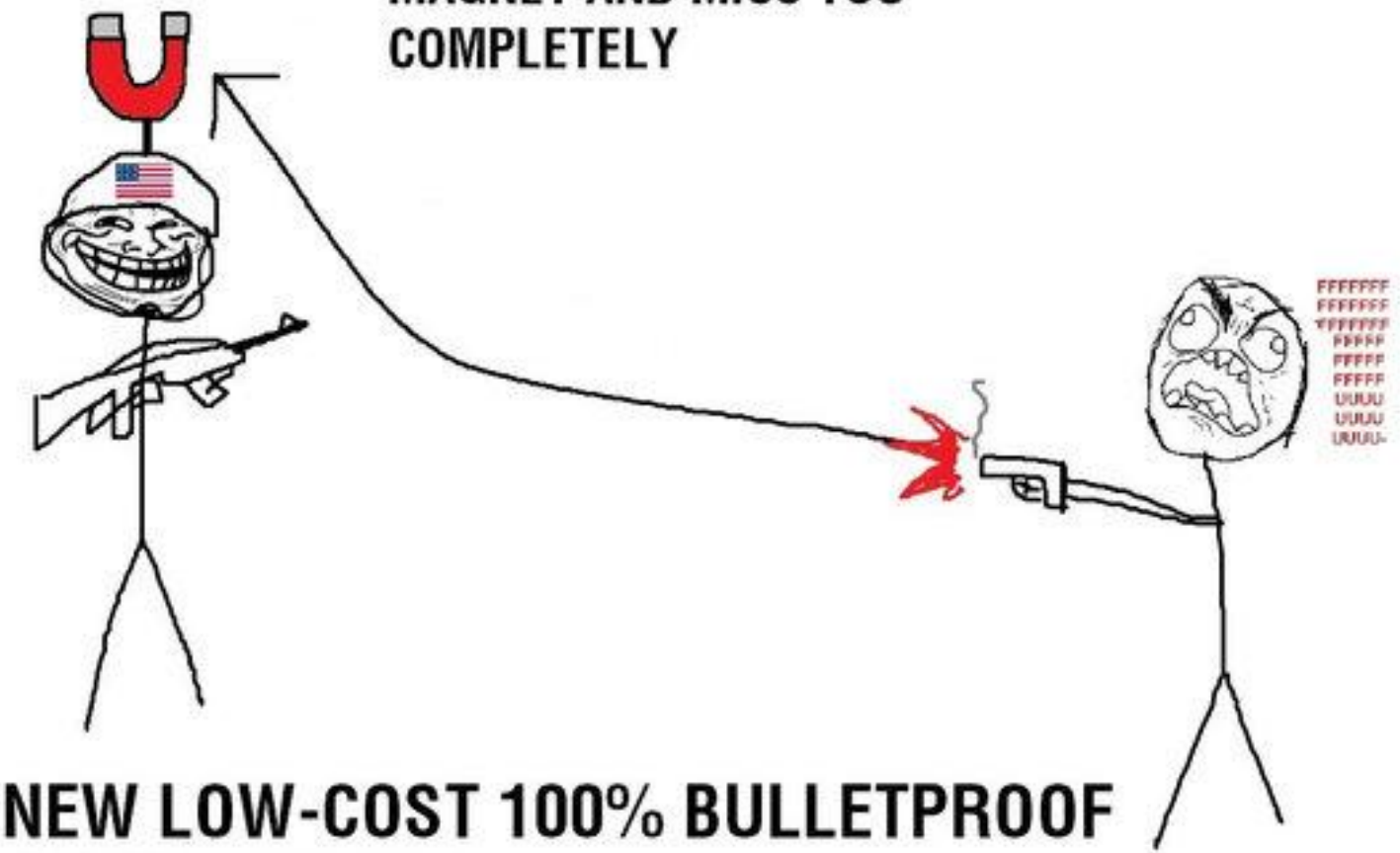

NEW LOW-COST 100% BULLETPROOF ARMOR/HELMET

HOW HAS THE ARMY NOT THOUGHT OF THIS YET?

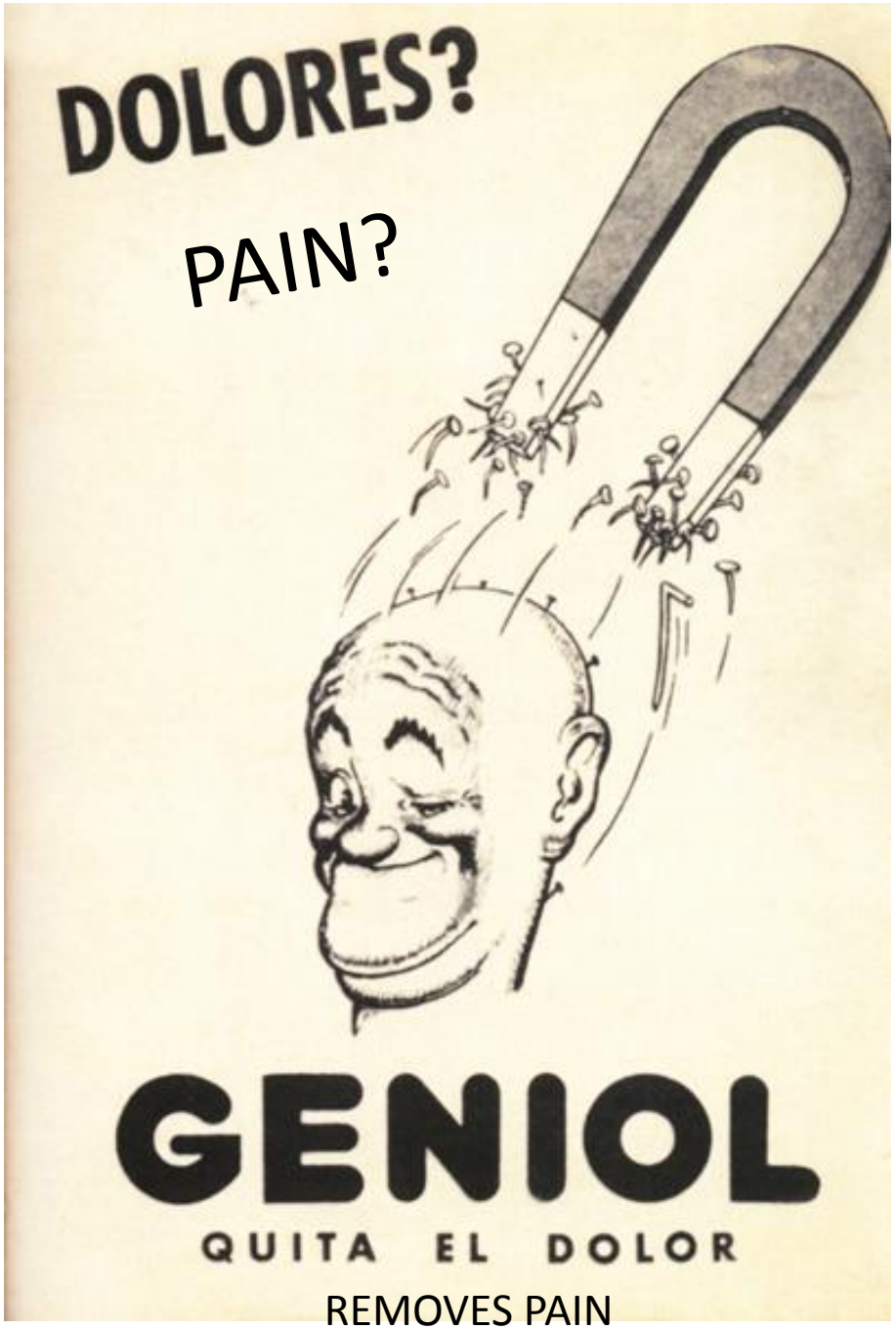

REMOVES PAIN

21st Century Childhood Pranks.

It does exist!!